Membrane coupled to the cytoskeleton: Fluctuations and stability

by

Sthembiso Reuben Gumede

Dissertation presented for the degree of Doctor of Philosophy in the Faculty of Science at Stellenbosch University

Prof. Kristian Müller-Nedebock

April 2019

Declaration

By submitting this dissertation electronically, I declare that the entirety of the work contained therein is my own, original work, that I am the sole author thereof (save to the extent explicitly otherwise stated), that reproduction and publication thereof by Stellenbosch University will not infringe any third party rights and that I have not previously in its entirety or in part submitted it for obtaining any qualification.

Date: April 2019

Abstract

Membrane coupled to the cytoskeleton: Fluctuations and stability

S.R. Gumede

Dissertation: PhD

April 2019

In erythrocytes the plasma membrane is coupled to the underlying two dimensional hexagonal network of spectrin filaments through protein node complexes. There are also other protein complexes that link an individual filament to the bilayer at a random point along its length. This network, together with a repulsive glycocalix, is responsible for large shape changes and shape transformation sequence of these erythrocytes. It has been experimentally shown that the stiffening of the erythrocytes after infection by malaria *Plasmodium falciparum* parasite, for instance, correlates with the structural transformation in the network.

We develop a model to treat the detachment of a membrane from such a substrate, which might be a model for structural failure of erythrocytes. We consider a flexible membrane elastically linked at random points to a substrate under an applied pressure differential across the membrane. This quenched randomness requires the use of the replica formalism, which we investigate from both replica symmetric and weakly broken replica symmetry perspectives. We compare these results with the continuum and the annealed adhesion models we first construct.

The fluctuation spectrum as function of the pressure, generally, shows that the average square fluctuations increases with the pressure. However, for the discrete inhomogeneous adhesion, when the position of tethers distribution is quenched the square fluctuation exhibit a non monotonic behavior. Our model characterize the role of the pressure and the disorder in the emergent non monotonic fluctuation spectrum for the different treatment of the tether position distribution randomness.

The annealed tether position distribution yields a monotonic relation of increase for the square fluctuations with the removal of tethers for nonzero pressure.

Uittreksel

Membrane coupled to the cytoskeleton: Fluctuations and stability

S.R. Gumede

Proefskrif: PhD

April 2019

In rooi bloedselle word die plasmamembraan aan die onderliggende tweedimensionele seskantige spektrin-netwerk gekoppel deur proteïenkomplekse. Daar bestaan ook ander proteïenkomplekse wat die membraandubbellagie op lukrake plekke verbind. Hierdie netwerk, saam met die afstotend wisselwerkende glikokaliks, is verantwoordelik vir die groot fluktuasies in vorm en volgorde in vormveranderinge van hierdie rooi bloedselle. Daar is deur anderes eksperimenteel bewys dat die verstywing van rooi bloedselle na infeksie deur *Plasmodium falciparum*, byvoorbeeld, met die strukturele veranderinge in die netwerk gekorreleer is.

Ons ontwikkel 'n model om die losmaking van die membraan van die substraat te behandel, wat 'n model kan wees vir die strukturele verval van rooi bloedselle. Ons beskou 'n buigsame membraan wat elasties vasgemaak is aan 'n substraat op lukrake posisies, en wat aan 'n drukverskil op die membraan onderwerp word. Hierdie ingevrore wanorde benodig die replika-formalisme, wat ons sowel uit die replika-simmetriese asook uit die swak replika-simmetrie brekende gesigspunte ondersoek. Ons vergelyk hierdie resultate met die modelle vir kontinue en nie-vaste wanorde, wat ons eers konstrueer.

Die spektrum van fluktuasies as funksie van druk, oor die algemeen, toon aan dat die gemiddelde-kwadraat fluktuasies met die druk toeneem. Maar, vir diskrete inhomogene adhesie, wanneer die posisies van die knooppunte vas is, vertoon die fluktuasies 'n nie-monotone gedrag. Ons model karakteriseer die rol van die druk en die wanorde in die daaruit ontstaande nie-monotoniese fluktuasiespektrum vir die verskillende behandelings van die knooppunte se wanorde in posisieverdelings.

Die nie-vaste wanorde posisieverdeling van knooppunte gee 'n diskontinue, Heaviside-agtige verband vir die toename in kwadratiese fluktuasies met die verwydering van die knooppunte vir nie-nul druk.

Acknowledgements

I would like to thank my supervisor Professor Kristian K. Müller-Nedebock for the guidance, cultivation and support. *Dankie* Kristian for the patience and facilitation for the completion of this thesis. It will be unjust not to mention here that part of the financial support came directly from you!

Professor Frederick G. Scholtz whom was the Head of the Department of Physics during the beginning of my journey at Stellenbosch has been instrumental to my development in various ways. Perhaps his etiquettes in leading the department and his teaching methodology are amongst the factors that I have found the Stellenbosch Physics Department an inspiring place.

I am grateful for the financial support from the National Institute for Theoretical Physics (NITheP) of the Republic of South Africa. Without their financial support I would not have been able to endeavour into this research project.

Lastly, I would like thank the many people whom The Subtle and Impeccable has aided me by in a critical period of my life. Only He, The Bestower of Forms, fully encompasses the value of your generosity.

Contents

List of Figures

Chapter 1

Introduction

1.1 Membrane and vesicle adhesion

Adhesion of biological lipid membranes or cell membranes is a ubiquitous fascinating phenomenon in nature. It is a process that controls many functions necessary for life. The lipid membranes are nearly two dimensional structures which form spontaneously out of aggregation of lipid molecules in aqueous solution. This is an example of what is termed *self-assembly* since the aggregation leads to a formation of a complex structure with a new length scale. The lipid molecules have a structure comprising of a head and a tail. They are natural, amphiphilic, forms of surfactants - surface active agents - which serve to reduce the interfacial tension. These lipid membranes can form higher dimensional large structures such as encapsulating structures called vesicles.

Lipid membranes and vesicles have of themselves acquired a great scientific interest. Inter alia, this can be attributed to their abundance in nature, ernomous number of shape conformations and the shape transformations they exhibit as well as the unique material properties associated with their molecular architecture. The vesicles also have a close resemblance to string theory models [1].

Biological lipid membranes form the boundary of all biological cells and cell organelles [2]. Amongst other things, they are embedded with proteins that enable them to fulfill functions such as ion pumping, converting light to chemical energy and, of the interest of this project, adhering, which is an essential step to the many other biological processes.

The cell-cell recognition is essentially adhesion - a process central to embryological development, tissue stability and immunology. Cell behaviour in a multi-cellular organism is affected by contacts with other cells or with substrata such as collagen. The contacts usually involve attachment of such specificity mediated by specific receptor molecules on the cells. An example, the

adhesion between specific cells in embryological development is attributed to cell receptors [3]. It is also established that lymphocytes posses surface receptors for antigenic determinants that enable antigen recognition leading to specific immune response [4]. Cell-cell adhesion can also be blocked as Berg *et al.* [5] showed in aggregating cells of *Dictyostelium discoideum* with univalent antibodies directed against specific membrane sites.

Further, after the observation that two strains of *Acanthamoeba castellani* have different adhesive properties. A study conducted by Hoover [6] cited the glycoprotein composition difference as responsible for the exponentially growing *amoebas*. In a different study, investigating the cytoadherence of malaria infected red blood cell under flow Xu *et al.* [7] showed that adhesiveness is strongly affected by the stiffness of the membrane. Adhesiveness of malaria infected red cells is amongst factors responsible for the fatality of malaria infection [8].

In vitro assays have been developed to study the mechanics of adhesion such as that of *rosette assays* where red blood cells (RBCs) may be bound to lymphocytes by means of specific antibodies [9].

Due to their simple structure lacking nucleus and organelles RBCs have been experimented and modeled extensively in membrane physics. Their various properties such as biconcave shapes [10], flickering phenomenon [11] and tank treading motion in shear flow [12] have been established based on a simple lipid bilayer bag models. However, internal specific adhesion through protein components of a network substructure - the cytoskeleton - to the lipid bilayer is found responsible for large scale shape changes under shear flow and shape transformation sequence[13]. This sequence can be effected systematically by agents such as high salt and adenosine triphosphate (ATP) depletion leading to a series of crenated shapes called echinocytes characterized by round protrusion or specules. Upon further loading, these protrusions eventually bud off as small network-free plasma membrane vesicles. In this process the normal biconcave state of the RBC becomes spherical -*spheroechinocyte*- with a reduced surface area and volume. In contrast, low salt and cholestrol depletion agents, amongst others, lead to concave shapes called stomatocytes. On further loading, multiple invaginations are produced which eventually bud off forming interior vesicles leaving a sphero *stomatocyte*. The agents are understood to cause defects on the cytoskeleton network substructure [14]. In experiments it has been shown that the stiffening of RBCs after being infected by malaria Plasmodium falciparum [15] correlates with the structural transformation in the cytoskeleton network [16].

The RBC cytoskeleton network is two dimensional in nature having on average a hexagonal symmetry of spectrin biopolymer filaments. These filaments are attached to the bilayer through a node of a protein complex. There are also other protein complexes that link an individual filament to the bilayer at a random point along its length [17].

Simplified model descriptions of the network and its effects on the bilayer

have been provided [18; 19; 20; 21]. However, a composite structure model has been introduced by Gov and coworkers [22] after their analysis of the fluctuation spectrum measured by Zilker and coworkers [23]. Gov *et al.*, through an empirical approach, claimed that the coupling of the bilayer to the cytoskeleton network induces a surface tension such that the effective bending modulus of the bilayer undergoes an abrupt jump at characteristic length [22].

This was further corroborated by Fournier *et al.* [24]. They modeled the cytoskeleton as a spring meshwork and examined the elastic energy of the meshwork as a function of the membrane area coarsely grained at mesh size. The tension contribution was found to vanish at at mesh size length scale.

There, however, exist variance with some experimental investigations. Yoon *et al.* [25] observed shape dependent fluctuations where the tension contribution is clearly visible for spherocype RBCs but almost unnoticeable for discocytes. Whilst Popescu *et al.* [26] observed the induced surface tension regardless of the shapes. Y. Park [20] only found a few samples of the RBCs to exhibit this tension in the intermediate tension dominated region. Whereas the short wavelength and long wavelength scales exhibited bending and confinment dominated fluctuations, respectively.

Choi and coworkers [27] recently also reached a contrary conclusion to the prediction of a sudden change of tension at characteristic length scale of [22; 24]. Instead, they have found that the tension appears gradually. Additionally, they found that the coupling modifies the fluctuation spectrum at wavelength longer than the mesh size of the network while leaving fluid like behaviour of the membrane intact at shorter wavelengths. The fluctuation spectra can be markedly different depending on, not only, the relative amplitude of the bilayer bending energy with respect to the cytoskeleton deformation energy but also the bilayer-cytoskeleton coupling strength.

1.2 Models and methods overview

Analytical models and descriptions [28; 29] of *free* fluid membranes and vesicles have grown since the early continuum formulation of Helfrich Halmitonian [30] for membranes. Biological membranes together with their applications, however, also require an understanding of the role of confinement and or the properties of solid membranes which can support a shear. The first mathematical models of membrane or cell adhesion were done by Bell, Dembo and Bongrad [31; 32]. What has become known as the Bell model describes such adhesion as a competition between lock and key specific adhesion with the repulsive pressure due to the *glycocalix*. This model is founded upon the assumption of ideal mixing. That is, the lock and key adhesion molecules are in chemical equilibrium. Further, the adhesion molecules are assumed to

have weak and rather negligible interactions. This reversible mobile lock and key model is, however, inadequate. Why? It has been observed in different studies [33; 34] that the adhesion disk connecting the cells is inhomogeneous with respect to the distribution of adhesion molecules. A simulation study conducted by Baljon and Robbins [35] also showed that when plates adhered by a polymer layer are pulled apart the layer decomposes into stress focussed regions with higher concentration of adhesion molecules.

A different treatment to the Bell ideal non-interacting adhesion molecules model was proposed by Braun, Abney and Owicki [36; 37]. They asserted that the adhesion molecules do interact, but indirectly. It is therefore understood that the adhesion molecules' higher concentration regions are a result of the repulsive glycocalix that generates a long-range attraction between adhesion molecules mediated by the cell membranes. A later study [38], upon introducing the Helfrich effective interaction term between the membranes in the Hamiltonian [30; 39] supported this assertion and predicted a logarithmic attractive potential between adhesion molecules. This assertion was incorporated in the model developed by Zuckerman and Bruinsma [40]. They mapped the interacting Bell model onto a two dimensional Coulomb plasma and treated this in a Debye-Hückel theory [41] which they also explored by Monte Carlo simulations.

Formation and stability of finite size adhesion domains by the mobile adhesion molecules has continued to attract investigations as shown in a review by Schwarz and Safran [42]. There is also a large body of work done by Schick [43; 44] on disorder-induced domain formation on membranes. A relatively recent study by Speck and Vink [45] followed the Zuckerman and Bruinsma [40] mapping approach. However, what is explored in this work is the role of the disorder of the environment due to compartmentalization or extra-cellular matrix pinning of the membranes thereby immobilizing a fraction of adhesion molecules. This mapping derived a two dimensional bond lattice Ising gas. The authors argue that the field is of a random field type. This is also argued with simulations. Hence, they apply the Imry-Ma argument [46; 47]: a system could try to lower its free energy by forming *domains* in which the order parameter takes advantage of local fluctuations in the random field. This is used as a justification of finite domains as opposed to a macroscopic one.

It has long been believed [48] that adhesion due to immobile stickers will lead to new critical behaviour. Interestingly, Mezard and Young [49] treated a random field Ising model using the technique of Replicas. This is a *method* we shall be concerned with. These authors discovered that the replica symmetric solution is unstable and obtained equations for solutions which break the replica symmetry. In the following sections we shall discuss some detail of the Replica Technique or Method.

The above mentioned Speck and Vink model contains elements of the context of our adhesion problem, that is of quenched pinning. However, an alter-

native analytical treatment of the quenched disorder is needed. In a different study motivating the phenomenological modelling of pinned membranes Gov and Safran had, themselves, earlier developed [22]. They constructed a discrete tethering or pinning mathematical model [50]. The objective of this model was to treat the random local discrete nature coupling of the cytoskeleton to the bilayer. Their calculation is based on an anology with the electronic wave equation in a periodic potential [51], which leads to a set of algebraic equations and thereby studied a smooth sinusoidal potential [51]. This was complemented with a study of a one dimensional series of delta potentials. A study of a similar model nature was done by Merath and Seifert [52] using a scheme developed by Lin and Brown [53].

1.3 Dissertation objective

Sophisticated lipid bilayer interfaces can be engineered using modern tools of biochemistry. These membrane interfaces are sometimes tethered by polymer layers or supported by solid supports. We can, for example, use infrared spectroscopy [54], surface plasmon resonance [55] and total interference fluorescence [56] to study structural and dynamic properties and function of cell membranes and their embedded proteins. These proteins acts as receptors for specific molecules or transport materials across the cell membrane. They also function as filters passing nutrients and metabolites whilst preventing toxic substances.

Watts *et al.* [57] using supported membranes containing reconstituted proteins showed that antigen cells recognition by T cells, for immune response activation, requires antigen association with the major histocompatibility complex. This immune response activation depends on dynamic features of the recognition and interaction that creates the immunological synapse [58]. Therefore tethered or supported membranes can serve as replacement cell surfaces.

The architecture of these tethered or supported membranes can be manipulated in order to control the membrane-support function and communication. Micro-nano patterned substrate supports involving silicon pillars and gold dots have been used to study the interaction with cell membranes [59]. Microfluidics technology that enable controlled delivery of analytes to membrane corrals in combination with field effect transistor semiconductor technology offers a powerful label free tool for high throughput screening. Semiconductor field effect transistors have been used to monitor activities of neuronal cells [60] and cardiac mycocytes [61].

These technological applications, and others, of tethered or supported membranes requires the understanding of **how thermal fluctuations are affected by tethering or pinning at the specific binding points as well as what critical behaviour can be harnessed**. In fig. 1.1 a simpli-

fied depiction of such pinning is shown. Now, in section 1 we started discussing supported membranes in the context of composite membranes such as that of the red blood cells which forms our model background into supported membranes. It is this context that shall be overaching in our model of tethered or supported membranes. Therefore, again, we are interested in understanding the role of the underlying polymer network support substrate, the cytoskeleton, in the observed properties or fluctuation spectra of the red blood cells. The fluid bilayer of the red blood cells is attached to the two dimensional spectrin network - the cytoskeleton - through membrane proteins. The cytoskeleton is generally stiffer than the lipid bilayer, and its solid like structure gives it a shear modulus [50].

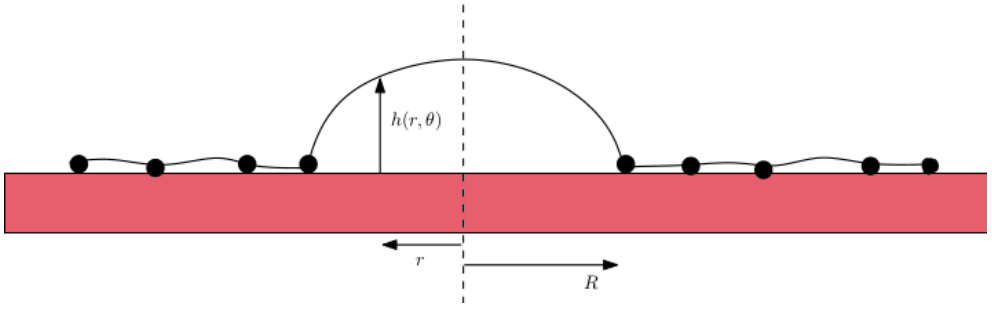

Figure 1.1: Sketch of a tethered or pinned membrane. Arc-segments, pinned to a substrate, the red section, at discrete sites of attachment, the black circles.

We have already mentioned that simplified model description of the network and its effects on the bilayer have been provided [18; 19; 20; 21]. Also that, a composite structure model was introduced by Gov and coworkers in the paper reference [22] after the analysis of the fluctuation spectrum measured by Zilker and coworkers [23]. As well as that Gov *et al.*, through an empirical approach, claimed that the coupling of the bilayer to the cytoskeleton network induces a surface tension such that the effective bending modulus of the bilayer undergoes an abrupt jump at characteristic length [22]. We highlighted the contrasting findings to these. These models do not address the following: that the stiffness of the red blood cells, after being infected by malaria Plasmodium falciparum [15], correlates with the structural transformation in the cytoskeleton network [16]. The network is two dimensional flexible-semiflexible network having on average a hexagonal symmetry of spectrin biopolymer filaments. These filaments are attached to the bilayer through a node of a protein complex. There are also other protein complexes that link an individual filament to the bilayer at a random point along its length [17]. This quenched random nature or quenched disordered distribution nature of attachment sites requires detailed consideration. This brings us to the statement of the objective of this dissertation:

In erythrocytes the plasma membrane is coupled to the underlying spectrin network. We develop a model in Monge parametrization to treat the detachment of a membrane from such a substrate, which might be a model for structural failure of the red blood cell. We consider a flexible membrane elastically linked at random points to a substrate. This quenched randomness requires the use of the replica formalism, which we investigate from both replica symmetric and weakly broken replica symmetry perspectives. Criteria for detachment under an applied pressure differential across the membrane are derived. We also sketch how a more detailed spectrin network can be included in this model.

1.4 Introduction to membranes

In the preceding section 1.1 we began the description of membranes as two dimensional surfaces that exhibit an enormous number of conformations and transformations. Subsequently, a physical description requires a background in elasticity physics of surfaces – how energy changes when the membrane undergoes some change – and thereby, in proper treatment, familiarity with differential geometry [64; 65]. In this brief introduction, however, we shall not delve very far in the formalisations. Our intent is to introduce a few primary concepts and the energy functional of membranes and their fluctuations.

The extension of the one dimensional concept of curvature $\kappa(s) = C(s) = \frac{1}{R(s)}$ where s is the arclength coordinate is that for surfaces there are now two principal curvatures $C_1 = \frac{1}{R_1}$ and $C_2 = \frac{1}{R_2}$. These curvatures enable us to define the extrinsic curvature $K = C_1 + C_2$ and thereby the mean curvature $H = \frac{1}{2}(C_1 + C_2)$. The intrinsic or Gaussian curvature is given by $K_{\mathrm{G}} = C_1 C_2$.

In the *Monge parametrization* – that is, the surface is assumed to have no overhangs and on average horizontal – the surface can be described with a height function $h(\mathbf{r})$, where $\mathbf{r}$ is a position vector on the projection reference plane. The curvature K can be expressed as $K \approx \nabla^2 h(\mathbf{r})$ for this gauge.

After Canham's [66] proposition that the bending energy density expression $E = \frac{1}{2}\kappa_{b_1} C_1^2 + \frac{1}{2}\kappa_{b_2} C_2^2$, with κ_{b_i} being the corresponding bending modulus, be generalized to

$$E = \frac{\kappa_b}{2}(C_1^2 + C_2^2) = \frac{\kappa_b}{2}(K^2 - 2K_{\mathrm{G}}) \tag{1.4.1}$$

for isotropic materials. With an addition of the characteristic or spontaneous curvature C_0, Helfrich [30] proposed the bending energy density

$$E = \frac{\kappa_b}{2}(C_1 + C_2 - C_0)^2 + \bar{\kappa} C_1 C_2 = \frac{\kappa_b}{2}(K - C_0)^2 + \bar{\kappa} K_{\mathrm{G}} \tag{1.4.2}$$

with a modulus $\bar{\kappa}$ called a saddle splay modulus. The condition of equivalence of these two formulations is established by the theorem called Gauss-Bonnet-

Theorem [64]. In conclusion, we can express the commonly used Helfrich Hamiltonian as given by

$$H = \int \mathrm{d}S[\frac{\kappa_b}{2}(K - C_0)^2 + \bar{\kappa}K_\mathrm{G} + \gamma] \tag{1.4.3}$$

where γ is the surface tension. The integral is over the membrane surface S. In the Monge parametrization this is equivalent to

$$H = H_0 + \int \mathrm{d}x\mathrm{d}y \left[\frac{\kappa_b}{2}(\nabla^2 h(\mathbf{r}))^2 + \gamma(\boldsymbol{\nabla} h(\mathbf{r}))^2\right]. \tag{1.4.4}$$

The other terms are absorbed into H_0. Fourier expanding $h(\mathbf{r})$ by $h(\mathbf{r}) = \sum_\mathbf{q} h_\mathbf{q} \exp(i\mathbf{q}\cdot\mathbf{r})$ with the wavevector $\mathbf{q}$ equivalent to $\mathbf{q} = \frac{2\pi}{L}\langle n_x, n_y\rangle$ the Helfrich Hamiltonian then becomes

$$H = L^2 \sum_\mathbf{q} |h_\mathbf{q}|^2 \left(\frac{\kappa_b}{2}q^4 + \frac{\gamma}{2}q^2\right). \tag{1.4.5}$$

Applying the energy equipartition theorem we obtain the fluctuation spectrum

$$\langle |h_\mathbf{q}|^2 \rangle = \frac{k_B T}{L^2\left(\frac{\kappa_b}{2}q^4 + \frac{\gamma}{2}q^2\right)}. \tag{1.4.6}$$

The parameters k_B, T and L are the Boltzmann constant, temperature and the side length of a square membrane.

1.5 Disordered systems

In this section we shall introduce concepts related to disordered systems. Disordered sytems at a simple level can be described in relation to pure metals or spatially regularly patterned systems such as gold. These are said to be *ordered* systems when there exist not any *random* void or alien impurities in their crystalline structure. In the contrary when such random defects or impurities exist these systems becomes *disordered*. In the context of magnetic systems, the transition metal impurities moments produce a magnetic polarization of the host conduction electrons around them which is positive at some distances and negative at others. Due to the random placement of the impurities, the field produced by the polarized conduction electrons felt by the other impurities creates interactions that for some favour parallel alignment and not for others [63].

Disorder can be categorized into *quenched* also called *frozen* and *self-generated* disorder [67]. In the quenched disorder systems the disorder is explicitly expressed in the Hamiltonian. A classic example, which formed the basis

of theoretical studies into spin glasses, is the Edwards-Anderson model [68] characterized by the Hamiltonian

$$H = -\sum_{\langle i,j \rangle}^{N} J_{ij}\sigma_i\sigma_j, \tag{1.5.1}$$

where the $\sigma_i = \pm 1$ are the Ising spins degrees of freedom. The quenched disorder is characterized by the relatively constant random coupling parameters J_{ij}. These remain constant over the timescale at which the systems degrees of freedom σ_i fluctuate.

When the random coupling parameters J_{ij} could not be satisfied, for example in a three spin spin model when either of the two spins have different orientation expectation of the third one, instantaneously the system becomes *frustrated* exhibiting degenarate ground state - an essential ingredient of glassy systems. Subsequently, the system cannot explore the phase space with equal likelihood, hence breaking the ergodicity, and thereby partitioning the phase space onto *metastable* states.

The second class of disorder, the self-generated, the disorder is not explicitly present in the Halmitonian. It usually takes the form $H = \sum_{ij} V(r_i - r_j)$ where r_i is the particle position degrees of freedom. $V(r_i - r_j)$ is not stochastic but a deterministic potential such as the interatomic Lennard-Jones potential. At low temperature, potentially a frozen configuration of the system occurs and thereby generating some disorder.

1.6 Averaging: annealed and quenched

In equilibrium statistical mechanics we are mainly interested in determining the free energy thermodynamic potential F. When there is quenched disorder in the system how do we determine such an observable? In the context of the above mentioned Edwards-Anderson model (1.5.1) we have to calculate the average

$$f = -\frac{1}{\beta N}\int \mathrm{d}J\; p(J) \log \int \mathcal{D}\sigma\; e^{-\beta H(\sigma;J)} = -\frac{1}{\beta N}\langle \log Z \rangle_{\text{disorder}} \tag{1.6.1}$$

where $\int \mathcal{D}\sigma \approx \lim_{N\to\infty} \int \prod_{n=1}^{N} \mathrm{d}\sigma_n$.

Mathematically, averaging over a log function makes this not an easy task. Is it then rather a good approximation to evaluate

$$f_{\text{approx}} = -\frac{1}{\beta N}\log \int \mathrm{d}J\; p(J) \int \mathcal{D}\sigma\; e^{-\beta H(\sigma;J)} = -\frac{1}{\beta N}\log \langle Z \rangle_{\text{disorder}} ? \tag{1.6.2}$$

This is certainly not what we want due to the role played by the disorder J. In such an approximation the disorder is no longer quenched as it simply

becomes another degree of freedom fluctuating at the same timescale as other degrees of freedom. This type of an average is called *annealed*. There exist, however, instances where such an approximation helps in the understanding of the problem. It has been argued that it sets an upper bound of the free energy [69]. We actually have to be careful that for each realization of the disorder we compute the free energy and thereafter determine the average over J. This is the *quenched* average of our interest. How do we then practically compute the quenched average of (1.6.1)? This is where the *replica approach* becomes expedient.

1.7 The replica approach

In this section, for completeness, we outline the background 'theory' into the replica technique. This background will hopefully elucidate the concepts and practical tools we shall need in handling our calculations and interpretations in following chapters in the context of tethered membranes. This outline is based on references [63; 67; 71; 69].

The replica approach is a method founded upon the mathematical identity

$$\ln Z = \lim_{n\to 0} \frac{Z^n - 1}{n} \tag{1.7.1}$$

derived from $Z^n = e^{n \ln Z} \approx 1 + n \ln Z$. The key ingredient of this approach is to initially assume the replica index n to be an integer such that we can write

$$\langle Z^n \rangle_{\text{disorder}} = \int \mathcal{D}\sigma_1 \cdots \mathcal{D}\sigma_n \left\langle e^{-\beta H(\sigma_1, J) \cdots - \beta H(\sigma_n, J)} \right\rangle_{\text{disorder}} \tag{1.7.2}$$

and hence the name replica method. We replicate the system n times whilst for every Halmitonian the realization of the quenched disorder is the same for all replicas. There also exist an alternative form of the replica method, namely

$$\begin{aligned} \langle A \rangle_{\text{disorder}} &= \left\langle \frac{1}{Z} \int \mathcal{D}\sigma \; A(\sigma) e^{-\beta H(\sigma, J)} \right\rangle_{\text{disorder}} \\ &= \lim_{n\to 0} \int \mathcal{D}\sigma_1 \cdots \mathcal{D}\sigma_n \; A(\sigma_1) \left\langle e^{-\beta H(\sigma_1, J) \cdots - \beta H(\sigma_n, J)} \right\rangle_{\text{disorder}} \end{aligned} \tag{1.7.3}$$

The physics result of the observable A must not be dependent on the choice of the index label σ_1 or σ_m in the parantheses of $A(\sigma)$.

1.7.1 Order parameter and overlap

As in normal magnetic systems in disordered systems also the concept of an order parameter is of essential importance. Normal magnetic systems have the

total average magnetization as the natural order parameter

$$m = \frac{1}{N}\sum_{i=1}\langle\sigma_i\rangle. \tag{1.7.4}$$

It is zero in the high temperature phase, and different from zero in the low temperature phase, where the symmetry is broken. In disordered systems it seems sensible to extend the above order parameter definition by simply including the disorder average such that

$$m = \frac{1}{N}\sum_{i=1}\langle\langle\sigma_i\rangle\rangle. \tag{1.7.5}$$

The second angular brackets $\langle\langle\cdots\rangle\rangle$ denotes the average over disorder whilst the inner ones are of thermal nature. We shall use both these notations $\langle\cdots\rangle_{\text{disorder}}$ and $\langle\langle\cdots\rangle\rangle$. Due to the disorder this extended order parameter is zero at all temperatures and thus not useful. Hence, Edwards and Anderson chose the disordered system order parameter as [68]

$$q_{EA} = \frac{1}{N}\sum_{i=1}\langle\langle\sigma_i\rangle^2\rangle. \tag{1.7.6}$$

This order parameter is non-zero if the local magnetizations m_i, are locally non-zero. Another important quantity to introduce in disordered systems is the *overlap*. Its value lies in determining the similarity or correlations of configurations or phase space states. For two configurations σ and τ, the overlap is defined as

$$q_{\sigma\tau} = \frac{1}{N}\sum_{i=1}\sigma_i\tau_i. \tag{1.7.7}$$

This overlap definition can be extended further such that it measures the similarity between partitioned phase space *states* α and β to

$$q_{\alpha\beta} = \frac{1}{N}\sum_{i=1}\langle\sigma_i\rangle_\alpha\langle\sigma_i\rangle_\beta \tag{1.7.8}$$

In the expanded form this expression is equivalent to

$$\begin{aligned} q_{\alpha\beta} &= \frac{1}{N}\sum_{i=1}\frac{1}{Z_\alpha}\int_{\sigma\epsilon\alpha}\sigma_i\; e^{-\beta H(\sigma)}\frac{1}{Z_\beta}\int_{\tau\epsilon\beta}\tau_i\; e^{-\beta H(\tau)} \\ &= \frac{1}{Z_\alpha Z_\beta}\int_{\sigma\epsilon\alpha}\int_{\tau\epsilon\beta}\mathcal{D}\sigma\;\mathcal{D}\tau\; e^{-\beta H(\sigma)}e^{-\beta H(\tau)}q_{\sigma\tau}. \end{aligned} \tag{1.7.9}$$

Therefore, by measuring states overlap we are actually probing the overlap between configurations belonging to the states each one weighted with its own

statistical weight. Disordered systems generally have many inequivalent *pure states* - unequal phase space states - such that we can express observables as

$$\langle \cdots \rangle = \sum_{\alpha} w_{\alpha} \langle \cdots \rangle_{\alpha} \quad \text{where} \quad w_{\alpha} = \sum_{\sigma \epsilon \alpha} \frac{e^{-\beta H(\sigma)}}{Z} \tag{1.7.10}$$

'at low temperatures'. Therefore it is sensible to introduce a probability distribution $P(q)$ of possible values of the overlaps among states [63]. For a system with only two phases $P(q)$ is simply a sum of a pair of delta functions. For two systems with the same disorder we can write [63]

$$P(q) = \frac{1}{Z^2} \int \mathcal{D}\sigma \mathcal{D}\tau e^{-\beta H(\sigma)} e^{-\beta H(\tau)} \delta(q - q_{\sigma\tau}). \tag{1.7.11}$$

This we can again expand as in the previous expression (1.7.9) to obtain

$$P(q) = \sum_{\alpha\beta} w_{\alpha} w_{\beta} \frac{1}{Z_{\alpha}} \int_{\sigma \epsilon \alpha} \frac{1}{Z_{\beta}} \int_{\tau \epsilon \beta} \mathcal{D}\sigma \mathcal{D}\tau e^{-\beta H(\sigma)} e^{-\beta H(\tau)} \delta(q - q_{\sigma\tau}), \tag{1.7.12}$$

with the conclusion

$$P(q) = \sum_{\alpha\beta} w_{\alpha} w_{\beta} \delta(q - q_{\alpha\beta}). \tag{1.7.13}$$

In this definition of the $P(q)$ the sum is over all the possible pairs of the states, including pairs of the same states, giving that state's self-overlap. In the Ising model example at low temperatures there are two pure states whilst there are four possible overlaps q_{++}, q_{--} and $q_{+-} = q_{-+}$ whereby

$$\begin{aligned} q_{++} &= \frac{1}{N} \sum_i \langle \sigma_i \rangle_+^2 = \frac{1}{N} \sum_i m_i^2 = \frac{1}{N} \sum_i \langle \sigma_i \rangle_-^2 = q_{--} = m^2, \\ q_{+-} &= q_{-+} = \frac{1}{N} \sum_i \langle \sigma_i \rangle_+ \langle \sigma_i \rangle_- = -\frac{1}{N} \sum_i m_i m_i = -m^2. \end{aligned} \tag{1.7.14}$$

Therefore for this model the overlap distribution function $P(q)$ has two peaks one at $-m^2$ and another at $+m^2$ each with the weight $1/2$. We note that the number of peaks of the $P(q)$ is *not* equal to the number of states.

Finally, $P(q)$ is not self-averaging since the particular structure of states of a given sample depends on the particular realization of the disorder J as such both the pure states weights and the overlap distribution $P(q)$ depend on the disorder J. Especially when the structure of states is non-trivial [63].

1.7.2 Replica symmetry

In this section we shall use the *p-spin spherical model* to detail an actual replica calculation. The reason we do this is that in this calculation the two

fundamental solutions of the replica approach, namely, the replica symmetry and the one step symmetry breaking solutions, are clearly expressed. The concept of the replicas overlap matrix also arise naturally in this elucidating example.

This model was explored by Crisanti and Sommers [72]. Its Hamiltonian is given by

$$H = -\sum_{i_1>\cdots>i_p=1} J_{i_1\cdots i_p}\sigma_{i_1}\cdots\sigma_{i_p} \qquad p \geq 3 \tag{1.7.15}$$

where the spins are *real* continuous variables. The model derives its name from the constraint

$$\sum_{i=1}^{N} {\sigma_i}^2 = N; \tag{1.7.16}$$

set to keep the energy finite for the system. Each random coupling J is a Gaussian variable, with the distribution

$$dp(J) = \exp\left(-\frac{1}{2}J^2\frac{2N^{p-1}}{p!}\right)dJ. \tag{1.7.17}$$

For the case $p = 3$ and with one replica $n = 1$ the annealed average partition function is given by

$$\begin{aligned}\langle\langle Z\rangle\rangle &= \int \mathcal{D}\sigma \int \prod_{1<j<k} dJ_{ijk} \exp\left[-{J_{ijk}}^2\frac{N^p}{p!} + J_{ijk}\beta\sigma_i\sigma_j\sigma_k\right] \\ \langle\langle Z\rangle\rangle &= \int \mathcal{D}\sigma \exp\left[\frac{\beta^2}{4N^{p-1}}\left(\sum_i \sigma_i^2\right)^p\right] = \exp\left[N\frac{\beta^2}{4}\right]\Omega,\end{aligned} \tag{1.7.18}$$

where the identity $p!\sum_{i<j<k}^{N} = \sum_{ijk}^{N}$ has been applied. Ω is the remaining surface integral. Therefore the annealed free energy in the thermodynamic limit is given by

$$\langle F\rangle_{ann} = -\beta/4 - TS_\infty, \tag{1.7.19}$$

where $S_\infty = \frac{\ln(\Omega)}{N}$.

In the correct treatment of the disorder we need to perform the quenched average $\langle \log Z\rangle_{\text{disorder}} = \lim_{n\to 0}\frac{1}{n}\log\langle Z^n\rangle_{\text{disorder}}$ as shown in (1.7.1). This is done below

$$\langle\langle Z^n\rangle\rangle = \int \mathcal{D}\sigma_i^a \prod_{ijk}\int \mathrm{d}J_{ijk} \exp\left[-{J_{ijk}}^2\frac{N^p}{p!} + J_{ijk}\beta\sum_a^n \sigma_i^a\sigma_j^a\sigma_k^a\right] \tag{1.7.20}$$

where a and b are replica indices and i and j are site indices. Upon performing the disorder average we obtain

$$\begin{aligned}\langle\langle Z^n\rangle\rangle &= \int \mathcal{D}\sigma_i^a \prod_{ijk} \exp\left[\frac{\beta^2 p!}{4N^{p-1}}\beta \sum_{ab}^{n} \sigma_i^a\sigma_i^b\sigma_j^a\sigma_j^b\sigma_k^a\sigma_k^b\right] \\ \langle\langle Z^n\rangle\rangle &= \int \mathcal{D}\sigma_i^a \exp\left[\frac{\beta^2}{4N^{p-1}}\beta \sum_{ab}^{n}\left(\sum_{i}^{N}\sigma_i^a\sigma_i^b\right)^p\right]. \end{aligned} \tag{1.7.21}$$

We can see here that the overlap between two different replicas a and b of the system appears naturally in the calculation:

$$Q_{ab} \equiv \frac{1}{N}\sum_i \sigma_i^a\sigma_i^b. \tag{1.7.22}$$

Implementing the overlap as a delta constraint we obtain

$$1 = \int \mathrm{d}Q_{ab}\delta\left(NQ_{ab} - \sum_i \sigma_i^a\sigma_i^b\right). \tag{1.7.23}$$

Expressing the δ-functional in the Fourier representation we have

$$\begin{aligned}\langle\langle Z^n\rangle\rangle &= \int \mathcal{D}Q_{ab}\mathcal{D}\lambda_{ab}\mathcal{D}\sigma_i^a \\ &\qquad \times \exp\left[\frac{\beta^2 N}{4}\sum_{ab}Q_{ab}^p + N\sum_{ab}\lambda_{ab}Q_{ab} - \sum_i\sum_{ab}\sigma_i^a\lambda_{ab}\sigma_i^b\right] \\ &= \int \mathcal{D}Q_{ab}\mathcal{D}\lambda_{ab}\exp\left[\frac{\beta^2 N}{4}\sum_{ab}Q_{ab}^p + N\sum_{ab}\lambda_{ab}Q_{ab} - \frac{N}{2}\log\det(2\lambda_{ab})\right] \\ &= \int \mathcal{D}Q_{ab}\mathcal{D}\lambda_{ab}\exp\left[-NS(Q,\lambda)\right] \end{aligned} \tag{1.7.24}$$

In the thermodynamic limit this can be solved using the saddle point approximation [69] . In this limit the saddle point approximation states that the integral (1.7.24) is concentrated in the minimum of the integrand [69]. That is

$$F = -\frac{1}{\beta n N}\log Z = \frac{1}{\beta n}\min[S(Q,\lambda)]. \tag{1.7.25}$$

It must also be noted, due to self averaging, that the free energy is in principle given by

$$-\beta F = \lim_{N\to\infty}\lim_{n\to 0}\frac{1}{nN}\log\int \mathcal{D}Q_{ab}\mathcal{D}\lambda_{ab}\exp\left[-NS(Q,\lambda)\right] \tag{1.7.26}$$

and therefore we should first take the replica limit $n \to 0$, and then take the thermodynamic limit $N \to \infty$. Self averaging nature of the observable means

that the results do not depend on the system size or specific realization of the disorder. In the case of the free energy this mathematically means

$$\lim_{N\to\infty} F_N(\beta, J) = F_\infty(\beta.) \tag{1.7.27}$$

Returning to the problem that we are concerned with (1.7.26), Unfortunately this order of limit taking is an impossible wish since S is not an explicit function of the replica index n. Also, it is difficult to solve the integral itself. Subsequently, we exchange the order of the two limits thereafter apply the saddle point approximation which requires that we find a parametrization of the matrix Q_{ab} and only then take the replica limit $n \to 0$. It should be noted that all the eigenvalues of Q_{ab} must be be positive since the first order corrections to this approximation include the square root of the determinant of the Hessian matrix.

What we now need to do is to apply this saddle point approximation (1.7.25). This means we need to minimize $S(Q, \lambda)$ both with respect to λ as well as the overlap Q. In order to achieve this we need the following identity

$$\frac{\partial}{\partial M_{ab}} \log\det M_{ab} = \left(M^{-1}\right)_{ab}. \tag{1.7.28}$$

Susequently, using the definition of $S(Q, \lambda)$ from equation (1.7.24) the λ minimization yields

$$2\lambda_{ab} = (Q^{-1})_{ab}. \tag{1.7.29}$$

Applying this result (1.7.29) upon the free energy expression (1.7.25) before the overlap Q minimization we obtain

$$F = \lim_{n\to 0} -\frac{1}{2\beta n}\left[\frac{\beta^2}{2}\sum_{ab} Q_{ab}^p + \log\det Q_{ab}\right]. \tag{1.7.30}$$

Upon minimization with respect to the overlap Q_{ab} we obtain the saddle point equation

$$0 = \frac{\partial F}{\partial Q_{ab}} = \frac{\beta^2 p}{2} Q_{ab}^{p-1} + (Q^{-1})_{ab} \tag{1.7.31}$$

where the identity (1.7.28) again was used. How do we find a solution for this saddle point equation? This is where we have to find suitable parametrization of the matrix Q_{ab} and subsequently express (1.7.31) as a function of the elements or parameters of Q_{ab} and dimension n.

It is at this juncture that the concept of replica symmetry enters into the picture. Sherrington and Kirkatrick assumed a *replica symmetric* [73] form for the matrix Q_{ab} in their spin glass problem. An intuitively simple parametrization it appears, that is

$$Q_{ab} = q_0 + (1 - q_0)\delta_{ab}. \tag{1.7.32}$$

Expressing this in a visual form we have

$$Q_{ab} = \begin{pmatrix} 1 & q_0 & q_0 & & \vdots & & \\ q_0 & 1 & q_0 & & q_0 & & \cdots \\ q_0 & q_0 & 1 & & \vdots & & \\ & \vdots & & 1 & q_0 & q_0 & \\ & q_0 & & q_0 & 1 & q_0 & \\ & & & q_0 & q_0 & 1 & \\ & \vdots & & & & & \ddots \end{pmatrix}$$

The task is to substitute this onto the saddle point equation (1.7.31) and find the value of q_0. The inverse of the replica symmetry matrix is given by

$$(Q^{-1})_{ab} = \frac{1}{1-q_0}\delta_{ab} - \frac{q_0}{(1-q_0)[1+(n-1)q_0]} \tag{1.7.33}$$

In the limit $n \to 0$ and $a \neq b$ we thus have (1.7.31) becoming,

$$\frac{\beta^2 p}{2} q_0^{p-1} - \frac{q_0}{(1-q_0)^2} = 0. \tag{1.7.34}$$

We observe that the trivial solution is $q_0 = 0$. A substitution of this result to (1.7.30) we obtain $F = -\frac{\beta}{4}$, a similar result to that obtained from the annealed calculation. That is, when the overlap matrix Q_{ab} is the identity the replication has no effect. Now, a graphical exploration shows that there is a another set of two solutions below some T^*. A problem with this non-trivial solution, however, exist. Crisanti and Sommers found that it is *unstable* [72]. Both solutions of equation (1.7.34) have a negative eigenvalue. This leads to the concept of *replica symmetry breaking*. The form of the order parameter Q_{ab} needs to be parametrized differently in order to find stable a stable solution. There exist different forms of replica symmetry breaking but it is the Parisi [74] construction that is standard We shall be concerned with the one step replica symmetry breaking (1RSB) solution also known as weak RSB developed by Parisi [74; 69].

1.7.2.1 The overlap order parameter physics

The generalization of the average magnetization $m = \frac{1}{N}\sum_{i=1}\langle\sigma_i\rangle$ to

$$q^{(1)} = \frac{1}{N}\sum_i \langle\langle\sigma_i\rangle^2\rangle \tag{1.7.35}$$

in the disordered systems, by decomposition, as we saw in the overlap distribution function (1.7.12), can be re-expressed as

$$q^{(1)} = \frac{1}{N}\sum_i \sum_{\alpha\beta} \langle w_\alpha w_\beta \langle\sigma_i\rangle_\alpha \langle\sigma_i\rangle_\beta\rangle = \sum_{\alpha\beta} \langle w_\alpha w_\beta q_{\alpha\beta}\rangle\,. \tag{1.7.36}$$

This can be expressed in terms of the overlap distribution function if one introduces a delta function as

$$q^{(1)} = \int \mathrm{d}q \sum_{\alpha\beta} \langle w_\alpha w_\beta \delta\left(q - q_{\alpha\beta}\right)\rangle \, q = \int \mathrm{d}q \, \langle P(q)\rangle \, q. \tag{1.7.37}$$

where $P(q) = \sum_{\alpha\beta} \langle w_\alpha w_\beta \delta\left(q - q_{\alpha\beta}\right)\rangle$ is the distribution function of the overlaps. This can be also expressed differently using the alternative replica trick form (1.7.3). That is,

$$q^{(1)} = \frac{1}{N} \sum_i \left\langle \langle \sigma_i \rangle^2 \right\rangle = \lim_{n\to 0} \left\langle \int \mathcal{D}\sigma_i^a \frac{1}{N} \sum_i \sigma_i^1 \cdot \sigma_i^2 \; e^{-\beta \sum_a H(\sigma^a)} \right\rangle. \tag{1.7.38}$$

Introducing the overlap matrix Q_{ab} we obtain

$$q^{(1)} = \int \mathcal{D}Q_{ab} e^{-NS(Q_{ab})} Q_{12} = Q_{12}^{SP} \tag{1.7.39}$$

where Q_{ab}^{SP} is the saddle point approxiamtion value of the overlap matrix. The general form of this expression for the arbitrary labels of the repiclas was derived by De Dominicis and Young [75]

$$q^{(1)} = \lim_{n\to 0} \frac{2}{n(n-1)} \sum_{a>b} Q_{ab}. \tag{1.7.40}$$

The saddle points Q_{34}^{SP} and so on are averaged. This establishes the key connection between the order parameter $q^{(1)}$ and the the replica overlap matrix Q_{ab}. Comparing this expression with the earlier one (1.7.37) for generic function $f(q)$ we have

$$\int \mathrm{d}q f(q) \, \langle P(q)\rangle_{\text{disorder}} = \lim_{n\to 0} \frac{2}{n(n-1)} \sum_{a>b} f(Q_{ab}) \tag{1.7.41}$$

Finally, when $f(q)$ is chosen to be $f(q) = \delta(q - q')$ we obtain:

$$\langle P(q)\rangle_{\text{disorder}} = \lim_{n\to 0} \frac{2}{n(n-1)} \sum_{a>b} \delta\left(q - Q_{ab}\right). \tag{1.7.42}$$

Therefore, the average probability that two pure states of the system have overlap q is equal to the fraction of elements of the overlap matrix Q_{ab} equal to q. This can be further translated to: the elements of the overlap matrix are the physical values of the overlap among pure states. In the replica symmetric solution, $Q_{ab} = q_0$ for each $a \neq b$ and according to (1.7.42)

$$\langle P(q)\rangle_{\text{disorder}} = \delta(q - q_0). \tag{1.7.43}$$

with a clear meaning that there can only be one single equilibrium state. When there is ergodicity breaking the correct form of Q_{ab} cannot be symmetric.

1.7.3 Weak replica symmetry breaking

As we already have mentioned that in order to attain a stable solution we must break the replica symmetry. The Parisi [74; 69] one step replica symmetry breaking comes to rescue. This is obtained by dividing the $n \times n$ matrix in $\frac{n}{m} \times \frac{n}{m}$ blocks of dimension $m \times m$. If $a \neq b$ belong to one of the $\frac{n}{m}$ diagonal blocks then $Q_{ab} = q_1$, otherwise $Q_{ab} = q_0 < q_1$. Therefore the matrix structure corresponding to this is [72]

$$Q_{ab} = \begin{pmatrix} 1 & q_1 & q_1 & & & \\ q_1 & 1 & q_1 & & q_0 & \cdots \\ q_1 & q_1 & 1 & & & \\ & & & 1 & q_1 & q_1 \\ & q_0 & & q_1 & 1 & q_1 \\ & & & q_1 & q_1 & 1 \\ & \vdots & & & & \ddots \end{pmatrix}$$

The parameter m is connected to the probability of having a given value of the overlap and hence it becomes a variational parameter in the saddle point equations, like q_1 and q_0. The overlap distribution associated with this first stage RSB structure of Q_{ab} from (1.7.42) is

$$\langle P(q) \rangle_{\text{disorder}} = \frac{m-1}{n-1}\delta(q-q_1) + \frac{n-m}{n-1}\delta(q-q_0) \tag{1.7.44}$$

with

$$1 \leq m \leq n. \tag{1.7.45}$$

The condition (1.7.45) cannot be met at the replica limit n going to zero. Since the probability (1.7.44)

$$\langle P(q) \rangle_{\text{disorder}} = (1-m)\delta(q-q_1) + m\delta(q-q_0). \tag{1.7.46}$$

at the replica limit $n \to 0$ the positive definition of the probability then requires $m < 1$ and $m > 0$. Alternatively, (1.7.45) for $n \to 0$ must be

$$0 \leq m \leq 1. \tag{1.7.47}$$

1.7.4 The weak replica symmetry breaking

We now have the structure of Q_{ab} in the first step symmetry breaking solution we must now calculate the free energy as a function of q_1, q_0, m. That is, we need to evaluate

$$F = \lim_{n\to 0} -\frac{1}{2\beta n}\left[\frac{\beta^2}{2}\sum_{ab} Q_{ab}^p + \log\det Q\right]. \tag{1.7.48}$$

Since the RSB matrix structure has the property $\sum_a Q_{ab}$ does not depend on b we have in the limit $n \to 0$,

$$\frac{1}{n}\sum_{ab} Q_{ab}^p = \sum_a Q_{ab}^p = 1 + (m-1)q_1^p - mq_0^p. \tag{1.7.49}$$

The 1RSB matrix Q_{ab} has three different eigenvalues and degeneracies [72]

$$\lambda_1 = 1 - q \qquad \text{deg.} = n - n/m \tag{1.7.50}$$

$$\lambda_2 = m(q_1 - q_0) + (1 - q) \qquad \text{deg.} = n/m - 1 \tag{1.7.51}$$

$$\lambda_3 = nq_0 + m(q_1 - q_0) + (1 - q) \qquad \text{deg.} = 1. \tag{1.7.52}$$

In the replica limit we subsequently obtain 1RSB free energy to be

$$\begin{aligned} -2\beta F_1 = \frac{\beta^2}{2}\left[1 + (m-1)q_1^p - mq_0^p\right] + \frac{m-1}{m}\log(1-q_1) \\ + \frac{1}{m}\log\left[m(q_1 - q_0) + (1 - q_1)\right] + \frac{q_0}{m(q_1 - q_0) + (1 - q_1)}. \end{aligned} \tag{1.7.53}$$

Interestingly, the replica symmetric (RS) solution

$$-2\beta F_0 = \frac{\beta^2}{2}\left[1 - q_0^p\right] + \log(1 - q_0) + \frac{q_0}{1 - q_0}. \tag{1.7.54}$$

can be derived from 1RSB by either taking the limit $q_1 \to q_0$ or $m \to 1$. Returning to the saddle point equations with respect to q_1, q_0, m for the 1RSB solution (1.7.53). The equation $\partial_{q_0} F_1 = 0$ has the solution $q_0 = 0$. The other saddle point equations $\partial_{q_1} F_1 = 0$ and $\partial_m F_1 = 0$ gives us

$$\begin{aligned} (1-m)\left(\frac{\beta^2}{2}pq_1^{p-1} - \frac{q_1}{(1-q_1)[(m-1)+1]}\right) = 0 \\ \frac{\beta^2}{2}pq_1^p + \frac{1}{m^2}\log\left(\frac{1-q_1}{1-(1-m)q_1}\right) + \frac{q_1}{m[1-(1-m)q_1]} = 0. \end{aligned} \tag{1.7.55}$$

Graphically, at high T the solution is $q_1 = 0$ and m undetermined which is a similar solution to the RS one. Now, the first equation in (1.7.55) has a solution $m = 1$. When this is substituted to the second equation of (1.7.55) we obtain

$$\frac{\beta^2}{2}pq_1^p + \log(1 - q_1) + q_1 \equiv g(q_1) = 0. \tag{1.7.56}$$

The graphical study of this equation for $0 \leq q_1 \leq 1$ shows that $g(0) = 0$ and $g(1) = -\infty$. At low temperature $g(q_1)$ developes a maximum, whose height diverges for decreasing $T$and therefore at T_s a new solution appears, with $q_1 = q_s$ and $m = 1$.

1.8 Summary of the dissertation results

For a composite system –polymer substrate attachment– we have investigated the role of the pressure, the nature of adhesion (homogeneous or inhomogeneous) as well as the role of a fluctuating substrate. In terms of the fluctuation spectrum $\langle h^2 \rangle$ as a measure function of the pressure μ parameter we, generally, observe that the average square fluctuations $\langle h^2 \rangle$ increases with the pressure. However, for the discrete inhomogeneous adhesion, when the position of tethers distribution is quenched this general behaviour is altered. The first stage Replica Symmetry Breaking is necessary in order to obtain these non-monotonic results.

The elastic substrate extension shows that the rate of entropic gain surpasses the rate of energetic loss at a lower tether density average. Therefore, the integrity of the system requires less average tether density in relation to the hard substrate when the substrate is elastic. The numerical exploration of these fluctuating substrates as a function of average tether density ρ_0 and pressure μ suggests that at least a second stage Replica Symmetry Breaking is necessary in order to observe multiple minima free energy F as a function of average tether density.

Chapter 2

Homogeneous adhesion of a polymer and of a membrane

We are interested in the physics of a membrane that is detaching from a substrate due the influence of a uniform pressure on one side of the membrane. This is in contrast to for example the works of Kierfeld [76] or Benetatos [77] where the effect of the pulling (by a force at the end) of a semiflexible chain from a substrate is investigated. We model in the approximation called Monge gauge for polymer chains and membranes which do not posses surface bending resistance and also with the inclusion of resistance. The competing statistical physical effects here are

- The energetic advantage of the membrane being attached to the substrate. In isolation of any other effects this would strive to keep the detached arclength or area – the blister – as small as possible.
- The entropic advantage of the fluctuations of the membrane itself. The freedom of the membrane to undergo fluctuations is associated with its entropy. In principle, the more of the membrane is detached from the substrate the larger this freedom, and the more advantageous it is to the system. The entropy of the membrane, therefore, competes directly with the attachment energy gain of the preceding entry.
- The third factor is the role of the pressure itself, that will want to stretch, and promote the detachment of the membrane. If the membrane is inextensible, it might again reverse the entropic freedom. The role of this is subtle depending on the type of the membrane we consider.

2.1 Flexible polymer chain

In this section we shall treat a flexible polymer chain of length L pinned at the two ends of a continuous homogeneous interaction potential substrate. The interaction energy per unit length is ϵ. Additional to this interaction, per unit length there is a pressure μ promoting detachment, with the units of per length squared, that is exerted upon the polymer. Our aim is then to determine the stability criteria or the fluctuation spectrum of the composite system—polymer-substrate. This criteria will allow us characterize the role of pressure in promoting the detachment and possibly in the fluctuation spectrum. We shall investigate this in the case of favourable energetic attachment and its contrary scenario. The partition function of such model description outlined is given by

$$\begin{aligned} Z &= \int \mathcal{D}h \exp\left\{-\kappa \int_0^L \mathrm{d}x \left(\frac{\partial h}{\partial x}\right)^2 + \mu \int_0^L \mathrm{d}x\, h + \beta\epsilon L\right\} \qquad (2.1.1)\\ Z &\equiv \int \mathcal{D}h \exp\left(-\int_0^L \mathcal{L}\,\mathrm{d}x\right), \text{ where } \mathcal{L} = \kappa\left(\frac{\partial h}{\partial x}\right)^2 - \mu h(x) - \beta\epsilon. \end{aligned}$$

This is subject to the constraint or boundary conditions $h(0) = h(L) = 0$. The parameter κ represents the material characteristic parameter viewed as per length elastic measure which is an inverse Kuhn length – the smallest length scale associated with interatomic bond length – with β being the inverse fundamental temperature with the units of per energy. $h(x)$ represent the displacements or undulations – a height function with the units of length where $h'(x)$ shall be used as shorthand for $\frac{\partial h}{\partial x}$. The first term represents the elastic thermal fluctuations term, the second the detachment favouring pressure whilst the last term represents the total adhesion energy. Our task is to calculate this partition function Z in equation (2.1.1) and thus the free energy F given by

$$\beta F = -\ln Z \qquad (2.1.2)$$

Calculating the partition function Z in the saddle point approximation we express $h(x)$ as

$$h(x) = h_0(x) + \eta(x) \qquad (2.1.3)$$

where $\eta(x)$ is the fluctuations component and $h_0(x)$ is a solution for the Euler-Lagrange equation

$$\frac{d}{dx}\frac{\partial \mathcal{L}}{\partial h_0'(x)} - \frac{\partial \mathcal{L}}{\partial h_0} = 0, \quad \text{with the conditions } h_0(0) = h_0(L) = 0. \qquad (2.1.4)$$

Subsequently, the differential equation that needs to be solved is

$$2\kappa h_0''(x) + \mu = 0. \qquad (2.1.5)$$

It has a solution

$$h_0(x) = -\frac{\mu}{4\kappa}x^2 + \frac{\mu L}{4\kappa}x. \tag{2.1.6}$$

After effecting the transformation (2.1.3) we therefore have the following for the partition function Z expression (2.1.1)

$$\begin{aligned} Z &= \int \mathcal{D}h \exp\left\{-\kappa \int_0^L \mathrm{d}x \left(\frac{\partial h}{\partial x}\right)^2 + \mu \int_0^L \mathrm{d}x\, h + \beta\epsilon L\right\} \\ &= \exp\left(-\kappa \int_0^L \mathrm{d}x \left(\frac{\partial h_0}{\partial x}\right)^2 + \mu \int_0^L \mathrm{d}x\, h_0(x) + \beta\epsilon L\right) \\ &\quad \times \int \mathcal{D}\eta \exp\left\{-\kappa \int_0^L \mathrm{d}x\, (\eta'(x))^2\right\}. \end{aligned} \tag{2.1.7}$$

After the evaluation of the fluctuation component $\int \mathcal{D}\eta \exp\left\{-\kappa \int_0^L \mathrm{d}x\, \eta'^2(x)\right\}$ we obtain

$$Z = \exp\left(\int_0^L \mathrm{d}x \left(-\kappa\left(\frac{\partial h_0}{\partial x}\right)^2 + \mu h_0(x)\right) + \beta\epsilon L - \frac{1}{2}\mathrm{tr}\ln A(x', x)\right). \tag{2.1.8}$$

After rescaling $h \to \frac{h}{\sqrt{\frac{L}{\kappa}}}$ and $x \to \frac{x}{L}$, therefore, we need to determine the eigenvalues of the operator $A(x, x')$ since

$$\mathrm{tr}\ln A(x', x) = \ln \det A(x', x) = \ln \prod_{i=n}^{\infty} \lambda_n = \sum_{n=1}^{\infty} \ln \lambda_n \tag{2.1.9}$$

where λ_n's are the eigenvalues of the operator

$$A(x', x) = -2\delta^{xx'} d_{xx}$$

. The eigenvalue equation $\int \mathrm{d}x\, A(x, x')\eta_n(x) = \lambda_n \eta_n(x')$ with the boundary conditions $\eta(0) = \eta(1) = 0$. This is solved by sinusoids, hence $\lambda_n = 2n^2\pi^2$. We subsequently obtain the free energy $F = -\frac{1}{\beta}\ln Z$, where we have substituted the saddle point solution $h_0(x)$ from equation (2.1.4), below

$$\begin{aligned} F &= -\left(\frac{\mu^2 L^3}{48\beta\kappa} + L\epsilon\right) + \frac{1}{2\beta}\sum_{n=1}^{\infty} \ln \lambda_n \approx -\left(\frac{\mu^2 L^3}{48\beta\kappa} + L\epsilon\right) + \frac{1}{2\beta}\sum_{n=1}^{q_c} \ln 2n^2\pi^2 \\ F &\approx -\frac{1}{\beta}\left(\frac{\mu^2 L^3}{48\kappa} + \beta L\epsilon\right) + \frac{1}{\beta}(q_c \ln q_c - q_c). \end{aligned} \tag{2.1.10}$$

The quantity q_c is a cut-off value related to the smallest length scale of the problem. We have applied the Stirling approximation, $\ln n! \approx n\ln n - n,\ n \to \infty$, to reach the final step of (2.1.10).

Since in the case of positive attachment energy ϵ the free energy is always a decreasing function of L we then concentrate on its opposite $\epsilon < 0$. This scenario reflects the attractive potential. Below we show the depiction of the free energy F as a function of length L for a choice of different values of pressure μ and attachment energy ϵ. In the case of a fixed value for attachment energy $\epsilon = -2$ units, we depict these in fig. 2.1 and fig. 2.2.

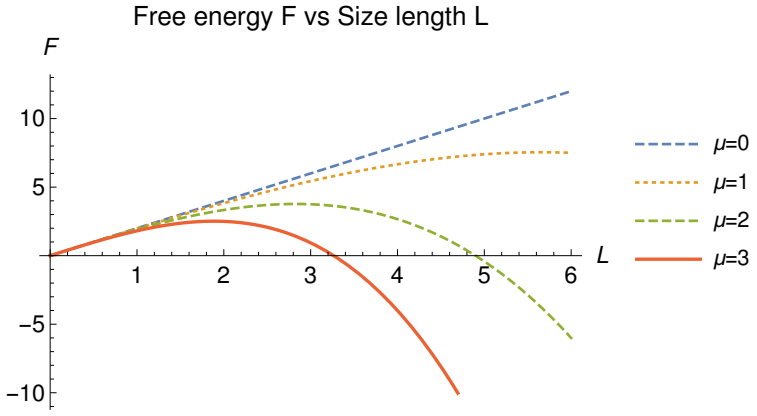

Figure 2.1: Free energy profiles of the chain polymer for the pressure values $\mu = \{0,\ 1,\ 3\}$ and attachment energy $\epsilon = -2$ units. β and κ are set to unity.

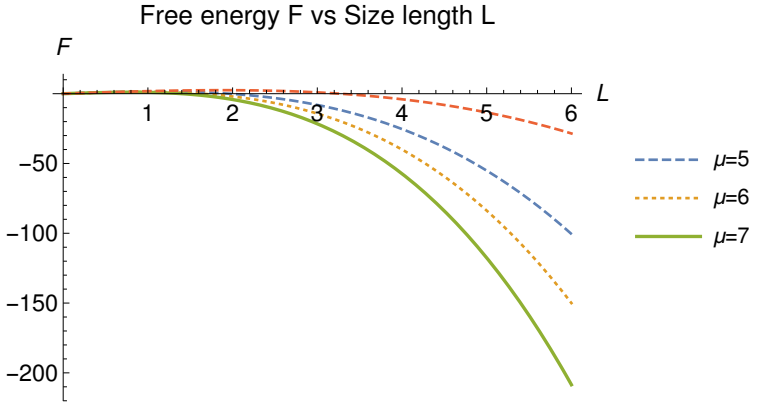

Figure 2.2: Free energy profiles of the chain polymer for the pressure values $\mu = \{5,\ 6,\ 7\}$ and attachment energy $\epsilon = -2$ units. β and κ are set to unity.

Our observation from these profiles under a similar attachment energy $\epsilon = -2$ units is that as we increase the pressure μ starting at zero units to 7 units is: the larger the length L the less pressure you require to debind the chain polymer. The thermal fluctuations associated with a larger length L promotes easier detachment. Alternatively, since the Helmholtz free energy is given by

$$F = E - TS. \tag{2.1.11}$$

such that

$$S \propto +\mu^2 L^3 \quad \text{and} \quad E \propto -\epsilon L.$$

Therefore, by increasing size L, one generally loses favourable energy E state but gains entropy S. When there is no pressure the entropy gain is a constant, however, this entropy gain becomes very large with the pressure μ bias.

From our free energy expression (2.1.10) we can deduce the critical pressure at which the polymer chain always detaches. The relationship between the detached length L_m, corresponding to the extremum of the derivative, and the pressure is given by

$$\mu_m = \frac{4\sqrt{\beta\kappa\,|\epsilon|}}{L_m}. \tag{2.1.12}$$

This is the solution expression of the derivative extremum with respect to L of the free energy F (2.1.10) expressed as an explicit function of pressure μ. Hence, the extreme pressure condition for the scenario depicted in fig. 2.2 is given by

$$\mu_m > \frac{4\sqrt{\beta\kappa\,|\epsilon|}}{L_m}. \tag{2.1.13}$$

Now, what happens when the pressure is kept constant and the attachment energy ϵ is varied? We depict this in fig. 2.3 below.

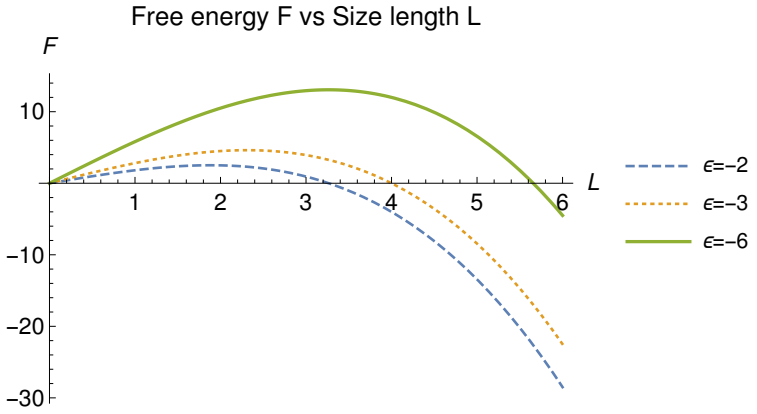

Figure 2.3: Free energy of the chain polymer where the pressure μ is 3 units and the attachment energy values $\epsilon = \{-2,\ -3,\ -6\}$ units.

In the preceding discussion we noted that larger pressure is required to for shorther length regions such that the fluctuations or entropy always dominate. In contrast here, for the given pressure the increase in the attractive potential shifts the maxima peak to right. This means that the same pressure that brought shorter, in detached length, runway now cannot. Instead a larger detached length that now can be "unbound" by this pressure. This grows with the adhesion energy.

2.2 Polymer chain with bending rigidity

In the preceding section 2.1 we treated the flexible polymer chain model without taking into account any rigidity or resistance to bending associated with the polymers and membranes. In this section we shall extend the model of the preceding section 2.1 to account for such resistance. The bending rigidity term is $\sigma \int_0^L dx\, \ddot{h}^2(x)$ [28] that we shall include in our Hamiltonian of (2.1.1), where σ is material characteristic cost of bending per unit length. κ now plays the role of a tension in a wormlike chain [78; 79] treated in the weak bending approximation which is valid when the tension is large or when the persistence length is much greater than the contour length of the chain. Subsequently we need to evaluate

$$Z = \int \mathcal{D}h \exp\left\{-\kappa \int_0^L \mathrm{d}x\, h'^2(x) - \sigma \int_0^L dx\, h''^2(x) + \mu \int_0^L \mathrm{d}x\, h + \beta\epsilon L\right\}. \tag{2.2.1}$$

From this point the evaluation proceeding is very much the same as before. We apply the saddle point approach we used in the model (2.1.1). However, in this case the Lagrangian becomes $\mathcal{L} = \sigma\left(\frac{\partial^2 h}{\partial x^2}\right)^2 + \kappa\left(\frac{\partial h}{\partial x}\right)^2 - \mu h(x) - \beta\epsilon$ for the Euler Lagrange equation we have to solve

$$-\frac{d^2}{dx^2}\frac{\partial \mathcal{L}}{\partial h_0''(x)} + \frac{d}{dx}\frac{\partial \mathcal{L}}{\partial h_0'(x)} - \frac{\partial \mathcal{L}}{\partial h_0} = 0, \tag{2.2.2}$$

upon the boundary conditions $h_0(0) = h_0(L) = h_0'(0) = h_0'(L) = 0$. The subsequent fourth order ordinary differential equation that then needs to be solved is

$$2\sigma h_0^{(4)}(x) - 2\kappa h_0^{(2)}(x) - \mu = 0. \tag{2.2.3}$$

The analytical solution is given by

$$h_0(x) = \frac{\mu}{4\kappa^{3/2}}\left[-L\sqrt{\sigma}\coth\left(\frac{\sqrt{\kappa}L}{2\sqrt{\sigma}}\right) + \sqrt{\kappa}x(L-x) + L\sqrt{\sigma}\,\mathrm{csch}\left(\frac{\sqrt{\kappa}L}{2\sqrt{\sigma}}\right)\cosh\left(\frac{\sqrt{\kappa}(L-2x)}{2\sqrt{\sigma}}\right)\right]. \tag{2.2.4}$$

Again, upon the substitution of $h(x) = h_0(x) + \eta(x)$ the expression for the partition function (2.2.1) becomes

$$\begin{aligned} Z &= \exp\left(\int_0^L \mathrm{d}x \, \left(-\kappa {h_0'}^2(x) - \sigma h_0''^2(x) + \mu h_0(x) + \beta\epsilon\right)\right) \\ &\quad \times \int \mathcal{D}\eta \exp\left\{-\kappa \int_0^L \mathrm{d}x \, \left(\eta'(x)\right)^2 - \sigma \int_0^L \mathrm{d}x \, \left(\eta''(x)\right)^2\right\} \\ Z &= \exp\left(\int_0^L \mathrm{d}x \, \left(-\kappa {h_0'}^2(x) - \sigma h_0''^2(x) + \mu h_0(x) + \beta\epsilon\right)\right) \\ &\quad \times \int \mathcal{D}\eta \exp\left\{-\kappa \int_0^L \mathrm{d}x \mathrm{d}x' \, \eta(x') \left[\delta(x'-x)\left(2\frac{d^2}{dx^2} + 2\frac{\sigma}{\kappa}\frac{d^4}{dx^4}\right)\right]\eta(x)\right\}. \end{aligned}$$

Finally obtaining

$$\begin{aligned} Z &= \exp\left(\int_0^L \mathrm{d}x \, \left(-\kappa {h_0'}^2(x) - \sigma h_0''^2(x) + \mu h_0(x) + \beta\epsilon\right)\right) \\ &\quad \times \exp\left(-\frac{1}{2}\mathrm{tr}\ln\left[2\delta(x'-x)\left(\frac{d^2}{dx^2} + \frac{\sigma}{\kappa L^2}\frac{d^4}{dx^4}\right)\right]\right). \end{aligned} \tag{2.2.5}$$

Therefore, after treating the eigenvalue problem as in (2.1.9), the free energy $F = -\frac{1}{\beta}\ln Z$ is given by

$$\begin{aligned} F &= -\frac{1}{\beta}\left(\int_0^L \mathrm{d}x \, \left(-\kappa {h_0'}^2(x) - \sigma h_0''^2(x) + \mu h_0(x) + \beta\epsilon\right)\right) \\ &\quad + \frac{1}{\beta}\sum_{n=1}^{\infty} \ln\left(2\frac{\sigma}{\kappa L^2}\left(n\pi\right)^4 + 2\left(n\pi\right)^2\right). \end{aligned} \tag{2.2.6}$$

The fluctuation contribution is evaluated as follows

$$\begin{aligned} &\frac{1}{\beta}\sum_{n=1}^{\infty} \ln\left(2\frac{\sigma}{\kappa L^2}\left(n\pi\right)^4 + 2\left(n\pi\right)^2\right) \\ &= \frac{2q_c}{\beta}\ln\pi + \frac{1}{\beta}\left(q_c\ln q_c - q_c\right) + \frac{q_c}{\beta}\int_0^1 \ln\left(\frac{\sigma}{\kappa L^2}q_c^2 q^2 + 1\right) dq \\ &= \frac{2q_c}{\beta}\ln\pi + \frac{1}{\beta}\left(q_c\ln q_c - q_c\right) \\ &\quad + \frac{q_c}{\beta}\left(\ln\left(\frac{\sigma\pi^2 q_c^2}{\kappa L^2} + 1\right) + \frac{2\tan^{-1}\left(\pi q_c\sqrt{\frac{\sigma}{\kappa L^2}}\right)}{\pi q_c\sqrt{\frac{\sigma}{\kappa L^2}}} - 2\right) \end{aligned} \tag{2.2.7}$$

Finally, upon the substitution of $h_0(x)$ in (2.2.6) and the above result (2.2.7) we obtain

$$\begin{aligned} F = &-\frac{L\left(48\beta\kappa^2\epsilon + \mu^2\left(\kappa L^2 + 12\sigma\right) - 6\sqrt{\kappa}\mu^2 L\sqrt{\sigma}\coth\left(\frac{\sqrt{\kappa}L}{2\sqrt{\sigma}}\right)\right)}{48\beta\kappa^2} + \frac{2q_c}{\beta}\ln\pi \\ &+ \frac{1}{\beta}\left(q_c\ln q_c - q_c\right) + \frac{q_c}{\beta}\left(\log\left(\frac{\pi^2\sigma q_c^2}{\kappa L^2} + 1\right) + \frac{2\tan^{-1}\left(\pi q_c\sqrt{\frac{\sigma}{\kappa L^2}}\right)}{\pi q_c\sqrt{\frac{\sigma}{\kappa L^2}}} - 2\right). \end{aligned} \tag{2.2.8}$$

The graphical depiction of this free energy is shown below on fig. 2.4 and fig. 2.5.

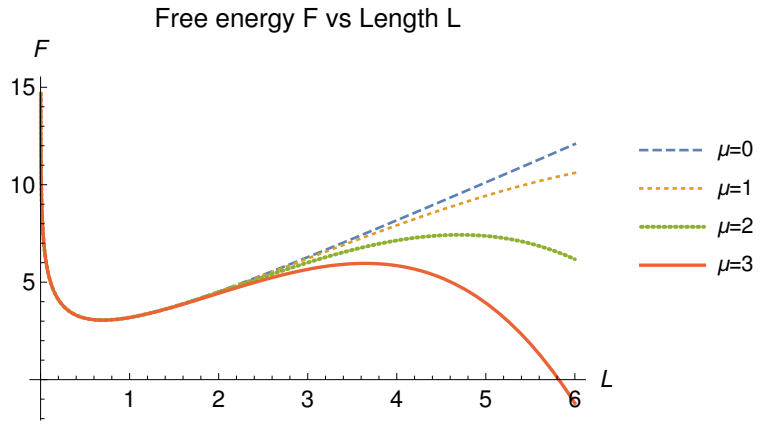

Figure 2.4: Free energy profiles of the chain polymer with bending for the pressure values $\mu = \{0,\ 1,\ 2,\ 3\}$ and attachment energy $\epsilon = -2$ units. β, σ and κ are set to unity.

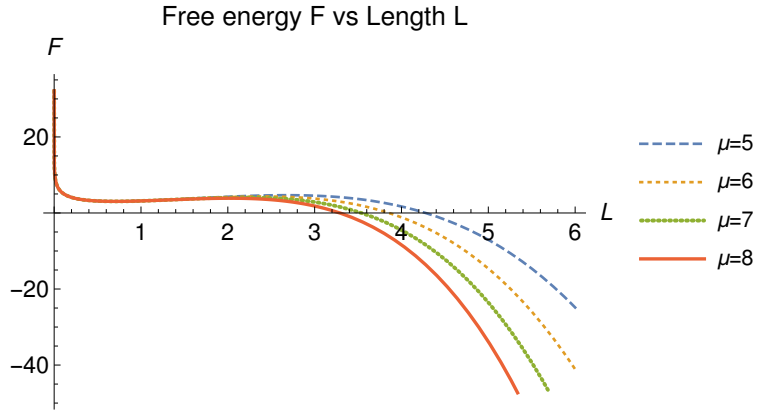

Figure 2.5: Free energy profiles of the chain polymer with bending for the pressure values $\mu = \{5,\ 6,\ 7,\ 8\}$ and attachment energy $\epsilon = -2$ units. β, σ and κ are set to unity.

A comparison between figs. 2.1 and 2.2 to this graph fig. 2.4 shows that the inclusion of the rigidity term increases or shifts the size of 'detached' length L_m to the right under similar pressure and attachment energy. This agrees with intuition about the role of this important quantity the bending resistance that it suppresses the bending fluctuations. In conclusion, the stiffer polymer chain will require more pressure to debind a similar sized chain of its counterpart. Alternatively, a similar amount of pressure applied to both flexible and less flexible chain can only unbind a more 'detached' or larger stiffer chain.

Similarly the critical pressure explicitly for this model unlike the preceding case of section 2.1, as we derived in equation (2.1.13) is given by

$$\mu > \frac{4\sqrt{-\frac{2q}{\beta L\left(\frac{\pi^2q^2\sigma}{\kappa L^2}+1\right)}+\frac{2\kappa L\sqrt{\frac{\sigma}{\kappa L^2}}\tan^{-1}\left(\pi q\sqrt{\frac{\sigma}{\kappa L^2}}\right)}{\pi\beta\sigma}-\frac{2\pi^2q^3\sigma}{\beta\kappa L^3\left(\frac{\pi^2q^2\sigma}{\kappa L^2}+1\right)}+|\epsilon|}}{\sqrt{\frac{4\sigma}{\beta\kappa^2}+\frac{L^2\operatorname{csch}^2\left(\frac{\sqrt{\kappa}L}{2\sqrt{\sigma}}\right)}{\beta\kappa}+\frac{L^2}{\beta\kappa}-\frac{4L\sqrt{\sigma}\coth\left(\frac{\sqrt{\kappa}L}{2\sqrt{\sigma}}\right)}{\beta\kappa^{3/2}}}}. \tag{2.2.9}$$

Including the bending term yields a condition that includes the trigonometric terms. Thus a complex relationship in length scales and possibly energy scales.

2.2.1 Average height fluctuations $\langle h\rangle$ and $\langle h^2\rangle$

The average height fluctuations by the chain quantity $\langle h\rangle$ is given by

$$\langle h\rangle \equiv \left\langle \int_0^L \mathrm{d}x\, h(x)\right\rangle = \frac{\partial \ln Z}{\partial \mu} \tag{2.2.10}$$

where $\ln Z = -\beta F$, where F is given by (2.1.10) and (2.2.8). For the model (2.1.1)

$$\ln Z = \left(\frac{\mu^2L^3}{48\kappa}+\beta L\epsilon\right) + \text{other terms} \tag{2.2.11}$$

and therefore

$$\mathcal{A}_{\text{sec:2.1}} = \frac{\mu L^3}{24\kappa}. \tag{2.2.12}$$

This shows us the relationship or the combination between the pressure μ and size L on the average area. The height fluctuations $\langle h\rangle$ by the chain, therefore, grows linearly with respect to the pressure μ whilst it grows exponentially with respect to the length L.

How does bending resistance affect this quantity? In this case, as derived from the second model (2.2.1),

$$\ln Z = \frac{L\left(48\beta\kappa^2\epsilon+\mu^2\left(\kappa L^2+12\sigma\right)-6\sqrt{\kappa}\mu^2L\sqrt{\sigma}\coth\left(\frac{\sqrt{\kappa}L}{2\sqrt{\sigma}}\right)\right)}{48\kappa^2} + \text{other terms} \tag{2.2.13}$$

and therefore

$$\mathcal{A}_{\text{sec:2.2}} = \frac{L\left(\mu\left(\kappa L^2+12\sigma\right)-6\sqrt{\kappa}\mu L\sqrt{\sigma}\coth\left(\frac{\sqrt{\kappa}L}{2\sqrt{\sigma}}\right)\right)}{24\kappa^2}. \tag{2.2.14}$$

The role of the resistance upon the average area $\mathcal{A}$ is depicted below in fig. 2.6

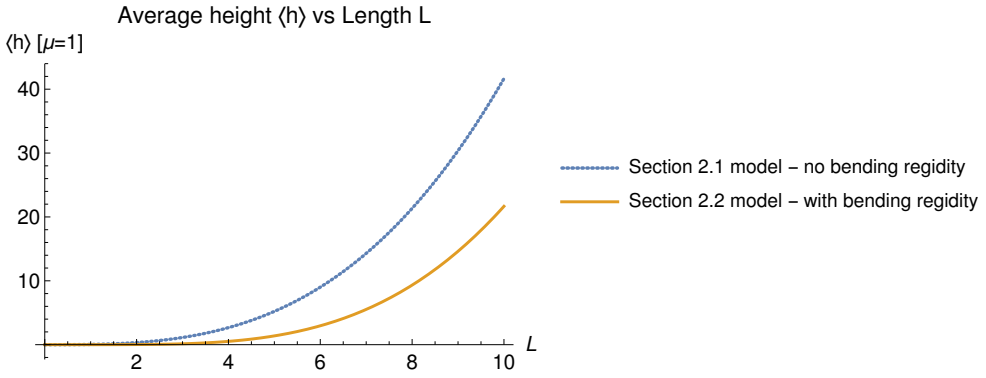

Figure 2.6: Average height $\langle h \rangle$ at fixed pressure $\mu = 1$ and attachment energy $\epsilon = -2$ units. β and κ are set to unity. The top graph is for the model (2.1.1) of the bending resistance free chain.

Figure fig. 2.6 demonstrate the relative reduction of the enclosed area growth with the size L when the chain has the bending resistance term. The pressure contribution to the average enclosed area remains linear with a different relationship to size L.

The average square fluctuations $\langle h^2 \rangle$ for the flexible polymer chain is given by equation (3.1.26)

$$\langle h^2 \rangle \;=\; \int_0^L \mathrm{d}x \;\left(h_0^2(x) + A^{-1}(x,x) \right). \tag{2.2.15}$$

The derivation of this equation is discussed in section 3.1. $h_0(x) = -\frac{\mu}{4}x^2 + \frac{\mu}{4}x$ for dimensionless pressure and x derived in the equation (2.1.6). However, the quantity $A^{-1}(x,x)$ is discussed in the section 3.1. The result is $A^{-1}(x,x) = -(-1+x)x$. Subsequently, for the bending resistance free chain

$$\langle h^2 \rangle \;=\; \int_0^L \mathrm{d}x \;\left(\left(-\frac{\mu}{4}x^2 + \frac{\mu}{4}x \right)^2 - (-1+x)x \right). \tag{2.2.16}$$

Therefore,

$$\langle h^2 \rangle = \frac{\mu^2}{480} + \frac{1}{6}. \tag{2.2.17}$$

Upon substituting the rescaled pressure with $L\sqrt{\frac{L}{\kappa}}\mu$ we obtain the graphical depiction of $\langle h^2 \rangle$ as shown below in figs. 2.7 and 2.8 as function of size L, and of pressure μ, respectively.

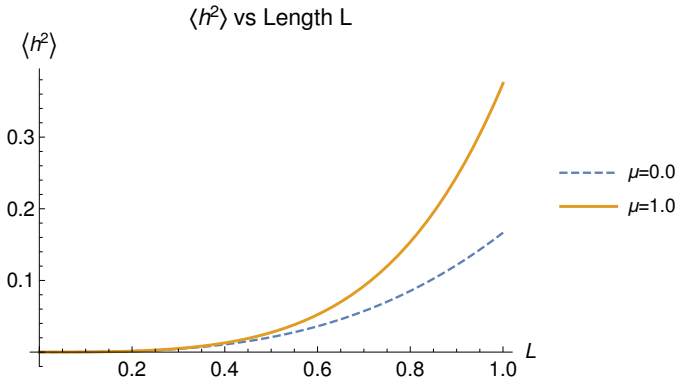

Figure 2.7: Average square fluctuations quantity $\langle h^2 \rangle$ as a function of the size L for the pressure $\mu = \{0,\ 1\}$ and attachment energy $\epsilon = -2$ units. β, σ and κ are set to unity.

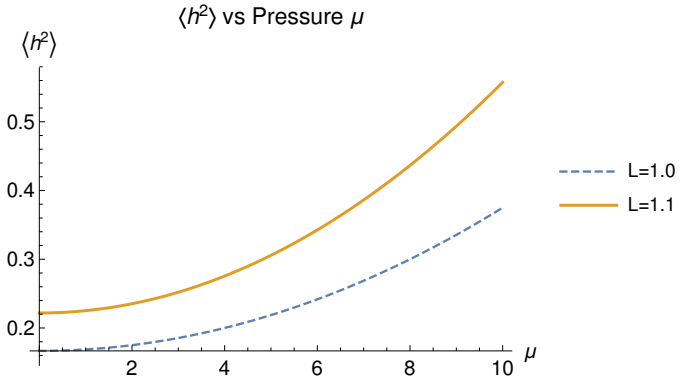

Figure 2.8: Average square fluctuations quantity $\langle h^2 \rangle$ as a function of the pressure μ for the size $L = \{1,\ 1.1\}$ and attachment energy $\epsilon = -2$ units. β, σ and κ are set to unity.

2.3 Flexible membrane

In this section we consider the higher dimensional model of the preceding section 2.1, that is, we now treat a two dimensional flexible membrane of surface area S around the edge of a continuous homogeneous interaction potential substrate of a circle of radius R. The interaction energy per unit length is ϵ. Additional to this interaction, there is a pressure μ promoting detachment that is exerted upon the polymer. Again our aim is to determine or understand the stability criteria or the fluctuation spectrum of the composite system–membrane-substrate. We wish to characterize the role of pressure in promoting the detachment and possibly in the fluctuation spectrum. We shall

investigate this in the case of favourable energetic attachment and its contrary scenario. The partition function of the model description outlined is given by

$$Z = \int \mathcal{D}h(r,\theta) \exp\left\{-\kappa \int_0^{2\pi}\int_0^R \mathrm{d}r\ \mathrm{d}\theta\ r\ (\boldsymbol{\nabla} h)^2 + \mu \int_0^{2\pi}\int_0^R \mathrm{d}r\ \mathrm{d}\theta\ r\ \ h(r,\theta) + \beta\epsilon\pi R^2\right\} \quad (2.3.1)$$

in polar coordinates. The parameters κ, μ, and β represents the 'bending' energy, the pressure and the inverse fundamental temperature. $h(r,\theta)$ represent the fluctuations or undulations as a height function. As in preceding models, the first term represents the thermal fluctuations with the second term being the detachment favouring pressure whereas the final term is the energetic energy adhesion contribution. The constraint of being around the circle of radius R is expressed as the boundary condition $h(R,\theta) = 0$ for every $\theta \in [0, 2\pi]$.

In this model (2.3.1) it is useful to start by reminding ourselves that

$$\boldsymbol{\nabla} h(r,\theta) = \partial_r h(r,\theta)\ \mathbf{i} + \frac{1}{r}\partial_\theta h(r,\theta)\ \mathbf{j} \quad (2.3.2)$$

in the polar coordinates. The $\mathbf{i}$ and $\mathbf{j}$ are the unit vectors $\langle 1,\ 0\rangle$ and $\langle 0,\ 1\rangle$, respectively. Therefore, the quantity of our need $(\boldsymbol{\nabla} h)^2$ becomes

$$(\boldsymbol{\nabla} h)^2 = (\partial_r h)^2 + \frac{1}{r^2}(\partial_\theta h)^2 = \dot{h}^2 + \frac{1}{r^2}h'^2. \quad (2.3.3)$$

The shorthand notation represents $\dot{h} = \partial_r h$ and $h' = \partial_\theta h$.

Substituting this expression (2.3.3) into (2.3.1) we obtain

$$Z = \int \mathcal{D}h(r,\theta) \exp\left\{-\kappa \int_0^{2\pi}\int_0^R \mathrm{d}r\ \mathrm{d}\theta\ r\ \left(\dot{h}^2(r,\theta) + \frac{1}{r^2}h'^2(r,\theta)\right) + \mu \int_0^{2\pi}\int_0^R \mathrm{d}r\ \mathrm{d}\theta\ r\ \ h(r,\theta) + \beta\epsilon\pi R^2\right\}. \quad (2.3.4)$$

How do we evaluate this object in order to determine the energy thermodynamic potential F? We turn to the saddle point approach as before. Again, in this approach we express $h(r,\theta)$ by the transformation

$$h(r,\theta) = h_0(r,\theta) + \eta(r,\theta) \quad (2.3.5)$$

where $\eta(r,\theta)$ is the fluctuations component and $h_0(r,\theta)$ is a solution for the Euler-Lagrange equation

$$\frac{d}{dr}\left(\frac{\partial \mathcal{L}}{\partial \dot{h}_0}\right) + \frac{d}{d\theta}\left(\frac{\partial \mathcal{L}}{\partial h_0'}\right) - \frac{\partial \mathcal{L}}{\partial h_0} = 0, \text{ with the condition } h_0(R,\theta) = 0. \quad (2.3.6)$$

The Lagrangian $\mathcal{L}$ is given by $\mathcal{L} = \kappa r\ (\boldsymbol{\nabla} h)^2 - r\mu h(r,\theta) - \beta\epsilon r$. Fortunately, the topology of the problem shows that there is symmetry associated with the angular coordinate θ for the stationary solution $h_0(r,\theta)$. That is, $h_0(r,\theta) = h_0(r)$. The differential equation that then needs to be solved is

$$2\kappa r\ddot{h}_0(r) + 2\kappa\dot{h}_0(r) + \mu r = 0. \tag{2.3.7}$$

The solution to this equation (2.3.7) is

$$h_0(r,\theta) = -\frac{\mu}{8\kappa}\left(r^2 - R^2\right). \tag{2.3.8}$$

The transformation (2.3.5) of $h(r,\theta)$ leads to equation (2.3.1) becoming

$$\begin{aligned} Z &= \int \mathcal{D}\eta(r,\theta)\exp\left\{-\kappa\int_0^{2\pi}\int_0^R \mathrm{d}r\ \mathrm{d}\theta\ r\ \left(\boldsymbol{\nabla}\left(h_0(r,\theta)+\eta(r,\theta)\right)\right)^2\right. \\ &\qquad \left. +\mu\int_0^{2\pi}\int_0^R \mathrm{d}r\ \mathrm{d}\theta\ r\ \ \left(h_0(r,\theta)+\eta(r,\theta)\right) + \beta\epsilon\pi R^2\right\} \\ &= \exp\left\{\int_0^{2\pi}\int_0^R \mathrm{d}r\ \mathrm{d}\theta\ \left(-\kappa r\left(\boldsymbol{\nabla}h_0(r,\theta)\right)^2 + \mu r\ \ h_0(r,\theta)\right) + \beta\epsilon\pi R^2\right\} \\ &\qquad \times \int \mathcal{D}\eta\exp\left\{\int_0^{2\pi}\int_0^R -\kappa r\left((\boldsymbol{\nabla}\eta)^2\right)\mathrm{d}r\mathrm{d}\theta\right\}. \end{aligned} \tag{2.3.9}$$

Upon substitution of the $h_0(r)$ solution together with the application of the first Green's identity

$$\int_S \boldsymbol{\nabla}u\boldsymbol{\nabla}v = \int_C u\boldsymbol{\nabla}v\cdot\hat{n}\,dC - \int_S u\boldsymbol{\nabla}^2 v\,\mathrm{d}S, \tag{2.3.10}$$

subject to the condition $\eta(R,\theta) = 0$ we obtain

$$Z = \exp\left\{\frac{\pi\mu^2R^4}{32\kappa} + \beta\epsilon\pi R^2 - \frac{1}{2}\mathrm{tr}\ln\left[-2\delta(\boldsymbol{r}'-\boldsymbol{r})\boldsymbol{\nabla}^2\right]\right\}. \tag{2.3.11}$$

in polar coordinates. Subsequently, we need to solve the eigenvalue problem

$$-2\boldsymbol{\nabla}^2\eta(r,\theta) - \lambda\eta(r,\theta) = 0 \quad \text{with the condition} \quad \eta(R,\theta) = 0. \tag{2.3.12}$$

In the expandend notation using equation (2.3.2) we need to solve

$$\partial_{rr}^2\eta(r,\theta) + r^{-1}\partial_r\eta(r,\theta) + r^{-2}\partial_{\theta\theta}^2\eta(r,\theta) + \lambda\eta(r,\theta) = 0. \tag{2.3.13}$$

Fortunately, this is a familiar problem. The solution can be attained by applying the separation of variables $\eta(r,\theta) = \psi(r)\Theta(\theta)$. As a result equation (2.3.13) becomes

$$r^2\ddot{\psi}(r) + r\dot{\psi}(r) + (\sqrt{\lambda}^2r^2 - m^2)\psi(r) = 0, \tag{2.3.14}$$

whilst

$$\ddot{\Theta}(\theta) + m^2\Theta(\theta) = 0. \tag{2.3.15}$$

The solution to the angular equation (2.3.15) is $\exp(-im\theta)$ and subsequently $m = 0, 1, \ldots$. The solution for the radial equation (2.3.14)is given by the Bessel functions $J_m(x)$. Upon scaling $r \to y/\sqrt{\lambda}$ the boundary condition yields $J_m(\sqrt{\lambda}R) = 0$. Therefore, $\sqrt{\frac{\lambda}{\kappa}}R$ is a root of $J_m(x)$. After considering the nature of the Bessel functions we noted that there are multiple solutions for each m and therefore $\lambda = \lambda_{m,n}$ where n designate the order number of the root for a specific m. The first eigenvalue corresponds to the first solution $m = 0$ and $n = 1$ which occurs at $2.4048 = \sqrt{\frac{\lambda}{2}}$. Therefore, $\lambda_{0,1} = 2 \cdot 2.4048^2$. Substituting these results upon (2.3.11), the free energy potential $F = -\beta^{-1} \ln Z$ is given by

$$F = -\frac{1}{\beta}\left(\frac{\pi\mu^2 R^4}{32\kappa} + \beta\epsilon\pi R^2\right) + \frac{\ln\lambda_{0,1}}{\beta} + \sum_{m=1} \ln\lambda_{m,1} + \sum_{m=0,n=2} \ln\lambda_{m,n}. \tag{2.3.16}$$

Approximating this free energy (2.3.16) to first order correction we obtain

$$F_{\text{approx}} \approx -\frac{1}{\beta}\left(\frac{\pi\mu^2 R^4}{32\kappa} + \beta\epsilon\pi R^2\right) + \frac{1}{\beta}\ln 2 \cdot 2.4048^2. \tag{2.3.17}$$

Since in the case of positive attachment energy ϵ the free energy is always a decreasing function of the radius R we then concentrate on the opposite which is physically relevant to a membrane that is energetically favoured to attach.

Below in figs. 2.9 and 2.10 we show the graphical depiction of the free energy F as a function of the diameter $d = 2R$ under a choice of different values of pressure μ and fixed attachment energy ϵ for illustration.

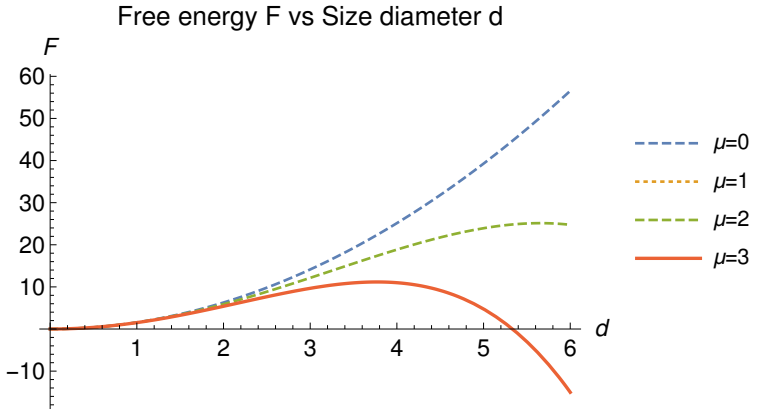

Figure 2.9: Free energy profiles of the blister membrane for the attachment $\epsilon = -2$ and pressure values $\mu = \{0,\ 1,\ 2,\ 3\}$ units. β and κ are set to unity.

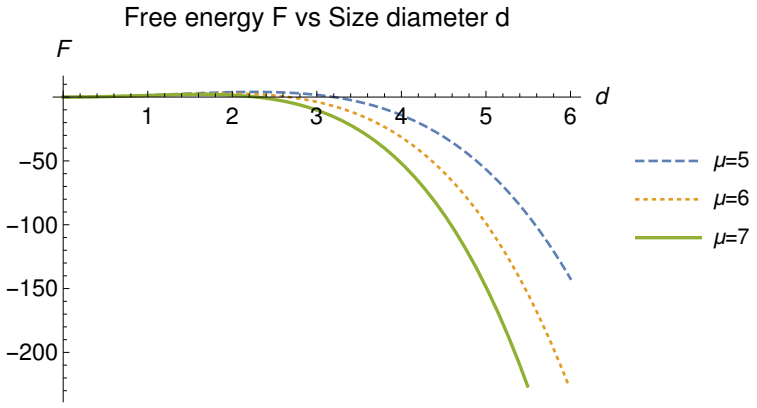

Figure 2.10: Free energy profiles of the blister membrane for the attachment $\epsilon = -2$ and pressure values $\mu = \{5,\ 6,\ 7\}$ units. β and κ are set to unity.

Our observations are quite similar to the one dimension less flexible polymer chain case with little variations. The profiles under a similar attachment energy $\epsilon = -2$ units at increasing pressure μ starting at zero units to 7 units show us again the role of the pressure μ bias as the larger the 'detached' area the less pressure you require to 'debind' the blister membrane. The thermal fluctuations associated with a larger detached blister promotes easier detachment. We observe that the extrema turning point is reached at smaller diameter in relation to the one dimensional polymer chain.

As we did in the flexible chain model in section 2.1 we here also determine the critical pressure from our free energy expression (2.3.17). This is the relationship between the critical radius R_m corresponding to the extremum of the derivative and the pressure. It is similar to the flexible polymer chain case given be equation (2.1.13) and it is given by

$$\mu > \frac{8\sqrt{\beta}\sqrt{\kappa}\sqrt{|\epsilon|}}{d}. \tag{2.3.18}$$

2.3.1 Average height over a volume $\mathcal{V}$

Similar to section 2.2.1 we here determine the quantity for the average volume enclosed by the blister membrane. It is, similarly to 2.2.10, given by

$$\mathcal{V} \ = \ \left\langle \int_0^{2\pi} \int_0^R \mathrm{d}r\ \mathrm{d}\theta\ r\ \ h(x) \right\rangle = \frac{\partial \ln Z}{\partial \mu} \tag{2.3.19}$$

where $\ln Z = -\beta F$, and F is given by (2.3.17) for the first order correction. Subsequently $\ln Z$ is given by

$$\ln Z = \left(\frac{\pi \mu^2 R^4}{32\kappa} + \beta \epsilon \pi R^2 \right) + \text{other terms} \tag{2.3.20}$$

and therefore

$$\mathcal{V} = \frac{\pi\mu R^4}{16\kappa}. \tag{2.3.21}$$

This result shows a similar behavior to the quantity $\mathcal{A}$ dervived in section 2.2.1 though for a volume as a function of the radius R and pressure μ. That is, we have linear relationship to the pressure μ and an exponential growth with the radius R.

2.4 Summary

We determined the analytical expressions (2.1.10) and (2.2.8) of the free energy F of an end constrained flexible chain with and without the bending rigidity term, respectively. These showed us that for every nonzero pressure μ the chain fluctuations or entropy always dominate at sufficiently large detachment region. The larger the pressure μ the smaller the size L that favours the entropy or fluctuations dominance. The critical pressure pressure such that no domain of energetic dominance occurs was derived in equation (2.1.13) for the polymer case without the bending term. This pressure relates the polymer characteristic/intrinsic properties κ, the energy advantage per length ϵ and the thermal energy k_BT. We also did similar investigations for the higher dimensional case of a flexible membrane 'blister', without the bending term, constrained on the edge of a circle of radius R as shown in figure 1.1. The free energy is shown in equation (2.3.17), whilst the critical pressure μ_c is shown in equation (2.3.18) The results are essentially similar in nature with a minor difference due to the different scales of the length differential in relation to the area differential. This difference is demonstrated in the free energy profiles figs. 2.1 and 2.9. In the one dimensional problem the rate of growth of the favourable energetic attachment is linear and much smaller compared to the membrane case of a quadratic growth due to a larger differential. Also, the entropy growth rate for the membrane with a growing diameter is smaller compared to the polymer chain entropy growth rate for a growing detached length. The point of free energy equivalence (the membrane case is the function of diameter) for the favourable energetic attachment term and the pressure (entropy) term is about two and half times that of the linear case.

In section 2.2 we modelled the polymer chain with an inclusion of the bending rigidity of the real polymer. The free energy of this model was derived in equation (2.2.8). The effect of the pressure was demonstrated in figs. 2.4 and 2.5. In relation to the bending resistance free polymer chain scenario, the amount of pressure that is required to detach the similar size constrained polymer is many folds. That is, the pressure bias to the entropy in this case is suppressed.

Chapter 3

Inhomogeneous adhesion of a polymer: annealed averaging

In this chapter we shall treat a model system of a Gaussian chain or polymer randomly tethered along its contour onto a substrate. This is in contrast to continuum (homogeneous) adhesion to a substrate as we encountered in the previous Chapter 2. We shall model the tethers as Hookean springs. In this chapter we shall limit ourselves to a model whereby the randomness associated with the tether positions is treated as *annealed* disorder discussed in the introductory Chapter 1. This means that the spatial tether density distribution $\rho(x)$ fluctuates at the same time scale as the height undulations degrees of freedom $h(x)$. Hence the disorder parameters are treated on an equal footing as the other degrees of freedom. We shall extend this model construction in the next chapter and treat the problem at a level of *quenched* (frozen) randomness. In mathematical terms, the disorder averaged thermodynamic potential F, the Helmholtz free energy, is taken as $-\beta\langle F\rangle_{\text{disorder}} = \langle \ln Z\rangle_{\text{disorder}}$. In the annealed average treatment this becomes $-\beta\langle F\rangle_{\text{disorder}} = \ln\langle Z\rangle_{\text{disorder}}$.

3.1 Gaussian chain randomly tethered

The statistical physical model that we shall treat is that of chain polymer over a region L tethered at random points along the chain. This chain polymer is also exerted with a detachment favouring upward pressure or force per unit

length. The partition function Z, in the path integral construction, is thus

$$Z = \int \mathcal{D}h(x) \exp\left\{-\frac{\kappa}{2}\int_0^L \mathrm{d}x \left(\frac{\partial h}{\partial x}\right)^2 - \frac{\beta k}{2}\int_0^L \mathrm{d}x\, \rho(x)h^2(x) + \mu\int_0^L \mathrm{d}x\, h(x)\right\}. \quad (3.1.1)$$

The parameters κ, k, μ, and β represents the elastic measure with the units: inverse length, the spring stiffness with the units: energy per inverse length squared, the pressure with the units: inverse length squared and the inverse fundamental temperature with the units : inverse energy. $h(x)$ represents the fluctuations or undulations as a height function with the substrate reference plane (axis) – with the units: length – while $\rho(x)$ represents the spatial tether density with the units: inverse length. The first term represents the thermal fluctuations term, the second term is the Hookean tethering contribution and the last term is the detachment favouring pressure contribution. Our task is to compute the annealed averaged free energy F_{disorder} given by

$$\beta F_{\text{ann}} = -\ln\langle Z\rangle_{\text{disorder}} \quad (3.1.2)$$

and thus the disorder averaged partition function $\langle Z\rangle_{\text{disorder}}$. We shall drop the subscript label on the average. We choose the spatial disorder distribution to be a Gaussian

$$P[\rho(x)] \sim \exp\left(-\frac{R}{2}\int_0^L \mathrm{d}x\,(\rho(x)-\rho_0)^2\right). \quad (3.1.3)$$

where R is measure of the disorder of the distribution with a average of ρ_0. This parameter has the units of length. This distribution form can be motivated for instance in the spin examples earlier encountered in section 1.6 when the central limit theorem is applied analogous to the coin tossing experiments distributions. Constraints or caution needs to be excercised though when applying such a continuous distribution in order to obtain physically sensible results. The entropy determined must always be positive. A more technical discussion of these issues in replica methods was introduced in the section 1.6

Applying this distribution (3.1.3) to the partition function (3.1.1) we obtain the following functional integral to evaluate

$$\langle Z\rangle = \int \mathcal{D}\rho(x)\mathcal{D}h(x) \exp\left\{-\frac{\kappa}{2}\int_0^L \mathrm{d}x \left(\frac{\partial h}{\partial x}\right)^2 - \frac{\beta k}{2}\int_0^L \mathrm{d}x\rho(x)h^2(x) + \mu\int_0^L \mathrm{d}x\, h(x) - \frac{R}{2}\int \mathrm{d}x\,(\rho(x)-\rho_0)^2\right\}$$

$$\langle Z\rangle = \int \mathcal{D}h(x) \exp\left\{-\frac{\kappa}{2}\int_0^L \mathrm{d}x \left(\frac{\partial h}{\partial x}\right)^2 + \mu\int_0^L \mathrm{d}x\, h(x) - \frac{\beta k\rho_0}{2}\int_0^L \mathrm{d}x\, h^2(x) + \frac{(\beta k)^2}{8R}\int_0^L \mathrm{d}x\, h^4(x)\right\}. \quad (3.1.4)$$

The consequence of the disorder average upon the partition function (3.1.1) is thus the quartic interaction term $\frac{(\beta k)^2}{8R}\int_0^L \mathrm{d}x\ h^4(x)$ upon the Hamiltonian H. We must maintain the consideration that this quartic term does not lead to a divergent contribution to the Hamiltonian due to its scale and sign – in order to maintain finite energy. This is realised in part by ensuring that R is sufficiently large together with a choice of the boundary conditions $h(0) = h(L) = 0$.

In order to solve this problem (3.1.4) we shall make use of the variational approach known as the Feynman-Bogoliubov variational approach. That is, we have to estimate the free energy (3.1.2) F_{ann} by minimizing $\tilde{F}(\zeta)$ with respect to ζ the variational parameter where

$$\tilde{F}(\zeta) = F_{\mathrm{var}} - \langle H_{\mathrm{var}} - H\rangle_{\mathrm{var}}. \tag{3.1.5}$$

This approach requires a good choice of the trial variational Hamiltonian H_{var}. In this instance the trial Hamiltonian we shall use is

$$H_{\mathrm{var}} = \frac{\kappa}{2}\int_0^L \mathrm{d}x \left(\frac{\partial h}{\partial x}\right)^2 + \frac{\zeta}{2}\int_0^L \mathrm{d}x\ h^2(x) - \mu\int_0^L \mathrm{d}x\ h(x). \tag{3.1.6}$$

where ζ is the variational parameter that we shall solve for and seek to minimize the variational free energy with respect to. Except for the parameters this trial Hamiltonian only differs by the quartic term from the true one in (3.1.4). Subsequently from (3.1.4) and (3.1.6),

$$\begin{aligned} F_{\mathrm{ann}} \leq \tilde{F}(\zeta) &= F_{\mathrm{var}}(\zeta) - \langle H_{\mathrm{var}}(\zeta) - H\rangle_{\mathrm{var}} \\ &= -\frac{1}{\beta}\ln Z_{\mathrm{var}} - \left[\left(\zeta - \frac{\beta k \rho_0}{2}\right)\int_0^L \mathrm{d}x\ \left\langle h^2(x)\right\rangle_{\mathrm{var}} + \frac{(\beta k)^2}{8R}\int_0^L \mathrm{d}x\ \left\langle h^4(x)\right\rangle_{\mathrm{var}}\right]. \end{aligned} \tag{3.1.7}$$

Thus we have reduced our problem to that of calculating the harmonic oscillator problem $F_{\mathrm{var}}(\zeta)$ and the expectation values $\langle h^2(x)\rangle_{\mathrm{var}}$ and $\langle h^4(x)\rangle_{\mathrm{var}}$ for the chosen harmonic oscillator trial Hamiltonian (3.1.6). We underline that the expectation values are computed using the variational distribution or Halmitonian (3.1.6). Upon the inclusion of the source term $\int_0^L \mathrm{d}x\ f(x)h(x)$ Z_{var} derived from the Hamiltonian (3.1.6) is given by

$$\begin{aligned} Z_{\mathrm{var}}(f) &= \exp\left(-\frac{1}{2}\int_0^1 \mathrm{d}x \left(\frac{\partial h_0}{\partial x}\right)^2 - \frac{\zeta L^2}{2\kappa}\int_0^1 \mathrm{d}x\ h_0^2(x) + \mu L\sqrt{\frac{L}{\kappa}}\int_0^1 \mathrm{d}x\ h_0(x)\right) \\ &\quad \times \int \mathcal{D}\eta(x) \exp\left\{-\frac{1}{2}\int_0^1 \mathrm{d}x \left(\frac{\partial \eta}{\partial x}\right)^2 - \frac{\zeta L^2}{\kappa}\int_0^1 \mathrm{d}x\ \eta^2(x)\right. \\ &\quad \left. + \int_0^1 \mathrm{d}x\ f(x)\eta(x) + \int_0^1 \mathrm{d}x\ f(x)h_0(x)\right\}. \end{aligned} \tag{3.1.8}$$

where we have applied the transformation $h(x) = h_0(x) + \eta(x)$ together with the rescaling $h \to \frac{h}{\sqrt{\frac{L}{\kappa}}}$ and $x \to \frac{x}{L}$. $h_0(x)$ is a solution for the Euler-Lagrange

equation

$$\frac{d}{dx}\frac{\partial \mathcal{L}}{\partial h_0'(x)} - \frac{\partial \mathcal{L}}{\partial x} = 0, \quad \text{with the conditions } h_0(0) = h_0(1) = 0. \tag{3.1.9}$$

where again $h'(x)$ shall be used as shorthand for $\frac{\partial h}{\partial x}$. The Lagrangian $\mathcal{L}$ is given by $\mathcal{L} = \frac{1}{2}\left(\frac{\partial h}{\partial x}\right)^2 + \frac{\zeta L^2}{\kappa}h^2(x) - \mu\sqrt{\frac{L^3}{\kappa}}h(x)$. Subsequently the differential equation that then needs to be solved is

$$h_0''(x) - \frac{\zeta L^2}{\kappa}h_0(x) + \mu\sqrt{\frac{L^3}{\kappa}} = 0 \tag{3.1.10}$$

which has a solution

$$h_0(x) = \frac{\mu - \mu\operatorname{sech}\left(\frac{\sqrt{\zeta}L}{2\sqrt{\kappa}}\right)\cosh\left(\frac{\sqrt{\zeta}L(2x-1)}{2\sqrt{\kappa}}\right)}{\zeta\sqrt{\frac{L}{\kappa}}}. \tag{3.1.11}$$

Substituting this result upon the stationary part $\exp(\cdots)$ of the equation (3.1.8) we obtain

$$\exp(\cdots) = \exp\left(\frac{\mu^2\left(\sqrt{\zeta}L - 2\sqrt{\kappa}\tanh\left(\frac{\sqrt{\zeta}L}{2\sqrt{\kappa}}\right)\right)}{2\zeta^{3/2}}\right) \tag{3.1.12}$$

The "stationary" contribution contained in the first factor is now complete. We now turn our focus onto the fluctuation contribution $\mathcal{F}$,

$$\begin{aligned}\mathcal{F} \;=\; & \int \mathcal{D}\eta(x)\exp\left\{-\frac{1}{2}\int_0^1 \mathrm{d}x\left(\frac{\partial\eta}{\partial x}\right)^2 - \frac{\zeta L^2}{\kappa}\int_0^1 \mathrm{d}x\,\eta^2(x)\right. \\ & \left. + \int_0^1 \mathrm{d}x\; f(x)\eta(x) + \int_0^1 \mathrm{d}x\; f(x)h_0(x)\right\}.\end{aligned} \tag{3.1.13}$$

After an integration by parts of the first term $\int \mathrm{d}x\left(\frac{\partial\eta}{\partial x}\right)^2$ with the boundary conditions $\eta(0) = \eta(1) = 0$ we obtain

$$\begin{aligned}\mathcal{F} \;=\; & \int \mathcal{D}\eta(x)\exp\left\{-\frac{1}{2}\int_0^1\int_0^1 \mathrm{d}x\,\mathrm{d}x'\eta(x')\underbrace{\left[\delta(x'-x)\left(\frac{\zeta L^2}{\kappa} - \partial_{xx}\right)\right]}_{A(x',x)}\eta(x)\right. \\ & \left. + \int_0^1 \mathrm{d}x\; f(x)\eta(x) + \int_0^1 \mathrm{d}x\; f(x)h_0(x)\right\} \\ =\; & \int \mathcal{D}\eta(x)\exp\left\{-\frac{1}{2}\int_0^1\int_0^1 \mathrm{d}x\,\mathrm{d}x'\eta(x')A(x',x)\eta(x)\right. \\ & \left. + \int_0^1 \mathrm{d}x\; f(x)\eta(x) + \int_0^1 \mathrm{d}x\; f(x)h_0(x)\right\}\end{aligned}$$

$$\mathcal{F} = \exp\left(-\frac{1}{2}\mathrm{tr}\ln A(x',x) + \frac{L^3}{\kappa}\int_0^1\int_0^1 \mathrm{d}x\,\mathrm{d}x' f(x')A^{-1}(x',x)f(x) + \int_0^1 \mathrm{d}x\; f(x)h_0(x)\right). \tag{3.1.14}$$

Combining this result (3.1.14) with the stationary factor from (3.1.8) we thus have

$$Z_{\mathrm{var}}(f) = \exp\left(\frac{\mu^2\left(\sqrt{\zeta}L - 2\sqrt{\kappa}\tanh\left(\frac{\sqrt{\zeta}L}{2\sqrt{\kappa}}\right)\right)}{2\zeta^{3/2}}\right) \times \exp\left(-\frac{1}{2}\mathrm{tr}\ln A(x',x) + \frac{1}{2}\int_0^1\int_0^1 \mathrm{d}x\;\mathrm{d}x' f(x')A^{-1}(x',x)f(x) + \int_0^1 \mathrm{d}x\; f(x)h_0(x)\right). \tag{3.1.15}$$

Now this result (3.1.15) still requires us to calculate the eigenvalues of the continuous operator $A(x',x)$ since

$$\mathrm{tr}\ln A(x',x) = \ln \det A(x',x) = \ln\prod_{i=1}^{\infty}\lambda_i = \sum_{i=1}^{\infty}\ln\lambda_i \tag{3.1.16}$$

where λ_i's are the eigenvalues of the operator $A(x',x)$. Also, due to the completeness relation and operator-inverse operator relation, found in standard texts, $A^{-1}(x',x) = \sum_{i=1}^{\infty}\lambda_i^{-1}u_i(x')u_i(x)$ where $u_i(x)$ are the eigenfunctions of the operator $A(x',x)$. Therefore, we need to solve

$$\int \mathrm{d}x\left[\delta(x'-x)\left(\frac{\zeta L^2}{\kappa} - \partial_{xx}\right)\right]u_i(x) = \lambda_i u_i(x'),\quad u_i(0) = u_i(1) = 0 \tag{3.1.17}$$

The solution to this problem is

$$u_n(x) = A\sin(n\pi x)\quad\text{and}\quad \lambda_n = \left(\frac{\zeta L^2}{\kappa} + (n\pi)^2\right). \tag{3.1.18}$$

With this we are almost done! Because

$$\begin{aligned}&\mathrm{tr}\ln A(x',x)\\ &= \sum_{n=1}^{\infty}\ln\lambda_n = \sum_{n=1}^{\infty}\ln\left(\frac{\zeta L^2}{\kappa} + (n\pi)^2\right) = c + \sum_{n=1}^{\infty}\ln\left(\frac{\zeta L^2}{\pi^2\kappa} + n^2\right)\\ &= c + \sum_{n=1}^{\infty}\int\frac{d}{d\alpha}\ln\left(\alpha^2+n^2\right)d\alpha = c + \int d\alpha\sum_{n=1}^{\infty}\frac{2\alpha}{(\alpha^2+n^2)}\end{aligned} \tag{3.1.19}$$

where $c = \infty \ln \pi$ and $\alpha^2 = \frac{\zeta L^2}{\pi^2 \kappa}$. Applying the identity [80]

$$\sum_{n=1}^{\infty} \frac{\cos nx}{n^2+\alpha^2} = \frac{\pi}{2\alpha}\frac{\cosh \alpha(\pi - x)}{\sinh \alpha\pi} - \frac{1}{2\alpha^2} \qquad \text{when} \quad x = 0, \tag{3.1.20}$$

we obtain

$$\begin{aligned} \operatorname{tr} \ln A(x', x) &= c + \int d\alpha \left(\pi \frac{\cosh \pi\alpha}{\sinh \pi\alpha} - \frac{1}{\alpha} \right) \\ \operatorname{tr} \ln A(x', x) &= c + \log \left(\sinh \left(\frac{\sqrt{\zeta} L}{\sqrt{\kappa}} \right) \right) - \log \left(\frac{\sqrt{\zeta} L}{\pi \sqrt{\kappa}} \right). \end{aligned} \tag{3.1.21}$$

What we are left to do now is to evaluate the object $A^{-1}(x', x)$. As can be seen on equation (3.1.14) this object is central to the evaluation of the correlation functions $\langle h^2(x) \rangle_{\text{var}}$ and $\langle h^4(x) \rangle_{\text{var}}$ that we need to achieve our goal (3.1.7).

$$A^{-1}(x', x) = \sum_{n=1}^{\infty} \lambda_n^{-1} u_n(x') u_n(x) = \sum_{n=1}^{\infty} \frac{\sin(n\pi x') \sin(n\pi x)}{\left(\frac{\zeta L^2}{\kappa} + n^2\pi^2 \right)}. \tag{3.1.22}$$

Fortunately, we can apply the identity [81]

$$2 \sum_{n=1}^{\infty} \frac{\sin(n\pi s') \sin(n\pi s)}{y^2 + n^2\pi^2} = \frac{\sinh(y \min(s, s')) \sinh(y(1 - \max(s, s')))}{y \sinh y}. \tag{3.1.23}$$

Subsequently,

$$A^{-1}(x, x) = \frac{1}{2} \frac{\sinh \left(\sqrt{\frac{\zeta L^2}{\kappa}} x \right) \sinh \sqrt{\frac{\zeta L^2}{\kappa}} (1 - x)}{\sqrt{\frac{\zeta L^2}{\kappa}} \sinh \sqrt{\frac{\zeta L^2}{\kappa}}}. \tag{3.1.24}$$

From (3.1.15) and (3.1.21) we effectively have determined $Z_{\text{var}} = Z_{\text{var}}[f = 0]$ from equation (3.1.7). This in effect is the first term $F_{\text{var}}(\zeta)$ of the free energy expression (3.1.5), that is

$$\begin{aligned} F_{\text{var}}(\zeta) &= -\frac{1}{\beta} \ln Z_{\text{var}} = -\frac{1}{\beta} \ln Z_{\text{var}}[f = 0] \\ &= -\frac{1}{\beta} \left(\frac{\mu^2 \left(\sqrt{\zeta} L - 2\sqrt{\kappa} \tanh \left(\frac{\sqrt{\zeta} L}{2\sqrt{\kappa}} \right) \right)}{2\zeta^{3/2}} \right) \\ &\qquad + \frac{1}{2\beta} \left(\log \left(\sinh \left(\frac{\sqrt{\zeta} L}{\sqrt{\kappa}} \right) \right) - \log \left(\frac{\sqrt{\zeta} L}{\pi \sqrt{\kappa}} \right) \right). \end{aligned} \tag{3.1.25}$$

We note here that the zero limit with respect to the variational parameter ζ reproduces the earlier encountered model 2.1.1 result. Whilst the opposite limit yield a divergence.

What we are left with is to determine the expressions for the correlation functions $\langle h^2(x)\rangle_{\text{var}}$ and $\langle h^4(x)\rangle_{\text{var}}$ and then substitute the result for $A^{-1}(x,x)$ and finally perform the integration. This shall give us $\tilde{F}(\zeta)$ of equation (3.1.7) that is larger or equal to the actual free energy according to the Feynman Bogoliubov inequality (3.1.7). Thereafter a minimization with respect to ζ will be implemented. The final expressions, see Appendix A, for $\langle h^2(x)\rangle_{\text{var}}$ and $\langle h^4(x)\rangle_{\text{var}}$ are

$$\left\langle h^2(x)\right\rangle_{\text{var}} = h_0^2(x) + A^{-1}(x,x) \tag{3.1.26}$$

and

$$\left\langle h^4(x)\right\rangle_{\text{var}} = h_0^4(x) + 6h_0^2(x)A^{-1}(x,x) + 3\left[A^{-1}(x,x)\right]^2 \tag{3.1.27}$$

where $h_0(x)$ and $A^{-1}(x,x)$ are given by (3.1.11) and (3.1.24), respectively. After the relabelling

$$\zeta_0 = \beta k \rho_0 \tag{3.1.28}$$

we have derived the terms $-\left(\zeta - \frac{\zeta_0}{2}\right)\int_0^1 \mathrm{d}x\, \langle h^2(x)\rangle_{\text{var}}$ and $-\frac{(\beta k)^2}{8R}\int_0^1 \mathrm{d}x\, \langle h^4(x)\rangle_{\text{var}}$ in equation (3.1.7) shown in the Appendices A.4 and A.5.

We are now in a position to express $\tilde{F}(\zeta)$ (3.1.7). That is,

$$\tilde{F}(\zeta) = -\frac{1}{\beta}\ln Z_{\text{var}}[f=0] - \left[\left(\zeta - \frac{\zeta_0}{2}\right)\int_0^1 \mathrm{d}x\, \left\langle h^2(x)\right\rangle_{\text{var}} + \frac{(\beta k)^2}{8R}\int_0^1 \mathrm{d}x\, \left\langle h^4(x)\right\rangle_{\text{var}}\right] \tag{3.1.29}$$

Substituting equations (3.1.25), (A.4.1) and equation (A.5.5) we obtain

$$\begin{aligned}\tilde{F}(\zeta) \;=\; & -\frac{1}{\beta}\left(\frac{\mu^2\left(\sqrt{\zeta}L-2\sqrt{\kappa}\tanh\left(\frac{\sqrt{\zeta}L}{2\sqrt{\kappa}}\right)\right)}{2\zeta^{3/2}}\right)\\ & +\frac{1}{2\beta}\left(\log\left(\sinh\left(\frac{\sqrt{\zeta}L}{\sqrt{\kappa}}\right)\right)-\frac{1}{2}\log\left(\frac{\sqrt{\zeta}L}{\pi\sqrt{\kappa}}\right)\right)\\ & +\frac{\left(\frac{\zeta_0}{2}-\zeta\right)\kappa\mu^2\left(\sqrt{\zeta}L\left(\operatorname{sech}^2\left(\frac{\sqrt{\zeta}L}{2\sqrt{\kappa}}\right)+2\right)-6\sqrt{\kappa}\tanh\left(\frac{\sqrt{\zeta}L}{2\sqrt{\kappa}}\right)\right)}{2\zeta^{5/2}L^2}\\ & -\frac{\left(\frac{\zeta_0}{2}-\zeta\right)\left(\kappa-\sqrt{\zeta}\sqrt{\kappa}L\coth\left(\frac{\sqrt{\zeta}L}{\sqrt{\kappa}}\right)\right)}{4\zeta L^2}\\ & -\frac{3\beta^2\kappa k^2\left(\sqrt{\zeta}L\left(3\operatorname{csch}^2\left(\frac{\sqrt{\zeta}L}{\sqrt{\kappa}}\right)+2\right)-3\sqrt{\kappa}\coth\left(\frac{\sqrt{\zeta}L}{\sqrt{\kappa}}\right)\right)}{64\zeta^{3/2}L^3R}\\ & -\frac{3\beta^2\kappa^{3/2}k^2\mu^2\left(4\cosh\left(\frac{\sqrt{\zeta}L}{\sqrt{\kappa}}\right)+\cosh\left(\frac{2\sqrt{\zeta}L}{\sqrt{\kappa}}\right)\right)\operatorname{csch}\left(\frac{\sqrt{\zeta}L}{\sqrt{\kappa}}\right)\operatorname{sech}^2\left(\frac{\sqrt{\zeta}L}{2\sqrt{\kappa}}\right)}{32\zeta^{5/2}L^2R}\\ & -\frac{\beta^2\kappa^2k^2\mu^2\left(4-19\cosh\left(\frac{\sqrt{\zeta}L}{\sqrt{\kappa}}\right)\right)\operatorname{sech}^2\left(\frac{\sqrt{\zeta}L}{2\sqrt{\kappa}}\right)}{32\zeta^3L^3R}\\ & -\frac{\beta^2\kappa^2k^2\mu^4\left(16\cosh\left(\frac{\sqrt{\zeta}L}{\sqrt{\kappa}}\right)+\cosh\left(\frac{2\sqrt{\zeta}L}{\sqrt{\kappa}}\right)+18\right)\operatorname{sech}^4\left(\frac{\sqrt{\zeta}L}{2\sqrt{\kappa}}\right)}{64\zeta^4L^2R}\\ & +\frac{5\beta^2\kappa^{5/2}k^2\mu^4\left(32\sinh\left(\frac{\sqrt{\zeta}L}{\sqrt{\kappa}}\right)+5\sinh\left(\frac{2\sqrt{\zeta}L}{\sqrt{\kappa}}\right)\right)\operatorname{sech}^4\left(\frac{\sqrt{\zeta}L}{2\sqrt{\kappa}}\right)}{384\zeta^{9/2}L^3R}. \qquad (3.1.30)\end{aligned}$$

3.2 Minimization of the free energy $\tilde{F}(\zeta)$

3.2.1 The attempt at an analytical solution for ζ

We have now derived the Feynman-Bogoliubov free energy $\tilde{F}(\zeta)$ (3.1.30). The task that remains is to minimize this expression, that is, determine the variational 'parameter' ζ, a function of L, μ, R, k, κ, β and $\zeta_0 = \rho_0\beta k$. In pursuit of this we express the free energy $\tilde{F}(\zeta)$ in terms of σ by the transformation

$$\zeta \to \frac{\kappa\sigma^2}{L^2} \qquad (3.2.1)$$

Hence,

$$\begin{aligned}\tilde{F}(\sigma) \;=\; & \frac{(\sigma\coth(\sigma)-1)\,(L^2\rho-2\kappa\sigma^2)}{8L^2\sigma^2}-\frac{3\beta^2k^2\left(\sigma\left(3\mathrm{csch}^2(\sigma)+2\right)-3\coth(\sigma)\right)}{64R\sigma^3}\\ &+\frac{\beta^2k^2\mu^2L^3\mathrm{sech}^2\left(\frac{\sigma}{2}\right)(19\cosh(\sigma)-3\sigma(4\cosh(\sigma)+\cosh(2\sigma))\mathrm{csch}(\sigma)-4)}{32\kappa R\sigma^6}\\ &-\frac{\beta^2k^2\mu^4L^6(16\cosh(\sigma)+\cosh(2\sigma)+18)\mathrm{sech}^4\left(\frac{\sigma}{2}\right)}{64\kappa^2R\sigma^8}\\ &+\frac{\mu^2L\mathrm{sech}^2\left(\frac{\sigma}{2}\right)(\sigma(\cosh(\sigma)+2)-3\sinh(\sigma))\,(L^2\rho-2\kappa\sigma^2)}{4\kappa\sigma^5}\\ &+\frac{5\beta^2k^2\mu^4L^6(32\sinh(\sigma)+5\sinh(2\sigma))\mathrm{sech}^4\left(\frac{\sigma}{2}\right)}{384\kappa^2R\sigma^9}\\ &-\frac{\mu^2L^3\left(\sigma-2\tanh\left(\frac{\sigma}{2}\right)\right)}{2\beta\kappa\sigma^3}+\frac{\log(\sinh(\sigma))+\log(\pi)}{2\beta}. \end{aligned}\tag{3.2.2}$$

The minimization requires that we find the derivative of $\tilde{F}(\zeta)$ with respect to the variational parameter ζ or rather σ in the transformed version (3.2.2) and thereafter solve for σ. The question that arises then is: does a minimum exist for the Feynman Bogoliubov free energy $\tilde{F}(\sigma)$ with respect to σ, the rescaled variational parameter ζ? Below in fig. 3.1 we show that indeed for certain values of parameters the minima does exist. In our explorations we shall often assume or set β, κ and k to be of unity order and we also here remind ourselves that $\zeta_0 = \rho_0\beta k$.

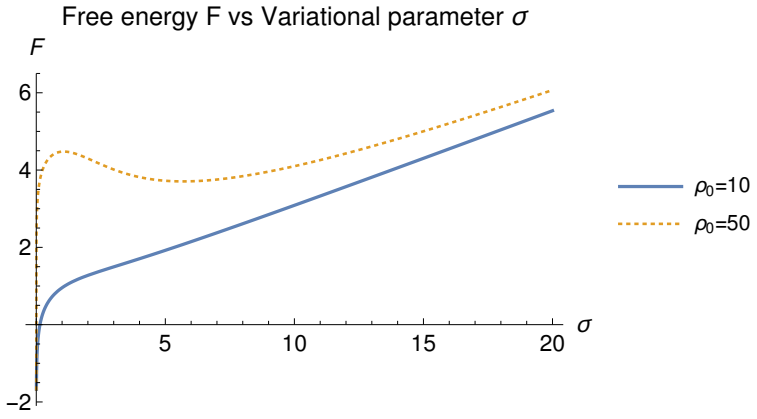

Figure 3.1: Feynman Bogoliubov free energy profile for pressure $\mu = 0$ dimensionless, average density $\rho_0 = \{10, 100\}$ units, distribution parameter $R = 1$ and length $L = 1$ units. β, κ and k are set to unity.

We observe from these figures that the minimum of the free energy's $\tilde{F}(\zeta)$ derivative exists in the small σ or ζ limit. Analytical approximate evaluation for the large σ or ζ limit corroborates this. The dominant term is of order

$\log(\sinh(\sigma))$. This minimum is dependent upon the other parameters such as pressure μ. For instance, we see in fig. 3.1 that this minimum vanishes with declining mean tether density ρ_0. Now, since the solution lies in the small σ domain we shall, therefore, perform a Taylor expansion approximation of the Feynman Bogoliubov free energy $\tilde{F}(\sigma)$ to fifth order from which we obtain a relatively simpler expression

$$\tilde{F}(\sigma) = A\sigma^4 + \frac{\log(\sigma)}{2\beta} + B\sigma^2 + C. \tag{3.2.3}$$

From this expression (3.2.3) we solve for the variational parameter $\sigma(\zeta)$ that minimizes this expression (3.2.3) from $\tilde{F}'(\sigma) = 0$,

$$\begin{aligned} A &= -\frac{1}{360\beta} - \frac{1193\beta^2k^2\mu^4L^6}{922521600\kappa^2R} - \frac{317\beta^2k^2\mu^2L^3}{4435200\kappa R} - \frac{\beta^2k^2}{4200R} - \frac{17\mu^2L^3}{40320\beta\kappa} \\ &\quad + \frac{31\mu^2L^3\rho}{241920\kappa} + \frac{\kappa}{180L^2} + \frac{17\mu^2L}{10080} + \frac{\rho}{3780} \end{aligned} \tag{3.2.4}$$

$$\begin{aligned} B &= \frac{1}{12\beta} + \frac{\beta^2k^2\mu^4L^6}{197120\kappa^2R} + \frac{\beta^2k^2\mu^2L^3}{2688\kappa R} + \frac{\beta^2k^2}{560R} + \frac{\mu^2L^3}{240\beta\kappa} - \frac{17\mu^2L^3\rho}{20160\kappa} - \frac{\kappa}{12L^2} \\ &\quad - \frac{\mu^2L}{120} - \frac{\rho}{360} \end{aligned} \tag{3.2.5}$$

$$\begin{aligned} C &= \frac{-1008\beta^3\kappa^2k^2 + \beta^3\left(-k^2\right)\mu^4L^6 - 108\beta^3\kappa k^2\mu^2L^3 - 3360\kappa\mu^2L^3R}{80640\beta\kappa^2R} \\ &\quad + \frac{336\beta\kappa\mu^2L^3\rho R + +3360\beta\kappa^2\rho R + 40320\kappa^2R\log(\pi)}{80640\beta\kappa^2R}. \end{aligned} \tag{3.2.6}$$

In the approximate free energy equation (3.2.3) we have a fourth order polynomial with the logarithmic term $\mathrm{Log}[\sigma]$. Minimization requires setting the gradient to zero. We have

$$D[\tilde{F}(\sigma)] = 4A\sigma^3 + 2B\sigma + \frac{1}{\sigma} = 0 \tag{3.2.7}$$

that we must solve for σ. This becomes a quadratic function of σ^2. On the physical basis the solution that we accept out of the four is

$$\sigma^2 = \frac{\sqrt{B^2 - 4A}}{A} - \frac{B}{A}, \quad \text{where} \quad \frac{\sqrt{B^2 - 4A}}{A} > \frac{B}{A}. \tag{3.2.8}$$

Therefore

$$\zeta = \frac{\kappa\sigma^2}{L^2} = \frac{\kappa}{L^2}\left(\frac{\sqrt{B^2 - 4A}}{A} - \frac{B}{A}\right). \tag{3.2.9}$$

Substituting this result (3.2.9) to obtain the approximate analytic minimized annealed free energy (3.1.7), the outcome is a gigantic expression of the rest of the parameters. This subsequent variational parameter ζ independent free energy expression must maintain the condition $\frac{\sqrt{B^2-4A}}{A} > \frac{B}{A}$. Further progress would now require a numerical strategy to draw the free energy and resulting functions such as the average height fluctuations.

3.2.2 The graphical solution for ζ

In this section we explore the solution for the variational parameter graphically. That is, for specific numerical values for parameters L, μ, R, k, κ, β and $\zeta_0 = \rho_0 \beta k$ we determine the interception numerical values of ζ. In order to do this we need the derivatives of $F_{\text{var}}(\zeta)$ and $\langle H_{\text{var}}[\zeta] - H \rangle_{\text{var}}$ – a function of $\langle h^2(x) \rangle_{\text{var}}$ and $\langle h^4(x) \rangle_{\text{var}}$ as can be seen in (3.1.7). These derivatives are listed below

$$\frac{\partial F_{\text{var}}(\zeta)}{\partial \zeta} = \frac{3\mu^2 \left(\sqrt{\zeta} L - 2\sqrt{\kappa} \tanh\left(\frac{\sqrt{\zeta} L}{2\sqrt{\kappa}} \right) \right)}{4\beta \zeta^{5/2}} - \frac{\mu^2 \left(\frac{L}{2\sqrt{\zeta}} - \frac{L \operatorname{sech}^2\left(\frac{\sqrt{\zeta} L}{2\sqrt{\kappa}} \right)}{2\sqrt{\zeta}} \right)}{2\beta \zeta^{3/2}} + \frac{\frac{L \coth\left(\frac{\sqrt{\zeta} L}{\sqrt{\kappa}} \right)}{2\sqrt{\zeta}\sqrt{\kappa}} - \frac{1}{2\zeta}}{2\beta} \tag{3.2.10}$$

$$\frac{\partial \langle H_{\text{var}}(\zeta) - H \rangle_{\text{var}}}{\partial \zeta} = \frac{\partial}{\partial \zeta} \left[\left(\zeta - \frac{\zeta_0}{2} \right) \int_0^1 \mathrm{d}x \, \langle h^2(x, \zeta) \rangle_{\text{var}} + \frac{(\beta k)^2}{8R} \int_0^1 \mathrm{d}x \, \langle h^4(x, \zeta) \rangle_{\text{var}} \right] \tag{3.2.11}$$

The derivative outcome is shown in Appendix A.6. From these expressions (3.2.10) and (3.2.11) with the final expression (A.6.1) we graphically determine the variational parameter ζ of the overestimated free energy (3.1.7). Below is a an example for a purpose of illustration. We note here also that the first expression (3.2.10) does not have the parameters ρ_0 and R.

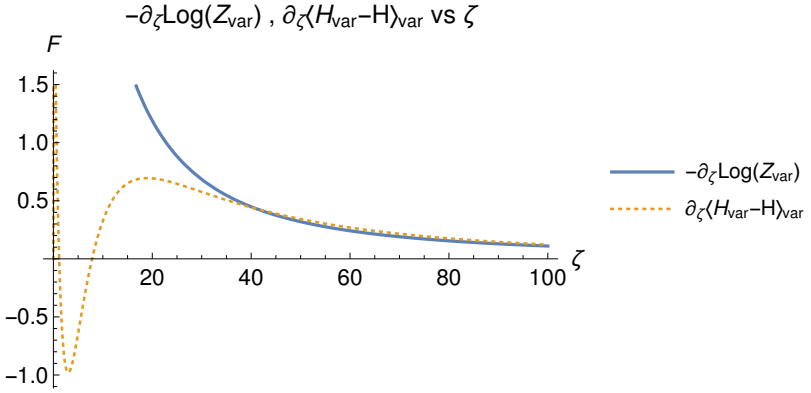

Figure 3.2: $-\frac{\partial \mathrm{Log} Z_{\mathrm{var}}}{\partial \zeta}, \frac{\partial \langle H_{\mathrm{var}} - H \rangle_{\mathrm{var}}}{\partial \zeta}$ as a function of ζ for pressure $\mu = 50$ dimensionless, average density $\rho_0 = 2$ units, distribution parameter $R = 1.15$ and length $L = 1$ units. In these choice of parameters we obtain $\zeta \approx 38$ units. β, κ and k are set to unity.

Smaller values of pressure require a discrete numerical treatment. The solutions for the intersections of the two plots occur at small values of ζ where there is a divergent behaviour. Subsequently, the superimposition of the two functions of ζ does not *show* the intersection output.

3.2.3 The numerical solution

In this section we treat the minimization of the variational free energy (3.1.7), that is, equation (3.1.30) numerically using *Mathematica* software. We determine the numerical value of the variational parameter ζ and also produce the subsequent list graph for specific numerical values for the parameters L, μ, R, k, κ, β. Below, figs. 3.3 and 3.4, the results of this computation are shown.

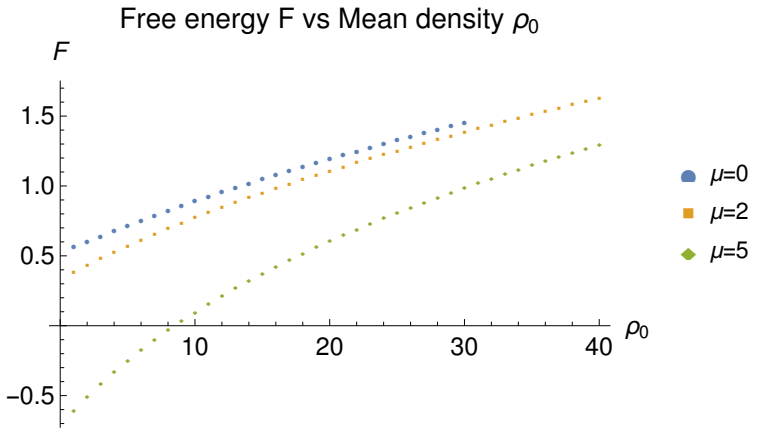

Figure 3.3: Free energy F as a function of the average density ρ_0, size $L = 1$ units and pressure $\mu = \{0, 3, 5\}$ dimensionless. β, κ and k are set to unity.

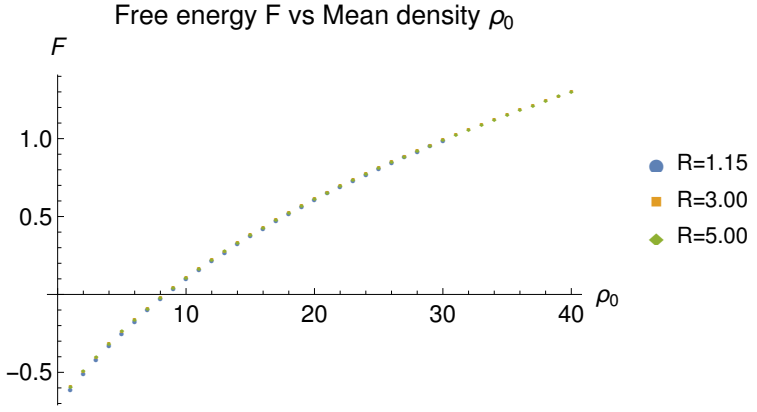

Figure 3.4: Free energy F as a function of the average density ρ_0, pressure $\mu = 5$ dimensionless, size $L = 1$ and $R = \{0, 3, 5\}$ units. β, κ and k are set to unity.

From these figures the annealed free energy has no minima for all pressure values. Instead we observe that for zero pressure μ we have a monotonic *constant gradient* linear relationship as we increase the average density ρ_0. However, for a pressure μ larger than zero this monotonic constant gradient picture changes. At smaller values of the average density ρ_0 the gradient is larger in relation to the larger values.

What role does the disorder parameter R play in this monotonic behaviour? The effect of the variation of this parameter upon the free energy is shown in the fig. 3.4. The figure reflects a similar profile with an increasing disorder parameter R. This is also true for a decreasing disorder parameter R.

Subsequent to fig. 3.3 and equation (3.1.4) the square height fluctuations $\langle h^2 \rangle = \frac{\partial F}{\partial \rho_0}$ are as follows – figs. 3.5 and 3.8.

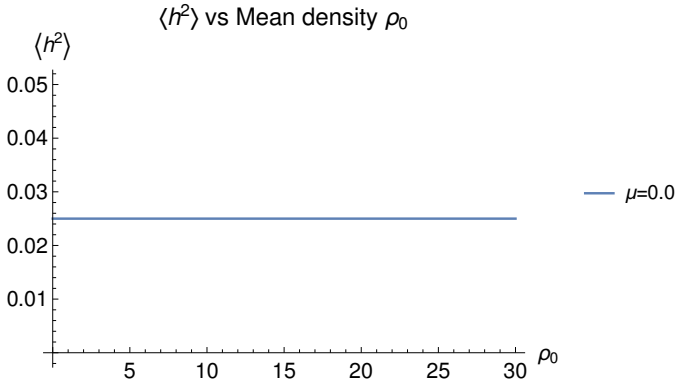

Figure 3.5: $\langle h^2 \rangle$ as a function of average density ρ_0 for the pressure $\mu = 0$ dimensionless. β, κ and k are set to unity.

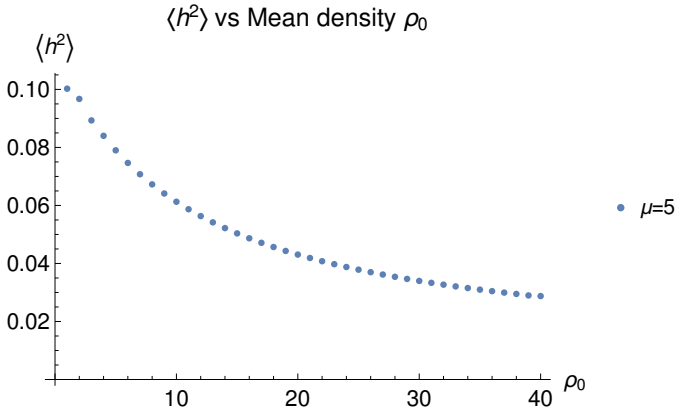

Figure 3.6: $\langle h^2 \rangle$ as a function of average density ρ_0 for the pressure $\mu = 5$ dimensionless. β, κ and k are set to unity.

In fig. 3.7 we draw the annealed free energy as a function of the pressure μ. From this figure we draw the subsequent average height function fig. 3.8 due to the equation (3.1.4) such that $\langle h \rangle = \frac{\partial F}{\partial \mu}$

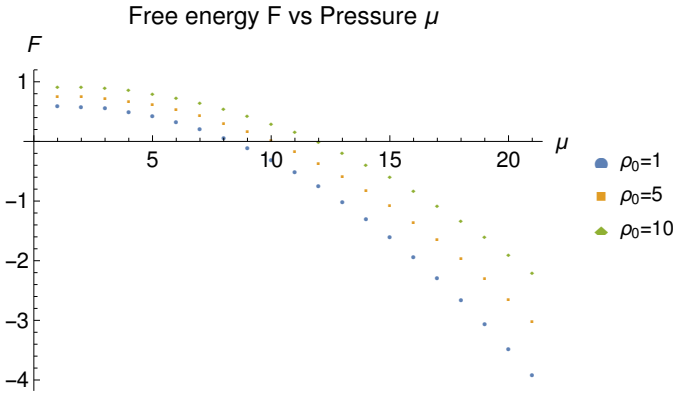

Figure 3.7: Free energy F as a function of the pressure μ for the average density $\rho_0 = \{1,\ 5,\ 10\}$ units. β, κ and k are set to unity.

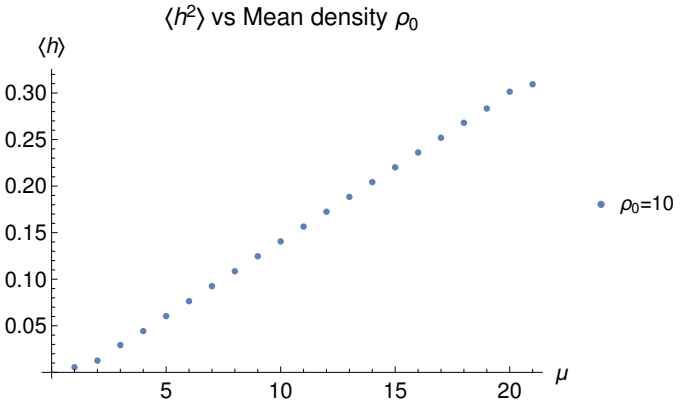

Figure 3.8: $\langle h \rangle$ as a function of the pressure μ for the average density $\rho_0 = 10$ units. β, κ and k are set to unity.

The above figs. 3.5 and 3.6 demonstrate that without any pressure μ applied the square fluctuation $\langle h^2 \rangle$ exhibits a flat response with the removal of the tethers. We view this as a manifestation of the annealed nature of the tether positions. However, when there is a nonzero uniform pressure μ applied this flat response with the removal of tethers exhibits monotonic growth from relatively small square fluctuations to large square fluctuations $\langle h^2 \rangle$.

In fig. 3.8 the average height $\langle h \rangle$ as a function of the pressure μ for a fixed tether density ρ_0 also exhibits a monotonic behaviour from small average height fluctuations to large height fluctuations at a higher pressure. We deduced this from the profile fig. 3.7. This exemplifies the polymer chain stretching as higher pressure is applied.

3.3 Tether adhesion energy ϵ effect

We have treated the random tethering model without an explicit account for the adhesion sticking energy associated with each tether. What happens when we, as in the homogeneous adhesion models encountered, associate each spring with adhesion sticking energy ϵ? This implies that the model that we have to treat is a modified version of (3.1.1) which now becomes

$$Z = \int \mathcal{D}h(x) \exp\left\{-\frac{\kappa}{2}\int_0^L \mathrm{d}x \left(\frac{\partial h}{\partial x}\right)^2 - \frac{\beta k}{2}\int_0^L \mathrm{d}x \rho(x) h^2(x) + \mu\int_0^L \mathrm{d}x\, h(x) - \beta\epsilon\int_0^L dx\, \rho(x)\right\}. \quad (3.3.1)$$

Similarly, upon applying (3.1.3)

$$\langle Z\rangle = \int \mathcal{D}h(x) \exp\left\{-\frac{\kappa}{2}\int_0^L \mathrm{d}x \left(\frac{\partial h}{\partial x}\right)^2 + \mu\int_0^L \mathrm{d}x\, h(x) - \left(\frac{\beta k\rho_0}{2} - \frac{\beta^2 k\epsilon}{R}\right) \times \int_0^L \mathrm{d}x\, h^2(x) + \frac{(\beta k)^2}{8R}\int_0^L \mathrm{d}x\, h^4(x) - \int_0^L dx\, \left(\beta\epsilon\rho_0 - \frac{\beta^2\epsilon^2}{R}\right)\right\}. \quad (3.3.2)$$

The consequence of this to the variational strategy we pursued is that (3.1.7) now becomes

$$\begin{aligned}\tilde{F}(\zeta) &= F_{\text{var}} - \langle H_{\text{var}} - H\rangle_{\text{var}} \\ \tilde{F}(\zeta) &= -\frac{1}{\beta}\ln Z_{\text{var}} - \left[\left(c - \frac{\bar{\zeta}_0}{2}\right)\int_0^L dx\, \left\langle h^2(x)\right\rangle_{\text{var}} \right. \\ &\quad \left. + \frac{(\beta k)^2}{8R}\int_0^L dx\, \left\langle h^4(x)\right\rangle_{\text{var}} - \int_0^L dx\, \left(\beta\epsilon\rho_0 - \frac{\beta^2\epsilon^2}{R}\right)\right].\end{aligned} \quad (3.3.3)$$

where now $\bar{\zeta}_0 = \left(\beta k\rho_0 - \frac{2\beta^2 k\epsilon}{R}\right) = \left(\beta k\rho_0 + \frac{2\beta^2 k|\epsilon|}{R}\right)$. Therefore (3.3.3) is equivalent to (3.1.30), however, with an extra term: $-\int_0^L dx\, \left(\beta\epsilon\rho_0 - \frac{\beta^2\epsilon^2}{R}\right)$ added upon it and a renormalized $\zeta_0 \to \bar{\zeta}_0$. This renormalized $\bar{\zeta}_0$ effectively affects the results listed above by translation. In one view this could be seen as rescaling the spring elastic coefficient. This rescaled elasticity also now depends on the disorder parameter R. The relationship with R means that for large R the rescaling is minimal. Large R corresponds to a uniform distribution of the tethers. Whereas smaller R corresponds with the inhomogeneous distribution. Hence, smaller R results in the ζ_0 rescaling that is relatively larger due the tether sticking adhesion energy ϵ. The effect of this will be a lateral translation towards the origin of the free energy profiles.

3.4 Summary

In this chapter we studied a one dimensional discrete random adhesion with a uniform applied pressure problem using the Feynman Bogoliubov variational approach. We treated this for an annealed scenario of the spatial distribution of the tethers. In our treatment we calculated analytically the annealed Feynman Bogoliubov free energy as the function of pressure μ, average density ρ_0 and global size L amongst other important parameters such as the tether stiffness k. The free energy displayed monotonic behaviour as shown and discussed in section 3.2.3. The representative graphs of this free energy are shown in figs. 3.3 and 3.7. The annealed nature of the distribution of the tethers results in the flat nature response of the square fluctuations $\langle h^2 \rangle$ with a removal of tethers when there is no applied pressure. The variations of the disorder parameter R display no changes to these profiles as shown in fig. 3.4. Applying pressure, the height square fluctuations $\langle h^2 \rangle$ display a monotonic growth behavior as shown in fig. 3.6 with the removal of tethers. This is only observed for pressure μ larger than zero. Therefore, it is the pressure that is reponsible for this behaviour. The pressure leads to an emergence of a polymer chain stretching regime exemplified by the higher square fluctuations $\langle h^2 \rangle$ for lower domain of tether density ρ_0. These collectively demonstrates the competition between the density of annealed nature tether positions distribution and the elasticity of the polymer chain in the presence of pressure.

Chapter 4

Adhesion of a polymer in 1+1 dimension: quenched averaging

4.1 Gaussian polymer randomly tethered onto hard substrate

In this chapter we shall introduce a more physically constrained model of inhomogeneous membrane adhesion in the context of our problem. Instead of a uniform continuous potential of surface attachment we take into account the fact that the tethers are spatially distant to each other and there is quenched disorder associated with the tether position distribution. The starting partition function still takes the form

$$Z = \int \mathcal{D}h \sum_{\{\tau=0,1\}} \exp\left\{-\frac{\kappa}{2}\int_0^L \mathrm{d}x \left(\frac{\partial h}{\partial x}\right)^2 + \mu\int_0^L \mathrm{d}x\, h - \frac{\beta k}{2}\sum_i^N \tau_i h^2(x_i) - \beta\epsilon\sum_i \tau_i\right\}. \quad (4.1.1)$$

In such a model scenario an account for the de/attachment permutations, expressed by the τ_i parameter, is needed as well as the constraint of frozen distribution of tether positions. That is, we shall be evaluating a free energy that accounts for the quenched disorder. Mathematically we need to determine

$$-\beta\langle F\rangle_{\text{disorder}} = \langle \ln Z\rangle_{\text{disorder}} \quad (4.1.2)$$

where the average is over the disorder distribution. The evaluation of average of a Log function is mathematically difficult. It is at this point that we turn

to the called Replica Method introduced in section 1.7 which is based on the identity

$$\ln Z = \lim_{n\to 0} \frac{Z^n - 1}{n}. \tag{4.1.3}$$

Our problem now is to evaluate $\langle Z^n \rangle$ over the spatial disorder. Expressing the density of tethers using the delta function as

$$\rho(x) = \sum_i^N \delta(x - x_i), \tag{4.1.4}$$

the partition function (4.1) then becomes

$$\begin{aligned} Z &= \int \mathcal{D}h \exp\left\{ -\frac{\kappa}{2}\int_0^L \mathrm{d}x \left(\frac{\partial h}{\partial x}\right)^2 + \mu \int_0^L \mathrm{d}x\ h(x) - \frac{\beta k}{2}\int \mathrm{d}x \rho(x) h^2(x) \right. \\ &\qquad \left. -\beta\epsilon \int \mathrm{d}x \rho(x) \right\} \end{aligned} \tag{4.1.5}$$

where we have ignored the de/attachment degree of freedom for the tethers. If we express the spatial distribution of the tethers to be a Gaussian

$$P[\rho(x)] \sim \exp\left(-\frac{R}{2} \int \mathrm{d}x \left(\rho(x) - \rho_0\right)^2 \right), \tag{4.1.6}$$

we are then able to determine $\langle Z^n \rangle$ over this distribution where the replicated partition function is

$$\begin{aligned} Z^n &= \int \prod_\alpha^n \mathcal{D}h_\alpha \exp\left\{ -\frac{\kappa}{2}\sum_{\alpha=1}^n \int_0^L \mathrm{d}x \left(\frac{\partial h_\alpha}{\partial x}\right)^2 + \mu \sum_{\alpha=1}^n \int_0^L \mathrm{d}x\ h_\alpha \right. \\ &\qquad \left. -\beta \sum_{\alpha=1}^n \int \mathrm{d}x \left(\frac{k}{2} h_\alpha^2(x) + \epsilon\right) \rho(x) \right\} \end{aligned} \tag{4.1.7}$$

The disorder averaged replicated partition function according to equation (4.1.6) is then

$$\begin{aligned} \langle Z^n \rangle &= \mathcal{N} \int \mathcal{D}\rho\ Z^n \exp\left(-\frac{R}{2} \int \mathrm{d}x \left(\rho(x) - \rho_0\right)^2 \right) \\ &= \mathcal{N} \int \prod_\alpha^n \mathcal{D}h_\alpha \exp\left\{ -\frac{1}{2}\sum_{\alpha=1}^n \int_0^1 \mathrm{d}x \left(\frac{\partial h_\alpha}{\partial x}\right)^2 + \mu L \sqrt{\frac{L}{\kappa}} \sum_{\alpha=1}^n \int_0^1 \mathrm{d}x\ h_\alpha(x) \right\} \\ &\quad \times \int \mathcal{D}\rho \exp\left\{ -\beta \sum_{\alpha=1}^n \int_0^1 \mathrm{d}x \left(\frac{kL^2}{2\sqrt{RL}\kappa} h_\alpha^2(x) + \frac{\epsilon L}{\sqrt{RL}} \right) \rho(x) \right. \\ &\qquad \left. -\frac{1}{2}\int_0^1 \mathrm{d}x \left(\rho(x) - \sqrt{RL}\rho_0\right)^2 \right\}. \end{aligned} \tag{4.1.8}$$

where we have performed rescaling $h \to \frac{h}{\sqrt{\frac{L}{\kappa}}}$ and $x \to \frac{x}{L}$.

We define the functional integral $\int \mathcal{D}\rho \ldots$ over the disorder distribution as I, where $\mathcal{N}$ is normalization constant. An emphasis is required upon the choice of the distribution as discussed in the text below equation (3.1.3). The evaluation of this expression is shown in Appendix B with the result (B.0.2)

$$\begin{aligned} I &= \mathcal{N}\int \mathcal{D}\rho \exp\left\{-\sum_{\alpha=1}^{n}\int_0^1 \mathrm{d}x \left(\frac{\beta k L^2}{2\sqrt{RL}\kappa}h_\alpha^2(x) + \frac{\beta\epsilon L}{\sqrt{RL}}\right)\rho(x) \right. \\ &\qquad \left. -\frac{1}{2}\int_0^1 \mathrm{d}x \left(\rho(x) - \sqrt{RL}\rho_0\right)^2\right\} \\ &= \exp\left(\frac{1}{2}\int \mathrm{d}x \left[\sum_{\alpha,\lambda}^{n}\frac{\beta^2k^2L^4}{4RL}h_\alpha^2(x)h_\lambda^2(x) \right.\right. \\ &\qquad \left.\left. + \frac{\rho_0\beta k L^2}{\kappa}\left(\frac{n\beta\epsilon}{\rho_0 R} - 1\right)\sum_{\alpha=1}^{n}h_\alpha^2(x) + n\beta\epsilon L\left(\frac{n\beta\epsilon}{R} - 2\rho_0\right)\right]\right). \quad (4.1.9) \end{aligned}$$

Inserting this result (4.1.9) into (4.1.8) we obtain for the averaged replicated partition functional

$$\begin{aligned} \langle Z^n\rangle &= \int \prod_{\alpha}^{n}\mathcal{D}h_\alpha \exp\left\{-\frac{1}{2}\sum_{\alpha=1}^{n}\int_0^1 \mathrm{d}x \left(\frac{\partial h_\alpha}{\partial x}\right)^2 + \mu\sum_{\alpha=1}^{n}\int_0^1 \mathrm{d}x\, h_\alpha\right\} \\ &= \times \exp\left(\frac{1}{2}\int_0^1 \mathrm{d}x \left[\sum_{\alpha,\lambda}^{n}\frac{\beta^2k^2L^4}{4RL}h_\alpha^2(x)h_\lambda^2(x) \right.\right. \\ &\qquad \left.\left. + \frac{\rho_0\beta k L^2}{\kappa}\left(\frac{n\beta\epsilon}{\rho_0 R} - 1\right)\sum_{\alpha=1}^{n}h_\alpha^2(x) + n\beta\epsilon L\left(\frac{n\beta\epsilon}{R} - 2\rho_0\right)\right]\right). \\ &\qquad (4.1.10) \end{aligned}$$

The effective replica Hamiltonian from this expression is thus

$$\begin{aligned} H_n = &-\frac{1}{2}\int \mathrm{d}x\, n\beta\epsilon L\left(\frac{n\beta\epsilon}{R} - 2\rho_0\right) + \frac{1}{2}\sum_{\alpha=1}^{n}\int \mathrm{d}x \left(\frac{\partial h_\alpha}{\partial x}\right)^2 - \mu\sum_{\alpha=1}^{n}\int \mathrm{d}x\, h_\alpha \\ &-\frac{1}{2}\frac{\rho_0\beta k L^2}{\kappa}\left(1 - \frac{n\beta\epsilon}{\rho_0 R}\right)\int \mathrm{d}x\sum_{\alpha=1}^{n}h_\alpha^2(x) - \frac{\beta^2k^2L^4}{8RL}\int \mathrm{d}x\sum_{\alpha,\lambda}^{n}h_\alpha^2(x)h_\lambda^2(x). \\ &\qquad (4.1.11) \end{aligned}$$

Now, the averaged replicated functional (4.1.10) cannot be evaluated exactly because of its non-Gaussian nature. Therefore, an appropriate approximation strategy needs to be determined. Before we pursue such we define the quantities shown below (4.1.12) for shorthand and neater expressions. These

are

$$\begin{aligned} \mathrm{C} &= \exp\left[\frac{1}{2}\int \mathrm{d}x\; n\beta\epsilon L\left(\frac{n\beta\epsilon}{R}-2\rho_0\right)\right] \\ \gamma &= \frac{\rho_0\beta k L^2}{\kappa}\left(1-\frac{n\beta\epsilon}{\rho_0 R}\right) \quad ; \quad \Delta=\frac{\beta^2k^2L^4}{4RL} \quad ; \quad \mu=-2\mu. \end{aligned} \tag{4.1.12}$$

Subsequently, the averaged replicated partition functional (4.1.10) becomes

$$\langle Z^n\rangle \propto \int\prod_\alpha^n \mathcal{D}h_\alpha \exp\left\{-\frac{1}{2}\int \mathrm{d}x\left[\sum_{\alpha=1}^n\left(\left(\frac{\partial h_\alpha}{\partial x}\right)^2+\mu\, h_\alpha(x)+\gamma h_\alpha^2(x)\right)-\Delta\left(\sum_{\alpha=1}^n h_\alpha^2(x)\right)^2\right]\right\}. \tag{4.1.13}$$

We shall pursue two approximations in evaluating this functional. The first shall be the Replica Symmetry (RS) approximation which we do in the next section 4.2. Thereafter, section 4.3, we shall follow with the weak Replica Symmetry Breaking (RSB) approximation.

4.2 Replica Symmetric Solution

In this section we shall explore the role of the quenched random disorder in the Replica Symmetry Approximation. The meaning of such an approximation for repiclas was introduced in section 1.7. In brief, the approximation refers to the symmetric parametrization of the replica matrix $\mathbb{Q}$ we shall introduce next, equation 4.2.2, in linearizing the quartic interaction term in the partition functional (4.1.13).

This replicated partition functional (4.1.13) is the object that we need to evaluate. It is now standard that our first goal in evaluating such objects is to turn them into Gaussian form. In order to fulfill this, in this context, an integration by part is applied to the integral containing $\left(\frac{\partial h_\alpha}{\partial x}\right)^2$ to yield a form $h_\alpha\frac{\partial^2 h_\alpha}{\partial x^2}$ due to the simplifying assumption, $h_\alpha(x)=0$ at the boundary, that we make. Therefore upon exercising this transformation (4.1.13) becomes

$$\langle Z^n\rangle = \mathrm{C}\int\prod_\alpha^n \mathcal{D}h_\alpha \exp\left\{-\frac{1}{2}\int \mathrm{d}x\left[\sum_{\alpha=1}^n\left(\gamma h_\alpha^2(x)-h_\alpha(x)\partial_{xx}h_\alpha(x)+\mu h_\alpha(x)\right)-\Delta\left(\sum_{\alpha=1}^n h_\alpha^2(x)\right)^2\right]\right\}. \tag{4.2.1}$$

The next step towards the quadratic form is the reduction of the quartic term $-\Delta\left(\sum_{\alpha=1}^{n} h_\alpha^2(x)\right)^2$ into a quadratic form at the expense of introducing an auxiliary matrix $\mathbb{Q}$ also known as the replica or overlap matrix, see section 1.7.1, by performing the transformation

$$\exp\left\{\frac{\Delta}{2}\int \mathrm{d}x \sum_{\alpha\beta} h_\alpha^2(x) h_\beta^2(x)\right\} = \int \prod_{\alpha}^{n}\prod_{\beta}^{n} \mathcal{D}Q_{\alpha\beta}(x) \times \exp\left\{-\frac{1}{2\Delta}\int \mathrm{d}x \sum_{\alpha\beta} Q_{\alpha\beta}^2(x) - \int \mathrm{d}x \sum_{\alpha\beta} Q_{\alpha\beta}(x) h_\alpha(x) h_\beta(x)\right\}. \quad (4.2.2)$$

A substitution of this result (4.2.2) upon (4.2.1) yields

$$\begin{aligned}\langle Z^n\rangle &= \mathrm{C}\int \prod_{\alpha}^{n}\prod_{\beta}^{n} \mathcal{D}Q_{\alpha\beta}(x) \exp\left\{-\frac{1}{2\Delta}\int \mathrm{d}x \sum_{\alpha\beta} Q_{\alpha\beta}^2(x)\right\} \int \prod_{\alpha}^{n} \mathcal{D}h_\alpha \\ &\quad \times \exp\left\{-\frac{1}{2}\int \mathrm{d}x \left[\sum_{\alpha=1}^{n}\left(\gamma h_\alpha^2(x) - h_\alpha(x)\partial_{xx} h_\alpha(x) + \mu\, h_\alpha(x)\right)\right.\right. \\ &\quad \left.\left. + 2\sum_{\alpha\beta} Q_{\alpha\beta}(x) h_\alpha(x) h_\beta(x)\right]\right\}. \quad (4.2.3)\end{aligned}$$

This is now the object that we need to evaluate. Fortunately, the $h_\alpha(x)$ functional has the form that we have encountered already but with a slight variation. We shall, therefore, first focus on the evaluation of the $h_\alpha(x)$ path integral we call H. That is,

$$\begin{aligned}H &= \int \prod_{i}^{n} \mathcal{D}h_i \exp\left\{-\frac{1}{2}\int \mathrm{d}x \left[\sum_{i}^{n}\left(\gamma h_i^2(x) - h_i(x)\partial_{xx} h_i(x) + \mu\, h_i(x)\right)\right.\right. \\ &\quad \left.\left. + 2\sum_{ij} Q_{ij}(x) h_i(x) h_j(x)\right]\right\} \quad (4.2.4)\end{aligned}$$

In order to attain a quadratic form of the exponential term we introduce the continuous and discrete identity matrices expressed as $\delta(x-x')$ and δ_{ij} such that

$$\begin{aligned}H &= \int \prod_{i}^{n} \mathcal{D}h_i \exp\left\{-\frac{1}{2}\int_{xx'} \sum_{ij} h_i(x')\left[\delta^{xx'}\left(\left(\gamma - \partial_{xx}\right)\delta_{ij}\right.\right.\right. \\ &\quad \left.\left.\left. + 2Q_{ij}(x)\right)\right] h_j(x) - \frac{1}{2}\int \mathrm{d}x \sum_{i} \mu h_i(x)\right\} \\ H &= \int \prod_{i}^{n} \mathcal{D}h_i \exp\left\{-\frac{1}{2}\int_{xx'} \sum_{ij} h_i(x') M_{ij}(x,x') h_j(x)\right. \\ &\quad \left. - \frac{1}{2}\int \mathrm{d}x \sum_{i} \mu h_i(x)\right\}, \quad (4.2.5)\end{aligned}$$

where $M_{ij}(x,x') = \delta^{xx'}\left((\gamma - \partial_{xx})\,\delta_{ij} + 2Q_{ij}(x)\right)$. This equation (4.2.5) can be expressed in matrix form such that we have

$$H = \int \mathcal{D}\mathbf{h}(x) \exp\left\{-\frac{1}{2}\int_{xx'} \mathbf{h}^{\mathsf{T}}(x')\mathbb{M}(x',x)\mathbf{h}(x) - \frac{1}{2}\int \mathrm{d}x\; \boldsymbol{\mu}^{\mathsf{T}}\,\mathbf{h}(x)\right\}. \tag{4.2.6}$$

The column and row vector will be distinguishable on the contexts that they are used. The exponential term now has the standard structure for which we need to complete the square so that we can evaluate this functional integral H. After making use of the identity $\int \mathrm{d}x\; \mathbb{M}^{-1}(x'',x)\mathbb{M}(x,x') = \delta(x''-x')$ we can express the exponential term (4.2.6) in the desired form

$$\begin{aligned} -\frac{1}{2}\int_{xx'} \mathbf{h}^{\mathsf{T}}(x')\mathbb{M}(x',x)\mathbf{h}(x) - \frac{1}{2}\int \mathrm{d}x\; \boldsymbol{\mu}^{\mathsf{T}}\,\mathbf{h}(x) = \\ -\frac{1}{2}\int \mathrm{d}x\mathrm{d}x'\; \tilde{\boldsymbol{h}}^{\mathsf{T}}(x')\mathbb{M}(x',x)\tilde{\boldsymbol{h}}(x) + \frac{1}{8}\int \mathrm{d}x\mathrm{d}x'\; \boldsymbol{\mu}^{\mathsf{T}}\mathbb{M}^{-1}(x,x')\boldsymbol{\mu}. \end{aligned} \tag{4.2.7}$$

Therefore,

$$H = C_\infty \exp\left(\frac{1}{8}\int \mathrm{d}x\mathrm{d}x'\; \boldsymbol{\mu}^{\mathsf{T}}\mathbb{M}^{-1}(x,x')\boldsymbol{\mu} - \frac{1}{2}\mathrm{tr}\ln\mathbb{M}(x,x')\right). \tag{4.2.8}$$

We here remind ourselves that the matrix $\mathbb{M}$ is a function of Q_{ij}. Therefore, we need to take this into account as we now evaluate the Q_{ij} functional (4.2.3) with this H result (4.2.8). The tr represents both the continuous and discrete tracing. After substituting this result (4.2.8) onto the expression (4.2.3) of the Q_{ij} functional we obtain

$$\begin{aligned} \langle Z^n\rangle = \mathrm{C}' \int \prod_{ij} \mathcal{D}Q_{ij}(x) \exp\left\{-\frac{1}{2\Delta}\int \mathrm{d}x \sum_{ij} Q_{ij}^2(x) - \frac{1}{2}\mathrm{tr}\ln\mathbb{M}(x',x)\right. \\ \left. +\frac{1}{8}\int \mathrm{d}x\mathrm{d}x'\; \boldsymbol{\mu}^{\mathsf{T}}\mathbb{M}^{-1}(x,x')\boldsymbol{\mu}\right\}. \end{aligned} \tag{4.2.9}$$

How do we evaluate such an object? The evaluation depends on the parametrization of the replica matrix $\mathbb{Q}(x)$ as we have seen in section 1.7. It is this parametrization that defines the Replica Symmetry solution. As we have encountered, the replica symmetry solution has the form shown in the composite matrix $\mathbb{M}(x,x')$

$$\mathbb{M}(x,x') = \begin{pmatrix} \delta_{ij}\delta^{xx'}\left(\gamma - \partial_{xx}\right) + 2\delta_{ij}Q_{ii}(x)\delta^{xx'} & 2Q_{ij}(x)\delta^{xx'} \\ 2Q_{ij}(x)\delta^{xx'} & \delta_{ij}\delta^{xx'}\left(\gamma - \partial_{xx}\right) + 2\delta_{ij}Q_{ii}(x)\delta^{xx'} \end{pmatrix} \tag{4.2.10}$$

where $Q_{ii}(x)$ are the diagonal elements and $Q_{ij}(x)$ are the off diagonal elements. Subsequently, we have

$$\begin{aligned}\langle Z^n\rangle &= \mathrm{C}'\int\prod_i \mathcal{D}Q_{ii}(x)\int\prod_{ij}\mathcal{D}Q_{ij}(x)\exp\left\{-\frac{1}{2\Delta}\int \mathrm{d}x\sum_i Q_{ii}^2(x)\right.\\ &\quad -\frac{1}{2\Delta}\int \mathrm{d}x\sum_{ij}Q_{ij}^2(x)-\frac{1}{2}\mathrm{tr}\ln\mathbb{M}(x',x)\\ &\quad \left.+\frac{1}{8}\int \mathrm{d}x\mathrm{d}x'\;\boldsymbol{\mu}^{\mathsf{T}}\mathbb{M}^{-1}(x,x')\boldsymbol{\mu}\right\} \qquad (4.2.11)\end{aligned}$$

Progressing in the evaluation of this functional we shall apply the factorization $\mathbb{M}=\mathbb{D}\left[1+\mathbb{D}^{-1}\mathbb{Q}\right]$. That is,

$$\begin{aligned}\mathbb{M}(x,x') &= \begin{pmatrix}\delta_{ij}\delta^{xx'}(\gamma-\partial_{xx}) & 0\\ 0 & \delta_{ij}\delta^{xx'}(\gamma-\partial_{xx})\end{pmatrix}\times\\ &\quad\left[\begin{pmatrix}1&0\\0&1\end{pmatrix}+\begin{pmatrix}\delta_{ij}\delta^{xx'}(\gamma-\partial_{xx}) & 0\\ 0 & \delta_{ij}\delta^{xx'}(\gamma-\partial_{xx})\end{pmatrix}^{-1}\right.\\ &\quad\left.\times\begin{pmatrix}2\delta_{ij}Q_{ii}(x)\delta^{xx'} & 2Q_{ij}(x)\delta^{xx'}\\ 2Q_{ij}(x)\delta^{xx'} & 2\delta_{ij}Q_{ii}(x)\delta^{xx'}\end{pmatrix}\right]. \qquad (4.2.12)\end{aligned}$$

Therefore, the first term $\mathrm{tr}\ln\mathbb{M}(x,x')$ becomes

$$\mathrm{tr}\ln\mathbb{M}(x,x') = \mathrm{tr}\ln\mathbb{D}+\mathrm{tr}\ln\left(1+\mathbb{D}^{-1}\mathbb{Q}\right). \qquad (4.2.13)$$

Upon performing a series expansion on $\ln\left(1+\mathbb{D}^{-1}\mathbb{Q}\right)$, to quadratic order, we obtain

$$\ln\left(1+\mathbb{D}^{-1}\mathbb{Q}\right)=\mathbb{D}^{-1}\mathbb{Q}-\frac{1}{2}\left(\mathbb{D}^{-1}\mathbb{Q}\right)^2+\ldots. \qquad (4.2.14)$$

Subsequently, we have (4.2.13) approximated to quadratic order to become

$$\mathrm{tr}\ln\mathbb{M}(x,x') \approx \mathrm{tr}\ln\mathbb{D}+\mathrm{tr}\left(\mathbb{D}^{-1}\mathbb{Q}\right)-\frac{1}{2}\mathrm{tr}\left(\mathbb{D}^{-1}\mathbb{Q}\right)^2. \qquad (4.2.15)$$

Similarly,

$$\begin{aligned}&\frac{1}{8}\int \mathrm{d}x\mathrm{d}x'\;\boldsymbol{\mu}^{\mathsf{T}}\mathbb{M}^{-1}(x,x')\boldsymbol{\mu}\\ &= \frac{1}{8}\int_{x,x'}\boldsymbol{\mu}^{\mathsf{T}}\left[\mathbb{D}\left(1+\mathbb{D}^{-1}\mathbb{Q}\right)\right]^{-1}\boldsymbol{\mu}\\ &= \frac{1}{8}\int_{xx'}\boldsymbol{\mu}^{\mathsf{T}}\left[\mathbb{D}^{-1}-\mathbb{D}^{-1}\mathbb{Q}\mathbb{D}^{-1}+\frac{1}{2}\left(\mathbb{D}^{-1}\mathbb{Q}\right)^2\mathbb{D}^{-1}\right]\boldsymbol{\mu}. \qquad (4.2.16)\end{aligned}$$

Our partition functional (4.2.11) then becomes

$$\begin{aligned}\langle Z^n\rangle &= \mathrm{C}'\exp\left(-\frac{1}{2}\mathrm{tr}\ln\mathbb{D}+\frac{1}{8}\int_{xx'}\boldsymbol{\mu}^{\mathsf{T}}\mathbb{D}^{-1}\boldsymbol{\mu}\right)\int\prod_i\mathcal{D}Q_{ii}(x)\int\prod_{ij}\mathcal{D}Q_{ij}(x)\\ &\exp\left\{-\frac{1}{2\Delta}\int\mathrm{d}x\sum_i Q_{ii}^2(x)-\frac{1}{2\Delta}\int\mathrm{d}x\sum_{ij}Q_{ij}^2(x)-\frac{1}{2}\mathrm{tr}\left(\mathbb{D}^{-1}\mathbb{Q}\right)\right.\\ &\left.+\frac{1}{4}\mathrm{tr}\left(\mathbb{D}^{-1}\mathbb{Q}\right)^2-\frac{1}{8}\int_{xx'}\boldsymbol{\mu}^{\mathsf{T}}\mathbb{D}^{-1}\mathbb{Q}\mathbb{D}^{-1}\boldsymbol{\mu}+\frac{1}{16}\int_{xx'}\boldsymbol{\mu}^{\mathsf{T}}\left(\mathbb{D}^{-1}\mathbb{Q}\right)^2\mathbb{D}^{-1}\boldsymbol{\mu}\right\}\end{aligned} \tag{4.2.17}$$

The evaluation of the constituents is shown in Appendix C. Substituting the results into the partition function (4.2.17) we obtain

$$\begin{aligned}\langle Z^n\rangle &= \exp\left(-\frac{2n}{2}\mathrm{tr}\ln A(x,x')+\frac{1}{8}\sum_a\int\frac{\mathrm{d}q}{(2\pi)^d}\mu_{1a}\mu_{a1}\frac{\delta(q)\delta(-q)}{q^2+\gamma}\right)\int\prod_i\mathcal{D}\tilde{Q}_{ii}(q)\\ &\prod_{ij}\mathcal{D}\tilde{Q}_{ij}(q)\exp\left[-\frac{1}{2}\int\frac{\mathrm{d}q}{(2\pi)^d}\sum_i\tilde{Q}_{ii}(q)\left(\frac{1}{\Delta}-2\Omega^{-1}(q)-\frac{\mu^2}{\gamma^2(q^2+\gamma)}\right)\tilde{Q}_{ii}(-q)\right.\\ &+\sum_{bf}\int\frac{\mathrm{d}q}{(2\pi)^d}\mu_{1b}\mu_{f1}\frac{\tilde{Q}_{bb}(q)\tilde{Q}_{bf}(-q)}{\gamma^2(q^2+\gamma)}-2\int\sum_m\frac{\mathrm{d}q}{(2\pi)^d}\frac{\tilde{Q}_{mm}(0)}{q^2+\gamma}\\ &\left.-\sum_b\mu_{1b}\mu_{b1}\frac{\tilde{Q}_{bb}(0)}{2\gamma^2}\right]\exp\left[-\frac{1}{2}\int\frac{\mathrm{d}q}{(2\pi)^d}\sum_{ij}\tilde{Q}_{ij}(q)\left(\frac{1}{\Delta}-2\Omega^{-1}(q)\right)\tilde{Q}_{ij}(-q)\right.\\ &\left.+\frac{1}{2}\sum_{bdf}\int\frac{\mathrm{d}q}{(2\pi)^d}\mu_{1b}\mu_{f1}\frac{\tilde{Q}_{bd}(q)\tilde{Q}_{df}(-q)}{\gamma^2(q^2+\gamma)}-\frac{1}{2\gamma^2}\sum_{bd}\mu_{1b}\mu_{d1}\tilde{Q}_{bd}(0)\right].\end{aligned} \tag{4.2.18}$$

where $\Omega^{-1}(q)$ is detailed from equation (4.2.22) and the Appendix C.2. Removing the zero mode, $q=0$, parameters from the yet to evaluate func-

tional (4.2.18) we have

$$\begin{aligned}\langle Z^n\rangle &= \exp\left(-\frac{2n}{2}\mathrm{tr}\ln A(x,x') + \frac{2n}{8}\frac{\mu^2\delta(0)}{\gamma}\right.\\
&\quad -2\int\sum_m \frac{\mathrm{d}q}{(2\pi)^d}\frac{\tilde{Q}_{mm}(0)}{q^2+\gamma} - \frac{1}{2\gamma^2}\sum_b \mu_{1b}\mu_{b1}\tilde{Q}_{bb}(0)\\
&\quad \left.-\frac{1}{2\gamma^2}\sum_{bd}\mu_{1b}\mu_{d1}\tilde{Q}_{bd}(0)\right)\int\prod_i \mathcal{D}\tilde{Q}_{ii}(q)\prod_{ij}\mathcal{D}\tilde{Q}_{ij}(q)\exp\\
&\quad \times\left[-\frac{1}{2}\int\frac{\mathrm{d}q}{(2\pi)^d}\sum_i \tilde{Q}_{ii}(q)\left(\frac{1}{\Delta}-2\Omega^{-1}(q)-\frac{\mu^2}{\gamma^2(q^2+\gamma)}\right)\tilde{Q}_{ii}(-q)\right.\\
&\qquad \left.+\sum_{bf}\int\frac{\mathrm{d}q}{(2\pi)^d}\mu_{1b}\mu_{f1}\frac{\tilde{Q}_{bb}(q)\tilde{Q}_{bf}(-q)}{\gamma^2(q^2+\gamma)}\right]\\
&\quad \times\exp\left[-\frac{1}{2}\int\frac{\mathrm{d}q}{(2\pi)^d}\sum_{ij}\tilde{Q}_{ij}(q)\left(\frac{1}{\Delta}-2\Omega^{-1}(q)\right)\tilde{Q}_{ij}(-q)\right.\\
&\qquad \left.+\frac{1}{2}\sum_{bdf}\int\frac{\mathrm{d}q}{(2\pi)^d}\mu_{1b}\mu_{f1}\frac{\tilde{Q}_{bd}(q)\tilde{Q}_{df}(-q)}{\gamma^2(q^2+\gamma)}\right] \quad (4.2.19)\end{aligned}$$

We shall now separately further simplify and evaluate where applicable the prefactor exponential called S_0, the Q_{ii} and Q_{ij} functionals called S_1 and S_2, respectively.

$$\begin{aligned}S_0 &= \exp\left(-\frac{2n}{2}\mathrm{tr}\ln A(x,x') + \frac{2n}{8}\frac{\mu^2\delta(0)}{\gamma} - 2(2n)\int\frac{\mathrm{d}q}{(2\pi)^d}\frac{\tilde{Q}_{ii}(0)}{q^2+\gamma}-\right.\\
&\qquad \left.\frac{(2n)\mu^2\tilde{Q}_{ii}(0)}{2\gamma^2} - \frac{((2n)^2-(2n))\mu^2}{2\gamma^2}\tilde{Q}_{ij}(0)\right). \quad (4.2.20)\end{aligned}$$

The term S_1 is given by

$$\begin{aligned} S_1 = & \int \prod_i \mathcal{D}\tilde{Q}_{ii}(q) \\ & \times \exp\left[-\frac{1}{2}\int \frac{\mathrm{d}q}{(2\pi)^d}\sum_i \tilde{Q}_{ii}(q)\left(\frac{1}{\Delta} - 2\Omega^{-1}(q) - \frac{\mu^2}{\gamma^2(q^2+\gamma)}\right)\tilde{Q}_{ii}(-q)\right. \\ & \qquad \left. + \sum_i \int \frac{\mathrm{d}q}{(2\pi)^d}\frac{\tilde{Q}_{ii}(q)\mu^2\sum_j \tilde{Q}_{ij}(-q)}{\gamma^2(q^2+\gamma)}\right] \\ = & \exp\left[-\frac{2n}{2}\sum_q \ln\left(\frac{1}{\Delta} - 2\Omega^{-1}(q) - \frac{\mu^2}{\gamma^2(q^2+\gamma)}\right)\right. \\ & \left. + \frac{1}{2}\sum_{ijk}\int \frac{\mathrm{d}q}{(2\pi)^d}\left(\frac{1}{\Delta} - 2\Omega^{-1}(q) - \frac{\mu^2}{\gamma^2(q^2+\gamma)}\right)^{-1}\frac{\tilde{Q}_{ij}(q)\mu^4\tilde{Q}_{jk}(-q)}{\gamma^4(q^2+\gamma)^2}\right]. \end{aligned} \tag{4.2.21}$$

Hence, we take the $\sum_{ijk}\int \frac{\mathrm{d}q}{(2\pi)^d}\left(\frac{1}{\Delta} - 2\Omega^{-1}(q) - \frac{\mu^2}{\gamma^2(q^2+\gamma)}\right)^{-1}\frac{\tilde{Q}_{ij}(q)\mu^4\tilde{Q}_{jk}(-q)}{\gamma^4(q^2+\gamma)^2}$ term into the evaluation of (4.2.29) below. Subsequently, what remains of S_1 to evaluate is $-\frac{2n}{2}\sum_q \ln\left(\frac{1}{\Delta} - 2\Omega^{-1}(q) - \frac{\mu^2}{\gamma^2(q^2+\gamma)}\right)$. In order to perform this sum we first simplify $\Omega^{-1}(q)$. This quantity is introduced in Appendix C equation (C.1.5). It is defined as

$$\Omega^{-1}(q) = \int \frac{\mathrm{d}^d p}{(2\pi)^d}\frac{1}{(p^2+\gamma)((q-p)^2+\gamma)} \tag{4.2.22}$$

The details of this are furnished in Appendix C.2. The result as derived in equation (C.2.12) is

$$\frac{1}{\Omega(q)} = \Gamma(2)\frac{\pi^{d/2}}{(2\pi)^d}\left[\frac{2}{\alpha} + \psi(1) - \ln(\gamma) + 2 - \sqrt{1+\frac{4\gamma}{q^2}}\ln\frac{\sqrt{1+\frac{4\gamma}{q^2}}+1}{\sqrt{1+\frac{4\gamma}{q^2}}-1}\right]. \tag{4.2.23}$$

$\Gamma(\mathrm{arg})$ is the Gamma function. $\alpha = 4-d$ and $\psi(1)$ is the Euler-Mascheroni constant equivalent to 0.5772. Applying this result (4.2.23) equation (4.2.21)

for S_1 becomes

$$\begin{aligned}
&-\frac{2n}{2}\sum_q \ln\left(\frac{1}{\Delta}-2\Omega^{-1}(q)-\frac{\mu^2}{\gamma^2(q^2+\gamma)}\right)\\
&= -\frac{2n}{2}\sum_q \ln\left(\frac{1}{\Delta}-2\left[\Gamma(2)\frac{\pi^{d/2}}{(2\pi)^d}\left[\frac{2}{\alpha}+\psi(1)-\ln(\gamma)+2\right.\right.\right.\\
&\qquad\left.\left.\left.-\sqrt{1+\frac{4\gamma}{q^2}}\ln\frac{\sqrt{1+\frac{4\gamma}{q^2}}+1}{\sqrt{1+\frac{4\gamma}{q^2}}-1}\right]\right]-\frac{\mu^2}{\gamma^2(q^2+\gamma)}\right)\\
&= -\frac{2n}{2}\frac{1}{(2\pi)^{d/2}\Gamma(d/2)}\int_q q^{d-1}\ln\left[\frac{1}{\Delta}-2\Gamma(2)\frac{\pi^{d/2}}{(2\pi)^d}\left[\frac{2}{\alpha}+\psi(1)-\ln(\gamma)\right.\right.\\
&\qquad\left.\left.+2-\sqrt{1+\frac{4\gamma}{q^2}}\ln\frac{\sqrt{1+\frac{4\gamma}{q^2}}+1}{\sqrt{1+\frac{4\gamma}{q^2}}-1}\right]-\frac{\mu^2}{\gamma^2(q^2+\gamma)}\right]. \qquad (4.2.24)
\end{aligned}$$

Performing a scale separation by the limits $\frac{1}{\sqrt{1/4\gamma^2\,q^2}} \gg 1$ or $\frac{4\gamma}{q^2} \gg 1$, thereby leading to, $\sqrt{1+\frac{4\gamma}{q^2}} \approx \sqrt{\frac{4\gamma}{q^2}}$ and $\frac{\mu^2}{\gamma^2(\gamma+q^2)} \approx \frac{\mu^2}{\gamma^3}-\frac{\mu^2 q^2}{\gamma^4}$ in this extreme. In the other extreme we have, $\frac{1}{\sqrt{1/4\gamma^2\,q^2}} \ll 1$ or $\frac{4\gamma}{q^2} \ll 1$, thereby leading to, $\sqrt{1+\frac{4\gamma}{q^2}} \approx 1+\frac{1}{2}\cdot\frac{4}{q^2}$ and $\frac{\mu^2}{\gamma^2(\gamma+q^2)} \approx \frac{\mu^2}{\gamma^2 q^2}$. Consequently the integral (4.2.24) can be expressed as two integrals as

$$\begin{aligned}
S_1 \approx\ & -\frac{2n}{2(2\pi)^{d/2}\Gamma(d/2)}\left\{\int_0^{\frac{1}{\sqrt{1/4\gamma}}} \mathrm{d}q\; q^{d-1}\ln\left[\frac{1}{\Delta}-\frac{\mu^2}{\gamma^3}+\frac{\mu^2 q^2}{\gamma^4}\right.\right.\\
&\left.\left.-\frac{(4\pi)^{\alpha/2}}{8\pi^2}\left\{\frac{2}{\alpha}+\psi(1)-\ln(\gamma)+2-\sqrt{\frac{4\gamma}{q^2}}\ln\frac{\sqrt{\frac{4\gamma}{q^2}}+1}{\sqrt{\frac{4\gamma}{q^2}}-1}\right\}\right]\right.\\
&\left.+\int_{\frac{1}{\sqrt{1/4\gamma}}}^{\Lambda} \mathrm{d}q\; q^{d-1}\ln\left[\frac{1}{\Delta}-\frac{\mu^2}{\gamma^2 q^2}-\frac{(4\pi)^{\alpha/2}}{8\pi^2}\right.\right.\\
&\left.\left.\times\left\{\frac{2}{\alpha}+\psi(1)-\ln(\gamma)+2-\left(1+\frac{1}{2}\frac{4}{q^2}\right)\ln\frac{\left(1+\frac{1}{2}\frac{4}{q^2}\right)+1}{\left(1+\frac{1}{2}\frac{4}{q^2}\right)-1}\right\}\right]\right\}. \qquad (4.2.25)
\end{aligned}$$

After algebraic re-arrangements equation (4.2.25) becomes

$$S_1 \approx -\frac{2n}{2(2\pi)^{d/2}\Gamma(d/2)}\left\{\int_0^{\frac{1}{\sqrt{1/4\gamma}}} \mathrm{d}q\, q^{d-1} \ln\left[\frac{1}{\Delta} - \frac{\mu^2}{\gamma^3} + \frac{\mu^2 q^2}{\gamma^4} - \frac{(4\pi)^{\alpha/2}}{8\pi^2} \times \left\{\frac{2}{\alpha} + \psi(1) - \ln(\gamma) + 2 - \frac{1}{q}\sqrt{4\gamma}\ln\frac{1+q/\sqrt{4\gamma}}{1-q/\sqrt{4\gamma}}\right\}\right] + \int_{\frac{1}{\sqrt{1/4\gamma}}}^{\Lambda} \mathrm{d}q\, q^{d-1}\ln\left[\frac{1}{\Delta} - \frac{\mu^2}{\gamma^2 q^2} - \frac{(4\pi)^{\alpha/2}}{8\pi^2}\times \left\{\frac{2}{\alpha} + \psi(1) - \ln(\gamma) + 2 - \left(1 + \frac{1}{2}\frac{4}{q^2}\right)\ln\left(1+\frac{q^2}{\gamma}\right)\right\}\right]\right\}. \quad (4.2.26)$$

Taking into account the scale separation arguments onto these integrals, that is, $\frac{4}{q^2} \gg 1$ in the first integral and its opposite on the second integral we can then further simplify these integrals. Applying the identity [80]

$$\ln\frac{1+q/\sqrt{4\gamma}}{1-q/\sqrt{4\gamma}} = 2\sum_{k=1}^{\infty}\frac{1}{2k-1}\left(q/\sqrt{4\gamma}\right)^{2k-1},$$

to quadratic order of q, equation (4.2.26) becomes

$$S_1 \approx -\frac{2n}{2(2\pi)^{d/2}\Gamma(d/2)}\left\{\int_0^{\frac{1}{\sqrt{1/4\gamma}}} \mathrm{d}q\, q^{d-1} \ln\left[\frac{1}{\Delta} - \frac{\mu^2}{\gamma^3} + \frac{\mu^2 q^2}{\gamma^4} - \frac{(4\pi)^{\alpha/2}}{8\pi^2}\left\{\frac{2}{\alpha} + \psi(1) - \ln(\gamma) + 2 - \left(2 + \frac{q^2}{6\gamma}\right)\right\}\right] + \int_{\frac{1}{\sqrt{1/4\gamma}}}^{\Lambda} \mathrm{d}q\, q^{d-1}\ln\left[\frac{1}{\Delta} - \frac{\mu^2}{\gamma^2 q^2} - \frac{(4\pi)^{\alpha/2}}{8\pi^2} \times \left\{\frac{2}{\alpha} + \psi(1) - \ln(\gamma) + 2 - \left(1 + \frac{1}{2}\frac{4}{q^2}\right)\ln\left(1+\frac{q^2}{2\gamma}\right)\right\}\right]\right\}. \quad (4.2.27)$$

After some algebraic recombinations we obtain

$$S_1 \approx -\frac{2n}{2(2\pi)^{d/2}\Gamma(d/2)}\left\{\int_0^{\frac{1}{\sqrt{1/4\gamma}}} \mathrm{d}q\, q^{d-1} \ln\left[\frac{1}{\Delta} - \frac{\mu^2}{\gamma^3} + \left(\frac{\mu^2}{\gamma^4} + \frac{(4\pi)^{\alpha/2}}{48\pi^2\gamma}\right)q^2 - \frac{(4\pi)^{\alpha/2}}{8\pi^2}\left\{\frac{2}{\alpha} + \psi(1) - \ln(\gamma)\right\}\right] + \int_{\frac{1}{\sqrt{1/4\gamma}}}^{\Lambda} \mathrm{d}q\, q^{d-1}\ln\left[\frac{1}{\Delta} - \frac{\mu^2}{\gamma^2 q^2} - \frac{(4\pi)^{\alpha/2}}{8\pi^2} \times \left\{\frac{2}{\alpha} + \psi(1) - \ln(\gamma) + 2 - \left(1 + \frac{1}{2}\frac{4}{q^2}\right)\ln\left(1+\frac{q^2}{2\gamma}\right)\right\}\right]\right\}. \quad (4.2.28)$$

Further evaluation of this integral in one dimension $S_1[d=1]$ is done in Appendix C.3.

We shall now evaluate S_2 from the expression (4.2.19) and the component of S_1 in equation (4.2.21). That is

$$\begin{aligned} S_2 = \int \prod_{ij} \mathcal{D}\tilde{Q}_{ij}(q) \exp\left\{ -\frac{1}{2}\int \frac{\mathrm{d}q}{(2\pi)^d} \sum_{ij} \tilde{Q}_{ij}(q)\left(\frac{1}{\Delta} - 2\Omega^{-1}(q)\right)\tilde{Q}_{ij}(-q) \right. \\ + \frac{1}{2}\sum_{ijk}\int \frac{\mathrm{d}q}{(2\pi)^d}\left[\left(\frac{1}{\Delta} - 2\Omega^{-1}(q) - \frac{\mu^2}{\gamma^2(q^2+\gamma)}\right)^{-1}\frac{\mu^4}{\gamma^4(q^2+\gamma)^2}\right. \\ \left.\left. + \frac{\mu^2}{\gamma^2(q^2+\gamma)}\right]\tilde{Q}_{ij}(q)\tilde{Q}_{jk}(-q) \right. \\ S_2 = \int \mathcal{D}\tilde{\boldsymbol{Q}}(q) \exp\left\{ -\frac{1}{2}\int \frac{\mathrm{d}q}{(2\pi)^d} \tilde{\boldsymbol{Q}}^{\mathsf{T}}(q)\mathbb{T}\left(X,Z\right)\tilde{\boldsymbol{Q}}(-q)\right\} \end{aligned} \tag{4.2.29}$$

$\tilde{\boldsymbol{Q}}^{\mathsf{T}}$ represents a vector $[Q_{12}\ \ Q_{13}\cdots\ \ Q_{1n}\ \ Q_{23}\ \ Q_{24}\cdots Q_{2n}\cdots\ \ Q_{n-1n}]$ whilst

$$\mathbb{T} = \begin{pmatrix} X+Z & Z & Z & & & & \\ Z & X+Z & Z & & Z & & \cdots \\ Z & Z & X+Z & & & & \\ & & & X+Z & Z & Z & \\ & Z & & Z & X+Z & Z & \\ & & & Z & Z & X+Z & \\ & \vdots & & & & & \ddots \end{pmatrix}. \tag{4.2.30}$$

The constituents Z and X of this matrix $\mathbb{T}$ are given by

$$\begin{aligned} Z &= -\left(\frac{1}{\Delta} - 2\Omega^{-1}(q) - \frac{\mu^2}{\gamma^2(q^2+\gamma)}\right)^{-1}\frac{\mu^4}{\gamma^4(q^2+\gamma)^2} - \frac{\mu^2}{\gamma^2(q^2+\gamma)} \\ X &= \left(\frac{1}{\Delta} - 2\Omega^{-1}(q)\right). \end{aligned} \tag{4.2.31}$$

The determinant of this matrix $\mathbb{T}$ of dimension $\frac{(2n)^2-(2n)}{2}$ is given by adding all the columns to the first column and subtracting the first row from the other rows such that

$$\begin{aligned} \det\mathbb{T} &= \left((X+Z) + \left(\frac{(2n)^2-(2n)}{2} - 1\right)Z\right)\left((X+Z)-Z\right)^{\frac{(2n)^2-(2n)}{2}-1} \\ \det\mathbb{T} &= \left(X + \left(\frac{(2n)^2-(2n)}{2}\right)Z\right)X^{\frac{(2n)^2-(2n)}{2}-1}. \end{aligned} \tag{4.2.32}$$

Subsequently, S_2 equation (4.2.29) becomes

$$S_2 = \exp\left(-\frac{1}{2}\sum_q \ln\left(X + \left(\frac{(2n)^2-(2n)}{2}\right)Z\right) - \frac{1}{2}\sum_q \ln X^{\frac{(2n)^2-(2n)}{2}-1}\right). \tag{4.2.33}$$

Upon expanding this expression (4.2.33) with respect to n up to linear order we obtain

$$S_2 = \exp\left(\frac{2n}{4}\sum_q \ln\left(\frac{1}{\Delta} - 2\Omega^{-1}(q)\right) - \frac{2n}{4}\sum_q \left\{\frac{1}{\frac{1}{\Delta} - 2\Omega^{-1}(q)} \left[\left(\frac{1}{\Delta} - 2\Omega^{-1}(q) - \frac{\mu^2}{\gamma^2(q^2+\gamma)}\right)^{-1} \frac{\mu^4}{\gamma^4(q^2+\gamma)^2} + \frac{\mu^2}{\gamma^2(q^2+\gamma)}\right]\right\}. \quad (4.2.34)$$

The first term $\frac{2n}{4}\sum_q \ln\left(\frac{1}{\Delta} - 2\Omega^{-1}(q)\right)$ is given by

$$\begin{aligned}\frac{2n}{4}\sum_q \ln\left(\frac{1}{\Delta} - 2\Omega^{-1}(q)\right) \approx{}& \frac{2n}{4(2\pi)^{d/2}\Gamma(d/2)} \\ &\left\{\int_0^{\frac{1}{\sqrt{1/4\gamma}}} \mathrm{d}q\, q^{d-1} \ln\left[\frac{1}{\Delta} + \frac{(4\pi)^{\alpha/2}q^2}{48\pi^2\gamma} - \frac{(4\pi)^{\alpha/2}}{8\pi^2}\left\{\frac{2}{\alpha} + \psi(1) - \ln(\gamma)\right\}\right]\right. \\ &+ \int_{\frac{1}{\sqrt{1/4\gamma}}}^{\Lambda} \mathrm{d}q\, q^{d-1} \ln\left[\frac{1}{\Delta} - \frac{(4\pi)^{\alpha/2}}{8\pi^2}\right. \\ &\left.\left.\times\left\{\frac{2}{\alpha} + \psi(1) - \ln(\gamma) + 2 - \left(1 + \frac{1}{2}\frac{4}{q^2}\right)\ln\left(1 + \frac{q^2}{2\gamma}\right)\right\}\right]\right\}. \quad (4.2.35)\end{aligned}$$

The further evaluation of this term in one dimension is furnished in Appendix C.4.

Finally, we now evaluate the second term of S_2 from equation (4.2.34). That is

$$-\frac{2n}{4}\sum_q \frac{\left(\frac{1}{\Delta} - 2\Omega^{-1}(q) - \frac{\mu^2}{\gamma^2(q^2+\gamma)}\right)^{-1}\frac{\mu^4}{\gamma^4(q^2+\gamma)^2} + \frac{\mu^2}{\gamma^2(q^2+\gamma)}}{\frac{1}{\Delta} - 2\Omega^{-1}(q)}. \quad (4.2.36)$$

As we have seen in the evaluation of S_1 from the step (4.2.24), this second term from (4.2.36), with the help of (4.2.27), becomes

$$\begin{aligned}&-\frac{2n}{4}\sum_q \frac{\left(\frac{1}{\Delta} - 2\Omega^{-1}(q) - \frac{\mu^2}{\gamma^2(q^2+\gamma)}\right)^{-1}\frac{\mu^4}{\gamma^4(q^2+\gamma)^2} + \frac{\mu^2}{\gamma^2(q^2+\gamma)}}{\frac{1}{\Delta} - 2\Omega^{-1}(q)} = \\ &\quad -\frac{2n}{4}\frac{1}{(2\pi)^{d/2}\Gamma(d/2)}\left\{\int_0^{\frac{1}{\sqrt{1/4\gamma}}} \mathrm{d}q\, q^{d-1}\right. \\ &\qquad \left.\frac{\left(\frac{\mu^4}{\gamma^6} - \frac{2\mu^4 q^2}{\gamma^7}\right)}{\left[\frac{1}{\Delta} - \frac{\mu^2}{\gamma^3} + \frac{\mu^2 q^2}{\gamma^4} - \frac{(4\pi)^{\alpha/2}}{8\pi^2}\left\{\frac{2}{\alpha} + \psi(1) - \ln(\gamma) + 2 - \left(2 + \frac{q^2}{6\gamma}\right)\right\}\right]} + \frac{\mu^2}{\gamma^3} - \frac{\mu^2 q^2}{\gamma^4}}{\left[\frac{1}{\Delta} + \frac{(4\pi)^{\alpha/2}q^2}{48\pi^2\gamma} - \frac{(4\pi)^{\alpha/2}}{8\pi^2}\left\{\frac{2}{\alpha} + \psi(1) - \ln(\gamma)\right\}\right]}\end{aligned}$$

$$+\int_{\frac{1}{\sqrt{1/4\gamma}}}^{\Lambda} \mathrm{d}q\, q^{d-1} \left.\frac{\frac{\mu^4}{\gamma^4 q^4}}{\left[\frac{1}{\Delta}-\frac{\mu^2}{\gamma^2 q^2}-\frac{(4\pi)^{\alpha/2}}{8\pi^2}\left\{\frac{2}{\alpha}+\psi(1)-\ln(\gamma)+2-\left(1+\frac{1}{2}\frac{4}{q^2}\right)\ln\left(1+\frac{q^2}{2\gamma}\right)\right\}\right]}+\frac{\mu^2}{\gamma^2 q^2}\right\}.$$

$$\left[\frac{1}{\Delta}-\frac{(4\pi)^{\alpha/2}}{8\pi^2}\left\{\frac{2}{\alpha}+\psi(1)-\ln(\gamma)+2-\left(1+\frac{1}{2}\frac{4}{q^2}\right)\ln\left(1+\frac{q^2}{2\gamma}\right)\right\}\right] \tag{4.2.37}$$

Its further evaluation in one dimension is also furnished in Appendix C.4.

We can now collect the terms S_0, S_1 and S_2 defined in (4.2.19) to express the free energy expression $\langle F\rangle$ as

$$\begin{aligned}
-\beta\langle F\rangle &= \lim_{n\to 0}\frac{\langle Z\rangle^{2n}-1}{2n} \\
&\approx \left(-\frac{1}{2}\mathrm{tr}\ln A(x,x')+\frac{1}{8}\frac{\mu^2\delta(0)}{\gamma}\right. \\
&\quad \left.-2\sum_i\int\frac{\mathrm{d}q}{(2\pi)^d}\frac{\tilde{Q}_{ii}(0)}{q^2+\gamma}-\frac{\mu^2\tilde{Q}_{ii}(0)}{2\gamma^2}+\frac{\mu^2}{2\gamma^2}\tilde{Q}_{ij}(0)\right) \\
&\quad -\frac{1}{2}\left(\sum_q\ln\left(\frac{1}{\Delta}-2\Omega^{-1}(q)-\frac{\mu^2}{\gamma^2(q^2+\gamma)}\right)\right) \\
&\quad +\frac{1}{4}\left(\sum_q\ln\left(\frac{1}{\Delta}-2\Omega^{-1}(q)\right)\right) \\
&\quad -\frac{1}{4}\sum_q\frac{\left[\left(\frac{1}{\Delta}-2\Omega^{-1}(q)-\frac{\mu^2}{\gamma^2(q^2+\gamma)}\right)^{-1}\frac{\mu^4}{\gamma^4(q^2+\gamma)^2}+\frac{\mu^2}{\gamma^2(q^2+\gamma)}\right]}{\frac{1}{\Delta}-2\Omega^{-1}(q)}.
\end{aligned} \tag{4.2.38}$$

$$\begin{aligned}
&\approx \left(-\frac{1}{2}\mathrm{tr}\ln A(x,x')+\frac{1}{8}\frac{\mu^2\delta(0)}{\gamma}-2\sum_i\int\frac{\mathrm{d}q}{(2\pi)^d}\frac{\tilde{Q}_{ii}(0)}{q^2+\gamma}-\frac{\mu^2\tilde{Q}_{ii}(0)}{2\gamma^2}+\frac{\mu^2}{2\gamma^2}\tilde{Q}_{ij}(0)\right) \\
&\quad -\frac{1}{2}\frac{1}{(2\pi)^{d/2}\Gamma(d/2)}\left\{\int_0^{\frac{1}{\sqrt{1/4\gamma}}}\mathrm{d}q\, q^{d-1}\ln\left[\frac{1}{\Delta}-\frac{\mu^2}{\gamma^3}+\left(\frac{\mu^2}{\gamma^4}+\frac{(4\pi)^{\alpha/2}}{48\pi^2\gamma}\right)q^2\right.\right. \\
&\qquad \left.\left.-\frac{(4\pi)^{\alpha/2}}{8\pi^2}\left\{\frac{2}{\alpha}+\psi(1)-\ln(\gamma)\right\}\right]\right.
\end{aligned}$$

$$
\begin{aligned}
&+\int_{\frac{1}{\sqrt{1/4\gamma}}}^{\Lambda} \mathrm{d}q\; q^{d-1} \ln\left[\frac{1}{\Delta} - \frac{\mu^2}{\gamma^2 q^2} - \frac{(4\pi)^{\alpha/2}}{8\pi^2}\right. \\
&\qquad\left.\times\left\{\frac{2}{\alpha} + \psi(1) - \ln(\gamma) + 2 - \left(1 + \frac{1}{2}\frac{4}{q^2}\right)\ln\left(1 + \frac{q^2}{2\gamma}\right)\right\}\right]\Bigg\} \\
&+\frac{1}{4(2\pi)^{d/2}\Gamma(d/2)}\left\{\int_0^{\frac{1}{\sqrt{1/4\gamma}}} \mathrm{d}q\; q^{d-1} \ln\left[\frac{1}{\Delta} + \frac{(4\pi)^{\alpha/2} q^2}{48\pi^2\gamma}\right.\right. \\
&\qquad\left.\left.-\frac{(4\pi)^{\alpha/2}}{8\pi^2}\left\{\frac{2}{\alpha} + \psi(1) - \ln(\gamma)\right\}\right] \right. \\
&+\int_{\frac{1}{\sqrt{1/4\gamma}}}^{\Lambda} \mathrm{d}q\; q^{d-1} \ln\left[\frac{1}{\Delta} - \frac{(4\pi)^{\alpha/2}}{8\pi^2}\left\{\frac{2}{\alpha} + \psi(1) - \ln(\gamma)\right.\right. \\
&\qquad\left.\left.\left.+2 - \left(1 + \frac{1}{2}\frac{4}{q^2}\right)\ln\left(1 + \frac{q^2}{2\gamma}\right)\right\}\right]\Bigg\} \\
&-\frac{1}{4}\frac{1}{(2\pi)^{d/2}\Gamma(d/2)}\left\{\int_0^{\frac{1}{\sqrt{1/4\gamma}}} \mathrm{d}q\; q^{d-1}\right. \\
&\qquad\left.\frac{\left(\frac{\mu^4}{\gamma^6} - \frac{2\mu^4 q^2}{\gamma^7}\right)}{\left[\frac{1}{\Delta} - \frac{\mu^2}{\gamma^3} + \frac{\mu^2 q^2}{\gamma^4} - \frac{(4\pi)^{\alpha/2}}{8\pi^2}\left\{\frac{2}{\alpha} + \psi(1) - \ln(\gamma) + 2 - \left(2 + \frac{q^2}{6\gamma}\right)\right\}\right]} + \frac{\mu^2}{\gamma^3} - \frac{\mu^2 q^2}{\gamma^4}}{\left[\frac{1}{\Delta} + \frac{(4\pi)^{\alpha/2} q^2}{48\pi^2\gamma} - \frac{(4\pi)^{\alpha/2}}{8\pi^2}\left\{\frac{2}{\alpha} + \psi(1) - \ln(\gamma)\right\}\right]} \\
&+\int_{\frac{1}{\sqrt{1/4\gamma}}}^{\Lambda} \mathrm{d}q\; q^{d-1} \\
&\left.\frac{\frac{\mu^4}{\gamma^4 q^4}}{\left[\frac{1}{\Delta} - \frac{\mu^2}{\gamma^2 q^2} - \frac{(4\pi)^{\alpha/2}}{8\pi^2}\left\{\frac{2}{\alpha} + \psi(1) - \ln(\gamma) + 2 - \left(1 + \frac{1}{2}\frac{4}{q^2}\right)\ln\left(1 + \frac{q^2}{2\gamma}\right)\right\}\right]} + \frac{\mu^2}{\gamma^2 q^2}}{\left[\frac{1}{\Delta} - \frac{(4\pi)^{\alpha/2}}{8\pi^2}\left\{\frac{2}{\alpha} + \psi(1) - \ln(\gamma) + 2 - \left(1 + \frac{1}{2}\frac{4}{q^2}\right)\ln\left(1 + \frac{q^2}{2\gamma}\right)\right\}\right]}\right\} \quad (4.2.39)
\end{aligned}
$$

In single dimension $d = 1$, where we apply results from the Appendices C.3, C.4, equations (3.1.19), (3.1.20) and (3.1.21) whilst also substituting $\gamma = \frac{\rho_0 \beta k L^2}{\kappa}\left(\frac{n\beta\epsilon}{\rho_0 R} - 1\right)$; $\Delta = \frac{\beta^2 k^2 L^4}{4RL}$ and $\mu = -2\mu$ from equation (4.1.12), we have the average free energy, of single dimension, $\langle F \rangle$ approximately equivalent to

4.2.1 The RS free energy profiles

The graphical depiction of this under various fixed input parameters is shown in figures figs. 4.1 to 4.3

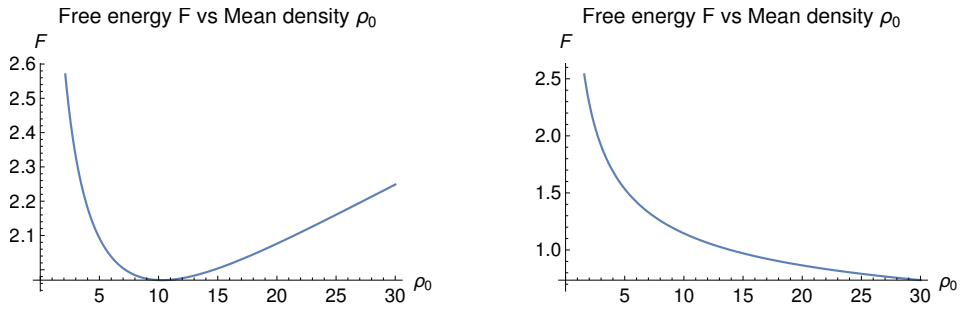

Figure 4.1: Free energy as a function of average density ρ_0, pressure $\mu = 0$ dimensionless and cut-off Λ. The other parameters were chosen to be $L = 1$, $R = 1.5$ (LHS) and $R = 2$ (RHS), $\Lambda = 2\sqrt{\frac{4\rho_0\beta k L^2}{\kappa}}$, $\beta = 1$, $k = 1$ and $\kappa = 1$ units. The zero mode parameters were chosen to be $\tilde{Q}_{ii}(0) = 1$ and $\tilde{Q}_{ij}(0) = 1$.

There is no specific scientific reason fot the unit value choice of the parameters $\tilde{Q}_{ii}(0) = 1$ and $\tilde{Q}_{ij}(0) = 1$.

These graphs shows us that in the inhomogeneous discrete adhesion the competition between the favourable energy E and entropy S at zero pressure μ has a different behaviour in contrast to the continuum adhesion case dealt with in Chapter 2. This different behaviour is exhibited for smaller values of the disorder parameter R. We observed, fig. 2.1, that for the continuum homogeneous adhesion when there is no pressure μ that the rate of energy loss E is always larger than the entropy S gain as the detached region grows. This corresponds with fig. 4.1. Large values of R reflects small variance of the tether position distribution. Thus, represents a homogeneous limit.

It was when we applied pressure μ that this picture changed in the continuum adhesion, sections 2.1 and 2.2. That is of the rate of energy loss E being always larger than the entropy S gain as the detached region grows. The pressure lead to an entropic growth bias whereby above a certain detached region size L the entropy gain dominates. In this discrete random adhesion scenario modelled here, however, the entropy growth exhibits the features we observed when there is an applied pressure μ in the continuum adhesion for smaller values of the disorder parameter R. We see that there exist two different behaviours of the competing energy E and entropy S. The disorder R effects the bias that we observed to be caused by the pressure in the continuum adhesion model. That is, above a certain tether density ρ_0, for the non-homogeneity case of large variance, there is an entropy gain dominance compared to the energetic gain. If one increases the disorder parameter R, that is a homogeneous limit, this behaviour vanishes.

What is then the role of pressure in this case? The graphs figs. 4.2 and 4.3 below help us to gain understanding to this.

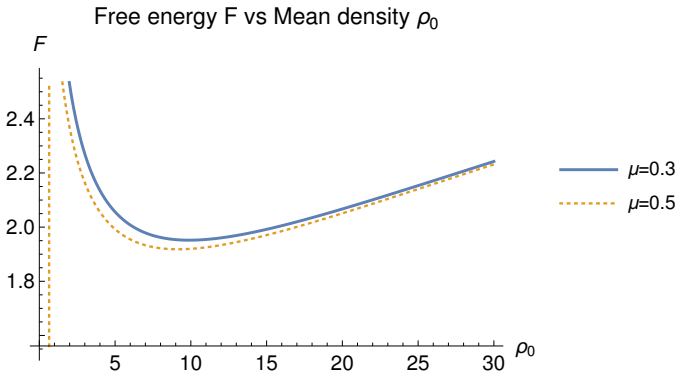

Figure 4.2: Free energy as a function of average density ρ_0, disorder parameter $R = 1$ unit, cut-off $\Lambda = 2\sqrt{\frac{4\rho_0\beta kL^2}{\kappa}}$, $\beta = 1$, $k = 1$ and $\kappa = 1$ units and for pressure values $\mu = \{0.3,\ 0.5\}$ dimensionless. The zero mode parameters were chosen to be $\tilde{Q}_{ii}(0) = 1$ and $\tilde{Q}_{ij}(0) = 1$.

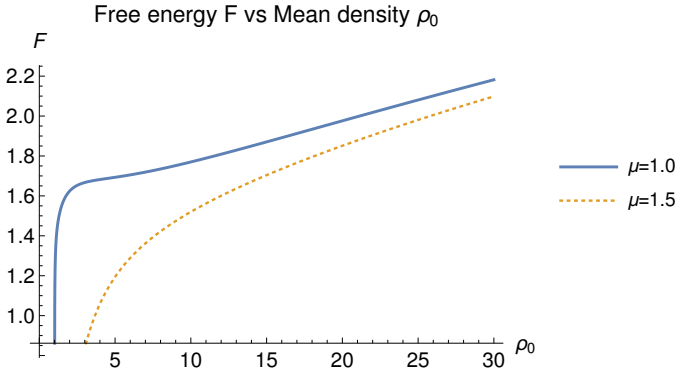

Figure 4.3: Free energy as a function of average density ρ_0, disorder parameter $R = 1$ unit, $\Lambda = 2\sqrt{\frac{4\rho_0\beta kL^2}{\kappa}}$, $\beta = 1$, $k = 1$ and $\kappa = 1$ units and for pressure values $\mu = \{1.0,\ 1.5\}$ dimensionless. The zero mode parameters were chosen to be $\tilde{Q}_{ii}(0) = 1$ and $\tilde{Q}_{ij}(0) = 1$.

At this level of replica treatment, the replica symmetry approximation, the moderate pressure μ increase leads to the appearance of the second domain of entropy dominance for small values of the tether density ρ_0. This appearance is similar to the continuum adhesion model 2.1. Therefore, there are now three competing factors, namely, the pressure μ, the sticking energy ϵ and the disorder R. However, a further increase of the pressure leads to the disappearance of the minima. This disappearance with the growing pressure finally leaves the profile depicted in the case of $\mu = 1.5$, fig. 4.3. Therefore, for larger values of the pressure μ the entropic gain always dominates upon the reduction of the tether density. This behaviour we also observed in the free energy F of

the continuum adhesion large pressure scenario in Chapter 2. Where we derived the free energy expressions for the homogeneously detethering polymer or membrane.

4.2.2 The disorder parameter R infinite and zero limits

The free energy F_T of multiple equal size bubbles is determined by the partition function $Z_T = Z^{N+1}(\frac{L}{N})$ where Z is the partition function of one bubble. N is the number of mid attachment points. Hence the number of bubbles is equivalent to $N+1$. Therefore, the free energy is given by $-\beta F_T = (N+1)\ln Z(\frac{L}{N})$. However, $N = \rho_0 L$. Hence, $-\beta F_T = (\rho_0 L + 1)\ln Z(\frac{1}{\rho_0})$. We can then extend or recast the equation result (2.1.10) $F \approx -\frac{1}{\beta}\left(\frac{\mu^2 L^3}{48\kappa} + \beta L\epsilon\right) + \frac{1}{\beta}(q_c \ln q_c - q_c)$ for the single bubble to this multiple equal bubbles case. The graphical depiction of this for the zero and 5.5 units pressure μ is shown below fig. 4.4, respectively.

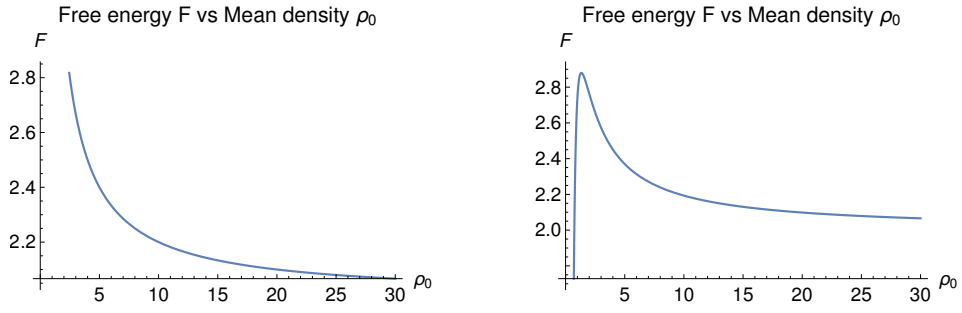

Figure 4.4: Free energy profile for a polymer as a function of average density ρ_0, pressure $\mu = \{0,\ 5.5\}$, respectively, derived from equation (2.1.10) of the continuum adhesion. The other parameters were chosen to be $L = 1$, $\beta = 1$, $\epsilon = -2$ and $\kappa = 1$ units.

This enable us to make the comparison with the result we have obtained in this section 4.2 result.

Now, we can investigate this Replica Symmetry Approximation free energy at the limit $R \to \infty$ or $\rho(x) \to \rho_0$. These limits corresponds to the uniform discrete adhesion scenario. We depict incrementally such a limit below in fig. 4.5 for the pressure $\mu = 0.8$ dimensionless.

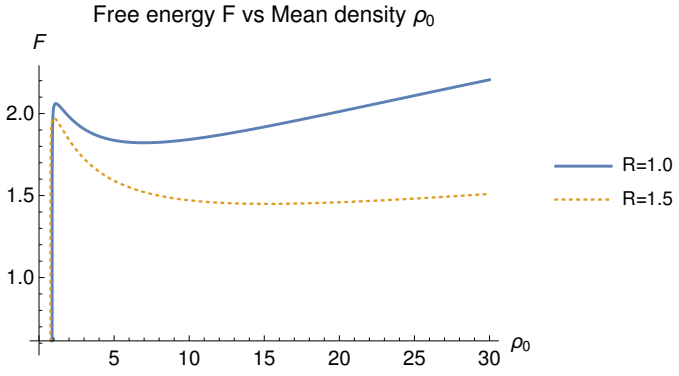

Figure 4.5: Free energy profile for a polymer as a function of average density ρ_0, pressure $\mu = 0.8$ dimensionless and cut-off $\Lambda = 2\sqrt{\frac{4\rho_0\beta k L^2}{\kappa}}$, $\beta = 1$, $k = 1$ and $\kappa = 1$ units. The zero mode parameters were chosen to be $\tilde{Q}_{ii}(0) = 1$ and $\tilde{Q}_{ij}(0) = 1$.

This graphical depiction, fig. 4.5, of the limit $R \to \infty$ (equivalent of $\rho(x) \to \rho_0$) are consistent with the recast result of equation (2.1.10) depicted in fig. 4.4. The opposite limit $R \to 0$ (equivalent of $\rho_0 \to 0$), by inspection, is also held.

In conclusion, the statistical properties of bubbles of different sizes are different to those of the uniform or homogeneous nature.

4.2.3 RS average fluctuations height $\langle h \rangle$ and $\langle h^2 \rangle$

In this subsection we shall plot the graphs of the average height and square fluctuations $\langle h \rangle = \langle \sum_i \int_0^L dx\ h_i(x) \rangle = \frac{\partial \ln Z}{\partial \mu}$ and $\langle h^2 \rangle = \langle \sum_i \int_0^L dx\ h_i^2(x) \rangle = \frac{\partial \ln Z}{\partial \gamma}$, respectively. These are depicted in the following graphs fig. 4.7 to fig. 4.9 as functions of either average density ρ_0 or pressure μ.

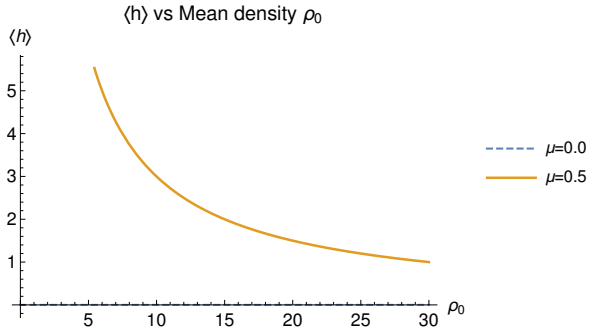

Figure 4.6: Average height $\langle h \rangle$ profile for a polymer as a function of average density ρ_0, pressure $\mu = 0.5$ dimensionless. The other parameters were chosen to be $L = 1$, $R = 1.6$, $\Lambda = 10\sqrt{\frac{4\rho_0\beta k L^2}{\kappa}}$, $\beta = 1$, $k = 0.91$ and $\kappa = 6$ units. The zero mode parameters were chosen to be $\tilde{Q}_{ii}(0) = 1$ and $\tilde{Q}_{ij}(0) = 1$.

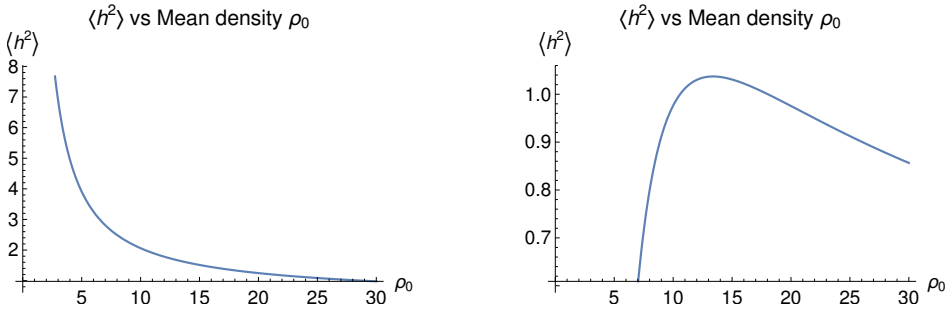

Figure 4.7: Average square fluctuations $\langle h^2 \rangle$ profile for a polymer as a function of average density ρ_0, pressure $\mu = \{0,\ 0.5\}$ dimensionless, respectively and the cut-off Λ. The other parameters were chosen to be $L = 1$, $R = 1.6$, $\Lambda = 10\sqrt{\frac{4\rho_0\beta k L^2}{\kappa}}$, $\beta = 1$, $k = 0.91$ and $\kappa = 6$ units. The zero mode parameters were chosen to be $\tilde{Q}_{ii}(0) = 1$ and $\tilde{Q}_{ij}(0) = 1$.

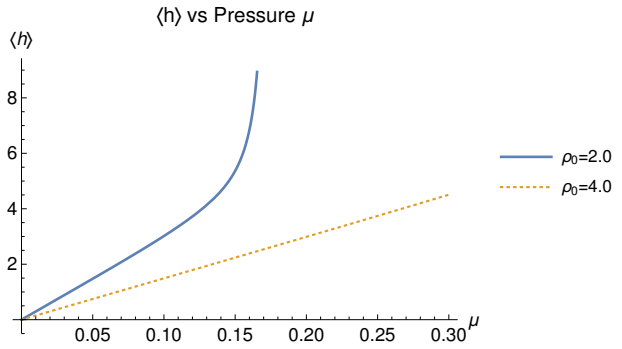

Figure 4.8: Average height $\langle h \rangle$ profile for a polymer as a function of pressure μ, tether density $\rho_0 = \{2.0,\ 4.0\}$ units. The other parameters were chosen to be $L = 1$, $R = 1.6$, $\Lambda = 10\sqrt{\frac{4\rho_0\beta k L^2}{\kappa}}$, $\beta = 1$, $k = 0.91$ and $\kappa = 6$ units. The zero mode parameters were chosen to be $\tilde{Q}_{ii}(0) = 1$ and $\tilde{Q}_{ij}(0) = 1$.

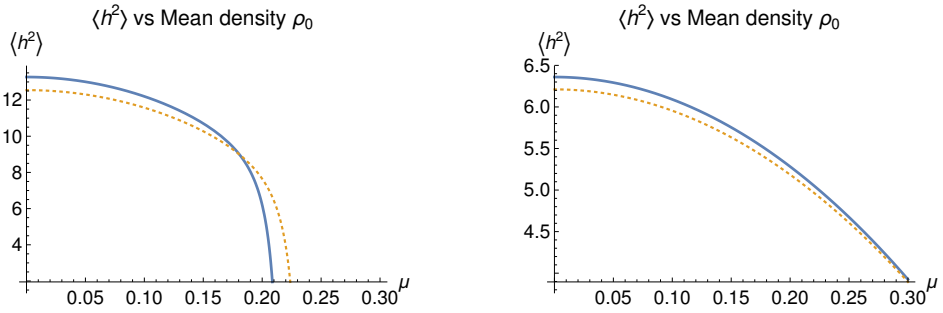

Figure 4.9: Average square fluctuations $\langle h^2 \rangle$ profile for a polymer as a function of pressure μ, average density $\rho_0 = \{(2.0,\ 2.1); (4.0,\ 4.1)\}$ units and $R = 1.6$. The other parameters were chosen to be $L = 1$, $R = 1.6$, $\Lambda = 10\sqrt{\frac{4\rho_0\beta k L^2}{\kappa}}$, $\beta = 1$, $k = 0.91$ and $\kappa = 6$ units. The zero mode parameters were chosen to be $\tilde{Q}_{ii}(0) = 1$ and $\tilde{Q}_{ij}(0) = 1$.

For relatively smaller choice values of the average density ρ_0 in fig. 4.9 we observe a lower pressure μ domain of almost flat square fluctuations $\langle h^2 \rangle$ before the decline. However, for relatively larger choice values of the average density ρ_0 an inverse relationship of monotonic decreasing behaviour of the square fluctuations $\langle h^2 \rangle$ with a growing pressure μ is displayed for the entire domain. Intermediate choice values of the average density ρ_0 values that lie in between the first two reflect a rescaled behavior of fig. 4.9. Similarly, altering the measure of the disorder, the parameter R, we only observe rescaling. So overall we observe a decreasing trend with the pressure. This is counter intuitive. These profiles of decreasing square fluctuations means that the pressure has a damping role. This behavior shows that this level of approximation of replica

symmetry is not adequately treating the problem. Certainly, there must be a growing region with inflation which is not reflected in this approximation. Therefore, we need to extend our approximation. The minor difference in these profiles arise due the average tether spacing ρ_0. Further, how do we contrast between the exhibited behavior from these figures of the square fluctuations as a function of the pressure? The almost flat response with the pressure for the smaller values of the tether density is similar the annealed treatment. However, the decline with further growth or for larger tether density means that the collective polymer intersegments acts as a drag at the right scale in relation to the pressure. This is due to the restricted fluctuations or stretching of the polymer intersegments.

4.3 Replica Symmetry Breaking Solution

In the previous section we explored the role of quenched random disorder in the Replica Symmetry Approximation. What happens when the replica matrix $\mathbb{Q}$ is not symmetric? Is this replica symmetry approximation sufficient for this problem. Does its physics depend on a or some conditions? In attempting to gain insight into these questions we explore a non-symmetric scenario albeit weak introduced in section 1.7.3. This is termed weak Replica Symmetry Breaking and was first constructed by Parisi [69].

How do we evaluate the object (4.1.13) equivalently (4.2.9) in the non Replica Symmetry scenario?

$$\langle Z^n \rangle = \mathrm{C}' \int \prod_{ij} \mathcal{D}Q_{ij}(x) \exp\left\{ -\frac{1}{2\Delta} \int \mathrm{d}x \sum_{ij} Q_{ij}^2(x) - \frac{1}{2}\mathrm{tr}\ln \mathbb{M}(x',x) + \frac{1}{8}\int \mathrm{d}x\mathrm{d}x'\ \boldsymbol{\mu}^{\mathsf{T}}\mathbb{M}^{-1}(x,x')\boldsymbol{\mu} \right\}. \tag{4.3.1}$$

The answer is the Replica Symmetry Breaking (RSB) scheme of Parisi [69]. This is executed by dividing the matrix $\mathbb{Q}$ into $n_1 \times n_1$ blocks along the diagonal. One of the $n_1 \times n_1$ is again divided into $n_2 \times n_2$ blocks and so on. However, in the approximation that we shall treat is the first step or *weak* RSB where

this procedure is stopped at first stage. Subsequently, we have

$$\begin{aligned}\langle Z^n\rangle &= \mathrm{C}'\int\prod_{ij}\mathcal{D}Q_{ii}^{(1)}(x)\mathcal{D}Q_{ii}^{(2)}(x)\mathcal{D}Q_{ij}^{(s)}(x)\mathcal{D}Q_{ij}^{(a)}(x)\\ &\exp\left\{-\frac{1}{2\Delta}\int \mathrm{d}x\sum_i\left(Q_{ii}^{(1)2}(x)+Q_{ii}^{(2)2}(x)\right)\right.\\ &\quad -\frac{1}{2\Delta}\int \mathrm{d}x\sum_{ij}\left(Q_{ij}^{(s)2}(x)+Q_{ij}^{(a)2}(x)\right)-\frac{1}{2}\mathrm{tr}\ln\mathbb{M}(x',x)\\ &\quad \left.+\frac{1}{2}\int \mathrm{d}x\mathrm{d}x'\,\boldsymbol{\mu}^{\mathsf{T}}\mathbb{M}^{-1}(x,x')\boldsymbol{\mu}\right\}.\end{aligned} \tag{4.3.2}$$

where [70]

$$\mathbb{M}(x,x') = \begin{pmatrix}\delta_{ij}\delta^{xx'}\left(\gamma-\partial_{xx}\right)+2\delta_{ij}Q_{ii}^{(1)}\delta^{xx'} & 2\left(Q_{ij}^{(s)}+Q_{ij}^{(a)}\right)\delta^{xx'}\\ 2\left(Q_{ij}^{(s)}-Q_{ij}^{(a)}\right)\delta^{xx'} & \delta_{ij}\delta^{xx'}\left(\gamma-\partial_{xx}\right)+2\delta_{ij}Q_{ii}^{(2)}\delta^{xx'}\end{pmatrix}. \tag{4.3.3}$$

$Q_{ij}^{(s)}$ represents a symmetric sub-matrix whilst $Q_{ij}^{(a)}$ represents its opposite. Alternatively, $Q_{ij}^{(s)}\to h_ih_j+h_jh_i$ and $Q_{ij}^{(a)}\to h_ih_j-h_jh_i$. Effectively, this is a block organization of the overlap matrix $\mathbb{Q}$ is in terms of the diagonal and anti/symmetric sub-matrices. In contrast to the RS solution (4.2.11) the replicated partition functional exponential (4.3.2) is now expressed in a quadratic form of the four sub-matrices.

With these considerations we now proceed to evaluate the functional $\langle Z^n\rangle$ (4.3.2). In oder to achieve this we now need to decipher the terms $\mathrm{tr}\ln\mathbb{M}(x,x')$ and $\int \mathrm{d}x\mathrm{d}x'\begin{pmatrix}\boldsymbol{\mu}\\ \boldsymbol{\mu}\end{pmatrix}\mathbb{M}^{-1}(x,x')\begin{pmatrix}\boldsymbol{\mu}\\ \boldsymbol{\mu}\end{pmatrix}$ as now functions of $Q_{ii}^{(1)}$, $Q_{ii}^{(2)}$, $Q_{ij}^{(s)}$ and $Q_{ij}^{(a)}$. In expressing these quantities in terms of Q_{ij} we shall treat them separately. In both cases we shall apply the factorization $\mathbb{M}=\mathbb{D}\left[1+\mathbb{D}^{-1}\mathbb{Q}\right]$. That is,

$$\begin{aligned}\mathbb{M}(x,x') = &\begin{pmatrix}\delta_{ij}\delta^{xx'}\left(\gamma-\partial_{xx}\right) & 0\\ 0 & \delta_{ij}\delta^{xx'}\left(\gamma-\partial_{xx}\right)\end{pmatrix}\times\\ &\left[\begin{pmatrix}1 & 0\\ 0 & 1\end{pmatrix}+\begin{pmatrix}\delta_{ij}\delta^{xx'}\left(\gamma-\partial_{xx}\right) & 0\\ 0 & \delta_{ij}\delta^{xx'}\left(\gamma-\partial_{xx}\right)\end{pmatrix}^{-1}\times\right.\\ &\left.\begin{pmatrix}2\delta_{ij}Q_{ii}^{(1)}(x)\delta^{xx'} & 2\left(\left(Q_{ij}^{(s)}(x)+Q_{ij}^{(a)}(x)\right)\delta^{xx'}\right)\\ 2\left(\left(Q_{ij}^{(s)}(x)-Q_{ij}^{(a)}(x)\right)\delta^{xx'}\right) & 2\delta_{ij}Q_{ii}^{(2)}(x)\delta^{xx'}\end{pmatrix}\right].\end{aligned} \tag{4.3.4}$$

The details of the evaluation or 'reduction' or decomposition of the terms $\operatorname{tr}\ln\mathbb{M}(x,x')$ and $\int \mathrm{d}x\mathrm{d}x' \begin{pmatrix} \boldsymbol{\mu} \\ \boldsymbol{\mu} \end{pmatrix}^{\mathsf{T}} \mathbb{M}^{-1}(x,x') \begin{pmatrix} \boldsymbol{\mu} \\ \boldsymbol{\mu} \end{pmatrix}$ are furnished in Appendix D. These results thereof bring us close to our goal of approximating the decomposed functional $\langle Z^n \rangle$ expressed in (4.3.2). Upon substituting these results (D.1.11) and (D.1.27) we have

$$\begin{aligned}
\langle Z^n \rangle = \int \prod_{ij} \mathcal{D}Q_{ii}^{(1)}(q)\mathcal{D}Q_{ii}^{(2)}(q)\mathcal{D}Q_{ij}^{(s)}(q)\mathcal{D}Q_{ij}^{(a)}(q) \\
\exp\Bigg(-n\,\operatorname{tr}\ln A(x,x') - \sum_i \int \frac{\mathrm{d}q}{(2\pi)^d} \frac{\left(\tilde{Q}_{ii}^{(1)}(0) + \tilde{Q}_{ii}^{(2)}(0)\right)}{q^2+\gamma} \\
+\frac{n\mu^2\delta(0)}{\gamma} - 2(n^2-n)\mu^2\frac{Q_{bc}^{(s)}(0)}{\gamma^2} - n\mu^2\frac{\left(Q_{ii}^{(1)}(0) + Q_{ii}^{(2)}(0)\right)}{\gamma^2}\Bigg) \\
\exp\Bigg\{\Bigg[-\frac{1}{2}\int \frac{\mathrm{d}q}{(2\pi)^d} \sum_{\substack{i \\ m=1,2}} Q_{ii}^{(m)}(q)\left(\frac{1}{\Delta} - 2\Omega^{-1}(q) - \frac{2\mu^2}{\gamma^2(q^2+\gamma)}\right) Q_{ii}^{(m)}(-q) \\
+\frac{1}{2}\int \frac{\mathrm{d}q}{(2\pi)^d} \sum_{\substack{ij \\ m=1,2}} \frac{Q_{ij}^{(s)}(q)4\mu^2 Q_{ii}^{(m)}(-q)}{\gamma^2(q^2+\gamma)}\Bigg] \\
\Bigg[-\frac{1}{2}\int \frac{\mathrm{d}q}{(2\pi)^d} \sum_{\substack{ij \\ m=s,a}} Q_{ij}^{(m)}(q)\left(\frac{1}{\Delta} - 4\Omega^{-1}(q)\right) Q_{ij}^{(m)}(-q) \\
+\frac{1}{2}\int \frac{\mathrm{d}q}{(2\pi)^d} \sum_{\substack{ijk \\ m=s,a}} \frac{Q_{ij}^{(m)}(q)4\mu^2 Q_{kj}^{(m)}(-q)}{\gamma^2(q^2+\gamma)}\Bigg]\Bigg\}. \qquad (4.3.5)
\end{aligned}$$

Defining $\chi(q) = \left(\frac{1}{\Delta} - 2\Omega^{-1}(q) - \frac{2\mu^2}{\gamma^2(q^2+\gamma)}\right)$, the Q_{ii} components of this ex-

pression (4.3.5) are evaluated by completing the square to obtain

$$\langle Z^n[Q_{ii}]\rangle = \int \prod_i \mathcal{D}Q_{ii}^{(1)}(q)\mathcal{D}Q_{ii}^{(2)}(q) \exp\left[-\frac{1}{2}\int \frac{\mathrm{d}q}{(2\pi)^d} \sum_{\substack{i \\ m=1,2}} Q_{ii}^{(m)}(q)\chi(q)Q_{ii}^{(m)}(-q) + \frac{1}{2}\int \frac{\mathrm{d}q}{(2\pi)^d} \sum_{\substack{ij \\ m=1,2}} \frac{Q_{ij}^{(s)}(q)4\mu^2 Q_{ii}^{(m)}(-q)}{\gamma^2(q^2+\gamma)}\right]$$

$$= \exp\left(-n\sum_q \ln\chi(q) + \underbrace{\frac{1}{2}\int \frac{\mathrm{d}q}{(2\pi)^d}\sum_{ijk} \frac{Q_{ij}^{(s)}(q)4\mu^4\chi^{-1}(q)Q_{jk}^{(s)}(-q)}{\left(\gamma^2(q^2+\gamma)\right)^2}}_{\text{combines in equation (4.3.8)}}\right). \quad (4.3.6)$$

The remaining term evaluates as

$$\begin{aligned}
\langle Z^n[Q_{ii}]\rangle &= \exp\left(-n\sum_q \ln\left(\frac{1}{\Delta} - 2\Omega^{-1}(q) - \frac{2\mu^2}{\gamma^2(q^2+\gamma)}\right)\right) \\
&= -n\sum_q \ln\left(\frac{1}{\Delta} - 2\left[\Gamma(2)\frac{\pi^{d/2}}{(2\pi)^d}\left[\frac{2}{\alpha} + \psi(1) - \ln(\gamma) + 2 - \sqrt{1+\frac{4\gamma}{q^2}}\ln\frac{\sqrt{1+\frac{4\gamma}{q^2}}+1}{\sqrt{1+\frac{4\gamma}{q^2}}-1}\right]\right] - \frac{2\mu^2}{\gamma^2(q^2+\gamma)}\right) \\
&= -\frac{n}{(2\pi)^{d/2}\Gamma(d/2)}\int_q q^{d-1}\ln\left[\frac{1}{\Delta} - 2\Gamma(2)\frac{\pi^{d/2}}{(2\pi)^d}\left[\frac{2}{\alpha} + \psi(1) - \ln(\gamma) + 2 - \sqrt{1+\frac{4\gamma}{q^2}}\ln\frac{\sqrt{1+\frac{4\gamma}{q^2}}+1}{\sqrt{1+\frac{4\gamma}{q^2}}-1}\right] - \frac{2\mu^2}{\gamma^2(q^2+\gamma)}\right] \\
&\approx -\frac{n}{(2\pi)^{d/2}\Gamma(d/2)}\left\{\int_0^{\frac{1}{\sqrt{1/4\gamma}}} \mathrm{d}q\, q^{d-1}\ln\left[\frac{1}{\Delta} - \frac{2\mu^2}{\gamma^3} + \left(\frac{2\mu^2}{\gamma^4} + \frac{(4\pi)^{\alpha/2}}{48\pi^2\gamma}\right)q^2 - \frac{(4\pi)^{\alpha/2}}{8\pi^2}\left\{\frac{2}{\alpha} + \psi(1) - \ln(\gamma)\right\}\right]\right. \\
&\quad \left. + \int_{\frac{1}{\sqrt{1/4\gamma}}}^{\Lambda} \mathrm{d}q\, q^{d-1}\ln\left[\frac{1}{\Delta} - \frac{2\mu^2}{\gamma^2 q^2} - \frac{(4\pi)^{\alpha/2}}{8\pi^2}\left\{\frac{2}{\alpha} + \psi(1) - \ln(\gamma) + 2 - \left(1+\frac{1}{2}\frac{4}{q^2}\right)\ln\left(1+\frac{q^2}{2\gamma}\right)\right\}\right]\right\}. \quad (4.3.7)
\end{aligned}$$

The further evaluation in the one dimension case is shown in Appendix D.2.

Proceeding to the subsequent equation (4.3.6), after defining $\mathrm{A}(q) = \frac{1}{\Delta} - 4\Omega^{-1}(q)$ we have

$$
\begin{aligned}
\langle Z^n[Q_{ij}^{(s)}]\rangle = \int \prod_{ij} \mathcal{D}Q_{ij}^{(s)}(q) \exp\Bigg\{ & -\frac{1}{2}\int \frac{\mathrm{d}q}{(2\pi)^d} \sum_{ij} Q_{ij}^{(s)}(q) A(q) Q_{ij}^{(s)}(-q) \\
& + \frac{1}{2}\int \frac{\mathrm{d}q}{(2\pi)^d} \sum_{ijk} Q_{ij}^{(s)}(q) \left(\frac{4\mu^2}{\gamma^2(q^2+\gamma)} + \frac{4\mu^4 \chi^{-1}(q)}{\left(\gamma^2(q^2+\gamma)\right)^2} \right) Q_{jk}^{(s)}(-q) \Bigg\} \\
= \quad & \exp\Bigg(\frac{n}{4} \sum_q \ln\left(\frac{1}{\Delta} - 4\Omega^{-1}(q) \right) - \frac{n}{4} \sum_q \Bigg\{ \frac{1}{\frac{1}{\Delta} - 4\Omega^{-1}(q)} \\
& \times \left[\left(\frac{1}{\Delta} - 2\Omega^{-1}(q) - \frac{2\mu^2}{\gamma^2(q^2+\gamma)} \right)^{-1} \frac{4\mu^4}{\gamma^4(q^2+\gamma)^2} + \frac{4\mu^2}{\gamma^2(q^2+\gamma)} \right] \Bigg\} \\
= \quad & \exp\Bigg(\frac{n}{4(2\pi)^{d/2}\Gamma(d/2)} \Bigg\{ \int_0^{\frac{1}{\sqrt{1/4\gamma}}} \mathrm{d}q\, q^{d-1} \ln\left[\frac{1}{\Delta} + \frac{(4\pi)^{\alpha/2} q^2}{24\pi^2\gamma} \right. \\
& \qquad \left. - \frac{(4\pi)^{\alpha/2}}{4\pi^2} \left\{ \frac{2}{\alpha} + \psi(1) - \ln(\gamma) \right\} \right] \\
& + \int_{\frac{1}{\sqrt{1/4\gamma}}}^{\Lambda} \mathrm{d}q\, q^{d-1} \ln\Bigg[\frac{1}{\Delta} - \frac{(4\pi)^{\alpha/2}}{4\pi^2} \\
& \times \left\{ \frac{2}{\alpha} + \psi(1) - \ln(\gamma) + 2 - \left(1 + \frac{1}{2}\frac{4}{q^2} \right) \ln\left(1 + \frac{q^2}{2\gamma} \right) \right\} \Bigg] \Bigg\} \\
& - \frac{n}{4} \frac{1}{(2\pi)^{d/2}\Gamma(d/2)} \Bigg\{ \int_0^{\frac{1}{\sqrt{1/4\gamma}}} \mathrm{d}q\, q^{d-1} \\
& \qquad \frac{\left(\frac{4\mu^4}{\gamma^6} - \frac{8\mu^4 q^2}{\gamma^7} \right)}{\left[\frac{1}{\Delta} - \frac{2\mu^2}{\gamma^3} + \frac{2\mu^2 q^2}{\gamma^4} - \frac{(4\pi)^{\alpha/2}}{8\pi^2} \left\{ \frac{2}{\alpha} + \psi(1) - \ln(\gamma) + 2 - \left(2 + \frac{q^2}{6\gamma} \right) \right\} \right]} + \frac{4\mu^2}{\gamma^3} - \frac{4\mu^2 q^2}{\gamma^4} \\
& \qquad \frac{}{\left[\frac{1}{\Delta} + \frac{(4\pi)^{\alpha/2} q^2}{24\pi^2\gamma} - \frac{(4\pi)^{\alpha/2}}{4\pi^2} \left\{ \frac{2}{\alpha} + \psi(1) - \ln(\gamma) \right\} \right]} \\
& + \int_{\frac{1}{\sqrt{1/4\gamma}}}^{\Lambda} \mathrm{d}q\, q^{d-1} \frac{\frac{4\mu^4}{\gamma^4 q^4}}{\left[\frac{1}{\Delta} - \frac{2\mu^2}{\gamma^2 q^2} - \frac{(4\pi)^{\alpha/2}}{8\pi^2} \left\{ \frac{2}{\alpha} + \psi(1) - \ln(\gamma) + 2 - \left(1 + \frac{1}{2}\frac{4}{q^2} \right) \ln\left(1 + \frac{q^2}{2\gamma} \right) \right\} \right]} + \frac{4\mu^2}{\gamma^2 q^2} \\
& \qquad \frac{}{\left[\frac{1}{\Delta} - \frac{(4\pi)^{\alpha/2}}{4\pi^2} \left\{ \frac{2}{\alpha} + \psi(1) - \ln(\gamma) + 2 - \left(1 + \frac{1}{2}\frac{4}{q^2} \right) \ln\left(1 + \frac{q^2}{2\gamma} \right) \right\} \right]} \Bigg\}
\end{aligned}
\tag{4.3.8}
$$

The further evaluation in the one dimension case is also shown in Appendix D.3.

Finally, the antisymmetric contribution is given by

$$\begin{aligned}\langle Z^n[Q_{ij}^{(a)}]\rangle &= \int\prod_{ij}\mathcal{D}Q_{ij}^{(a)}(q)\exp\left\{-\frac{1}{2}\int\frac{\mathrm{d}q}{(2\pi)^d}\sum_{ij}Q_{ij}^{(a)}(q)A(q)Q_{ij}^{(a)}(-q)\right.\\ &\quad\left.+\frac{1}{2}\int\frac{\mathrm{d}q}{(2\pi)^d}\sum_{ijk}Q_{ij}^{(a)}(q)\left(\frac{4\mu^2}{\gamma^2(q^2+\gamma)}\right)Q_{kj}^{(a)}(-q)\right\}\\ &= \int\prod_{ij}\mathcal{D}Q_{ij}^{(a)}(q)\exp\left\{-\frac{1}{2}\int\frac{\mathrm{d}q}{(2\pi)^d}\sum_{ij}Q_{ij}^{(a)}(q)A(q)Q_{ij}^{(a)}(-q)\right.\\ &\quad\left.-\frac{1}{2}\int\frac{\mathrm{d}q}{(2\pi)^d}\sum_{ijk}Q_{ij}^{(a)}(q)\left(\frac{4\mu^2}{\gamma^2(q^2+\gamma)}\right)Q_{jk}^{(a)}(-q)\right\}\\ &= \int\mathcal{D}\tilde{\boldsymbol{Q}}^a(q)\exp\left\{-\frac{1}{2}\int\frac{\mathrm{d}q}{(2\pi)^d}\tilde{\boldsymbol{Q}}^{a\,\mathsf{T}}(q)\mathbb{T}(W,R)\tilde{\boldsymbol{Q}}^a(-q)\right\}\end{aligned}\tag{4.3.9}$$

where

$$\mathbb{T}=\begin{pmatrix}W+R & R & R & & & & \\ R & W+R & R & & & R & \dots\\ R & R & W+R & & & & \\ & & & W+R & R & & \\ & R & & R & W+R & & \\ & & & R & R & & \\ & \vdots & & & & & \ddots\end{pmatrix}.\tag{4.3.10}$$

In this case the constituents W and R of this matrix $\mathbb{T}$ represents

$$W=\left(\frac{1}{\Delta}-4\Omega^{-1}(q)\right)\ \text{and}\ R=\left(\frac{4\mu^2}{\gamma^2(q^2+\gamma)}\right).\tag{4.3.11}$$

Similar to the evaluation of S_2 in equations (4.2.29), (4.2.33) and (4.2.34) we have

$$\langle Z^n[Q_{ij}^{(a)}]\rangle = \exp\left(\frac{n}{4}\sum_q \ln\left(\frac{1}{\Delta} - 4\Omega^{-1}(q)\right) + \frac{n}{4}\sum_q \frac{\frac{4\mu^2}{\gamma^2(q^2+\gamma)}}{\frac{1}{\Delta} - 4\Omega^{-1}(q)}\right)$$

$$= \exp\left(+\frac{n}{4}\frac{1}{(2\pi)^{d/2}\Gamma(d/2)}\right.$$

$$\left\{\int_0^{\frac{1}{\sqrt{1/4\gamma}}} \mathrm{d}q\, q^{d-1}\, \frac{\frac{4\mu^2}{\gamma^3} - \frac{4\mu^2 q^2}{\gamma^4}}{\left[\frac{1}{\Delta} + \frac{(4\pi)^{\alpha/2}q^2}{24\pi^2\gamma} - \frac{(4\pi)^{\alpha/2}}{4\pi^2}\left\{\frac{2}{\alpha} + \psi(1) - \ln(\gamma)\right\}\right]} + \int_{\frac{1}{\sqrt{1/4\gamma}}}^{\Lambda} \mathrm{d}q\right.$$

$$\left.\left. q^{d-1}\, \frac{\frac{4\mu^2}{\gamma^2 q^2}}{\left[\frac{1}{\Delta} - \frac{(4\pi)^{\alpha/2}}{4\pi^2}\left\{\frac{2}{\alpha} + \psi(1) - \ln(\gamma) + 2 - \left(1 + \frac{1}{2}\frac{4}{q^2}\right)\ln\left(1 + \frac{q^2}{2\gamma}\right)\right\}\right]}\right\}\right). \tag{4.3.12}$$

The further evaluation for the one dimension case is shown in Appendix D.4. Collecting terms together according to equation (4.3.5) we have now dervived in one dimension, $d = 1$, where we have used the result equation (3.1.21) upon the $\mathrm{tr}\ln A(x, x')$ term, the free energy F expression.

4.3.1 The RSB free energy profiles

The illustrative graphical depictions of the free energy result from the equations (4.3.7), (4.3.8) and (4.3.12) under various input parameters are shown in figs. 4.10 to 4.12 below.

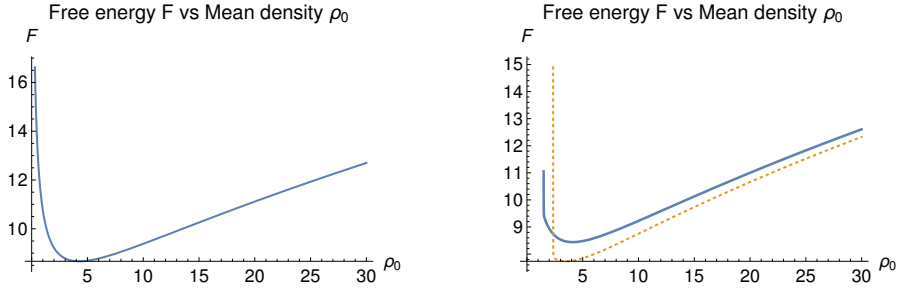

Figure 4.10: Free energy as a function of average density ρ_0, pressure $\mu = 0$ and cut-off Λ. The other parameters were chosen to be $L = 1$, $R = 1.6$, $\Lambda = 10\sqrt{\frac{4\rho_0\beta k L^2}{\kappa}}$, $\beta = 1$, $k = 0.91$ and $\kappa = 6$. The zero mode parameters were chosen to be $\tilde{Q}_{ii}^{(1)}(0) = 1$, $\tilde{Q}_{ii}^{(2)}(0) = 1$ and $\tilde{Q}_{ij}^{(s)}(0) = 1$.

We interested in the role of the pressure, is it similar to the Replica Symmetry Approximation? We explore this on the free energy for different parameter settings to see how the profile varies.

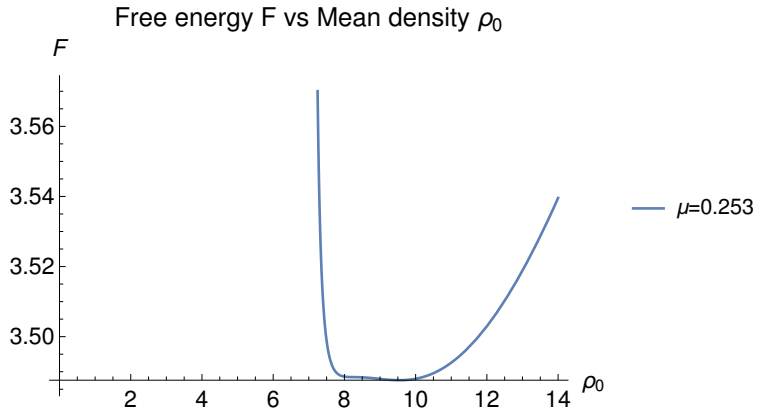

Figure 4.11: Free energy profile for a polymer as a function of average density ρ_0, for the pressure $\mu = 0.253$ dimensionless and disorder parameter $R = 0.347$, spring stiffness $k = 1.2$ units, $\kappa = 10$ units and cut-off Λ. The zero mode parameters were chosen to be $\tilde{Q}^{(1)}_{ii}(0) = 1$, $\tilde{Q}^{(2)}_{ii}(0) = 1$ and $\tilde{Q}^{(s)}_{ij}(0) = 1$.

The figure fig. 4.12 below represents the increase and decrese of the pressure μ, respectively, with respect to the previous profile fig. 4.11.

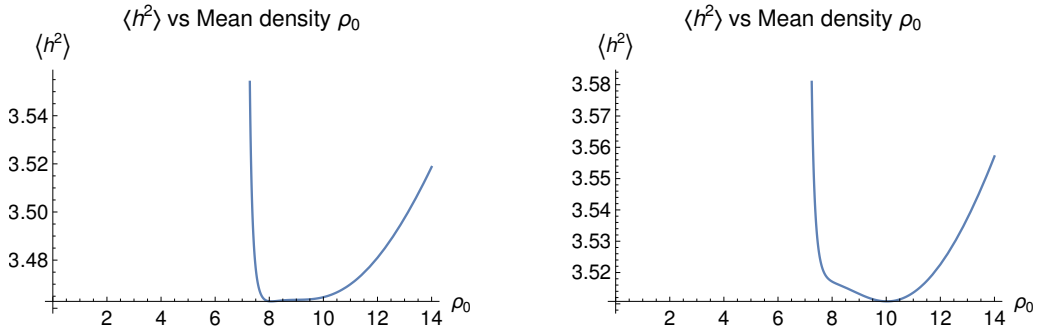

Figure 4.12: Free energy profile for a polymer as a function of average density ρ_0, for the pressure $\mu = \{0.256,\ 0.251\}$ dimensionless, respectively and disorder parameter $R = 0.347$, spring stiffness $k = 1.2$ units, $\kappa = 10$ units , and cut-off Λ. The zero mode parameters were chosen to be $\tilde{Q}^{(1)}_{ii}(0) = 1$, $\tilde{Q}^{(2)}_{ii}(0) = 1$ and $\tilde{Q}^{(s)}_{ij}(0) = 1$.

4.3.2 The zero and infinite limits effect of the disorder parameter R on the free energy profile

The limit $R \to \infty$ which is equivalent to $\rho(x) \to \rho_0$ representing the uniform discrete adhesion scenario is shown below in fig. 4.13.

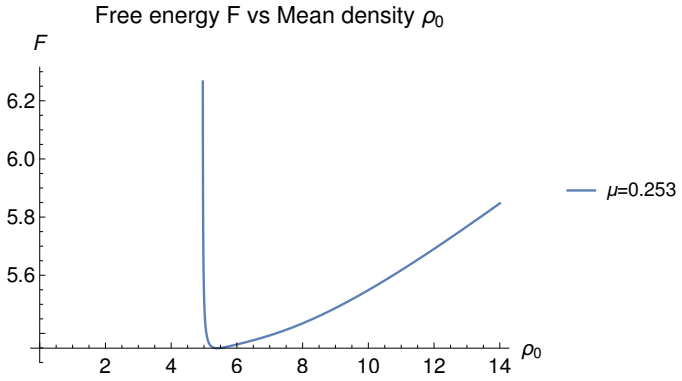

Figure 4.13: Free energy profile for a polymer as a function of average density ρ_0, for the pressure $\mu = 0.253$ and disorder parameter $R = 1$, and cut-off Λ. The zero mode parameters were chosen to be $\tilde{Q}^{(1)}_{ii}(0) = 1$, $\tilde{Q}^{(2)}_{ii}(0) = 1$ and $\tilde{Q}^{(s)}_{ij}(0) = 1$.

This graphical depiction, fig. 4.13, of the limit $R \to \infty$ (equivalent of $\rho(x) \to \rho_0$) is consistent with the recast result of equation (2.1.10) depicted in fig. 4.4. The opposite limit $R \to 0$ (equivalent of $\rho_0 \to 0$) is also held.

4.3.3 RSB average height fluctuations $\langle h \rangle$ and $\langle h^2 \rangle$

Similar to the section 4.2.3 for the RSB solution we plot the graphs of the average height and square fluctuations $\langle h \rangle = \langle \sum_i \int_0^L dx \; h_i(x) \rangle = \frac{\partial \ln Z}{\partial \mu}$ and $\langle h^2 \rangle = \langle \sum_i \int_0^L dx \; h_i^2(x) \rangle = \frac{\partial \ln Z}{\partial \gamma}$, respectively. These are depicted in the following graphs fig. 4.14 to fig. 4.18 as functions of either average density ρ_0 or pressure μ. The cut

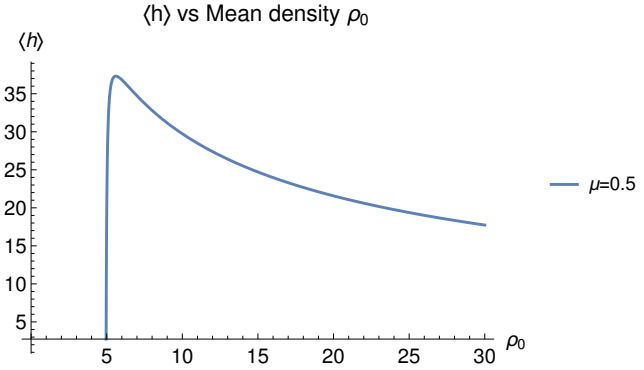

Figure 4.14: Average height $\langle h \rangle$ profile for a polymer chain as a function of average density ρ_0, pressure $\mu = 0.5$ dimensionless, disorder parameter $R = 1.0$ units and $\Lambda = 10\sqrt{\frac{4\rho_0\beta k L^2}{\kappa}}$, $\beta = 1$, $k = 0.91$ and $\kappa = 6$ units. The zero mode parameters were chosen to be $\tilde{Q}_{ii}^{(1)}(0) = 1$, $\tilde{Q}_{ii}^{(2)}(0) = 1$ and $\tilde{Q}_{ij}^{(s)}(0) = 1$.

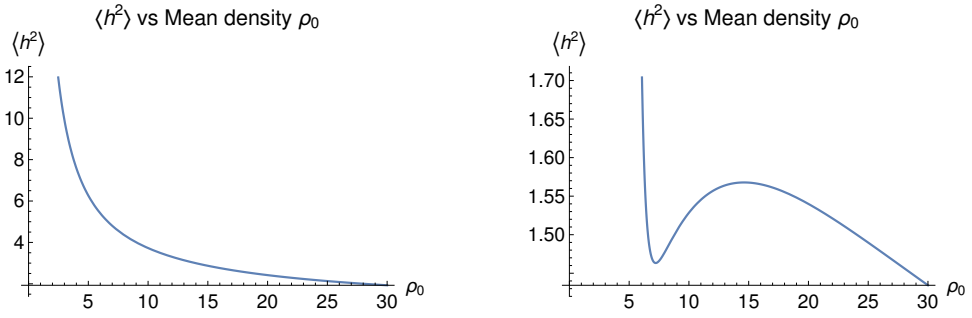

Figure 4.15: Average square fluctuations $\langle h^2 \rangle$ profile for a polymer chain as a function of average density ρ_0, pressure $\mu = \{0,\ 0.5\}$ dimensionless, disorder parameter $R = 1.0$ units and $\Lambda = 10\sqrt{\frac{4\rho_0\beta k L^2}{\kappa}}$, $\beta = 1$, $k = 0.91$ and $\kappa = 6$ units. The zero mode parameters were chosen to be $\tilde{Q}_{ii}^{(1)}(0) = 1$, $\tilde{Q}_{ii}^{(2)}(0) = 1$ and $\tilde{Q}_{ij}^{(s)}(0) = 1$.

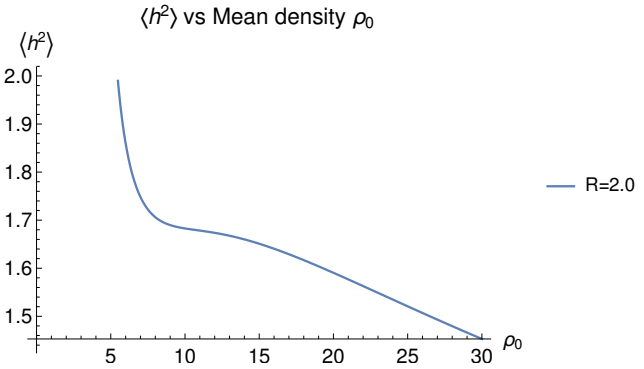

Figure 4.16: The role of the disorder R on the average square fluctuations $\langle h^2 \rangle$ profile for a polymer chain as a function of density ρ_0 for the pressure $\mu = 0.5$, disorder parameter $R = 2.0$ units and $\Lambda = 10\sqrt{\frac{4\rho_0\beta k L^2}{\kappa}}$, $\beta = 1$, $k = 0.91$ and $\kappa = 6$ units. The zero mode parameters were chosen to be $\tilde{Q}_{ii}^{(1)}(0) = 1$, $\tilde{Q}_{ii}^{(2)}(0) = 1$ and $\tilde{Q}_{ij}^{(s)}(0) = 1$.

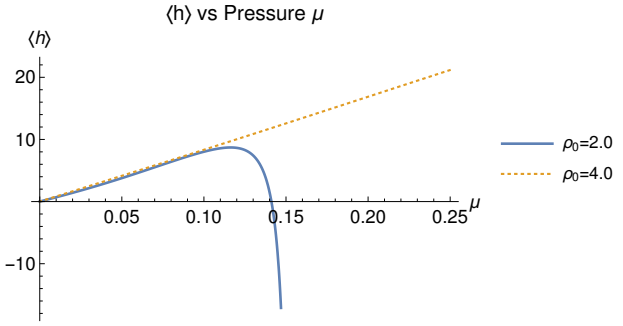

Figure 4.17: Average height $\langle h \rangle$ profile for a polymer chain as a function of pressure μ, tether density $\rho_0 = \{2.0,\ 4.0\}$ units, disorder parameter $R = 1.6$ units and $\Lambda = 10\sqrt{\frac{4\rho_0\beta k L^2}{\kappa}}$, $\beta = 1$, $k = 0.91$ and $\kappa = 6$ units. The zero mode parameters were chosen to be $\tilde{Q}_{ii}^{(1)}(0) = 1$, $\tilde{Q}_{ii}^{(2)}(0) = 1$ and $\tilde{Q}_{ij}^{(s)}(0) = 1$.

The reversal of the growing trend of the average height fluctuation $\langle h \rangle$ at higher pressure μ for fewer tethers signals the stretching limit in our model. Stiffer tethers or higher tether density can hold for larger pressure domain. Larger polymer intersegments require lesser pressure to increase their effective height.

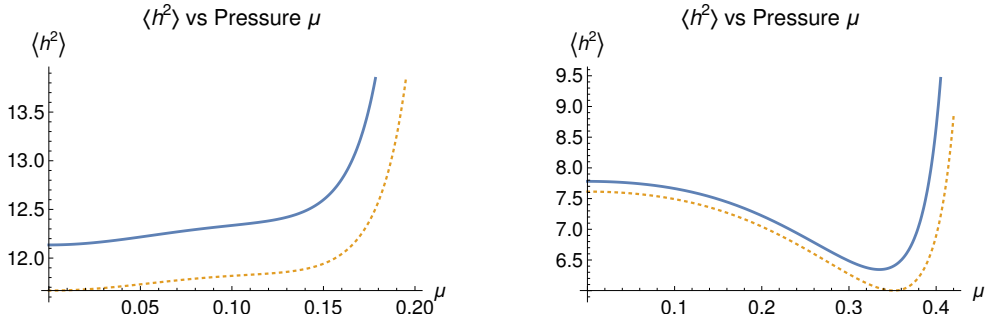

Figure 4.18: Average square fluctuations $\langle h^2 \rangle$ profile for a polymer chain as a function of pressure μ, tether density $\rho_0 = \{(2.0, 2.1);\ (4.0, 4.1)\}$ units respectively, disorder parameter $R = 1.6$ units and $\Lambda = 10\sqrt{\frac{4\rho_0 \beta k L^2}{\kappa}}$, $\beta = 1$, $k = 0.91$ and $\kappa = 6$ units. The zero mode parameters were chosen to be $\tilde{Q}_{ii}^{(1)}(0) = 1$, $\tilde{Q}_{ii}^{(2)}(0) = 1$ and $\tilde{Q}_{ij}^{(s)}(0) = 1$.

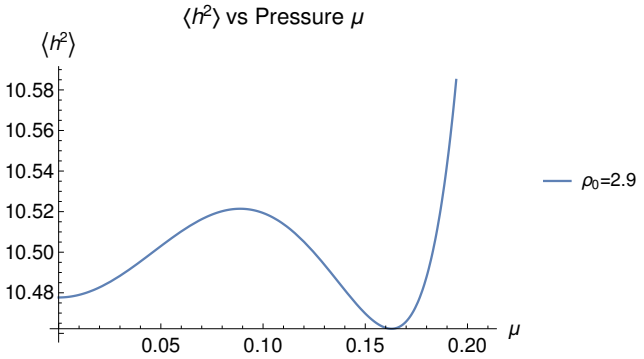

Figure 4.19: Average square fluctuations $\langle h^2 \rangle$ profile for a polymer chain as a function of pressure μ, the tether density $\rho_0 = 2.9$ units, disorder parameter $R = 1.6$ units and $\Lambda = 10\sqrt{\frac{4\rho_0 \beta k L^2}{\kappa}}$, $\beta = 1$, $k = 0.91$ and $\kappa = 6$ units. The zero mode parameters were chosen to be $\tilde{Q}_{ii}^{(1)}(0) = 1$, $\tilde{Q}_{ii}^{(2)}(0) = 1$ and $\tilde{Q}_{ij}^{(s)}(0) = 1$.

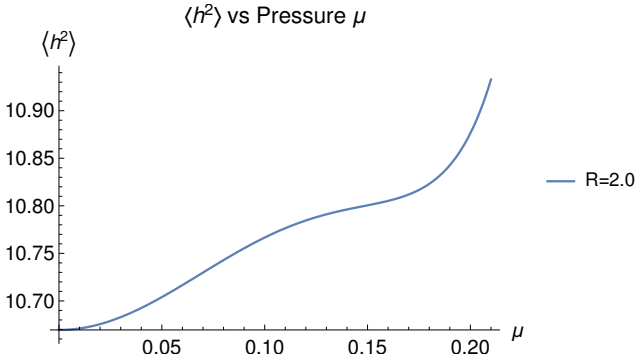

Figure 4.20: The role of the disorder parameter R if increased to $R = 2.0$ units on the average square fluctuations $\langle h^2 \rangle$ profile for a polymer chain as a function of pressure μ, the tether density $\rho_0 = 2.9$ units and $\Lambda = 10\sqrt{\frac{4\rho_0 \beta k L^2}{\kappa}}$, $\beta = 1$, $k = 0.91$ and $\kappa = 6$ units. The zero mode parameters were chosen to be $\tilde{Q}_{ii}^{(1)}(0) = 1$, $\tilde{Q}_{ii}^{(2)}(0) = 1$ and $\tilde{Q}_{ij}^{(s)}(0) = 1$.

In fig. 4.18 we observe an increasing monotonic behavior of the square fluctuations $\langle h^2 \rangle$ with the growing pressure μ for some relatively smaller choice values of the average density ρ_0. However, for relatively larger choice values of the average density ρ_0 this monotonic behaviour changes. A decrease of the square fluctuations $\langle h^2 \rangle$ is now exhibited for the lower domain of the pressure μ before the increasing behaviour for the upper domain of the pressure. In fig. 4.19 we see these behaviours combined for a choice of average density ρ_0 values that lie in between the first two. That is, we observe a non-monotonic relationship between the square fluctuations $\langle h^2 \rangle$ and the pressure μ that has both the growing domain of the square fluctuations and the decreasing domain of the square fluctuations before the again growing domain that is displayed in the figure fig. 4.18. When we increase the measure of the disorder, the parameter R – fig. 4.20, we recover a monotonic square fluctuations pressure relationship. These figures demonstrates a clear role of the pressure μ in the square fluctuations $\langle h^2 \rangle$. Collectively, for the bubbles of varying sizes, there exist a tether density ρ_0 domain such that the pressure μ acts anologous to a dissipative force in non-equilibrium statistical physics of damped harmonic oscillator. This happens for a higher tether density. At such a level of tether density the polymer chain segments are short yet still possessing its stretchable (flexible) nature, therefore with minimal fluctuations. This is in contrast to the lower density scenario where the pressure stretches the intersegment polymers. Beyond these characteristic behaviours the further stretching of the polymer segments inclunding the smaller sized ones into *bubbles* is exhibited. This is evidenced by the average height fluctuations $\langle h \rangle$ in fig. 4.17.

4.4 RS and RSB relative results observations

We have derived *analytic* free energy functions or generating functions for both the RSA and wRSB scenarios. Whilst we observed a minima disappearance trend to a monotonic function of average density ρ_0 with the pressure increase in the RSA this is however not always true for the wRSB. In figure fig. 4.11, the wRSB free energy, this function is rather displaying two minima at some pressure domain larger than zero.

We also derived the fluctuation functions, $\langle h \rangle$ and $\langle h^2 \rangle$, in both approximations as a function of average density ρ_0. A comparitive figure fig. 4.21 of the $\langle h^2 \rangle$ functions as a function of the tether density ρ_0 in both evaluation is shown below.

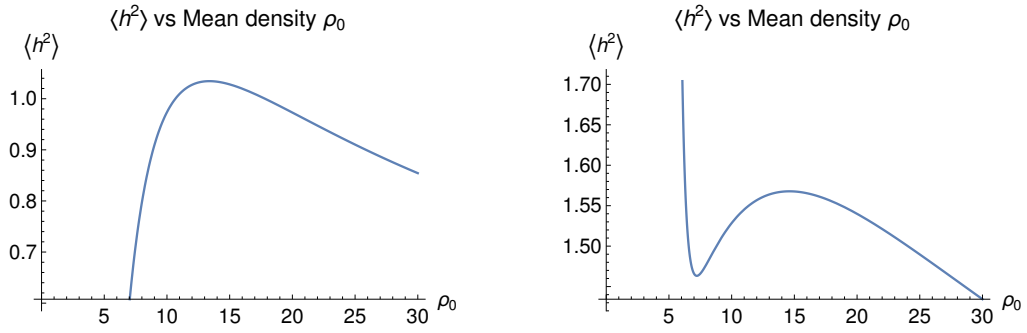

Figure 4.21: Replica Symmetry (Left) and Breaking (Right) square fluctuations $\langle h^2 \rangle$ profiles for a polymer chain as a function of tether density ρ_0 for the pressure $\mu = 0.5$ dimensionless and the disorder parameter $R = 1$ units and $\Lambda = 10\sqrt{\frac{4\rho_0 \beta k L^2}{\kappa}}$, $\beta = 1$, $k = 0.91$ and $\kappa = 6$ units. The zero mode parameters were chosen to be $\tilde{Q}_{ii}^{(1)}(0) = 1$, $\tilde{Q}_{ii}^{(2)}(0) = 1$ and $\tilde{Q}_{ij}^{(s)}(0) = 1$.

A further comparitive figure fig. 4.22 of the $\langle h^2 \rangle$ functions in both evaluation is shown below. However, here we demonstrate the effect of reduction of the disorder towards a homogeneous system in the two evaluations by increasing the parameter R .

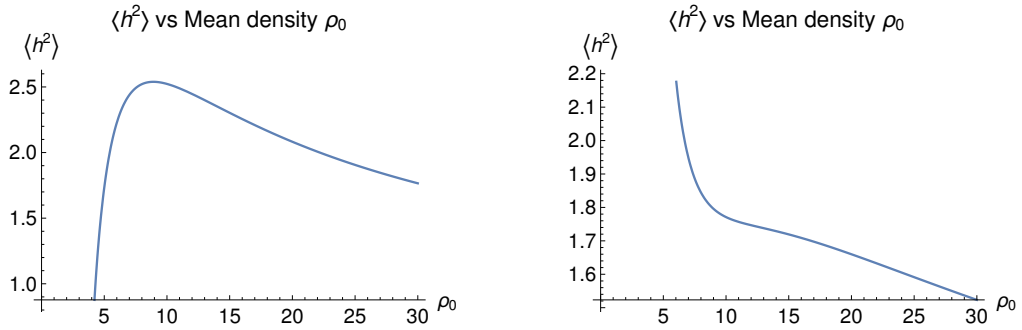

Figure 4.22: Effect of increasing the disorder parameter $R = 1.6$ to $R = 2$ units. Replica Symmetry (Left) and Breaking (Right) square fluctuations $\langle h^2 \rangle$ profiles for a polymer chain as a function of tether density ρ_0 for the pressure $\mu = 0.5$ dimensionless and $\Lambda = 10\sqrt{\frac{4\rho_0\beta k L^2}{\kappa}}$, $\beta = 1$, $k = 0.91$ and $\kappa = 6$ units. The zero mode parameters were chosen to be $\tilde{Q}_{ii}^{(1)}(0) = 1$, $\tilde{Q}_{ii}^{(2)}(0) = 1$ and $\tilde{Q}_{ij}^{(s)}(0) = 1$.

A similar comparitive figure fig. 4.23 of the $\langle h^2 \rangle$ functions, however, as a function of the pressure μ in both evaluation is shown below.

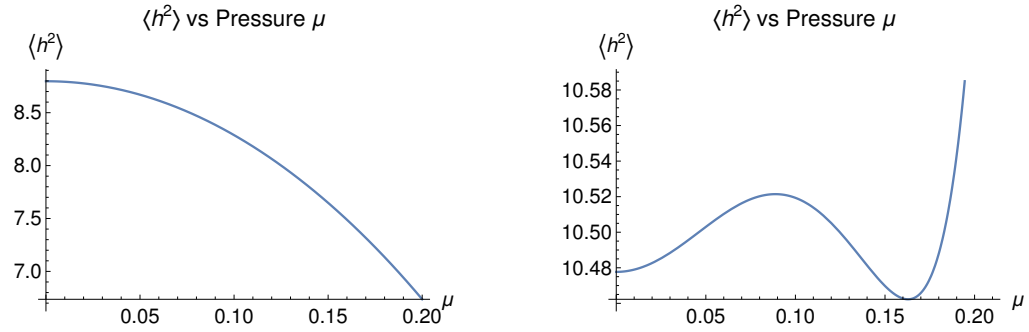

Figure 4.23: Replica Symmetry (Left) and Breaking (Right) square fluctuations $\langle h^2 \rangle$ profiles for a polymer chain as a function of pressure μ for the tether density $\rho_0 = 2.9$ and the disorder parameter $R = 1.6$ units and $\Lambda = 10\sqrt{\frac{4\rho_0\beta k L^2}{\kappa}}$, $\beta = 1$, $k = 0.91$ and $\kappa = 6$ units. The zero mode parameters were chosen to be $\tilde{Q}_{ii}^{(1)}(0) = 1$, $\tilde{Q}_{ii}^{(2)}(0) = 1$ and $\tilde{Q}_{ij}^{(s)}(0) = 1$.

If we increase the tether elasticity by choosing the lower value for k to be 0.88 units instead of 0.91 units we obtain fig. 4.24

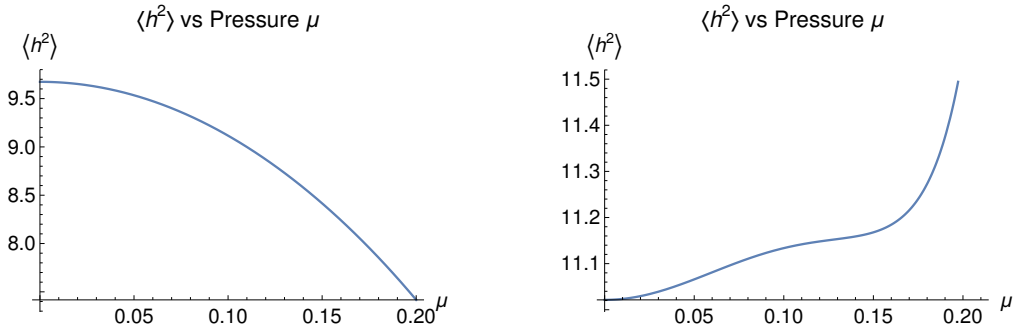

Figure 4.24: Replica Symmetry (Left) and Breaking (Right) square fluctuations $\langle h^2 \rangle$ profiles for a polymer chain as a function of pressure μ for the tether density $\rho_0 = 2.9$ and the disorder parameter $R = 1.6$ units and $\Lambda = 10\sqrt{\frac{4\rho_0 \beta k L^2}{\kappa}}$, $\beta = 1$, $k = 0.88$ and $\kappa = 6$ units. The zero mode parameters were chosen to be $\tilde{Q}_{ii}^{(1)}(0) = 1$, $\tilde{Q}_{ii}^{(2)}(0) = 1$ and $\tilde{Q}_{ij}^{(s)}(0) = 1$.

Therefore, the softnening of the tethers yields a monotonic behavior of the height square fluctuations $\langle h^2 \rangle(\mu)$ for the RSB construction. This figure also shows the $\langle h^2 \rangle(\mu = 0)$ upward translation.

A further comparitive figure fig. 4.25 of the $\langle h^2 \rangle$ functions in both evaluation is shown below. However, here we demonstrate the effect of reduction of the disorder towards a homogeneous system in the two evaluations by increasing the parameter R .

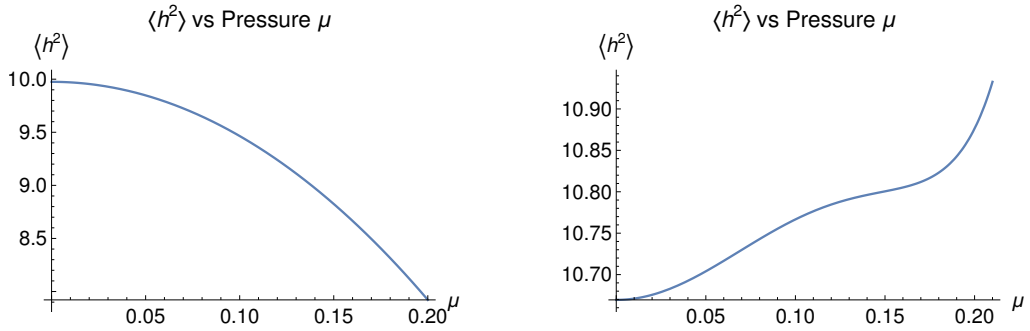

Figure 4.25: Effect of increasing the disorder parameter $R = 1.6$ to $R = 2$ units. Replica Symmetry (Left) and Breaking (Right) square fluctuations $\langle h^2 \rangle$ profiles for a polymer chain as a function of pressure μ for the tether density $\rho_0 = 2.9$ and $\Lambda = 10\sqrt{\frac{4\rho_0 \beta k L^2}{\kappa}}$, $\beta = 1$, $k = 0.91$ and $\kappa = 6$ units. The zero mode parameters were chosen to be $\tilde{Q}_{ii}^{(1)}(0) = 1$, $\tilde{Q}_{ii}^{(2)}(0) = 1$ and $\tilde{Q}_{ij}^{(s)}(0) = 1$.

$\langle h^2 \rangle$ for the RSA exhibits a monotonic decrease towards zero for all pressure. In the wRSB, however, we observe a non-monotonic relationship as

shown in fig. 4.23 for specific pressure value(s) larger than zero. The monotonicity can be recovered by increasing the disorder parameter R, effectively reducing the tether distribution variance, as shown in fig. 4.25.

Similar observations are made for the case now of $\langle h^2 \rangle$ as function of the pressure μ. That is, there exist non-monotonic behavior in the wRSB as the pressure is increased for specific value(s) of the average density ρ_0. By reducing the average density ρ_0 or increasing the disorder parameter R the monotonicity is recovered.

This behaviour reflects the subtle interplay of the quenched discrete harmonic confinement with the pressure. That is the interplay of the elasticity of the tethers, the polymer chain (and arguably a membrane) as well as the pressure. The quenched *random* distribution of the finite stretching tethers is responsible for this behavior. This behavior is not observable upon the RS approximation thus, as often understood – see section 1.7, RSA cannot comprehensively capture the disordered nature physics.

The length scales in this problem are the average tether separation ρ_0, the tether elasticity k and the membrane elasticity κ. In the quenched tether position distribution scenario the pressure μ cannot change the average separation ρ_0 length scale. When the polymer (or membrane) arcsegments are inflated by growing the pressure it is only those of large tether separation that will be first to exhibit greater height fluctuations. For the smaller separation length scale arcsegments a large pressure is required in order to grow the height fluctuations. Interestingly, our results show that, a larger pressure also reduces the tether elasticity length scale k.

This is in contrast to the annealed tether position distribution whereby the pressure μ can possibly reduce the multiple bubbles to a single large bubble.

4.5 The effect of a fluctuating substrate

Our overaching goal is to model a composite system of a membrane tethered onto a two dimensional elastic network. Such a system has to treat the collective properties of an elastic network associated with disorder in its crosslinking. That is, a system of combined fluctuations and disorder associated with tether distribution and disorder associated with crosslinking. In the preceding section we have modelled a limit case where the substrate is a hard in the sense that the tether *positions* do not posess the transverse degree of freedom. However, this does not treat a hardwall often model by delta function in excluded volume problems in treatment of a repulsive potential. In this chapter we shall treat the aspect of an elastic substrate albeit of a polymer substrate represented by the second field $h^{(2)}(x)$ rather than a network.

Subsequently, extending the model 4.1.1, we now have to treat

$$\begin{aligned} Z &= \int \mathcal{D}h^{(1)}\mathcal{D}h^{(2)} \sum_{\{\tau=0,\,1\}} \exp\left\{ -\frac{\kappa_1}{2}\int_0^L \mathrm{d}x \left(\frac{\partial h^{(1)}}{\partial x}\right)^2 - \frac{\kappa_2}{2}\int_0^L \mathrm{d}x \left(\frac{\partial h^{(2)}}{\partial x}\right)^2 \right. \\ &\quad +\mu\int_0^L \mathrm{d}x\ \left(h^{(1)}(x) - h^{(2)}(x)\right) - \frac{\beta k}{2}\sum_i^N \int_0^L \mathrm{d}x\ \tau_i^2 \left(h^{(1)}(x_i) - h^{(2)}(x_i)\right)^2 \\ &\quad \left. -\beta\epsilon\sum_i \tau_i \right\}. \end{aligned} \tag{4.5.1}$$

The study of this model shall follow closely to that of the models of the previous sections 4.2 and 4.3. Hence, we undertake the replica approach to determine the disordered free energy F. Our goal, yet again, becomes that of evaluating

$$-\beta\langle F\rangle = \lim_{n\to 0}\frac{\langle Z^n\rangle - 1}{n} \tag{4.5.2}$$

upon the Gaussian disorder distribution

$$P[\rho(x)] \sim \exp\left(-\frac{R}{2}\int_0^L \mathrm{d}x\,(\rho(x)-\rho_0)^2\right). \tag{4.5.3}$$

The tether density is defined by $\rho(x) = \sum_i^N \delta(x - x_i)$. The partition function then becomes

$$\begin{aligned} Z &= \int \mathcal{D}h^{(1)}\mathcal{D}h^{(2)} \exp\left\{ -\frac{\kappa_1}{2}\int \mathrm{d}x \left(\frac{\partial h^{(1)}}{\partial x}\right)^2 - \frac{\kappa_2}{2}\int \mathrm{d}x \left(\frac{\partial h^{(2)}}{\partial x}\right)^2 \right. \\ &\quad -\mu\int_0^L \mathrm{d}x\ \left(h^{(1)}(x) - h^{(2)}(x)\right) - \frac{\beta k}{2}\int \mathrm{d}x\ \rho(x)\left(h^{(1)}(x) - h^{(2)}(x)\right)^2 \\ &\quad \left. -\beta\epsilon\int \mathrm{d}x\ \rho(x) \right\}. \end{aligned} \tag{4.5.4}$$

If we perform a transformation

$$f(x) = \frac{1}{2}\left(h^{(1)}(x) - h^{(2)}(x)\right) \text{ and } g(x) = \frac{1}{2}\left(h^{(1)}(x) + h^{(2)}(x)\right), \tag{4.5.5}$$

we obtain

$$\begin{aligned} Z &= \int \mathcal{D}f(x)\mathcal{D}g(x) \exp\left\{ -\frac{\kappa_1+\kappa_2}{2}\int \mathrm{d}x \left(\frac{\partial f(x)}{\partial x}\right)^2 \right. \\ &\quad -\frac{\kappa_1+\kappa_2}{2}\int \mathrm{d}x \left(\frac{\partial g(x)}{\partial x}\right)^2 - \frac{\kappa_1-\kappa_2}{2}\int \mathrm{d}x \left(\frac{\partial f(x)}{\partial x}\right)\left(\frac{\partial g(x)}{\partial x}\right) \\ &\quad \left. -2\mu\int \mathrm{d}x\ f(x) - 2\beta k\int \mathrm{d}x\ \rho(x) f^2(x) - \beta\epsilon\int \mathrm{d}x\ \rho(x) \right\}. \end{aligned} \tag{4.5.6}$$

Therefore this equation (4.5.6) leads to the disorder averaged replicated partition function

$$\begin{aligned}\langle Z^n\rangle &= \int\prod_\alpha \mathcal{D}f_\alpha(x)\mathcal{D}g_\alpha(x)\exp\left\{-\frac{1}{2}\sum_\alpha\int \mathrm{d}x\left[\tilde{\kappa}\left[\left(\frac{\partial f_\alpha(x)}{\partial x}\right)^2\right.\right.\right.\\ &\left.\left.\left.+\left(\frac{\partial g_\alpha(x)}{\partial x}\right)^2\right]+2\bar{\kappa}\left(\frac{\partial f_\alpha(x)}{\partial x}\right)\left(\frac{\partial g_\alpha(x)}{\partial x}\right)+\mu f_\alpha(x)+\gamma f_\alpha^2(x)\right]\right.\\ &\left.+\frac{\Delta}{2}\int \mathrm{d}x\left(\sum_\alpha f_\alpha^2(x)\right)^2\right\}. \quad (4.5.7)\end{aligned}$$

The parameters $\tilde{\kappa}$, $\bar{\kappa}$, μ, γ and Δ represents $\tilde{\kappa}=\kappa_1+\kappa_2$, $\bar{\kappa}=\kappa_1-\kappa_2$, $\tilde{\mu}=-4\mu$, $\tilde{\gamma}=4\rho_0\beta k\left(1-\frac{2n\beta\epsilon}{R}\right)$ and $\tilde{\Delta}=16\frac{\beta^2k^2}{4R}$. This can be seen, effectively, as a doubling of the pressure μ and a quadrupling of the spring coefficient k.

If we now complete the square with respect to the $g(x)$ function we obtain

$$\begin{aligned}\langle Z^n\rangle &= \text{const.}\times\exp\left(-\frac{n}{2}\mathrm{tr}\ln[-\tilde{\kappa}\delta(x-x')\partial_{xx}]\right)\int\prod_\alpha\mathcal{D}f_\alpha(x)\\ &\exp\left\{-\frac{1}{2}\sum_\alpha\int\mathrm{d}x\left[\left(\tilde{\kappa}-\frac{\bar{\kappa}^2}{\tilde{\kappa}}\right)\left(\frac{\partial f_\alpha(x)}{\partial x}\right)^2+\tilde{\mu}f_\alpha(x)+\tilde{\gamma}f_\alpha^2(x)\right]\right.\\ &\left.+\frac{\tilde{\Delta}}{2}\int\mathrm{d}x\left(\sum_\alpha f_\alpha^2(x)\right)^2\right\}. \quad (4.5.8)\end{aligned}$$

Except for the renormalization of the parameters, this expression is similar to the one of the hard substrate equation (4.1.13) with an additional term $\exp\left(-\frac{n}{2}\mathrm{tr}\ln[-\tilde{\kappa}\delta(x-x')\partial_{xx}]\right)$. Therefore we obtain a similar form of both the Replica Symmetry (and Breaking) disordered free energy $\langle F\rangle$.

In the case of the Replica Symmetry the free energy F is given by (4.2.38).

Therefore,

$$
\begin{aligned}
-\beta\langle F\rangle \approx & \left(-\frac{1}{2}\mathrm{tr}\ln[-\tilde{\kappa}\delta(x-x')\partial_{xx}] - \frac{1}{2}\mathrm{tr}\ln A(x,x') + \frac{1}{8}\frac{\tilde{\mu}^2\delta(0)}{\tilde{\gamma}}\right. \\
& \left. -2\sum_i \int \frac{\mathrm{d}q}{(2\pi)^d}\frac{\tilde{Q}_{ii}(0)}{\kappa q^2+\tilde{\gamma}} - \frac{\tilde{\mu}^2\tilde{Q}_{ii}(0)}{2\tilde{\gamma}^2} + \frac{\tilde{\mu}^2}{2\tilde{\gamma}^2}\tilde{Q}_{ij}(0)\right) \\
& -\frac{1}{2}\left(\sum_q \ln\left(\frac{1}{\tilde{\Delta}} - 2\Omega^{-1}(q) - \frac{\tilde{\mu}^2}{\tilde{\gamma}^2(\kappa q^2+\tilde{\gamma})}\right)\right) \\
& +\frac{1}{4}\left(\sum_q \ln\left(\frac{1}{\tilde{\Delta}} - 2\Omega^{-1}(q)\right)\right) \\
& -\frac{1}{4}\sum_q \frac{\left[\left(\frac{1}{\tilde{\Delta}} - 2\Omega^{-1}(q) - \frac{\tilde{\mu}^2}{\tilde{\gamma}^2(\kappa q^2+\tilde{\gamma})}\right)^{-1}\frac{\tilde{\mu}^4}{\tilde{\gamma}^4(\kappa q^2+\tilde{\gamma})^2} + \frac{\tilde{\mu}^2}{\tilde{\gamma}^2(\kappa q^2+\tilde{\gamma})}\right]}{\frac{1}{\tilde{\Delta}} - 2\Omega^{-1}(q)}. \qquad (4.5.9)
\end{aligned}
$$

In the complementary case of the weak Replica Symmetry Breaking $\langle F\rangle$ is given by (4.3.5). Therefore,

$$
\begin{aligned}
-\beta\langle F\rangle \approx & -\frac{1}{2}\mathrm{tr}\ln[-\tilde{\kappa}\delta(x-x')\partial_{xx}] - \ \mathrm{tr}\ln A(x,x') + \frac{\tilde{\mu}^2\delta(0)}{\tilde{\gamma}} + 2\tilde{\mu}^2\frac{Q^{(s)}_{bc}(0)}{\tilde{\gamma}^2} \\
& -\tilde{\mu}^2\frac{\left(Q^{(1)}_{ii}(0)+Q^{(2)}_{ii}(0)\right)}{\tilde{\gamma}^2} - \sum_i \int \frac{\mathrm{d}q}{(2\pi)^d}\frac{\left(\tilde{Q}^{(1)}_{ii}(0)+\tilde{Q}^{(2)}_{ii}(0)\right)}{\kappa q^2+\tilde{\gamma}} \\
& -\sum_q \ln\left(\frac{1}{\tilde{\Delta}} - 2\Omega^{-1}(q) - \frac{2\tilde{\mu}^2}{\tilde{\gamma}^2(\kappa q^2+\tilde{\gamma})}\right) + \frac{1}{4}\sum_q \ln\left(\frac{1}{\tilde{\Delta}} - 4\Omega^{-1}(q)\right) \\
& -\frac{1}{4}\sum_q \frac{\left[\left(\frac{1}{\tilde{\Delta}} - 2\Omega^{-1}(q) - \frac{2\tilde{\mu}^2}{\tilde{\gamma}^2(\kappa q^2+\tilde{\gamma})}\right)^{-1}\frac{4\tilde{\mu}^4}{\tilde{\gamma}^4(\kappa q^2+\tilde{\gamma})^2} + \frac{4\tilde{\mu}^2}{\tilde{\gamma}^2(\kappa q^2+\tilde{\gamma})}\right]}{\frac{1}{\tilde{\Delta}} - 4\Omega^{-1}(q)} \\
& +\frac{1}{4}\sum_q \frac{\frac{4\tilde{\mu}^2}{\tilde{\gamma}^2(\kappa q^2+\tilde{\gamma})}}{\frac{1}{\tilde{\Delta}} - 4\Omega^{-1}(q)}. \qquad (4.5.10)
\end{aligned}
$$

where $\kappa = \left(\tilde{\kappa} - \frac{\bar{\kappa}^2}{\tilde{\kappa}}\right)$ is the effective elastic measure.

4.6 Summary

In this chapter we have explored the quenched inhomogeneous coupling of a polymer or membrane to a substrate under a spatially uniform pressue μ. This is in contrast to the earlier treatment of Chapter 3 where the tethers still had the lateral fluctuation degree of freedom.We investigated this for a

hard substrate and an elastic substrate modelled by a polymer or membrane. The substrate is hard in the sense that the tether *position* do not posess the transverse degree of freedom. The hardwall repulsive potential often model by delta function in excluded volume problems is not treated. Given the nature of the spatial distribution we treated the statics of this problem by the replica method. This replica treatment was pursued to first stage or weak Replica Symmetry Breaking (wRSB). We derived the associated generic free energies F in equations (4.2.39) and (4.3.5)–(D.4.1), for the hard substrate case, for the Replica Symmetry Approximation (RSA) and its extension, respectively. In the elastic or fluctuating substrate case the generic free energies F are given by equations (4.5.9) and (4.5.10) where the pressure, spring stiffness and bending rigidity parameters μ, k and κ, respectively, are now renomarlized in relation to the hard substrate model.

In the RSA we observed a single intermediate minimum. In the extension of wRSB a second intermediate minimum appears. The elastic substrate model consideration of coupled fluctuations has a similar structure as that of the hard substrate. However, there exist an additional term that is reponsible for the transverse translation of the energy profiles. More important is the renormalization of the parameters μ, k and κ. The relative physics of the different models arise from this. The pressure μ becomes doubled, the spring coefficient or elasticity k quadrupled and the effective elastic measure or 'Kuhn length/area' is given by $\kappa = \frac{4\,\kappa_1\kappa_2}{\kappa_1+\kappa_2}$. Therefore, the critical behaviour observed in the hard substrate case is now defined by the relationship between the pressure and the elasticity of the tethers. At a simple analysis, less pressure μ, specifically, half of the hard substrate case pressure will now be required to observe a similar critical behaviour if the tether elasticity was softened by a factor of 4 or the disorder R parameter is increased sufficiently for the membrane-substrate of equivalent elasticity. The increase of the disorder parameter R means more homogeneity in the tether distribution. This elasticity can be viewed in context of the tether density ρ_0! One may ask. At a similar pressure μ revealing the basic double well behaviour as function of ρ_0 in the hard substrate case. How many tethers N do we need to add given certain relative bending rigidities of the membranes or polymers? Effectively the average tether density ρ_0. Alternatively, we observe that the rate of entropic gain surpasses the rate of energetic loss at a lower tether density average. Therefore the integrity of the system requires less average tether density in relation to the hard substrate when the substrate is elastic. The numerical exploration of these fluctuating substrate results in equation (4.5.10) as a function of average tether density ρ_0 and pressure μ exhibits similar features to the Replica Symmetry calculation that lead us to the Symmetry Breaking calculation. Subsequently, we suggests that at least a second stage Replica Symmetry Breaking is necessary in order to observe the type of results we obtained in the Symmetry Breaking calculation.

In terms of the fluctuation spectrum $\langle h^2 \rangle$ as a measure function of the pres-

sure μ parameter. We observe that the monotonicity of the average square fluctuations $\langle h^2 \rangle$ with pressure becomes non-monotonic. The Replica Symmetry Breaking treatment of the quenched distribution of tether positions is responsible for this.

The Replica Symmetry Breaking provides more accurate, reliable, consistent results of the measurable quantities over a wide range of testing values in comparison to its counterpart. The subtle relationship between tether and membrane elasticity for a quenched random position distribution of the tethers is well articulated.

Chapter 5

Conclusion and outlook

We have investigated the role of the pressure, the nature of adhesion (homogeneous or inhomogeneous) as well as the role of a soft substrate. In terms of the fluctuation spectrum $\langle h^2 \rangle$ as a measure function of the pressure μ parameter. We, generally, observe that the average square fluctuations $\langle h^2 \rangle$ increases with the pressure. However, for the discrete inhomogeneous adhesion, when the positions of tethers distribution is quenched this general behaviour is altered.

We observe that for the elastic substrate the rate of entropic gain surpasses the rate of energetic loss at a lower tether density average. Therefore the integrity of the system requires less average tether density in relation to the hard substrate when the substrate is elastic. The numerical exploration of these fluctuating substrate results in equation (4.5.10) as a function of average tether density ρ_0 and pressure μ suggests that at least a second stage Replica Symmetry Breaking is necessary in order to observe the double well free energy F as a function of average tether density.

If time permitted we would have furthered this study as follows. We would have extended the current models for surfaces and include the attached-detach degree of freedom to the tethers as suggested [84] in the biological problem of cells. Secondly, the quest of our study is the detail modelling of structure of a surface-cytoskeleton network system, this needs a more detailed treatment of the elastic two dimensional *network*. This network treatment must account for the spectrin elastic properties. That is, the small stretching and the large stretching behaviour of these filaments. The ideas that we would have explored would probably centre on the grand canonical treatment or monomer ensemble technique [85; 86]. This we would have combined with the field theory constructed by Edwards [87; 88; 89].

Further, the remodelling or structural transformation [16] of this network requires innovative treatment.

Finally, we would have reformulated this problem in the dynamical or

Langevin treatment of Martin Siggia Rose [90]. This is partly motivated by the result of multiple ground states we obtained in the weak replica symmetry treatment. Secondly, it would have been more appropriate in order to account for the treatment of the dynamic dissociations of the tethers.

List of References

[1] J.F. Wheather, J. Phys. A **27**, 3323 (1994).

[2] B. Alberts, D. Bray, J. Lewis, M. Raff, and K. Roberts, and J.D. Watson, *Molecular Biology of the Cell*, Second edition, (New York: Garland, 1989)

[3] R.E. Hausman and A. A. Moscona, Proc. Natl. Acad. Sci. U.S.A. **73**, 3594 (1976).

[4] M.F. Greaves, J. J. T. Owen, and M. C. Raff, *T and B Lymphocytes: Origins, Properties and Roles in Immune Responses* (American Elsevier, New York, 1974)

[5] H. Berg, F.E. Katz, A. Stein, and G. Gerisch, Proc. Natl. Acad. Sci. U.S.A. **70**, 3150 (1973).

[6] R.L. Hoover, Exp. Cell Res. **87**, 265 (1974).

[7] X. Xu, A. K. Efremov, A. Li, L. Lai, M. Dao, C. T. Lim, and J. Cao, PloS One **8**, e6473 (2013).

[8] K.R. Hughes, G.A. Biagini, and A.G. Craig, Mol. Biochem. Parasitol **169**, 71 (2010).

[9] V. Nussenzweig, Adv. Immunol. **19**, 217 (1974).

[10] H.J. Deuling and W. Helfrich, Biophys. J. **16**, 861 (1976).

[11] F. Brochard and J.F. Lennon,unpublished J. Phys. France **36**, 1035 (1975).

[12] S.R. Keller and R. Skalak, J. Fluid Mech. **120**, 27 (1982).

[13] H. W. Gerald Lim, M. Wortis, and R. Mukhopadhyay, Proc. Natl. Acad. Sci. USA **99**, 16766 (2002).

[14] S. Levin, and R. Korenstein, Biophys. J. **60**, 733 (1991).

[15] M. Paulitschke and G.B. Nash, J. Lab. Clin. Med. **122**, 581 (1993).

[16] H. Shi, Z. Liu, A. Li, J. Yin, A. G. L. Chong, K. S. W. Tan, Y. Zhang, and C.T. Lim, PloS One **8**, e61170 (2013).

[17] W. T. Tse and S.E. Lux, Br Haematol **104**, 2 (1999).

[18] T. Auth and S.A. Safran, Phys. Rev. E **76**, 051910 (2007).

[19] J. Paulose, G.A. Vliegenthart, G. Gommper, and D.R. Nelson, Proc. Natl. Acad. Sci. USA **109**, 19551 (2012).

[20] Y. Park, C. A. Best, K. B. Ramachandra, R. Dasaria, M. S. Felda, T. Kuriabovad, M. L. Henlee, A. J. Levine, and G. Popescu, Proc. Natl. Acad. Sci. USA **107**, 6731 (2010).

[21] J. Li, M. Dao, C.T. Lim and S. Suresh, Biophys. J. **88**, 3707 (2005).

[22] N. Gov, A.G. Zilman, and S. Safran, Phys. Rev. Lett. **90**, 228101 (2003).

[23] A. Zilker, H. Engelhardt, and E. Sackmann, J. Phys. **48**, 2139 (1997).

[24] J.-B. Fournier, D. Lacoste, E. Raphaël, Phys. Rev. Lett. **92**, 018102 (2004).

[25] Y.-Z. Yoon, H. Hong, A. Brown, D. C. Kim, D. J. Kang, V. L. Lew, and P. Cicuta, Biophys. J. **97**, 1606 (2009).

[26] G. Popescu, T. Ikeda, K. Goda, C. A. Best-Popescu, M. Laposata, S. Manley, R. R. Dasari, K. Badizadegan, and M. S. Feld, Phys. Rev. Lett. **97**. 218101 (2006).

[27] W. Choi, J. Yi, and Y. W. Kim, Phys. Rev. E. **92**, 012727 (2015).

[28] S.A. Safran., *Statistical thermodynamics of Surfaces, Interfaces, and Membranes* (Westview Press, Boulder, 2003).

[29] U. Seifert, Advances in Physics **46**, 13 (1997).

[30] W. Helfrich, Z. Naturforsch. C **28**, 693 (1973).

[31] G.I. Bell, Science **200**, 618 (1978).

[32] G.I. Bell, M. Dembo, and P. Bongrad, Biophys. J. **45**, 1051 (1984).

[33] A. Tozeren, K.-L. Sung and S. Chien, Biophys. J. **55**, 479 (1989).

[34] V.L. Chen, C. Helm, and J. Israelachevilli, J. Phys. Chem. **95**, 10726 (1991).

[35] A. Baljon and M. Robbins, Science **271**, 482 (1996).

[36] J. Braun, J. Abney and J. Owicki, Nature (London) **310**, 316 (1984).

[37] J. Abney, J. Braun and J. Owicki, Biophys. J. **52**, 441 (1987).

[38] R. Bruinsma, M. Goulian and P. Pincus, Biophys. J. **67**, 746 (1994).

[39] W. Helfrich and R.M. Servuss, II Nuovo Cimento D **3**, 137 (1984).

[40] D. Zuckerman and R. Bruinsma, Phys. Rev. E. **57**, 964 (1998).

[41] D.A. McQuarrie, *Statistical Mechanics* (Harper Collins, New York 1976).

[42] U. Schwarz and S. Safran, Rev. Mod. Phys. **85**, 1327 (2013).

[43] M. Schick, Progr. Surf. Sci. **11**, 245 (1981).

[44] E. Domany, M. Schick, J. S. Walker, Phys. Rev. Lett. **38**, 1148 (1977).

[45] T. Speck and R.L.C. Vink, Phys. Rev. E **86**, 031923 (2012).

[46] Y. Imry and S.K. Ma, Phys. Rev. Lett. **35**, 1399 (1975).

[47] M. Aizenman and J. Wehr, Phys. Rev. Lett. **62**, 2503 (1989).

[48] R. Lipowsky, Phys. Rev. Lett. **77**, 1652 (1996).

[49] M. Mezard and A. P. Young, EPL **18**, 653 (1992).

[50] N. Gov, S.A. Safran, Phys. Rev. E **69**, 011101 (2004).

[51] C. Kittel, *Introduction to Solid State Physics*, 5th edition, (J. Wiley & Sons 1976).

[52] R.-J. Merath and U. Seifert, Eur. Phys. J. E **23** 103 (1976).

[53] L.C.-L. Lin and F.L.H. Brown, Biophys. J. **86** 764 (2004).

[54] S.A Tatulian, P. Hinterdorfer, G. Baber, and L.K. Tamm, EMBO J. **14**, 5514 (1995).

[55] S.Terrettaz, T. Stora, C. Duschl, and H. Vogel, Langmuir **9**, 1361 (1993).

[56] E. Kalb, J. Engel, and L.K. Tamm, Biochemistry **29**, 1607 (1990).

[57] T.H. Watts, H.E. Gaub, and H.M. McConell, Nature **320**, 179 (1986).

[58] A. Grakoui, S.K. Bromley, C. Sumen, M.M. Davis, A.S. Shaw, P.M. Allen, and M.L. Dustin, Science **285**, 221 (1999).

[59] M. Arnold, E.A. Cavalcanti-Adam, R. Glass, J. Blümmel, W. Eck, M. Kantlehner, H. Kessler, and J.P. Spatz, ChemPhysChem **5**, 383 (2004).

[60] P. Fromherz, A. Offenhausser, T. Vetter, and J. Weis, Science **252**, 1290 (1991).

[61] G. Steinhoff, B. Baur, G. Wrobel, S. Ingebrandt, A. Offenhauser, A. Dadgar, A. Krost, M. Stutzmann, and M. Eickhoff, Appl. Phys. Lett. **86**, 033901 (2005).

[62] F.F. Abraham and D.R. Nelson, J. Phys. (Paris) **51**, 2653 (1990).

[63] Fischer K.H. and Hertz J.A., *Spin Glasses* (Cambridge University Press, 1991).

[64] M.P. do Carmo, *Differential Geometry of Curves and Surfaces* (Prentice Hall, EnglewoodCliffs, 1976).

[65] E. Kreyszig, *Differential Geometry* (Dover, New York, 1991).

[66] P.B. Canham, J. Theoret. Biol. **26**, 61 (1970).

[67] D. Chowdhury and A. Mookerjee, Phys. Rep. **114**, 1 (1984).

[68] S. F. Edwards and P. W. Anderson, J. Phys. F: Met. Phys. **5** 965 (1975).

[69] M. Mezard and G. Parisi, J. Phys. I **1**, 809, (1991).

[70] P. Haronska and T. Vilgis, J. Chem. Phys. **101**, 3104, (1994).

[71] T. Castellani and A. Cavagna, J. Stat. Mech. Theory Exp. **2005**, 05012 (2005).

[72] A. Crisanti and H.-J. Sommers, Z. Phys. B **87**, (1992).

[73] D. Sherrington and S. Kirkpatrick, Phys. Rev. Lett. **35**, 1792 (1975).

[74] G. Parisi, Phys. Lett. **73**, 203 (1979).

[75] C. DeDominicis and P. Young, J. Phys. A: Math. Gen. **16**, 2063 (1992).

[76] J. Keirfield, Phys. Rev. Lett. **97**, 058302 (2006).

[77] P. Benetatos and E. Frey, J. Phys. Rev. E **67**, 051108 (2003).

[78] J. F. Marko and E. D. Siggia, Macromolecules **28**, 8759 (1995).

[79] P. Benetatos, Phys. Rev. E **96**, 042502 (2017).

[80] I.S. Gradshteyn and I.M. Ryzhik, *Table of Integrals, Series, and Products* (Elsevier Inc., 1943).

[81] M. Chaichian and A. Demichev, *Path Integrals in Physics, Vol. 2: Quantum Field Theory, Statistical Physics and Other Modern Applications* (IOP, Bristol, UK, 2001).

[82] H. Kleinert and V. Schulte-Frohlinde, *Critical Properties of* ϕ^4 *-Theories* (World Scientific 2001).

[83] P. Ramond, *Field Theory, A Modern Primer* (Benjamin/Cummings, Reading, MA, 1981).

[84] N. S. Gov and S. Safran, Biophys. J. **88**, 1859 (2005).

[85] S. Pasquali and J.K. Percus, Mol. Phys. **107**, 1303 (2009).

[86] K. K. Müller-Nedebock and J.L. Frisch, Phys. Rev. E **67**, 011801 (2003).

[87] S.F. Edwards, J. Phys. France **49**, 1673 (1988).

[88] S.I. Kuchanov, S.V. Korolev and S.V. Panyukov, Adv. Chem. Phys. **72**, 115 (1988).

[89] R.Fantoni and K. Müller-Nedebock, Phys. Rev. E **84**, 011808 (2011).

[90] P. C. Martin, E.D. Siggia and H.A. Rose, Phys. Rev. A **8**, 423 (1973).

Appendices

Appendix A

Correlation functions

In this section we show how we obtained the expressions for the correlation functions $\langle h^2(x)\rangle_{\text{var}}$ and $\langle h^2(x)\rangle_{\text{var}}$ needed in the evaluation of the free energy (3.1.7) using functional differentiation.

A.1 Functionals and functional derivative

A functional, in contrast to a function, is a transformation from function space to a number. A basic example is the integral $\int_0^L h(x)\,dx$. Mathematically,

$$F[h(x)] = \lim_{\Delta x \to 0} F(\cdots, h_{-1}, h_0, h_1, \cdots) \tag{A.1.1}$$

where h_i is the value $h(x_i)$. The operation of our interest, the functional derivative, has various definitions. We choose an intuitive version which closely resemble that of the ordinary function derivative, namely

$$\frac{\delta F[h(x)]}{\delta h(x')} = \lim_{\epsilon \to 0} \frac{F[h(x) + \epsilon\delta(x - x')] - F[h(x)]}{\epsilon}. \tag{A.1.2}$$

This determines the change of F due to an infinitesimal change in $h(x)$ at a point x'.

A.2 The correlation function $\langle h(x_2)h(x_1)\rangle_{\mathbf{var}}$

We can now use the above definition of the functional derivative to determine the correlation function $\langle h(x_2)h(x_1)\rangle_{\text{var}}$ as follows

$$\begin{aligned}
&\langle h(x_2)h(x_1)\rangle_{\text{var}} \\
&= \frac{1}{\mathcal{N}}\int \mathcal{D}h(x)\, h(x_2)h(x_1) \\
&\quad \times \exp\left\{-\frac{\kappa}{2}\int \mathrm{d}x \left(\frac{\partial h}{\partial x}\right)^2 - \frac{\zeta}{2}\int \mathrm{d}x\, h^2(x) + \mu\int \mathrm{d}x\, h(x)\right\} \\
&= \frac{\delta^2 \ln Z_{\text{var}}(f)}{\delta f(x_2)\delta f(x_1)}_{f=0} \\
&= \frac{\delta^2}{\delta f(x_2)\delta f(x_1)} \exp\left(+\frac{1}{2}\int_x\int_{x'} f(x')A^{-1}(x',x)f(x) + \int_x f(x)h_0(x)\right)
\end{aligned} \tag{A.2.1}$$

Now,

$$\begin{aligned}
\frac{\delta Z_{\text{var}}(f)}{\delta f(x_1)} &= \left(h_0(x_1) + \int_x f(x)A^{-1}(x,x_1)\right) \\
&\quad \times \exp\left(+\frac{1}{2}\int_x\int_{x'} f(x')A^{-1}(x',x)f(x) + \int_x f(x)h_0(x)\right).
\end{aligned} \tag{A.2.2}$$

Subsequently,

$$\begin{aligned}
\frac{\delta^2 Z_{\text{var}}(f)}{\delta f(x_2)\delta f(x_1)} &= \exp\left(+\frac{1}{2}\int_x\int_{x'} f(x')A^{-1}(x',x)f(x) + \int_x f(x)h_0(x)\right) \\
&\quad \left(A^{-1}(x_2,x_1) + \left(h_0(x_1) + \int_x f(x)A^{-1}(x,x_1)\right)\right. \\
&\quad \left.\times \left(h_0(x_2) + \int_x f(x)A^{-1}(x,x_2)\right)\right).
\end{aligned} \tag{A.2.3}$$

Therefore,

$$\langle h(x_2)h(x_1)\rangle_{\text{var}} = A^{-1}(x_2,x_1) + h_0(x_2)h_0(x_1). \tag{A.2.4}$$

A.3 The correlation function

$$\langle h(x_4)h(x_3)h(x_2)h(x_1)\rangle_{\mathbf{var}}$$

After the second order correlation function what we still need to evaluate is $\langle h(x_4)h(x_3)h(x_2)h(x_1)\rangle_{\text{var}}$. This is the extension of the previous result (A.2.3)

since

$$\langle h(x_4)h(x_3)h(x_2)h(x_1)\rangle_{\text{var}} = \frac{\delta^4 Z_{\text{var}}(f)}{\delta f(x_4)\delta f(x_3)\delta f(x_2)\delta f(x_1)}.$$

Starting with the third order evaluation we have

$$\begin{aligned}
&\frac{\delta^3 Z_{\text{var}}(f)}{\delta f(x_3)\delta f(x_2)\delta f(x_1)} \\
&= \frac{\delta}{\delta f(x_3)} \exp\left(+\frac{1}{2}\int_x\int_{x'} f(x')A^{-1}(x',x)f(x) + \int_x f(x)h_0(x)\right) \\
&\quad \left(A^{-1}(x_2,x_1) + \left(h_0(x_1) + \int_x f(x)A^{-1}(x,x_1)\right)\right. \\
&\qquad \left.\times\left(h_0(x_2) + \int_x f(x)A^{-1}(x,x_2)\right)\right) \qquad \text{(A.3.1)}
\end{aligned}$$

which is equivalent to

$$\begin{aligned}
&\frac{\delta^3 Z_{\text{var}}(f)}{\delta f(x_3)\delta f(x_2)\delta f(x_1)} = \exp\left(+\frac{1}{2}\int_x\int_{x'} f(x')A^{-1}(x',x)f(x) + \int_x f(x)h_0(x)\right) \\
&\quad \left[A^{-1}(x_2,x_1)\left(h_0(x_3) + \int_x f(x)A^{-1}(x,x_3)\right)\right. \\
&\quad +h_0(x_2)h_0(x_1)\left(h_0(x_3) + \int_x f(x)A^{-1}(x,x_3)\right) \\
&\quad +h_0(x_1)\left(h_0(x_3) + \int_x f(x)A^{-1}(x,x_3)\right)\int_x f(x)A^{-1}(x,x_2) \\
&\quad +h_0(x_2)\left(h_0(x_3) + \int_x f(x)A^{-1}(x,x_3)\right)\int_x f(x)A^{-1}(x,x_1) \\
&\quad \left(h_0(x_3) + \int_x f(x)A^{-1}(x,x_3)\right)\int_x\int_{x'} f(x)f(x')A^{-1}(x,x_2)A^{-1}(x,x_1) \\
&\quad +h_0(x_1)A^{-1}(x_3,x_2) + h_0(x_2)A^{-1}(x_3,x_1) \\
&\quad \left.+\int_x f(x)A^{-1}(x,x_2)A^{-1}(x_3,x_1) + \int_x f(x)A^{-1}(x_3,x_2)A^{-1}(x,x_1)\right]. \\
&\qquad\qquad\qquad\qquad\qquad\qquad\qquad\qquad\qquad\qquad\qquad\qquad \text{(A.3.2)}
\end{aligned}$$

Finally, taking advantage of the condition that we set $f = 0$ afterwards, after applying the chain rule, we obtain

$$\begin{aligned}\langle h(x_4)h(x_3)h(x_2)h(x_1)\rangle_{\text{var}} &= \frac{\delta^4 Z_{\text{var}}(f)}{\delta f(x_4)\delta f(x_3)\delta f(x_2)\delta f(x_1)} \\ &= A^{-1}(x_2,x_1)h_0(x_4)h_0(x_3) + h_0(x_4)h_0(x_3)h_0(x_2)h_0(x_1) \\ &\quad + h_0(x_4)h_0(x_1)A^{-1}(x_3,x_2) + h_0(x_4)h_0(x_2)A^{-1}(x_3,x_1) \\ &\quad + A^{-1}(x_2,x_1)A^{-1}(x_4,x_3) + A^{-1}(x_4,x_2)A^{-1}(x_3,x_1) \\ &\quad + A^{-1}(x_3,x_2)A^{-1}(x_4,x_1) + h_0(x_2)h_0(x_3)A^{-1}(x_4,x_1) \\ &\quad + h_0(x_1)h_0(x_3)A^{-1}(x_4,x_2) + h_0(x_2)h_0(x_1)A^{-1}(x_4,x_3). \end{aligned} \tag{A.3.3}$$

A.4 The $-\left(\zeta - \frac{\zeta_0}{2}\right)\int_0^1 \mathrm{d}x\, \left\langle h^2(x)\right\rangle_{\text{var}}$ term

$$\begin{aligned}-\left(\zeta - \frac{\zeta_0}{2}\right)\int_0^1 \mathrm{d}x\, \left\langle h^2(x)\right\rangle_{\text{var}} &= -\left(\zeta - \frac{\zeta_0}{2}\right)\int_0^1 \mathrm{d}x\, \left(h_0^2(x) + A^{-1}(x,x)\right) \\ &= -\left(\zeta - \frac{\zeta_0}{2}\right)\int_0^1 \left[\left(\frac{\mu - \mu\operatorname{sech}\left(\frac{\sqrt{\zeta}L}{2\sqrt{\kappa}}\right)\cosh\left(\frac{\sqrt{\zeta}L(2x-1)}{2\sqrt{\kappa}}\right)}{\zeta\sqrt{\frac{L}{\kappa}}}\right)^2\right. \\ &\qquad \left. + \frac{\sinh\left(\frac{x\left(\sqrt{\zeta}L\right)}{\sqrt{\kappa}}\right)\sinh\left(\frac{(1-x)\left(\sqrt{\zeta}L\right)}{\sqrt{\kappa}}\right)}{\frac{2\left(\left(\sqrt{\zeta}L\right)\sinh\left(\frac{\sqrt{\zeta}L}{\sqrt{\kappa}}\right)\right)}{\sqrt{\kappa}}}\right] dx \\ &= \frac{\left(\frac{\zeta_0}{2} - \zeta\right)\kappa\mu^2\left(\sqrt{\zeta}L\left(\operatorname{sech}^2\left(\frac{\sqrt{\zeta}L}{2\sqrt{\kappa}}\right) + 2\right) - 6\sqrt{\kappa}\tanh\left(\frac{\sqrt{\zeta}L}{2\sqrt{\kappa}}\right)\right)}{2\zeta^{5/2}L^2} \\ &\quad - \frac{\left(\frac{\zeta_0}{2} - \zeta\right)\left(\kappa - \sqrt{\zeta}\sqrt{\kappa}L\coth\left(\frac{\sqrt{\zeta}L}{\sqrt{\kappa}}\right)\right)}{4\zeta L^2} \end{aligned} \tag{A.4.1}$$

A.5 The $-\frac{(\beta k)^2}{8R}\int_0^1 \mathrm{d}x\,\left\langle h^4(x)\right\rangle_{\mathbf{var}}$ term

$$
\begin{aligned}
&-\frac{(\beta k)^2}{8R}\int_0^1 \mathrm{d}x\,\left\langle h^4(x)\right\rangle_{\mathrm{var}} \\
&= -\frac{(\beta k)^2}{8R}\int_0^1 \mathrm{d}x\,\left(h_0^4(x)+6h_0^2(x)A^{-1}(x,x)+3\left[A^{-1}(x,x)\right]^2\right) \\
&= -\frac{(\beta k)^2}{8R}\int_0^1 \left(3\frac{\kappa\mathrm{csch}^2\left(\frac{\sqrt{\zeta}L}{\sqrt{\kappa}}\right)\sinh^2\left(\frac{\sqrt{\zeta}L(1-x)}{\sqrt{\kappa}}\right)\sinh^2\left(\frac{\sqrt{\zeta}Lx}{\sqrt{\kappa}}\right)}{\zeta L^2}\right. \\
&\quad +6\frac{\left(\sinh\left(\frac{x\left(\sqrt{\zeta}L\right)}{\sqrt{\kappa}}\right)\sinh\left(\frac{(1-x)\left(\sqrt{\zeta}L\right)}{\sqrt{\kappa}}\right)\right)\left(\frac{\mu-\mu\mathrm{sech}\left(\frac{\sqrt{\zeta}L}{2\sqrt{\kappa}}\right)\cosh\left(\frac{\sqrt{\zeta}L(2x-1)}{2\sqrt{\kappa}}\right)}{\zeta\sqrt{\frac{L}{\kappa}}}\right)^2}{\frac{\left(\sqrt{\zeta}L\right)\sinh\left(\frac{\sqrt{\zeta}L}{\sqrt{\kappa}}\right)}{\sqrt{\kappa}}} \\
&\quad \left.+\frac{\kappa^2\left(\mu-\mu\mathrm{sech}\left(\frac{\sqrt{\zeta}L}{2\sqrt{\kappa}}\right)\cosh\left(\frac{\sqrt{\zeta}L(2x-1)}{2\sqrt{\kappa}}\right)\right)^4}{\zeta^4L^2}\right)dx. \qquad \text{(A.5.1)}
\end{aligned}
$$

We shall perform the integration term by term as follows. The first term evaluates to

$$
\begin{aligned}
&-\frac{(\beta k)^2}{8R}\int_0^1 3\frac{\kappa\mathrm{csch}^2\left(\frac{\sqrt{\zeta}L}{\sqrt{\kappa}}\right)\sinh^2\left(\frac{\sqrt{\zeta}L(1-x)}{\sqrt{\kappa}}\right)\sinh^2\left(\frac{\sqrt{\zeta}Lx}{\sqrt{\kappa}}\right)}{\zeta L^2}dx \\
&= -\frac{3\beta^2\kappa k^2\left(\sqrt{\zeta}L\left(3\mathrm{csch}^2\left(\frac{\sqrt{\zeta}L}{\sqrt{\kappa}}\right)+2\right)-3\sqrt{\kappa}\coth\left(\frac{\sqrt{\zeta}L}{\sqrt{\kappa}}\right)\right)}{64\zeta^{3/2}L^3R}. \qquad \text{(A.5.2)}
\end{aligned}
$$

The third term evaluates to

$$
\begin{aligned}
&-\frac{(\beta k)^2}{8R}\int_0^1 \frac{\kappa^2\left(\mu-\mu\mathrm{sech}\left(\frac{\sqrt{\zeta}L}{2\sqrt{\kappa}}\right)\cosh\left(\frac{\sqrt{\zeta}L(2x-1)}{2\sqrt{\kappa}}\right)\right)^4}{\zeta^4L^2}dx \\
&= -\frac{\beta^2\kappa^2k^2\mu^4\left(16\cosh\left(\frac{\sqrt{\zeta}L}{\sqrt{\kappa}}\right)+\cosh\left(\frac{2\sqrt{\zeta}L}{\sqrt{\kappa}}\right)+18\right)\mathrm{sech}^4\left(\frac{\sqrt{\zeta}L}{2\sqrt{\kappa}}\right)}{64\zeta^4L^2R} \\
&\quad +\frac{5\beta^2\kappa^{5/2}k^2\mu^4\left(32\sinh\left(\frac{\sqrt{\zeta}L}{\sqrt{\kappa}}\right)+5\sinh\left(\frac{2\sqrt{\zeta}L}{\sqrt{\kappa}}\right)\right)\mathrm{sech}^4\left(\frac{\sqrt{\zeta}L}{2\sqrt{\kappa}}\right)}{384\zeta^{9/2}L^3R} \qquad \text{(A.5.3)}
\end{aligned}
$$

Finally, the second term evaluates to

$$
\begin{aligned}
&-\frac{(\beta k)^2}{8R}\int_0^1 \frac{\kappa^{3/2}\operatorname{csch}\left(\frac{\sqrt{\zeta}L}{\sqrt{\kappa}}\right)\left(\mu-\mu\operatorname{sech}\left(\frac{\sqrt{\zeta}L}{2\sqrt{\kappa}}\right)\cosh\left(\frac{\sqrt{\zeta}L(2x-1)}{2\sqrt{\kappa}}\right)\right)^2}{\zeta^{5/2}L^2} \\
&\qquad\qquad \times \sinh\left(\frac{\sqrt{\zeta}L(1-x)}{\sqrt{\kappa}}\right)\sinh\left(\frac{\sqrt{\zeta}Lx}{\sqrt{\kappa}}\right) \\
&= -\frac{3\beta^2\kappa^{3/2}k^2\mu^2\left(4\cosh\left(\frac{\sqrt{\zeta}L}{\sqrt{\kappa}}\right)+\cosh\left(\frac{2\sqrt{\zeta}L}{\sqrt{\kappa}}\right)\right)\operatorname{csch}\left(\frac{\sqrt{\zeta}L}{\sqrt{\kappa}}\right)\operatorname{sech}^2\left(\frac{\sqrt{\zeta}L}{2\sqrt{\kappa}}\right)}{32\zeta^{5/2}L^2R} \\
&\qquad -\frac{\beta^2\kappa^2k^2\mu^2\left(4-19\cosh\left(\frac{\sqrt{\zeta}L}{\sqrt{\kappa}}\right)\right)\operatorname{sech}^2\left(\frac{\sqrt{\zeta}L}{2\sqrt{\kappa}}\right)}{32\zeta^3L^3R}. \qquad \text{(A.5.4)}
\end{aligned}
$$

Collecting all terms together we therefore have

$$
\begin{aligned}
&-\frac{(\beta k)^2}{8R}\int_0^1 \mathrm{d}x\,\left\langle h^4(x)\right\rangle_{\text{var}} \\
&= -\frac{3\beta^2\kappa k^2\left(\sqrt{\zeta}L\left(3\operatorname{csch}^2\left(\frac{\sqrt{\zeta}L}{\sqrt{\kappa}}\right)+2\right)-3\sqrt{\kappa}\coth\left(\frac{\sqrt{\zeta}L}{\sqrt{\kappa}}\right)\right)}{64\zeta^{3/2}L^3R} \\
&= -\frac{3\beta^2\kappa^{3/2}k^2\mu^2\left(4\cosh\left(\frac{\sqrt{\zeta}L}{\sqrt{\kappa}}\right)+\cosh\left(\frac{2\sqrt{\zeta}L}{\sqrt{\kappa}}\right)\right)\operatorname{csch}\left(\frac{\sqrt{\zeta}L}{\sqrt{\kappa}}\right)\operatorname{sech}^2\left(\frac{\sqrt{\zeta}L}{2\sqrt{\kappa}}\right)}{32\zeta^{5/2}L^2R} \\
&\qquad -\frac{\beta^2\kappa^2k^2\mu^2\left(4-19\cosh\left(\frac{\sqrt{\zeta}L}{\sqrt{\kappa}}\right)\right)\operatorname{sech}^2\left(\frac{\sqrt{\zeta}L}{2\sqrt{\kappa}}\right)}{32\zeta^3L^3R} \\
&= -\frac{\beta^2\kappa^2k^2\mu^4\left(16\cosh\left(\frac{\sqrt{\zeta}L}{\sqrt{\kappa}}\right)+\cosh\left(\frac{2\sqrt{\zeta}L}{\sqrt{\kappa}}\right)+18\right)\operatorname{sech}^4\left(\frac{\sqrt{\zeta}L}{2\sqrt{\kappa}}\right)}{64\zeta^4L^2R} \\
&\quad +\frac{5\beta^2\kappa^{5/2}k^2\mu^4\left(32\sinh\left(\frac{\sqrt{\zeta}L}{\sqrt{\kappa}}\right)+5\sinh\left(\frac{2\sqrt{\zeta}L}{\sqrt{\kappa}}\right)\right)\operatorname{sech}^4\left(\frac{\sqrt{\zeta}L}{2\sqrt{\kappa}}\right)}{384\zeta^{9/2}L^3R}. \qquad \text{(A.5.5)}
\end{aligned}
$$

A.6 The $\frac{\partial\langle H_{\mathbf{var}}[\zeta]-H\rangle_{\mathbf{var}}}{\partial\zeta}$ term

$$\frac{\partial\langle H_{\mathrm{var}}[\zeta]-H\rangle_{\mathrm{var}}}{\partial\zeta} = \frac{9\beta^2k^2\mu^2L\left(L\sqrt{\frac{\zeta}{\kappa}}\coth\left(L\sqrt{\frac{\zeta}{\kappa}}\right)-1\right)}{2\zeta^4R}$$
$$-\frac{3\beta^2k^2\mu^2L\left(\frac{L\coth\left(L\sqrt{\frac{\zeta}{\kappa}}\right)}{2\kappa\sqrt{\frac{\zeta}{\kappa}}}-\frac{L^2\mathrm{csch}^2\left(L\sqrt{\frac{\zeta}{\kappa}}\right)}{2\kappa}\right)}{2\zeta^3R}$$
$$+\frac{9\beta^2k^2L^2\left(L\sqrt{\frac{\zeta}{\kappa}}\left(3\mathrm{csch}^2\left(L\sqrt{\frac{\zeta}{\kappa}}\right)+2\right)-3\coth\left(L\sqrt{\frac{\zeta}{\kappa}}\right)\right)}{64\kappa^3R\left(\frac{\zeta}{\kappa}\right)^{5/2}}$$
$$-\frac{3\beta^2k^2L^2\left(-\frac{3L^2\coth\left(L\sqrt{\frac{\zeta}{\kappa}}\right)\mathrm{csch}^2\left(L\sqrt{\frac{\zeta}{\kappa}}\right)}{\kappa}+\frac{3L\mathrm{csch}^2\left(L\sqrt{\frac{\zeta}{\kappa}}\right)}{2\kappa\sqrt{\frac{\zeta}{\kappa}}}+\frac{L\left(3\mathrm{csch}^2\left(L\sqrt{\frac{\zeta}{\kappa}}\right)+2\right)}{2\kappa\sqrt{\frac{\zeta}{\kappa}}}\right)}{32\kappa^2R\left(\frac{\zeta}{\kappa}\right)^{3/2}}$$
$$-\frac{3\beta^2k^2\mu^2L^3\mathrm{sech}^2\left(\frac{\sqrt{\zeta}L}{2\sqrt{\kappa}}\right)}{8\zeta^3\kappa R}+\frac{9\beta^2k^2\mu^2L\left(\cosh\left(\frac{\sqrt{\zeta}L}{\sqrt{\kappa}}\right)-2\right)\mathrm{sech}^2\left(\frac{\sqrt{\zeta}L}{2\sqrt{\kappa}}\right)}{8\zeta^4R}$$
$$\frac{15\beta^2k^2\mu^2L^2\left(2\cosh\left(\frac{\sqrt{\zeta}L}{\sqrt{\kappa}}\right)-1\right)\mathrm{csch}\left(\frac{\sqrt{\zeta}L}{\sqrt{\kappa}}\right)\mathrm{sech}^2\left(\frac{\sqrt{\zeta}L}{2\sqrt{\kappa}}\right)}{16\zeta^{7/2}\sqrt{\kappa}R}$$

$$
\begin{aligned}
&+\frac{3\beta^2k^2\mu^2L^3\left(2\cosh\left(\frac{\sqrt{\zeta}L}{\sqrt{\kappa}}\right)-1\right)\coth\left(\frac{\sqrt{\zeta}L}{\sqrt{\kappa}}\right)\operatorname{csch}\left(\frac{\sqrt{\zeta}L}{\sqrt{\kappa}}\right)\operatorname{sech}^2\left(\frac{\sqrt{\zeta}L}{2\sqrt{\kappa}}\right)}{16\zeta^3\kappa R}\\
&+\frac{\beta^2k^2\mu^4L\left(16\cosh\left(\frac{\sqrt{\zeta}L}{\sqrt{\kappa}}\right)+\cosh\left(\frac{2\sqrt{\zeta}L}{\sqrt{\kappa}}\right)+18\right)\operatorname{sech}^4\left(\frac{\sqrt{\zeta}L}{2\sqrt{\kappa}}\right)}{2\zeta^5R}\\
&+\frac{5\beta^2\sqrt{\kappa}k^2\mu^4\left(\frac{16L\cosh\left(\frac{\sqrt{\zeta}L}{\sqrt{\kappa}}\right)}{\sqrt{\zeta}\sqrt{\kappa}}+\frac{5L\cosh\left(\frac{2\sqrt{\zeta}L}{\sqrt{\kappa}}\right)}{\sqrt{\zeta}\sqrt{\kappa}}\right)\operatorname{sech}^4\left(\frac{\sqrt{\zeta}L}{2\sqrt{\kappa}}\right)}{48\zeta^{9/2}R}\\
&-\frac{3\beta^2k^2\mu^2L^2\sinh\left(\frac{\sqrt{\zeta}L}{\sqrt{\kappa}}\right)\operatorname{sech}^2\left(\frac{\sqrt{\zeta}L}{2\sqrt{\kappa}}\right)}{16\zeta^{7/2}\sqrt{\kappa}R}\\
&-\frac{15\beta^2\sqrt{\kappa}k^2\mu^4\left(32\sinh\left(\frac{\sqrt{\zeta}L}{\sqrt{\kappa}}\right)+5\sinh\left(\frac{2\sqrt{\zeta}L}{\sqrt{\kappa}}\right)\right)\operatorname{sech}^4\left(\frac{\sqrt{\zeta}L}{2\sqrt{\kappa}}\right)}{32\zeta^{11/2}R}\\
&-\frac{\beta^2k^2\mu^4L\left(\frac{8L\sinh\left(\frac{\sqrt{\zeta}L}{\sqrt{\kappa}}\right)}{\sqrt{\zeta}\sqrt{\kappa}}+\frac{L\sinh\left(\frac{2\sqrt{\zeta}L}{\sqrt{\kappa}}\right)}{\sqrt{\zeta}\sqrt{\kappa}}\right)\operatorname{sech}^4\left(\frac{\sqrt{\zeta}L}{2\sqrt{\kappa}}\right)}{8\zeta^4R}\\
&+\frac{2\beta^2k^2\mu^2L^2\tanh\left(\frac{\sqrt{\zeta}L}{2\sqrt{\kappa}}\right)\operatorname{sech}^2\left(\frac{\sqrt{\zeta}L}{2\sqrt{\kappa}}\right)}{\zeta^{7/2}\sqrt{\kappa}R}\\
&+\frac{3\beta^2k^2\mu^2L^2\left(\cosh\left(\frac{\sqrt{\zeta}L}{\sqrt{\kappa}}\right)-2\right)\tanh\left(\frac{\sqrt{\zeta}L}{2\sqrt{\kappa}}\right)\operatorname{sech}^2\left(\frac{\sqrt{\zeta}L}{2\sqrt{\kappa}}\right)}{16\zeta^{7/2}\sqrt{\kappa}R}\\
&+\frac{3\beta^2k^2\mu^2L^3\left(2\cosh\left(\frac{\sqrt{\zeta}L}{\sqrt{\kappa}}\right)-1\right)\tanh\left(\frac{\sqrt{\zeta}L}{2\sqrt{\kappa}}\right)\operatorname{csch}\left(\frac{\sqrt{\zeta}L}{\sqrt{\kappa}}\right)\operatorname{sech}^2\left(\frac{\sqrt{\zeta}L}{2\sqrt{\kappa}}\right)}{16\zeta^3\kappa R}\\
&+\frac{\beta^2k^2\mu^4L^2\left(16\cosh\left(\frac{\sqrt{\zeta}L}{\sqrt{\kappa}}\right)+\cosh\left(\frac{2\sqrt{\zeta}L}{\sqrt{\kappa}}\right)+18\right)\tanh\left(\frac{\sqrt{\zeta}L}{2\sqrt{\kappa}}\right)\operatorname{sech}^4\left(\frac{\sqrt{\zeta}L}{2\sqrt{\kappa}}\right)}{8\zeta^{9/2}\sqrt{\kappa}R}\\
&-\frac{5\beta^2k^2\mu^4L\left(32\sinh\left(\frac{\sqrt{\zeta}L}{\sqrt{\kappa}}\right)+5\sinh\left(\frac{2\sqrt{\zeta}L}{\sqrt{\kappa}}\right)\right)\tanh\left(\frac{\sqrt{\zeta}L}{2\sqrt{\kappa}}\right)\operatorname{sech}^4\left(\frac{\sqrt{\zeta}L}{2\sqrt{\kappa}}\right)}{48\zeta^5R}\\
&-\frac{12\beta^2k^2\mu^2L\tanh^2\left(\frac{\sqrt{\zeta}L}{2\sqrt{\kappa}}\right)}{\zeta^4R}\\
&-\frac{\zeta^{3/2}L\left(L\sqrt{\frac{\zeta}{\kappa}}\coth\left(L\sqrt{\frac{\zeta}{\kappa}}\right)-1\right)-12\sqrt{\kappa}\mu^2\tanh\left(\frac{\sqrt{\zeta}L}{2\sqrt{\kappa}}\right)}{4\zeta^{5/2}}\\
&+\frac{2\sqrt{\zeta}\mu^2L\left(\cosh\left(\frac{\sqrt{\zeta}L}{\sqrt{\kappa}}\right)+2\right)\operatorname{sech}^2\left(\frac{\sqrt{\zeta}L}{2\sqrt{\kappa}}\right)}{4\zeta^{5/2}}
\end{aligned}
$$

$$
\begin{aligned}
&+\frac{5(\zeta-\beta k\rho)\left(\zeta^{3/2}L\left(L\sqrt{\frac{\zeta}{\kappa}}\coth\left(L\sqrt{\frac{\zeta}{\kappa}}\right)-1\right)-12\sqrt{\kappa}\mu^2\tanh\left(\frac{\sqrt{\zeta}L}{2\sqrt{\kappa}}\right)\right.}{8\zeta^{7/2}}\\
&\left.\frac{+2\sqrt{\zeta}\mu^2L\left(\cosh\left(\frac{\sqrt{\zeta}L}{\sqrt{\kappa}}\right)+2\right)\operatorname{sech}^2\left(\frac{\sqrt{\zeta}L}{2\sqrt{\kappa}}\right)}{8\zeta^{7/2}}\right)\\
&-\frac{(\zeta-\beta k\rho)\left(\zeta^{3/2}L\left(\frac{L\coth\left(L\sqrt{\frac{\zeta}{\kappa}}\right)}{2\kappa\sqrt{\frac{\zeta}{\kappa}}}-\frac{L^2\operatorname{csch}^2\left(L\sqrt{\frac{\zeta}{\kappa}}\right)}{2\kappa}\right)\right.}{4\zeta^{5/2}}\\
&\frac{+\frac{\mu^2L^2\sinh\left(\frac{\sqrt{\zeta}L}{\sqrt{\kappa}}\right)\operatorname{sech}^2\left(\frac{\sqrt{\zeta}L}{2\sqrt{\kappa}}\right)}{\sqrt{\kappa}}}{4\zeta^{5/2}}\\
&\frac{-\frac{\mu^2L^2\left(\cosh\left(\frac{\sqrt{\zeta}L}{\sqrt{\kappa}}\right)+2\right)\tanh\left(\frac{\sqrt{\zeta}L}{2\sqrt{\kappa}}\right)\operatorname{sech}^2\left(\frac{\sqrt{\zeta}L}{2\sqrt{\kappa}}\right)}{\sqrt{\kappa}}-\frac{3\mu^2L\operatorname{sech}^2\left(\frac{\sqrt{\zeta}L}{2\sqrt{\kappa}}\right)}{\sqrt{\zeta}}}{4\zeta^{5/2}}\\
&\left.\frac{+\frac{\mu^2L\left(\cosh\left(\frac{\sqrt{\zeta}L}{\sqrt{\kappa}}\right)+2\right)\operatorname{sech}^2\left(\frac{\sqrt{\zeta}L}{2\sqrt{\kappa}}\right)}{\sqrt{\zeta}}+\frac{3}{2}\sqrt{\zeta}L\left(L\sqrt{\frac{\zeta}{\kappa}}\coth\left(L\sqrt{\frac{\zeta}{\kappa}}\right)-1\right)}{4\zeta^{5/2}}\right).
\end{aligned}
\tag{A.6.1}
$$

Appendix B

Disorder distribution functional I

In this appendix we evaluate the disorder functional I without rescaling

$$
\begin{aligned}
I &= \mathcal{N}\int \mathcal{D}\rho \exp\left\{\int \mathrm{d}x \left(-\beta \sum_{\alpha=1}^{n}\left(\frac{k}{2}h_\alpha^2(x)+\epsilon\right)\rho(x) - \frac{R}{2}\left(\rho(x)-\rho_0\right)^2\right)\right\} \\
I &= \mathcal{N}\int \mathcal{D}\rho \exp\left\{-\frac{R}{2}\int \mathrm{d}x \left(\frac{2}{R}\beta\sum_{\alpha=1}^{n}\left(\frac{k}{2}h_\alpha^2(x)+\epsilon\right)\rho(x) + \rho^2(x)\right.\right. \\
&\qquad\qquad \left.\left. -2\rho_0\rho(x)+\rho_0^2\right)\right\} \\
I &\propto \int \mathcal{D}\rho \exp\left\{-\frac{R}{2}\int_x \left(\rho^2(x) + \frac{2\beta}{R}\sum_{\alpha=1}^{n}\left(\frac{k}{2}h_\alpha^2(x)+\epsilon\right)\rho(x) - 2\rho_0\rho(x)+\rho_0^2\right)\right. \\
I &= \mathcal{N}\int \mathcal{D}\rho \exp\left\{-\frac{R}{2}\int \mathrm{d}x \left[\left(\rho(x)+\frac{\beta}{R}\sum_{\alpha=1}^{n}\left(\frac{k}{2}h_\alpha^2(x)+\epsilon\right)\right)^2 + \rho_0^2\right.\right. \\
&\quad -2\rho_0\left(\rho(x)+\frac{\beta}{R}\sum_{\alpha=1}^{n}\left(\frac{k}{2}h_\alpha^2(x)+\epsilon\right)\right) - \left(\frac{\beta}{R}\sum_{\alpha=1}^{n}\left(\frac{k}{2}h_\alpha^2(x)+\epsilon\right)\right)^2 \\
&\qquad\qquad \left.\left. +2\frac{\rho_0\beta}{R}\sum_{\alpha=1}^{n}\left(\frac{k}{2}h_\alpha^2(x)+\epsilon\right)\right]\right\} \\
I &= \mathcal{N}\int \mathcal{D}\tilde{\rho} \exp\left\{-\frac{R}{2}\int \mathrm{d}x \left(\tilde{\rho}^2(x) - 2\rho_0\tilde{\rho}(x) + \rho_0^2 - \left(\frac{\beta}{R}\sum_{\alpha=1}^{n}\left(\frac{k}{2}h_\alpha^2(x)+\epsilon\right)\right)^2\right.\right. \\
&\qquad\qquad \left.\left. +2\frac{\rho_0\beta}{R}\sum_{\alpha=1}^{n}\left(\frac{k}{2}h_\alpha^2(x)+\epsilon\right)\right)\right\}. \qquad \text{(B.0.1)}
\end{aligned}
$$

Substituting the normalization constant $\mathcal{N} = \int \mathcal{D}\rho \exp\left(-\frac{R}{2}\int \mathrm{d}x\,(\rho(x)-\rho_0)^2\right)$, to the equation (B.0.1) for I we obtain

$$\begin{aligned} I &= \exp\left(-\frac{R}{2}\int \mathrm{d}x\left[-\left(\frac{\beta}{R}\sum_{\alpha=1}^{n}\left(\frac{k}{2}h_\alpha^2(x)+\epsilon\right)\right)^2 + 2\frac{\rho_0\beta}{R}\sum_{\alpha=1}^{n}\left(\frac{k}{2}h_\alpha^2(x)+\epsilon\right)\right]\right) \\ &= \exp\left(\frac{R}{2}\int \mathrm{d}x\left[\sum_{\alpha,\lambda}^{n}\frac{\beta^2k^2}{4R^2}h_\alpha^2(x)h_\lambda^2(x)\right.\right. \\ &\qquad \left.\left. + \frac{\rho_0\beta k}{R}\left(\frac{n\beta\epsilon}{R}-1\right)\sum_{\alpha=1}^{n}h_\alpha^2(x) + \frac{n\beta\epsilon}{R}\left(\frac{n\beta\epsilon}{R}-2\rho_0\right)\right]\right). \end{aligned} \tag{B.0.2}$$

Appendix C

Components of Replica Symmetry

C.1 $\mathbf{tr}\ln\mathbb{M}$ and $\int \mathbf{d}x\mathrm{d}x'\ \boldsymbol{\mu}^{\mathsf{T}}\mathbb{M}^{-1}(x,x')\boldsymbol{\mu}$

$$\mathrm{tr}\ln\mathbb{M}(x,x') \approx \mathrm{tr}\ln\mathbb{D} + \mathrm{tr}\left(\mathbb{D}^{-1}\mathbb{Q}\right) - \frac{1}{2}\mathrm{tr}\left(\mathbb{D}^{-1}\mathbb{Q}\right)^2. \tag{C.1.1}$$

We shall begin by evaluating $\mathrm{tr}\left(\mathbb{D}^{-1}\mathbb{Q}\right)$ term. We therefore need to determine the product $\mathbb{D}^{-1}\mathbb{Q}$. This is given by

$$\mathbb{D}^{-1}\mathbb{Q} = \begin{pmatrix} \left[\delta_{ij}\delta^{xx'}\left(\gamma - \partial_{xx}\right)\right]^{-1} & 0 \\ 0 & \left[\delta_{ij}\delta^{xx'}\left(\gamma - \partial_{xx}\right)\right]^{-1} \end{pmatrix} \times \begin{pmatrix} 2\delta_{ij}Q_{ii}(x)\delta^{xx'} & 2Q_{ij}(x)\delta^{xx'} \\ 2Q_{ij}(x)\delta^{xx'} & 2\delta_{ij}Q_{ii}(x)\delta^{xx'} \end{pmatrix}. \tag{C.1.2}$$

Adopting a shorthand notation we have

$$\mathbb{D}^{-1}\mathbb{Q} = \begin{pmatrix} \mathbb{A}^{-1}(x,x') & 0 \\ 0 & \mathbb{A}^{-1}(x,x') \end{pmatrix} \begin{pmatrix} \mathbb{C}(x,x') & \mathbb{D}(x,x') \\ \mathbb{D}(x,x') & \mathbb{C}(x,x') \end{pmatrix}$$

$$\mathbb{D}^{-1}\mathbb{Q} = 2\int \mathrm{d}x'' \sum_l \times \begin{pmatrix} (\mathbb{A}^{-1})_{il}(x,x'')\mathbb{C}_{lj}(x'',x') & (\mathbb{A}^{-1})_{il}(x,x'')\mathbb{D}_{lj}(x'',x') \\ (\mathbb{A}^{-1})_{il}(x,x'')\mathbb{D}_{lj}(x'',x') & (\mathbb{A}^{-1})_{il}(x,x'')\mathbb{C}_{lj}(x'',x') \end{pmatrix}. \tag{C.1.3}$$

Therefore $\mathrm{tr}\,(\mathbb{D}^{-1}\mathbb{Q})$ is given by

$$\begin{aligned}
&\mathrm{tr}\left(\mathbb{D}^{-1}\mathbb{Q}\right)\\
&= 4\int \mathrm{d}x'dx''\sum_{lm}\left[(\mathbb{A}^{-1})_{ml}(x',x'')[\delta_{lm}Q_{ll}(x'')\delta^{x''x'}\right]\\
&= 4\int \mathrm{d}x'dx''\sum_{lm}\int\frac{dpdq}{(2\pi)^{2d}}\frac{\mathrm{e}^{iq(x'-x'')+ip(x''-x')}}{q^2+\gamma}\delta^{-1}_{ml}\delta_{lm}Q_{mm}(x'')\\
&= 4\int\sum_{m}\frac{\mathrm{d}q}{(2\pi)^d}\frac{Q_{mm}(0)}{q^2+\gamma}. \qquad \text{(C.1.4)}
\end{aligned}$$

We now proceed to $\mathrm{tr}\,(\mathbb{D}^{-1}\mathbb{Q})^2 = \mathrm{tr}\,(\mathbb{D}^{-1}\mathbb{Q}\mathbb{D}^{-1}\mathbb{Q}) = 2\ \mathrm{tr}\,(\mathbb{A}^{-1}\mathbb{C}\mathbb{A}^{-1}\mathbb{C}) + 2\,\mathrm{tr}\,(\mathbb{A}^{-1}\mathbb{D}\mathbb{A}^{-1}\mathbb{D})$

$$\begin{aligned}
\mathrm{tr}\left(\mathbb{D}^{-1}\mathbb{Q}\right)^2 &= 4\int_{x''\ldots x''''}\sum_{fghi}(\mathbb{A}^{-1})_{fg}(x',x'')\left[\delta_{gh}Q_{gg}(x'')\delta^{x''x'''}\right]\\
&\qquad\times(\mathbb{A}^{-1})_{hi}(x''',x'''')\left[\delta_{if}Q_{ii}(x'''')\delta^{x''''x'}\right]\\
&\quad+4\int_{x''\ldots x''''}\sum_{fghi}(\mathbb{A}^{-1})_{fg}(x,x'')\left[Q_{gh}(x'')\delta^{x''x'''}\right]\\
&\qquad\times(\mathbb{A}^{-1})_{hi}(x''',x'''')\left[(Q_{if}(x''''))\,\delta^{x''''x'}\right]\\
&= 4\int_{x'\ldots x''''}\sum_{fghi}\int\frac{dp}{(2\pi)^d}\frac{\mathrm{d}q}{(2\pi)^d}\frac{dr}{(2\pi)^d}\frac{ds}{(2\pi)^d}\delta^{-1}_{fg}\delta^{-1}_{hi}\delta_{gh}\delta_{if}\\
&\quad\times\frac{\mathrm{e}^{ip(x'-x'')+iq(x'''-x'''')+ir(x''-x''')+is(x''''-x')}}{(q^2+\gamma)(p^2+\gamma)}Q_{gg}(x'')Q_{ii}(x'''')\\
&\quad+4\int_{x'\ldots x''''}\sum_{fghi}\int\frac{dp}{(2\pi)^d}\frac{\mathrm{d}q}{(2\pi)^d}\frac{dr}{(2\pi)^d}\frac{ds}{(2\pi)^d}\delta^{-1}_{fg}\delta^{-1}_{hi}\\
&\quad\times\frac{\mathrm{e}^{ip(x'-x'')+iq(x'''-x'''')+ir(x''-x''')+is(x''''-x')}}{(q^2+\gamma)(p^2+\gamma)}Q_{gh}(x'')Q_{if}(x'''')\\
&= 4\sum_i\int\frac{dp\,dq}{(2\pi)^{2d}}\frac{Q_{ii}(q)Q_{ii}(-q)}{(p^2+\gamma)((q-p)^2+\gamma)}\\
&\qquad+4\sum_{ig}\int\frac{dp\,dq}{(2\pi)^{2d}}\frac{Q_{ig}(q)Q_{ig}(-q)}{(p^2+\gamma)((q-p)^2+\gamma)}\\
&= 4\sum_i\int\frac{\mathrm{d}q}{(2\pi)^d}Q_{ii}(q)\Omega^{-1}Q_{ii}(-q)\\
&\qquad+4\sum_{ig}\int\frac{\mathrm{d}q}{(2\pi)^{2d}}\,Q_{ig}(q)\Omega^{-1}(q)Q_{ig}(-q). \qquad \text{(C.1.5)}
\end{aligned}$$

The $\int \mathrm{d}x\mathrm{d}x'\ \boldsymbol{\mu}^{\mathsf{T}}\mathbb{M}^{-1}(x,x')\boldsymbol{\mu}$ term is our next object of evaluation.

$$\begin{aligned}
&\frac{1}{8}\int \mathrm{d}x\mathrm{d}x'\ \boldsymbol{\mu}^{\mathsf{T}}\mathbb{M}^{-1}(x,x')\boldsymbol{\mu} \\
&\quad = \frac{1}{8}\int_{x,x'} \boldsymbol{\mu}^{\mathsf{T}}\left[\mathbb{D}\left(1+\mathbb{D}^{-1}\mathbb{Q}\right)\right]^{-1}\boldsymbol{\mu} \\
&\qquad = \frac{1}{8}\int_{xx'} \boldsymbol{\mu}^{\mathsf{T}}\left[\mathbb{D}^{-1}-\mathbb{D}^{-1}\mathbb{Q}\mathbb{D}^{-1}+\frac{1}{2}\left(\mathbb{D}^{-1}\mathbb{Q}\right)^2\mathbb{D}^{-1}\right]\boldsymbol{\mu} \qquad \text{(C.1.6)}
\end{aligned}$$

We proceed by starting with the evaluation of $\int_{xx'}\ \boldsymbol{\mu}^{\mathsf{T}}\mathbb{D}^{-1}\mathbb{Q}\mathbb{D}^{-1}\boldsymbol{\mu}$ and $\int_{xx'}\ \boldsymbol{\mu}^{\mathsf{T}}\left(\mathbb{D}^{-1}\mathbb{Q}\right)^2\mathbb{D}^{-1}\boldsymbol{\mu}$. The first term is given by

$$\begin{aligned}
&\int_{xx'}\ \boldsymbol{\mu}^{\mathsf{T}}\mathbb{D}^{-1}\mathbb{Q}\mathbb{D}^{-1}\boldsymbol{\mu} = 2\int_{xx'}\ \boldsymbol{\mu}^{\mathsf{T}}\mathbb{A}^{-1}\mathbb{C}\mathbb{A}^{-1}\boldsymbol{\mu} + 2\int_{xx'}\ \boldsymbol{\mu}^{\mathsf{T}}\mathbb{A}^{-1}\mathbb{D}\mathbb{A}^{-1}\boldsymbol{\mu} \\
&= 2\int_{xx'x''x'''}\sum_{abcd}\boldsymbol{\mu}_{ia}(\mathbb{A}^{-1})_{ab}(x,x'')\left[2Q_{bb}(x'')\delta_{bc}(x'')\delta^{x''x'''}\right](\mathbb{A}^{-1})_{cd}(x''',x')\boldsymbol{\mu}_{dj} \\
&\quad +2\int_{xx'x''x'''}\sum_{abcd}\boldsymbol{\mu}_{ia}(\mathbb{A}^{-1})_{ab}(x,x'')\left[2Q_{bc}(x'')\delta^{x''x'''}\right](\mathbb{A}^{-1})_{cd}(x''',x')\boldsymbol{\mu}_{dj} \\
&= 4\int_{xx'x'''}\sum_{abcd}\int\frac{dp}{(2\pi)^d}\frac{\mathrm{d}q}{(2\pi)^d}\boldsymbol{\mu}_{ia}\boldsymbol{\mu}_{dj}\delta^{-1}_{ab}\delta_{bc}\delta^{-1}_{cd}\frac{\mathrm{e}^{ip(x'-x''')+iq(x'''-x')}}{(q^2+\gamma)(p^2+\gamma)}Q_{bb}(x''') \\
&\quad +4\int_{xx'x'''}\sum_{abcd}\int\frac{dp}{(2\pi)^d}\frac{\mathrm{d}q}{(2\pi)^d}\boldsymbol{\mu}_{ia}\boldsymbol{\mu}_{dj}\delta^{-1}_{ab}\delta^{-1}_{cd}\frac{\mathrm{e}^{ip(x-x''')+iq(x'''-x')}}{(q^2+\gamma)(p^2+\gamma)}Q_{bc}(x''') \\
&= \frac{4}{\gamma^2}\sum_b\boldsymbol{\mu}_{1b}\boldsymbol{\mu}_{b1}Q_{bb}(0)+\frac{4}{\gamma^2}\sum_{bd}\boldsymbol{\mu}_{1b}\boldsymbol{\mu}_{d1}Q_{bd}(0) \\
&\int_{xx'}\ \boldsymbol{\mu}^{\mathsf{T}}\mathbb{D}^{-1}\mathbb{Q}\mathbb{D}^{-1}\boldsymbol{\mu} = \frac{4(2n)Q_{bb}(0)+4((2n)^2-(2n))Q_{bd}(0)}{\gamma^2} \qquad \text{(C.1.7)}
\end{aligned}$$

The second term $\int_{xx'}\ \boldsymbol{\mu}^{\mathsf{T}}\left(\mathbb{D}^{-1}\mathbb{Q}\right)^2\mathbb{D}^{-1}\boldsymbol{\mu}$ is given by

$$\begin{aligned}
&\int_{xx'}\ \boldsymbol{\mu}^{\mathsf{T}}\left(\mathbb{D}^{-1}\mathbb{Q}\right)^2\mathbb{D}^{-1}\boldsymbol{\mu} = 2\int_{xx'}\ \boldsymbol{\mu}^{\mathsf{T}}\mathbb{A}^{-1}\mathbb{C}\mathbb{A}^{-1}\mathbb{C}^{-1}\mathbb{A}^{-1}\boldsymbol{\mu} \\
&\quad +2\int_{xx'}\ \boldsymbol{\mu}^{\mathsf{T}}\mathbb{A}^{-1}\mathbb{D}\mathbb{A}^{-1}\mathbb{D}\mathbb{A}^{-1}\boldsymbol{\mu}+4\int_{xx'}\ \boldsymbol{\mu}^{\mathsf{T}}\mathbb{A}^{-1}\mathbb{C}\mathbb{A}^{-1}\mathbb{D}\mathbb{A}^{-1}\boldsymbol{\mu}. \qquad \text{(C.1.8)}
\end{aligned}$$

Now,

$$\begin{aligned}
&\int_{xx'} \boldsymbol{\mu}^{\mathsf{T}}\mathbb{A}^{-1}\mathbb{C}\mathbb{A}^{-1}\mathbb{C}^{-1}\mathbb{A}^{-1}\boldsymbol{\mu} \\
&= 4\sum_{abcdef}\int_{\substack{xx'x''\\ x'''x''''x'''''}} \boldsymbol{\mu}_{ia}(\mathbb{A}^{-1}(x,x''))_{ab}\left[\delta_{bc}Q_{bb}(x'')\delta^{x''x'''}\right] \\
&\quad\times(\mathbb{A}^{-1}(x''',x''''))_{cd}\left[\delta_{de}Q_{dd}(x'''')\delta^{x''''x'''''}\right](\mathbb{A}^{-1}(x'''',x'))_{ef}\boldsymbol{\mu}_{fj} \\
&= 4\sum_{abcdef}\int_{\substack{xx'x''\\ x'''x''''x'''''}} \boldsymbol{\mu}_{ia}\left(\delta_{ab}\right)^{-1}\left(\delta_{cd}\right)^{-1}\left(\delta_{ef}\right)^{-1}\delta_{bc}\delta_{de} \\
&\quad\times\int\frac{dp}{(2\pi)^d}\frac{e^{ip(x-x'')}}{p^2+\gamma}\int\frac{\mathrm{d}q}{(2\pi)^d}\frac{e^{iq(x'''-x'''')}}{q^2+\gamma}\int\frac{dr}{(2\pi)^d}\frac{e^{ir(x'''''-x')}}{r^2+\gamma} \\
&\qquad\qquad\times\left[Q_{bb}(x'')\delta^{x''x'''}Q_{dd}(x'''')\delta^{x''''x'''''}\right]\boldsymbol{\mu}_{fj}
\end{aligned}$$

$$\begin{aligned}
&\int_{xx'} \boldsymbol{\mu}^{\mathsf{T}}\mathbb{A}^{-1}\mathbb{C}\mathbb{A}^{-1}\mathbb{C}^{-1}\mathbb{A}^{-1}\boldsymbol{\mu} \\
&= 4\sum_{a}\int\frac{dp}{(2\pi)^d}\frac{\mathrm{d}q}{(2\pi)^d}\frac{dr}{(2\pi)^d}\boldsymbol{\mu}_{1a}\boldsymbol{\mu}_{a1}\frac{Q_{aa}(q-p)Q_{aa}(r-q)\delta(p)\delta(r)}{(p^2+\gamma)(q^2+\gamma)(r^2+\gamma)} \\
&= 4\sum_{a}\int\frac{\mathrm{d}q}{(2\pi)^d}\boldsymbol{\mu}_{1a}\boldsymbol{\mu}_{a1}\frac{Q_{aa}(q)Q_{aa}(-q)}{\gamma^2(q^2+\gamma)}. \qquad \text{(C.1.9)}
\end{aligned}$$

Also,

$$\begin{aligned}
&\int_{xx'} \boldsymbol{\mu}^{\mathsf{T}}\mathbb{A}^{-1}\mathbb{D}\mathbb{A}^{-1}\mathbb{D}\mathbb{A}^{-1}\boldsymbol{\mu} \\
&= 4\sum_{abcdef}\int_{\substack{xx'x''\\ x'''x''''x'''''}} \boldsymbol{\mu}_{ia}(\mathbb{A}^{-1}(x,x''))_{ab}\left[Q_{bc}(x'')\delta^{x''x'''}\right] \\
&\quad\times(\mathbb{A}^{-1}(x''',x''''))_{cd}\left[Q_{de}(x'''')\delta^{x''''x'''''}\right](\mathbb{A}^{-1}(x'''',x'))_{ef}\boldsymbol{\mu}_{fj} \\
&= 4\sum_{abcdef}\int_{\substack{xx'x''\\ x'''x''''x'''''}} \boldsymbol{\mu}_{ia}\left(\delta_{ab}\right)^{-1}\left(\delta_{cd}\right)^{-1}\left(\delta_{ef}\right)^{-1} \\
&\quad\times\int\frac{dp}{(2\pi)^d}\frac{e^{ip(x-x'')}}{p^2+\gamma}\int\frac{\mathrm{d}q}{(2\pi)^d}\frac{e^{iq(x'''-x'''')}}{q^2+\gamma}\int\frac{dr}{(2\pi)^d}\frac{e^{ir(x'''''-x')}}{r^2+\gamma} \\
&\qquad\qquad\times\left[Q_{bc}(x'')\delta^{x''x'''}Q_{de}(x'''')\delta^{x''''x'''''}\right]\boldsymbol{\mu}_{fj} \\
&= 4\sum_{bdf}\int\frac{dp}{(2\pi)^d}\frac{\mathrm{d}q}{(2\pi)^d}\frac{dr}{(2\pi)^d}\boldsymbol{\mu}_{1b}\boldsymbol{\mu}_{f1}\frac{Q_{bd}(q-p)Q_{df}(r-q)\delta(p)\delta(r)}{(p^2+\gamma)(q^2+\gamma)(r^2+\gamma)} \\
&= 4\sum_{bdf}\int\frac{\mathrm{d}q}{(2\pi)^d}\boldsymbol{\mu}_{1b}\boldsymbol{\mu}_{f1}\frac{Q_{bd}(q)Q_{df}(-q)}{\gamma^2(q^2+\gamma)}. \qquad \text{(C.1.10)}
\end{aligned}$$

Finally,

$$\begin{aligned}
&\int_{xx'} \boldsymbol{\mu}^{\mathsf{T}}\mathbb{A}^{-1}\mathbb{C}\mathbb{A}^{-1}\mathbb{D}\mathbb{A}^{-1}\boldsymbol{\mu} \\
&= 4\sum_{abcdef}\int_{\substack{xx'x''\\x'''x''''x'''''}} \boldsymbol{\mu}_{ia}(\mathbb{A}^{-1}(x,x''))_{ab}\left[\delta_{bc}Q_{bb}(x'')\delta^{x''x'''}\right] \\
&\quad\times(\mathbb{A}^{-1}(x''',x''''))_{cd}\left[Q_{de}(x'''')\delta^{x''''x'''''}\right](\mathbb{A}^{-1}(x'''',x'))_{ef}\boldsymbol{\mu}_{fj} \\
&= 4\sum_{abcdef}\int_{\substack{xx'x''\\x'''x''''x'''''}} \boldsymbol{\mu}_{ia}\left(\delta_{ab}\right)^{-1}\left(\delta_{cd}\right)^{-1}\left(\delta_{ef}\right)^{-1}\delta_{bc} \\
&\quad\times\int\frac{dp}{(2\pi)^d}\frac{e^{ip(x-x'')}}{p^2+\gamma}\int\frac{\mathrm{d}q}{(2\pi)^d}\frac{e^{iq(x'''-x'''')}}{q^2+\gamma}\int\frac{dr}{(2\pi)^d}\frac{e^{ir(x''''-x')}}{r^2+\gamma} \\
&\qquad\qquad\times\left[Q_{bb}(x'')\delta^{x''x'''}Q_{de}(x'''')\delta^{x''''x'''''}\right]\boldsymbol{\mu}_{fj} \\
&= 4\sum_{bf}\int\frac{dp}{(2\pi)^d}\frac{\mathrm{d}q}{(2\pi)^d}\frac{dr}{(2\pi)^d}\boldsymbol{\mu}_{1b}\boldsymbol{\mu}_{f1}\frac{Q_{bb}(q-p)Q_{bf}(r-q)\delta(p)\delta(r)}{(p^2+\gamma)(q^2+\gamma)(r^2+\gamma)} \\
&= 4\sum_{bf}\int\frac{\mathrm{d}q}{(2\pi)^d}\boldsymbol{\mu}_{1b}\boldsymbol{\mu}_{f1}\frac{Q_{bb}(q)Q_{bf}(-q)}{\gamma^2(q^2+\gamma)}. \qquad \text{(C.1.11)}
\end{aligned}$$

Therefore,

$$\begin{aligned}
\int_{xx'}\boldsymbol{\mu}^{\mathsf{T}}\left(\mathbb{D}^{-1}\mathbb{Q}\right)^2\mathbb{D}^{-1}\boldsymbol{\mu} &= 8\sum_{a}\int\frac{\mathrm{d}q}{(2\pi)^d}\boldsymbol{\mu}_{1a}\boldsymbol{\mu}_{a1}\frac{Q_{aa}(q)Q_{aa}(-q)}{\gamma^2(q^2+\gamma)} \\
&+8\sum_{bdf}\int\frac{\mathrm{d}q}{(2\pi)^d}\boldsymbol{\mu}_{1b}\boldsymbol{\mu}_{f1}\frac{Q_{bd}(q)Q_{df}(-q)}{\gamma^2(q^2+\gamma)} \\
&+16\sum_{bf}\int\frac{\mathrm{d}q}{(2\pi)^d}\boldsymbol{\mu}_{1b}\boldsymbol{\mu}_{f1}\frac{Q_{bb}(q)Q_{bf}(-q)}{\gamma^2(q^2+\gamma)}. \qquad \text{(C.1.12)}
\end{aligned}$$

We shall now evaluate the prefactor terms $-\frac{1}{2}\mathrm{tr}\ln\mathbb{D}$ and $\frac{1}{8}\int_{xx'}\boldsymbol{\mu}^{\mathsf{T}}\mathbb{D}^{-1}\boldsymbol{\mu}$ of our partition functional (4.2.17). According to (3.1.21), in one dimension $d=1$, we have

$$\mathrm{tr}\ln\mathbb{D} = 2n\ \mathrm{tr}\ln\mathbb{A}(x,x') = 2n\left(\log\left(\sinh\left(\frac{\sqrt{\zeta}L}{\sqrt{\kappa}}\right)\right)-\log\left(\frac{\sqrt{\zeta}L}{\pi\sqrt{\kappa}}\right)\right). \qquad \text{(C.1.13)}$$

The pressure term is given by

$$\begin{aligned}\int_{xx'} \boldsymbol{\mu}^{\mathsf{T}}\mathbb{D}^{-1}\boldsymbol{\mu} &= \sum_{a,b}\int \mathrm{d}x\mathrm{d}x'\ \boldsymbol{\mu}_{ia}\left(\mathbb{A}^{-1}(x,x')\right)_{ab}\boldsymbol{\mu}_{bj} \\ &= \sum_{a,b}\int \mathrm{d}x\mathrm{d}x'\boldsymbol{\mu}_{ia}\boldsymbol{\mu}_{bj}\delta_{ab}{}^{-1}\int\frac{\mathrm{d}q}{(2\pi)^d}\frac{e^{iq(x-x')}}{q^2+\gamma} \\ &= \sum_{a}\int\frac{\mathrm{d}q}{(2\pi)^d}\boldsymbol{\mu}_{ia}\boldsymbol{\mu}_{bj}\frac{\delta(q)\delta(-q)}{q^2+\gamma} = \frac{2n\mu^2\delta(0)}{\gamma}\end{aligned} \tag{C.1.14}$$

C.2 Evaluation of $\Omega^{-1}(q)$

In this appendix we evaluate or simplify the quantity $\frac{1}{\Omega(q)}$. This requires Feynman's parametric integral formula [82]

$$\frac{1}{A^aB^b} = \frac{\Gamma(a+b)}{\Gamma(a)\Gamma(b)}\int_0^1 \mathrm{d}x\frac{x^{a-1}(1-x)^{b-1}}{(Ax+B(1-x))^{a+b}}. \tag{C.2.1}$$

Applying this result (C.2.1) to the expression

$$\Omega^{-1}(q) = \int\frac{dp}{(2\pi)^d}\frac{1}{(p^2+\gamma)((q-p)^2+\gamma)} \tag{C.2.2}$$

we obtain

$$\begin{aligned}\frac{1}{\Omega(q)} &= \frac{\Gamma(2)}{}\int_p\int_0^1 \mathrm{d}x\frac{1}{((p^2+\gamma)-(p^2+\gamma)x+((q-p)^2+\gamma)x)^2} \\ &= \frac{\Gamma(2)}{}\int_0^1\mathrm{d}x\int\frac{dp}{(2\pi)^d}\frac{1}{((q^2-2pq)x+p^2+\gamma)^2}.\end{aligned} \tag{C.2.3}$$

A completion of the square upon (p^2-2pqx) result in

$$\frac{1}{\Omega(q)} = \frac{\Gamma(2)}{}\int_0^1\mathrm{d}x\int\frac{dp}{(2\pi)^d}\frac{1}{(p^2+\gamma+q^2x(1-x))^2}. \tag{C.2.4}$$

Analogous to

$$\int\frac{dp}{(2\pi)^d}\frac{1}{p^2+m^2} = \int_p\int_0^\infty du\exp\left(-u(p^2+m^2)\right) = \frac{\pi^{d/2}m^{d-2}}{(2\pi)^d}\Gamma(1-d/2) \tag{C.2.5}$$

where the integral representation for $\Gamma(z)$ is

$$\Gamma(z) = \int_0^\infty du\ u^{z-1}e^{-u}. \tag{C.2.6}$$

The expression for $\frac{1}{\Omega(q)}$ (C.2.4) becomes

$$\frac{1}{\Omega(q)} = \frac{\Gamma(2)}{} \int_0^1 \mathrm{d}x \int \frac{dp}{(2\pi)^d} \int_0^\infty du\; u \exp\left(-u(x(1-x)q^2+\gamma+p^2)\right)$$
$$= \frac{\Gamma(2)}{} \int_0^1 dx \int_0^\infty du \frac{(\pi/u)^{d/2}}{(2\pi)^d}\; u \exp\left(-u(x(1-x)q^2+\gamma)\right). \quad \text{(C.2.7)}$$

After a change of variables transformation on the exponential quantity we obtain

$$\begin{aligned}
\frac{1}{\Omega(q)} &= \Gamma(2)\frac{\pi^{d/2}}{(2\pi)^d} \int_0^\infty du\; u^{1-d/2} e^{-u} \int_0^1 dx \frac{1}{(x(1-x)q^2+\gamma)^{\frac{4-d}{2}}} \\
&= \Gamma(2)\frac{\pi^{d/2}}{(2\pi)^d} \Gamma\left(\frac{4-d}{2}\right) \int_0^1 dx \frac{1}{(x(1-x)q^2+\gamma)^{\frac{4-d}{2}}} \\
\frac{1}{\Omega(q)} &= \Gamma(2)\frac{\pi^{d/2}}{(2\pi)^d} \Gamma\left(\frac{\alpha}{2}\right) \int_0^1 dx \frac{1}{(x(1-x)q^2+\gamma)^{\frac{\alpha}{2}}}. \qquad \text{(C.2.8)}
\end{aligned}$$

After the approximate expansion of the following terms

$$\frac{1}{(\gamma+q^2x(1-x))^{\alpha/2}}$$
$$= \exp\left\{-\frac{\alpha}{2}\ln(\gamma+q^2x(1-x))\right\} \approx 1-\frac{\alpha}{2}\ln(\gamma+q^2x(1-x))$$

and from the Table of Integrals [80]

$$\Gamma(-m+\alpha/2)$$
$$\approx \frac{(-1)^m}{m!}\left\{\frac{2}{\alpha}+\psi(m+1)+\frac{\alpha}{4}\left[\frac{\pi^2}{3}+\psi^2(m+1)-\psi'(m+1)\right]\right\}$$

where $\psi(m+1) = 1+\frac{1}{2}+\cdots+\frac{1}{m}-0.5772$, $\psi'(m+1) = \frac{\pi^2}{6}-\Sigma_{k=1}^m\frac{1}{k^2}$. Substituting these (C.2.9) and (C.2.9) on (C.2.8) yields

$$\frac{1}{\Omega(q)} = \Gamma(2)\frac{\pi^{d/2}}{(2\pi)^d}\left[\frac{2}{\alpha}+\psi(1)-\int_0^1 dx \ln(x(1-x)q^2+\gamma)\right]. \qquad \text{(C.2.9)}$$

The task that now remains is of evaluating the integral contained in (C.2.9). Fortunately, we can evaluate this integral term $\int_0^1 \mathrm{d}x\;\ln(\gamma+q^2x(1-x))$ using the identity [83]

$$\int_0^1 \mathrm{d}x\;\ln\left(1+\frac{4}{a}x(1-x)\right) = -2+\sqrt{1+a}\ln\frac{\sqrt{1+a}+1}{\sqrt{1+a}-1}. \qquad \text{(C.2.10)}$$

Therefore

$$\int_0^1 \mathrm{d}x\ \ln\left(\gamma + q^2 x(1-x)\right) = \ln\gamma + \int_0^1 \mathrm{d}x\ \ln\left(1 + 4\frac{1}{4\gamma}q^2 x(1-x)\right)$$
$$= \ln(\gamma) - 2 + \sqrt{1+\frac{4\gamma}{q^2}}\ln\frac{\sqrt{1+\frac{4\gamma}{q^2}}+1}{\sqrt{1+\frac{4\gamma}{q^2}}-1}. \qquad \text{(C.2.11)}$$

Substituting this result into (C.2.9) we have

$$\frac{1}{\Omega(q)} = \Gamma(2)\frac{\pi^{d/2}}{(2\pi)^d}\left[\frac{2}{\alpha} + \psi(1) - \int_0^1 dx \ln(x(1-x)q^2+\gamma)\right]$$
$$\frac{1}{\Omega(q)} = \Gamma(2)\frac{\pi^{d/2}}{(2\pi)^d}\left[\frac{2}{\alpha} + \psi(1) - \ln(\gamma) + 2 - \sqrt{1+\frac{4\gamma}{q^2}}\ln\frac{\sqrt{1+\frac{4\gamma}{q^2}}+1}{\sqrt{1+\frac{4\gamma}{q^2}}-1}\right] \qquad \text{(C.2.12)}$$

C.3 Evaluation of $S_1[d=1]$

In this section we perform substitution to the conclusion of the integration evaluation of the below quantity

$$S_1 \approx -\frac{2n}{2(2\pi)^{d/2}\Gamma(d/2)}\left\{\int_0^{\frac{1}{\sqrt{1/4\gamma}}} \mathrm{d}q\ q^{d-1}\ln\left[\frac{1}{\Delta} - \frac{\mu^2}{\gamma^3} + \left(\frac{\mu^2}{\gamma^4} + \frac{(4\pi)^{\alpha/2}}{48\pi^2\gamma}\right)q^2 - \frac{(4\pi)^{\alpha/2}}{8\pi^2}\left\{\frac{2}{\alpha} + \psi(1) - \ln(\gamma)\right\}\right] + \int_{\frac{1}{\sqrt{1/4\gamma}}}^{\Lambda} \mathrm{d}q\ q^{d-1}\ln\left[\frac{1}{\Delta} - \frac{\mu^2}{\gamma^2 q^2} - \frac{(4\pi)^{\alpha/2}}{8\pi^2} \times \left\{\frac{2}{\alpha} + \psi(1) - \ln(\gamma) + 2 - \left(1 + \frac{1}{2}\frac{4}{q^2}\right)\ln\left(1+\frac{q^2}{2\gamma}\right)\right\}\right]\right\}. \qquad \text{(C.3.1)}$$

In the one dimension, $d=1$, scenario we have

$$S_1[d=1] \approx -\frac{(2n)L}{\sqrt{8}\pi}\left\{\int_0^{\frac{1}{\sqrt{1/4\gamma}}} \mathrm{d}q\ \ln\left[\frac{1}{\Delta} - \frac{\mu^2}{\gamma^3} + \left(\frac{\mu^2}{\gamma^4} + \frac{(4\pi)^{3/2}}{48\pi^2\gamma}\right)q^2 - \frac{(4\pi)^{3/2}}{8\pi^2}\left\{\frac{2}{3} - 0.577 - \ln(\gamma)\right\}\right] + \int_{\frac{1}{\sqrt{1/4\gamma}}}^{\Lambda} \mathrm{d}q\ \ln\left[\frac{1}{\Delta} - \frac{\mu^2}{\gamma^2 q^2} - \frac{(4\pi)^{3/2}}{8\pi^2} \times \left\{\frac{2}{3} - 0.577 - \ln(\gamma) + 2 - \left(1 + \frac{1}{2}\frac{4}{q^2}\right)\ln\left(1+\frac{q^2}{2\gamma}\right)\right\}\right]\right\}.$$

$$
\begin{aligned}
S_1[d=1] \approx & -\frac{(2n)L}{\sqrt{8}\pi}\left\{-4\sqrt{\frac{\beta k\rho_0}{1}}+\frac{4\sqrt{6}\sqrt{\beta k\rho_0}}{\sqrt{1}\sqrt{\frac{\beta^2k^2}{R}}\sqrt{24\sqrt{\pi}^2\mu^2+\beta^3k^3\rho_0^3}}\right. \\
& \times\tan^{-1}\left(\frac{\sqrt{\frac{\beta^2k^2}{R}}\sqrt{\beta k\rho_0}\sqrt{24\sqrt{\pi}\mu^2+\beta^3k^3\rho_0^3}}{\sqrt{6}\sqrt{\beta k\rho_0}\sqrt{-\frac{\beta^5ck^5\rho_0^3}{4R}+\frac{\beta^5k^5\rho_0^3\log(\beta k\rho_0)}{4R}+\sqrt{\pi}\left(\beta^3k^3\rho_0^3-\frac{\beta^2k^2\mu^2}{R}\right)}}\right) \\
& \times\sqrt{-\frac{\beta^5ck^5\rho_0^3}{4R}+\frac{\beta^5k^5\rho_0^3\log(\beta k\rho_0)}{4R}+\sqrt{\pi}\left(\beta^3k^3\rho_0^3-\frac{\beta^2k^2\mu^2}{R}\right)} \\
& +2\sqrt{\beta k\rho_0}\log\left(\frac{\log(\beta k\rho_0)-c}{\sqrt{\pi}}+\frac{4\beta k\rho_0\left(\frac{4\mu^2}{\beta^4k^4\rho_0^4}+\frac{1}{6\sqrt{\pi}\beta k\rho_0}\right)}{1}-\frac{4\mu^2}{\beta^3k^3\rho_0^3}+\frac{4R}{\beta^2k^2}\right) \\
& -\frac{(2n)L}{\sqrt{8}\pi}\int_{\frac{1}{\sqrt{1/4\gamma}}}^{\Lambda}\mathrm{d}q\ \ln\left[\frac{1}{\Delta}-\frac{\mu^2}{\gamma^21q^2}-\frac{(4\pi)^{3/2}}{8\pi^2}\right. \\
& \left.\left.\times\left\{\frac{2}{3}-0.577-\ln(\gamma)+2-\left(1+\frac{1}{2}\frac{4}{q^2}\right)\ln\left(1+\frac{q^2}{2\gamma}\right)\right\}\right]\right\}. \qquad \text{(C.3.2)}
\end{aligned}
$$

The cut-off Λ integral component we shall evaluate numerically.

C.4 Evaluation of $S_2[d=1]$

In this section we perform substitution to the integration evaluation of the below quantity. In dimension $d=1$. The component $\frac{2n}{4}\sum_q \ln\left(\frac{1}{\Delta}-2\Omega^{-1}(q)\right)$ is further given by

$$
\begin{aligned}
\frac{2n}{4}\sum_q\ln\left(\frac{1}{\Delta}-2\Omega^{-1}(q)\right) &= \frac{2n}{4}\sum_q\ln\left(\frac{1}{\Delta}-2\Omega^{-1}(q)\right)\approx\frac{(2n)L}{\sqrt{32}\pi} \\
&\left\{\int_0^{\frac{1}{\sqrt{1/4\gamma}}}\mathrm{d}q\ \ln\left[\frac{1}{\Delta}+\frac{(4\pi)^{3/2}q^2}{48\pi^2\gamma}-\frac{(4\pi)^{3/2}}{8\pi^2}\left\{\frac{2}{3}-0.577-\ln(\gamma)\right\}\right]\right. \\
&+\int_{\frac{1}{\sqrt{1/4\gamma}}}^{\Lambda}\mathrm{d}q\ \ln\left[\frac{1}{\Delta}-\frac{(4\pi)^{3/2}}{8\pi^2}\right. \\
&\left.\left.\times\left\{\frac{2}{3}-0.577-\ln(\gamma)+2-\left(1+\frac{1}{2}\frac{4}{q^2}\right)\ln\left(1+\frac{q^2}{2\gamma}\right)\right\}\right]\right\}
\end{aligned}
$$

$$
\begin{aligned}
\approx \quad & \frac{(2n)L}{\sqrt{32\pi}}\left[2\sqrt{\beta k\rho}\log\left(\frac{\log(\beta k\rho)-c}{\sqrt{\pi}}+\frac{2}{3\sqrt{\pi}}+\frac{4R}{\beta^2k^2}\right)\right. \\
& +\frac{4\sqrt{6}\sqrt{\beta k\rho}\sqrt{-\frac{\beta^2ck^2}{4R}+\sqrt{\pi}+\frac{\beta^2k^2\log(\beta k\rho)}{4R}}}{\sqrt{\kappa}\sqrt{\frac{\beta^2k^2}{R}}} \\
& \qquad \times\tan^{-1}\left(\frac{\sqrt{\kappa}\sqrt{\frac{\beta^2k^2}{R}}\sqrt{\beta k\rho}}{\sqrt{6}\sqrt{\beta k\rho}\sqrt{-\frac{\beta^2ck^2}{4R}+\sqrt{\pi}+\frac{\beta^2k^2\log(\beta k\rho)}{4R}}}\right) \\
& \left.-4\sqrt{\beta k\rho}\right]+\frac{(2n)L}{\sqrt{32\pi}}\int_{\frac{1}{\sqrt{1/4\gamma}}}^{\Lambda}\mathrm{d}q\ \ln\left[\frac{1}{\Delta}-\frac{(4\pi)^{3/2}}{8\pi^2}\left\{\frac{2}{\alpha}+\psi(1)-\ln(\gamma)\right.\right. \\
& \qquad \left.\left.+2-\left(1+\frac{1}{2}\frac{4}{q^2}\right)\ln\left(1+\frac{q^2}{2\gamma}\right)\right\}\right]\Bigg\}. \qquad \text{(C.4.1)}
\end{aligned}
$$

The component $-\frac{2n}{4}\sum_q \frac{\left(\frac{1}{\Delta}-2\Omega^{-1}(q)-\frac{\mu^2}{\gamma^2(q^2+\gamma)}\right)^{-1}\frac{\mu^4}{\gamma^4(q^2+\gamma)^2}+\frac{\mu^2}{\gamma^2(q^2+\gamma)}}{\frac{1}{\Delta}-2\Omega^{-1}(q)}$, that is, equation (4.2.37) becomes equivalent to

$$
\begin{aligned}
&-\frac{(2n)L}{\sqrt{32}\pi}\left\{\int_0^{\frac{1}{\sqrt{1/4\gamma}}}\mathrm{d}q\right.\\
&\qquad\frac{\left(\frac{\mu^4}{\gamma^6}-\frac{2\mu^4\kappa q^2}{\gamma^7}\right)}{\left[\frac{1}{\Delta}-\frac{\mu^2}{\gamma^3}+\left(\frac{\mu^2\kappa}{\gamma^4}+\frac{(4\pi)^{3/2}}{48\pi^2\gamma\kappa}\right)q^2-\frac{(4\pi)^{3/2}}{8\pi^2}\left\{\frac{2}{3}-0.577-\ln(\gamma)\right\}\right]}+\frac{\mu^2}{\gamma^3}-\frac{\mu^2\kappa q^2}{\gamma^4}\\
&\qquad\overline{\left[\frac{1}{\Delta}+\frac{(4\pi)^{3/2}q^2}{48\pi^2\gamma\kappa}-\frac{(4\pi)^{3/2}}{8\pi^2}\left\{\frac{2}{3}-0.577-\ln(\gamma)\right\}\right]}\\
&+\int_{\frac{1}{\sqrt{1/4\gamma}}}^{\Lambda}\mathrm{d}q\\
&\qquad\left.\frac{\frac{\mu^4}{\gamma^4q^4}}{\left[\frac{1}{\Delta}-\frac{\mu^2}{\gamma^2\kappa q^2}-\frac{(4\pi)^{3/2}}{8\pi^2}\left\{\frac{2}{3}-0.577-\ln(\gamma)+2-\left(1+\frac{1}{2}\frac{4}{q^2}\right)\ln\left(1+\frac{q^2}{2\gamma}\right)\right\}\right]}+\frac{\mu^2}{\gamma^2\kappa q^2}}{\left[\frac{1}{\Delta}-\frac{(4\pi)^{3/2}}{8\pi^2}\left\{\frac{2}{3}-0.577-\ln(\gamma)+2-\left(1+\frac{1}{2}\frac{4}{q^2}\right)\ln\left(1+\frac{q^2}{2\gamma}\right)\right\}\right]}\right\}\\
\approx\;&-\frac{(2n)L}{\sqrt{32}\pi}\frac{6\sqrt{\pi}\mu^2}{\beta k\rho_0^3R}\left\{\frac{48\sqrt{6}\sqrt{\beta k\rho_0}\left(-\frac{\beta^2ck^2}{4R}+\sqrt{\pi}+\frac{\beta^2k^2\log(\beta k\rho_0)}{4R}\right)^{3/2}}{\sqrt{\kappa}\left(\frac{\beta^2k^2}{R}\right)^{3/2}\left(-\frac{3\beta^2ck^2}{2R}+6\sqrt{\pi}+\frac{3\beta^2k^2\log(\beta k\rho_0)}{2R}+\frac{\beta^2k^2}{4R}\right)}\right.\\
&\qquad\left.\times\tan^{-1}\left(\frac{\sqrt{\kappa}\sqrt{\frac{\beta^2k^2}{R}}\sqrt{\beta k\rho_0}}{\sqrt{6}\sqrt{\beta k\rho_0}\sqrt{-\frac{\beta^2ck^2}{4R}+\sqrt{\pi}+\frac{\beta^2k^2\log(\beta k\rho_0)}{4R}}}\right)-\frac{8R\sqrt{\beta k\rho_0}}{\beta^2k^2}\right.\\
&+\frac{\sqrt{\frac{2}{3}}\sqrt{\beta k\rho_0}\left(\beta^3k^3\rho_0^3\left(-\frac{3\beta^2ck^2}{R}+12\sqrt{\pi}+\frac{\beta^2k^2}{4R}\right)+\frac{3\beta^5k^5\rho_0^3\log(\beta k\rho_0)}{R}-\frac{6\sqrt{\pi}\beta^2k^2\mu^2}{R}\right)}{\sqrt{\kappa}\sqrt{\frac{\beta^2k^2}{R}}\sqrt{24\sqrt{\pi}\mu^2+\beta^3k^3\rho_0^3}\left(-\frac{3\beta^2ck^2}{2R}+6\sqrt{\pi}+\frac{3\beta^2k^2\log(\beta k\rho_0)}{2R}+\frac{\beta^2k^2}{4R}\right)}\\
&\times\frac{\tan^{-1}\left(\frac{\sqrt{\kappa}\sqrt{\frac{\beta^2k^2}{R}}\sqrt{\beta k\rho_0}\sqrt{24\sqrt{\pi}\mu^2+\beta^3k^3\rho_0^3}}{\sqrt{6}\sqrt{\beta k\rho_0}\sqrt{-\frac{\beta^5ck^5\rho_0^3}{4R}+\frac{\beta^5k^5\rho_0^3\log(\beta k\rho_0)}{4R}+\sqrt{\pi}\left(\beta^3k^3\rho_0^3-\frac{\beta^2k^2\mu^2}{R}\right)}}\right)}{\sqrt{-\frac{\beta^5ck^5\rho_0^3}{4R}+\frac{\beta^5k^5\rho_0^3\log(\beta k\rho_0)}{4R}+\sqrt{\pi}\left(\beta^3k^3\rho_0^3-\frac{\beta^2k^2\mu^2}{R}\right)}}\\
&-\frac{(2n)L}{\sqrt{32}\pi}\int_{\frac{1}{\sqrt{1/4\gamma}}}^{\Lambda}\mathrm{d}q\;\frac{\frac{\frac{\mu^4}{\gamma^4q^4}}{\left[\frac{1}{\Delta}-\frac{\mu^2}{\gamma^2\kappa q^2}-\frac{(4\pi)^{3/2}}{8\pi^2}\left\{\frac{2}{3}-0.577-\ln(\gamma)+2-\left(1+\frac{1}{2}\frac{4}{q^2}\right)\ln\left(1+\frac{q^2}{2\gamma}\right)\right\}\right]}+\frac{\mu^2}{\gamma^2\kappa q^2}}{\left[\frac{1}{\Delta}-\frac{(4\pi)^{3/2}}{8\pi^2}\left\{\frac{2}{3}-0.577-\ln(\gamma)+2-\left(1+\frac{1}{2}\frac{4}{q^2}\right)\ln\left(1+\frac{q^2}{2\gamma}\right)\right\}\right]}
\end{aligned}
\tag{C.4.2}
$$

Appendix D

Components for wRSB

D.1 $\mathbf{tr}\ln\mathbb{M}$ and $\int \mathbf{d}x\mathrm{d}x'\ \boldsymbol{\mu}^{\mathsf{T}}\mathbb{M}^{-1}(x,x')\boldsymbol{\mu}$

$$\mathrm{tr}\ln\mathbb{M}(x,x') \approx \mathrm{tr}\ln\mathbb{D} + \mathrm{tr}\left(\mathbb{D}^{-1}\mathbb{Q}\right) - \frac{1}{2}\mathrm{tr}\left(\mathbb{D}^{-1}\mathbb{Q}\right)^2. \tag{D.1.1}$$

We shall begin with the $\mathrm{tr}\left(\mathbb{D}^{-1}\mathbb{Q}\right)$ term. This requires the determination of the product $\mathbb{D}^{-1}\mathbb{Q}$. This is given by

$$\mathbb{D}^{-1}\mathbb{Q} = \begin{pmatrix} \left[\delta_{ij}\delta^{xx'}\left(\gamma - \partial_{xx}\right)\right]^{-1} & 0 \\ 0 & \left[\delta_{ij}\delta^{xx'}\left(\gamma - \partial_{xx}\right)\right]^{-1} \end{pmatrix} \times \begin{pmatrix} 2\delta_{ij}Q_{ii}^{(1)}(x)\delta^{xx'} & 2\left(\left(Q_{ij}^{(s)}(x) + Q_{ij}^{(a)}(x)\right)\delta^{xx'}\right) \\ 2\left(\left(Q_{ij}^{(s)}(x) - Q_{ij}^{(a)}(x)\right)\delta^{xx'}\right) & 2\delta_{ij}Q_{ii}^{(2)}(x)\delta^{xx'} \end{pmatrix}. \tag{D.1.2}$$

In shorthand notation

$$\mathbb{D}^{-1}\mathbb{Q} = \begin{pmatrix} \mathbb{A}^{-1}(x,x') & 0 \\ 0 & \mathbb{B}^{-1}(x,x') \end{pmatrix}\begin{pmatrix} \mathbb{C}(x,x') & \mathbb{D}(x,x') \\ \mathbb{E}(x,x') & \mathbb{F}(x,x') \end{pmatrix}$$

$$= 2\int \mathrm{d}x'' \sum_l \begin{pmatrix} (\mathbb{A}^{-1})_{il}(x,x'')\mathbb{C}_{lj}(x'',x') & (\mathbb{A}^{-1})_{il}(x,x'')\mathbb{D}_{lj}(x'',x') \\ (\mathbb{B}^{-1})_{il}(x,x'')\mathbb{E}_{lj}(x'',x') & (\mathbb{B}^{-1})_{il}(x,x'')\mathbb{F}_{lj}(x'',x') \end{pmatrix}. \tag{D.1.3}$$

Upon performing a partial re-substitution on equation(D.1.3) in order to organize the important elements when tracing we have

$$\mathbb{D}^{-1}\mathbb{Q} = 2\int \mathrm{d}x'' \sum_l \times$$

$$\begin{pmatrix} (\mathbb{A}^{-1})_{il}(x,x'')[\delta_{lj}Q^{(1)}_{ll}(x'')\delta^{x''x'}] & (\mathbb{A}^{-1})_{il}(x,x'')[(Q^{(s)}_{lj}(x'')+Q^{(a)}_{lj}(x''))\delta^{x''x'}] \\ (\mathbb{A}^{-1})_{il}(x,x'')[(Q^{(s)}_{lj}(x'')-Q^{(a)}_{lj}(x''))\delta^{x''x'}] & (\mathbb{A}^{-1})_{il}(x,x'')[\delta_{lj}Q^{(2)}_{ll}(x'')\delta^{x''x'}] \end{pmatrix} \tag{D.1.4}$$

Subsequently, $\mathrm{tr}\,(\mathbb{D}^{-1}\mathbb{Q})$ in the expression of $\mathrm{tr}\ln\mathbb{M}(x,x')$ equation (D.1.1) becomes

$$\begin{aligned}
&\mathrm{tr}\left(\mathbb{D}^{-1}\mathbb{Q}\right)\\
&= 2\int \mathrm{d}x'dx''\sum_{lm}\Big[(\mathbb{A}^{-1})_{ml}(x',x'')[\delta_{lm}Q^{(1)}_{ll}(x'')\delta^{x''x'}]\\
&\qquad\qquad +(\mathbb{A}^{-1})_{ml}(x',x'')[\delta_{lm}Q^{(2)}_{ll}(x'')\delta^{x''x'}]\Big]\\
&= 2\int \mathrm{d}x'dx''\sum_{lm}\int\frac{dqdr}{(2\pi)^{2d}}\frac{\mathrm{e}^{iq(x'-x'')+ir(x''-x')}}{\kappa q^2+\gamma}\delta^{-1}_{ml}\delta_{ml}\\
&\qquad\qquad \times\left(Q^{(1)}_{mm}(x'')+Q^{(2)}_{mm}(x'')\right)\delta^{x''x'}\\
&= 2\sum_i\int\frac{\mathrm{d}q}{(2\pi)^d}\frac{\left(\tilde{Q}^{(1)}_{ii}(0)+\tilde{Q}^{(2)}_{ii}(0)\right)}{\kappa q^2+\gamma}.
\end{aligned}\tag{D.1.5}$$

We have, again, made used of the identity $(\mathbb{A}^{-1})_{fg}(x',x'')=\int\frac{dp}{(2\pi)^d}\frac{e^{ip(x'-x'')}}{(\kappa p^2+\gamma)}\delta^{-1}_{fg}$ and the Fourier representation of the delta function $\delta^{x''x'}$. We take note that the term is linear in Q_{ii} and has no contribution from Q_{ij}. We now proceed to $\mathrm{tr}\,(\mathbb{D}^{-1}\mathbb{Q})^2=\mathrm{tr}\,\mathbb{D}^{-1}\mathbb{Q}\mathbb{D}^{-1}\mathbb{Q}$ starting with the product $(\mathbb{D}^{-1}\mathbb{Q})^2$ given by

$$\left(\mathbb{D}^{-1}\mathbb{Q}\right)^2 \equiv 4\int \mathrm{d}x''\ldots dx''''\sum_{ghi}\begin{pmatrix} m_{aghib}(x,\ldots,x') & n_{aghib}(x,\ldots,x') \\ o_{aghib}(x,\ldots,x') & p_{aghib}(x,\ldots,x')\end{pmatrix}. \tag{D.1.6}$$

Since our goal is calculating the trace $\mathrm{tr}\,(\mathbb{D}^{-1}\mathbb{Q})^2$ we shall here only determine the diagonal terms $4\int \mathrm{d}x''\ldots dx''''\sum_{ghi}m_{aghib}(x,\ldots,x')$ and $4\int \mathrm{d}x''\ldots dx''''\sum_{ghi}p_{aghib}(x,\ldots,x')$ of this product $(\mathbb{D}^{-1}\mathbb{Q})^2$. The first term is given by

$$\begin{aligned}
&4\int \mathrm{d}x''\ldots dx''''\sum_{ghi}m_{aghib}(x,\ldots,x')\\
&= 4\int \mathrm{d}x''\ldots dx''''\sum_{ghi}(\mathbb{A}^{-1})_{ag}(x,x'')[\delta_{gh}Q^{(1)}_{gg}(x'')\delta^{x''x'''}]\\
&\qquad\qquad\times(\mathbb{A}^{-1})_{hi}(x''',x'''')[\delta_{ib}Q^{(1)}_{ii}(x'''')\delta^{x''''x'}]\\
&\quad +4\int \mathrm{d}x''\ldots dx''''\sum_{ghi}(\mathbb{A}^{-1})_{ag}(x,x'')\left[\left(Q^{(s)}_{gh}(x'')+Q^{(a)}_{gh}(x'')\right)\delta^{x''x'''}\right]\\
&\qquad\qquad\times(\mathbb{A}^{-1})_{hi}(x''',x'''')\left[\left(Q^{(s)}_{ib}(x'''')-Q^{(a)}_{ib}(x'''')\right)\delta^{x''''x'}\right].
\end{aligned}\tag{D.1.7}$$

Similarly, the second term is given by

$$
\begin{aligned}
&4\int \mathrm{d}x''\ldots dx''''\sum_{ghi} p_{aghib}(x,\ldots,x') \\
&\quad= \quad 4\int \mathrm{d}x''\ldots dx''''\sum_{ghi}(\mathbb{A}^{-1})_{ag}(x,x'')\left[\left(Q^{(s)}_{gh}(x'')-Q^{(a)}_{gh}(x'')\right)\delta^{x''x'''}\right] \\
&\qquad\qquad\qquad\qquad\times(\mathbb{A}^{-1})_{hi}(x''',x'''')\left[\left(Q^{(s)}_{ib}(x'''')+Q^{(a)}_{ib}(x'''')\right)\delta^{x''''x'}\right] \\
&\qquad+4\int \mathrm{d}x''\ldots dx''''\sum_{ghi}(\mathbb{A}^{-1})_{ag}(x,x'')[\delta_{gh}Q^{(2)}_{gg}(x'')\delta^{x''x'''}] \\
&\qquad\qquad\qquad\qquad\times(\mathbb{A}^{-1})_{hi}(x''',x'''')[\delta_{ib}Q^{(2)}_{ii}(x'''')\delta^{x''''x'}] \qquad \text{(D.1.8)}
\end{aligned}
$$

Performing the trace tr the term $-\frac{1}{2}\mathrm{tr}\left(\mathbb{D}^{-1}\mathbb{Q}\right)^2$ in the expression of $\mathrm{tr}\ln\mathbb{M}(x,x')$ (D.1.1) then becomes

$$
\begin{aligned}
&-\frac{1}{2}\mathrm{tr}\left(\mathbb{D}^{-1}\mathbb{Q}\right)^2 \\
&\quad= \quad -2\int \mathrm{d}x'dx''\ldots dx''''\sum_{fghi}\Big\{(\mathbb{A}^{-1})_{fg}(x',x'')[\delta_{gh}Q^{(1)}_{gg}(x'')\delta^{x''x'''}] \\
&\qquad\times(\mathbb{A}^{-1})_{hi}(x''',x'''')[\delta_{if}Q^{(1)}_{ii}(x'''')\delta^{x''''x'}]+(\mathbb{A}^{-1})_{fg}(x',x'')[\delta_{gh}Q^{(2)}_{gg}(x'')\delta^{x''x'''}] \\
&\qquad\qquad\qquad\qquad\times\ (\mathbb{A}^{-1})_{hi}(x''',x'''')[\delta_{if}Q^{(2)}_{ii}(x'''')\delta^{x''''x'}]\Big\} \\
&\qquad-2\int \mathrm{d}x'dx''\ldots dx''''\sum_{fghi}\Big\{(\mathbb{A}^{-1})_{fg}(x',x'')\left[\left(Q^{(s)}_{gh}(x'')+Q^{(a)}_{gh}(x'')\right)\delta^{x''x'''}\right] \\
&\qquad\qquad\qquad\qquad\times(\mathbb{A}^{-1})_{hi}(x''',x'''')\left[\left(Q^{(s)}_{if}(x'''')-Q^{(a)}_{if}(x'''')\right)\delta^{x''''x'}\right] \\
&\qquad\qquad\qquad\qquad+(\mathbb{A}^{-1})_{fg}(x',x'')\left[\left(Q^{(s)}_{gh}(x'')-Q^{(a)}_{gh}(x'')\right)\delta^{x''x'''}\right] \\
&\qquad\qquad\times\ (\mathbb{A}^{-1})_{hi}(x''',x'''')\left[\left(Q^{(s)}_{if}(x'''')+Q^{(a)}_{if}(x'''')\right)\delta^{x''''x'}\right]\Big\}. \qquad \text{(D.1.9)}
\end{aligned}
$$

Yet again upon the application of the identity $(\mathbb{A}^{-1})_{fg}(x',x'')=\frac{1}{(2\pi)^d}\int \mathrm{d}p\frac{e^{ip(x'-x'')}}{(\kappa p^2+\gamma)}\delta^{-1}_{fg}$ and the Fourier representation of the delta function $\delta^{x''x'''}$ we obtain

$$
\begin{aligned}
&-\frac{1}{2}\mathrm{tr}\left(\mathbb{D}^{-1}\mathbb{Q}\right)^2 \\
&= -2\int \mathrm{d}x'\ldots dx'''' \sum_{fghi}\left(\int \frac{dp}{(2\pi)^d}\frac{\mathrm{d}q}{(2\pi)^d}\frac{dr}{(2\pi)^d}\frac{ds}{(2\pi)^d}\delta_{fg}^{-1}\delta_{hi}^{-1}\delta_{gh}\delta_{if}\right. \\
&\quad \times \frac{\mathrm{e}^{ip(x'-x'')+iq(x'''-x'''')+ir(x''-x''')+is(x''''-x')}}{(q^2+\gamma)(\kappa p^2+\gamma)}\left(Q_{ii}^{(1)}(x'')Q_{ii}^{(1)}(x'''')\right. \\
&\qquad\qquad \left.\left. +Q_{ii}^{(2)}(x'')Q_{ii}^{(2)}(x'''')\right)\right) \\
&\quad -4\int_{\substack{x' \\ x'''}}^{\substack{x'' \\ x''''}} \sum_{gi}\frac{1}{(2\pi)^{2d}}\int \mathrm{d}p\, dq \frac{e^{ip(x'-x'')+iq(x'''-x'''')}}{(\kappa p^2+\gamma)(q^2+\gamma)} \\
&\qquad\qquad \times\left(Q_{gi}^{(s)}(x'')Q_{ig}^{(s)}(x'''') - Q_{gi}^{(a)}(x'')Q_{ig}^{(a)}(x'''')\right)\delta^{x''x'''}\delta^{x''''x'} \\
&= -2\sum_i \int \frac{dp\, dq}{(2\pi)^{2d}}\frac{\left(\tilde{Q}_{ii}^{(1)}(q)\tilde{Q}_{ii}^{(1)}(-q)+\tilde{Q}_{ii}^{(2)}(q)\tilde{Q}_{ii}^{(2)}(-q)\right)}{(\kappa p^2+\gamma)(\kappa(q-p)^2+\gamma)} \\
&\qquad -4\sum_{gi}\int \frac{dp\, dq}{(2\pi)^{2d}}\frac{\left(\tilde{Q}_{ig}^{(s)}(q)\tilde{Q}_{ig}^{(s)}(-q)+\tilde{Q}_{ig}^{(a)}(q)\tilde{Q}_{ig}^{(a)}(-q)\right)}{(\kappa p^2+\gamma)(\kappa(q-p)^2+\gamma)}. \qquad \text{(D.1.10)}
\end{aligned}
$$

Collecting the results (D.1.5) and (D.1.10) of $\mathrm{tr}\left(\mathbb{D}^{-1}\mathbb{Q}\right)$ and $-\frac{1}{2}\mathrm{tr}\left(\mathbb{D}^{-1}\mathbb{Q}\right)^2$, respectively, we obtain for $\mathrm{tr}\ln\mathbb{M}(x,x')$ equation (D.1.1)

$$
\begin{aligned}
&\mathrm{tr}\ln\mathbb{M}(x,x') \\
&\quad \approx \mathrm{tr}\ln\mathbb{D} + \mathrm{tr}\left(\mathbb{D}^{-1}\mathbb{Q}\right) - \frac{1}{2}\mathrm{tr}\left(\mathbb{D}^{-1}\mathbb{Q}\right)^2 \\
&\quad \approx 2n\ \mathrm{tr}\ln\mathbb{A}(x,x') + 2\int \sum_m \frac{\mathrm{d}q}{(2\pi)^d}\frac{\left(\tilde{Q}_{mm}^{(1)}(0)+\tilde{Q}_{mm}^{(2)}(0)\right)}{\kappa q^2+\gamma} \\
&\qquad -2\sum_{\substack{i \\ m=1,2}}\int \frac{\mathrm{d}q}{(2\pi)^d}\tilde{Q}_{ii}^{(m)}(q)\Omega^{-1}(q)\tilde{Q}_{ii}^{(m)}(-q) \\
&\qquad\qquad -4\sum_{\substack{gi \\ m=s,a}}\int \frac{\mathrm{d}q}{(2\pi)^d}\tilde{Q}_{ig}^{(m)}(q)\Omega^{-1}(q)\tilde{Q}_{ig}^{(m)}(-q). \qquad \text{(D.1.11)}
\end{aligned}
$$

where $\Omega^{-1}(q) = \int \frac{dp}{(2\pi)^d}\frac{1}{(\kappa p^2+\gamma)(\kappa(q-p)^2+\gamma)}$.

Since we have now achieved our goal with the $\mathrm{tr}\ln\mathbb{M}(x,x')$ term in (4.3.2). We shall now proceed to the next term $\int \mathrm{d}x\mathrm{d}x' \begin{pmatrix} \boldsymbol{\mu} \\ \boldsymbol{\mu} \end{pmatrix}^{\mathsf{T}} \mathbb{M}^{-1}(x,x') \begin{pmatrix} \boldsymbol{\mu} \\ \boldsymbol{\mu} \end{pmatrix}$. The basis of the evaluation of this term is similar to the previous one. That

is,

$$\begin{aligned}
\int \mathrm{d}x\mathrm{d}x' \begin{pmatrix} \boldsymbol{\mu} \\ \boldsymbol{\mu} \end{pmatrix}^{\mathsf{T}} \mathbb{M}^{-1}(x,x') \begin{pmatrix} \boldsymbol{\mu} \\ \boldsymbol{\mu} \end{pmatrix} &= \\
&= \int \mathrm{d}x\mathrm{d}x' \begin{pmatrix} \boldsymbol{\mu} \\ \boldsymbol{\mu} \end{pmatrix}^{\mathsf{T}} \left[\mathbb{D}\left(1+\mathbb{D}^{-1}\mathbb{Q}\right)\right]^{-1} \begin{pmatrix} \boldsymbol{\mu} \\ \boldsymbol{\mu} \end{pmatrix} \\
&= \int \mathrm{d}x\mathrm{d}x' \begin{pmatrix} \boldsymbol{\mu} \\ \boldsymbol{\mu} \end{pmatrix}^{\mathsf{T}} \left[\left(1+\mathbb{D}^{-1}\mathbb{Q}\right)^{-1}\mathbb{D}^{-1}\right] \begin{pmatrix} \boldsymbol{\mu} \\ \boldsymbol{\mu} \end{pmatrix} \\
&\approx \int \mathrm{d}x\mathrm{d}x' \begin{pmatrix} \boldsymbol{\mu} \\ \boldsymbol{\mu} \end{pmatrix}^{\mathsf{T}} \left[\left(1-\mathbb{D}^{-1}\mathbb{Q}+\frac{1}{2}\left(\mathbb{D}^{-1}\mathbb{Q}\right)^2\right)\mathbb{D}^{-1}\right] \begin{pmatrix} \boldsymbol{\mu} \\ \boldsymbol{\mu} \end{pmatrix} \quad \text{(D.1.12)}
\end{aligned}$$

Therefore, the integrals that we need to evaluate are
$\Theta = \int \mathrm{d}x\mathrm{d}x' \begin{pmatrix} \boldsymbol{\mu} \\ \boldsymbol{\mu} \end{pmatrix}^{\mathsf{T}} \mathbb{D}^{-1} \begin{pmatrix} \boldsymbol{\mu} \\ \boldsymbol{\mu} \end{pmatrix}$ and $\Lambda = \int \mathrm{d}x\mathrm{d}x' \begin{pmatrix} \boldsymbol{\mu} \\ \boldsymbol{\mu} \end{pmatrix}^{\mathsf{T}} (\mathbb{D}^{-1}\mathbb{Q})\mathbb{D}^{-1} \begin{pmatrix} \boldsymbol{\mu} \\ \boldsymbol{\mu} \end{pmatrix}$
as well as $\Xi = \int \mathrm{d}x\mathrm{d}x' \begin{pmatrix} \boldsymbol{\mu} \\ \boldsymbol{\mu} \end{pmatrix}^{\mathsf{T}} (\mathbb{D}^{-1}\mathbb{Q})^2\,\mathbb{D}^{-1} \begin{pmatrix} \boldsymbol{\mu} \\ \boldsymbol{\mu} \end{pmatrix}$.

The first term Θ is evaluated as follows

$$\begin{aligned}
\Theta &= \int \mathrm{d}x\mathrm{d}x' \begin{pmatrix} \boldsymbol{\mu} \\ \boldsymbol{\mu} \end{pmatrix}^{\mathsf{T}} \mathbb{D}^{-1} \begin{pmatrix} \boldsymbol{\mu} \\ \boldsymbol{\mu} \end{pmatrix} \\
&= \int \mathrm{d}x\mathrm{d}x' \begin{pmatrix} \boldsymbol{\mu} \\ \boldsymbol{\mu} \end{pmatrix}^{\mathsf{T}} \begin{pmatrix} \mathbb{A}^{-1}(x,x') & 0 \\ 0 & \mathbb{A}^{-1}(x,x') \end{pmatrix} \begin{pmatrix} \boldsymbol{\mu} \\ \boldsymbol{\mu} \end{pmatrix} \\
&= 2\int \mathrm{d}x\mathrm{d}x'\, \boldsymbol{\mu}^{\mathsf{T}}\mathbb{A}^{-1}(x,x')\boldsymbol{\mu} = 2\sum_{ab}\int \mathrm{d}x\mathrm{d}x'\, \boldsymbol{\mu}_{ia}\left(\mathbb{A}^{-1}(x,x')\right)_{ab}\boldsymbol{\mu}_{bj} \\
\Theta &= 2\mu^2\sum_{ab}\int \mathrm{d}x\mathrm{d}x' \int \frac{\mathrm{d}q}{(2\pi)^d}\frac{e^{iq(x-x')}}{\kappa q^2+\gamma}\delta_{ab}^{-1} = 2n\mu^2\frac{\delta(0)}{\gamma}. \qquad \text{(D.1.13)}
\end{aligned}$$

We then proceed to the second term Λ evaluation. Fortunately, we have already determined the product $\mathbb{D}^{-1}\mathbb{Q}$ in equation (D.1.4). Subsequently we

have, where a partial substitution has been implemented,

$$\begin{aligned}
\Lambda &= \int \mathrm{d}x\mathrm{d}x' \begin{pmatrix} \boldsymbol{\mu} \\ \boldsymbol{\mu} \end{pmatrix}^{\mathsf{T}} (\mathbb{D}^{-1}\mathbb{Q})\mathbb{D}^{-1} \begin{pmatrix} \boldsymbol{\mu} \\ \boldsymbol{\mu} \end{pmatrix} \\
&= 2\int_{xx'} \begin{pmatrix} \boldsymbol{\mu} \\ \boldsymbol{\mu} \end{pmatrix}^{\mathsf{T}} \times \\
&\quad \begin{pmatrix} \mathbb{A}^{-1}(x,x')\left[\delta_{ij}Q_{ii}^{(1)}\delta^{xx'}\right]\mathbb{A}^{-1}(x,x') \\ \mathbb{A}^{-1}(x,x')\left[\left(Q_{ij}^{(s)}-Q_{ij}^{(a)}\right)\delta^{xx'}\right]\mathbb{A}^{-1}(x,x') \\ \qquad\qquad \mathbb{A}^{-1}(x,x')\left[\left(Q_{ij}^{(s)}+Q_{ij}^{(a)}\right)\delta^{xx'}\right]\mathbb{A}^{-1}(x,x') \\ \qquad\qquad \mathbb{A}^{-1}(x,x')\left[\delta_{ij}Q_{ii}^{(2)}\delta^{xx'}\right]\mathbb{A}^{-1}(x,x') \end{pmatrix} \begin{pmatrix} \boldsymbol{\mu} \\ \boldsymbol{\mu} \end{pmatrix}.
\end{aligned}$$

After performing the matrix product we obtain the following expression for Λ.

$$\begin{aligned}
\Lambda &= 2\int_{xx'} \Big\{ \boldsymbol{\mu}^{\mathsf{T}}\mathbb{A}^{-1}(x,x')\left[\delta_{ij}Q_{ii}^{(1)}\delta^{xx'}\right]\mathbb{A}^{-1}(x,x')\boldsymbol{\mu} \\
&\qquad +\boldsymbol{\mu}^{\mathsf{T}}\mathbb{A}^{-1}(x,x')\left[\left(Q_{ij}^{(s)}+Q_{ij}^{(a)}\right)\delta^{xx'}\right]\mathbb{A}^{-1}(x,x')\boldsymbol{\mu} \\
&\qquad +\boldsymbol{\mu}^{\mathsf{T}}\mathbb{A}^{-1}(x,x')\left[\delta_{ij}Q_{ii}^{(2)}\delta^{xx'}\right]\mathbb{A}^{-1}(x,x')\boldsymbol{\mu} \\
&\qquad +\boldsymbol{\mu}^{\mathsf{T}}\mathbb{A}^{-1}(x,x')\left[\left(Q_{ij}^{(s)}-Q_{ij}^{(a)}\right)\delta^{xx'}\right]\mathbb{A}^{-1}(x,x')\boldsymbol{\mu}\Big\} \\
&= 2\int_{xx'} \Big\{\boldsymbol{\mu}^{\mathsf{T}}\mathbb{A}^{-1}(x,x')\left[\delta_{ij}\left(Q_{ii}^{(1)}+Q_{ii}^{(2)}\right)\delta^{xx'}\right]\mathbb{A}^{-1}(x,x')\boldsymbol{\mu} \\
&\qquad +\boldsymbol{\mu}^{\mathsf{T}}\mathbb{A}^{-1}(x,x')\left[2Q_{ij}^{(s)}\delta^{xx'}\right]\mathbb{A}^{-1}(x,x')\boldsymbol{\mu}\Big\}.
\end{aligned} \tag{D.1.14}$$

Performing the detailed element wise product of the matrices we obtain

$$\begin{aligned}
\Lambda &= 2\sum_{abcd}\int_{\substack{xx'\\x''x'''}} \boldsymbol{\mu}_{ia}(\mathbb{A}^{-1}(x,x''))_{ab}\left[\delta_{bc}\left(Q_{bb}^{(1)}(x'')+Q_{bb}^{(2)}(x'')\right)\delta^{x''x'''}\right] \\
&\qquad \times(\mathbb{A}^{-1}(x''',x'))_{cd}\boldsymbol{\mu}_{dj} \\
&\quad +4\sum_{abcd}\int_{\substack{xx'\\x''x'''}} \boldsymbol{\mu}_{ia}(\mathbb{A}^{-1}(x,x''))_{ab}\left[Q_{bc}^{(s)}(x'')\delta^{x''x'''}\right](\mathbb{A}^{-1}(x''',x'))_{cd}\boldsymbol{\mu}_{dj}.
\end{aligned} \tag{D.1.15}$$

Once again, upon the application identity for $(\mathbb{A}^{-1}(x,x''))_{ab}$ we obtain

$$\begin{aligned}\Lambda &= 2\mu^2\sum_{abcd}\int_{\substack{xx'\\x''x'''}}(\delta_{ab})^{-1}(\delta_{cd})^{-1}\delta_{bc}\int\frac{dp}{(2\pi)^d}\frac{e^{ip(x-x'')}}{\kappa p^2+\gamma}\int\frac{dp}{(2\pi)^d}\frac{e^{iq(x'''-x')}}{\kappa q^2+\gamma}\\ &\qquad\times\left[\left(Q^{(1)}_{bb}(x'')+Q^{(2)}_{bb}(x'')\right)\delta^{x''x'''}\right]\\ &\quad+4\mu^2\sum_{abcd}\int_{\substack{xx'\\x''x'''}}(\delta_{ab})^{-1}(\delta_{cd})^{-1}\int\frac{dp}{(2\pi)^d}\frac{e^{ip(x-x'')}}{\kappa p^2+\gamma}\int\frac{dp}{(2\pi)^d}\frac{e^{iq(x'''-x')}}{\kappa q^2+\gamma}\\ &\qquad\left[Q^{(s)}_{bc}(x'')\delta^{x''x'''}\right],\end{aligned}\tag{D.1.16}$$

further,

$$\begin{aligned}\Lambda &= 2\mu^2\sum_{a}\int_{\substack{xx'\\x'''}}\int\frac{dp}{(2\pi)^d}\frac{e^{ip(x-x''')}}{\kappa p^2+\gamma}\int\frac{dp}{(2\pi)^d}\frac{e^{iq(x'''-x')}}{\kappa q^2+\gamma}\\ &\qquad\times\left(Q^{(1)}_{aa}(x''')+Q^{(2)}_{aa}(x''')\right)\\ &\quad+4\mu^2\sum_{bc}\int_{\substack{xx'\\x'''}}\int\frac{dp}{(2\pi)^d}\frac{e^{ip(x-x''')}}{\kappa p^2+\gamma}\int\frac{dp}{(2\pi)^d}\frac{e^{iq(x'''-x')}}{\kappa q^2+\gamma}Q^{(s)}_{bc}(x''')\\ &= 2\mu^2\sum_{a}\int\frac{dp\,dq}{(2\pi)^{2d}}\frac{\delta(p)\delta(-q)}{(\kappa p^2+\gamma)(q^2+\gamma)}\left(Q^{(1)}_{aa}(q-p)+Q^{(2)}_{aa}(q-p)\right)\\ &\quad+4\mu^2\sum_{bc}\int\frac{dp\,dq}{(2\pi)^{2d}}\frac{\delta(p)\delta(-q)}{(\kappa p^2+\gamma)(q^2+\gamma)}Q^{(s)}_{bc}(q-p)\\ &= 2\mu^2\sum_{a}\frac{\left(Q^{(1)}_{aa}(0)+Q^{(2)}_{aa}(0)\right)}{\gamma^2}+4\mu^2\sum_{bc}\frac{Q^{(s)}_{bc}(0)}{\gamma^2}\\ \Lambda &= 2n\mu^2\frac{\left(Q^{(1)}_{aa}(0)+Q^{(2)}_{aa}(0)\right)}{\gamma^2}+4(n^2-n)\mu^2\frac{Q^{(s)}_{bc}(0)}{\gamma^2}.\end{aligned}\tag{D.1.17}$$

We are now left with the final term Ξ to evaluate. In condensed form

$$\begin{aligned}\Xi &= \int \mathrm{d}x\mathrm{d}x'\begin{pmatrix}\boldsymbol{\mu}\\ \boldsymbol{\mu}\end{pmatrix}^{\mathsf{T}}\left(\mathbb{D}^{-1}\mathbb{Q}\right)^2\mathbb{D}^{-1}\begin{pmatrix}\boldsymbol{\mu}\\ \boldsymbol{\mu}\end{pmatrix}\\ &= \int \mathrm{d}x\mathrm{d}x'\begin{pmatrix}\boldsymbol{\mu}\\ \boldsymbol{\mu}\end{pmatrix}^{\mathsf{T}}\begin{pmatrix}\mathbb{I} & \mathbb{J}\\ \mathbb{K} & \mathbb{L}\end{pmatrix}\begin{pmatrix}\boldsymbol{\mu}\\ \boldsymbol{\mu}\end{pmatrix},\end{aligned}\tag{D.1.18}$$

where according to (D.1.3)

$$\begin{aligned}
\mathbb{I} &= \mathbb{A}^{-1}(x,x')\mathbb{C}(x,x')\mathbb{A}^{-1}(x,x')\mathbb{C}(x,x')\mathbb{A}^{-1}(x,x') \\
&\quad +\mathbb{A}^{-1}(x,x')\mathbb{D}(x,x')\mathbb{A}^{-1}(x,x')\mathbb{E}(x,x')\mathbb{A}^{-1}(x,x') \\
\mathbb{J} &= \mathbb{A}^{-1}(x,x')\mathbb{C}(x,x')\mathbb{A}^{-1}(x,x')\mathbb{D}(x,x')\mathbb{A}^{-1}(x,x') \\
&\quad +\mathbb{A}^{-1}(x,x')\mathbb{D}(x,x')\mathbb{A}^{-1}(x,x')\mathbb{F}(x,x')\mathbb{A}^{-1}(x,x') \\
\mathbb{K} &= \mathbb{A}^{-1}(x,x')\mathbb{E}(x,x')\mathbb{A}^{-1}(x,x')\mathbb{C}(x,x')\mathbb{A}^{-1}(x,x') \\
&\quad +\mathbb{A}^{-1}(x,x')\mathbb{F}(x,x')\mathbb{A}^{-1}(x,x')\mathbb{E}(x,x')\mathbb{A}^{-1}(x,x') \\
\mathbb{L} &= \mathbb{A}^{-1}(x,x')\mathbb{E}(x,x')\mathbb{A}^{-1}(x,x')\mathbb{D}(x,x')\mathbb{A}^{-1}(x,x') \\
&\quad +\mathbb{A}^{-1}(x,x')\mathbb{F}(x,x')\mathbb{A}^{-1}(x,x')\mathbb{F}(x,x')\mathbb{A}^{-1}(x,x').
\end{aligned} \tag{D.1.19}$$

Therefore,

$$\Xi = \int \mathrm{d}x\mathrm{d}x' \begin{pmatrix} \boldsymbol{\mu} \\ \boldsymbol{\mu} \end{pmatrix}^{\mathsf{T}} \begin{pmatrix} \mathbb{I} & \mathbb{J} \\ \mathbb{K} & \mathbb{L} \end{pmatrix} \begin{pmatrix} \boldsymbol{\mu} \\ \boldsymbol{\mu} \end{pmatrix}$$

$$
\begin{aligned}
= \sum_{abcdef} \int_{x'''x''''x'''''}^{xx'x''} & \Big\{ \boldsymbol{\mu}_{ia} (\mathbb{A}^{-1}(x,x''))_{ab} \mathbb{C}_{bc}(x'',x''') (\mathbb{A}^{-1}(x''',x''''))_{cd} \\
& \times \mathbb{C}_{de}(x'''',x''''') (\mathbb{A}^{-1}(x''''',x'))_{ef} \boldsymbol{\mu}_{fj} \\
& + \boldsymbol{\mu}_{ia} (\mathbb{A}^{-1}(x,x''))_{ab} \mathbb{D}_{bc}(x'',x''') (\mathbb{A}^{-1}(x''',x''''))_{cd} \\
& \times \mathbb{E}_{de}(x'''',x''''') (\mathbb{A}^{-1}(x''''',x'))_{ef} \boldsymbol{\mu}_{fj} \\
& + \boldsymbol{\mu}_{ia} (\mathbb{A}^{-1}(x,x''))_{ab} \mathbb{C}_{bc}(x'',x''') (\mathbb{A}^{-1}(x''',x''''))_{cd} \\
& \times \mathbb{D}_{de}(x'''',x''''') (\mathbb{A}^{-1}(x''''',x'))_{ef} \boldsymbol{\mu}_{fj} \\
& + \boldsymbol{\mu}_{ia} (\mathbb{A}^{-1}(x,x''))_{ab} \mathbb{D}_{bc}(x'',x''') (\mathbb{A}^{-1}(x''',x''''))_{cd} \\
& \times \mathbb{F}_{de}(x'''',x''''') (\mathbb{A}^{-1}(x''''',x'))_{ef} \boldsymbol{\mu}_{fj} \\
& + \boldsymbol{\mu}_{ia} (\mathbb{A}^{-1}(x,x''))_{ab} \mathbb{E}_{bc}(x'',x''') (\mathbb{A}^{-1}(x''',x''''))_{cd} \\
& \times \mathbb{C}_{de}(x'''',x''''') (\mathbb{A}^{-1}(x''''',x'))_{ef} \boldsymbol{\mu}_{fj} \\
& + \boldsymbol{\mu}_{ia} (\mathbb{A}^{-1}(x,x''))_{ab} \mathbb{F}_{bc}(x'',x''') (\mathbb{A}^{-1}(x''',x''''))_{cd} \\
& \times \mathbb{E}_{de}(x'''',x''''') (\mathbb{A}^{-1}(x''''',x'))_{ef} \boldsymbol{\mu}_{fj} \\
& + \boldsymbol{\mu}_{ia} (\mathbb{A}^{-1}(x,x''))_{ab} \mathbb{E}_{bc}(x'',x''') (\mathbb{A}^{-1}(x''',x''''))_{cd} \\
& \times \mathbb{D}_{de}(x'''',x''''') (\mathbb{A}^{-1}(x''''',x'))_{ef} \boldsymbol{\mu}_{fj} \\
& + \boldsymbol{\mu}_{ia} (\mathbb{A}^{-1}(x,x''))_{ab} \mathbb{F}_{bc}(x'',x''') (\mathbb{A}^{-1}(x''',x''''))_{cd} \\
& \times \mathbb{F}_{de}(x'''',x''''') (\mathbb{A}^{-1}(x''''',x'))_{ef} \boldsymbol{\mu}_{fj} \Big\} . \qquad \text{(D.1.20)}
\end{aligned}
$$

We shall now combine terms of similar structure with the application of the identity for $(\mathbb{A}^{-1}(x,x''))_{ab}$. Beginning with terms 2 and 7 we have

$$
\begin{aligned}
T_{2+7} = \; & 4\mu^2 \sum_{abcdef} \int_{x'''x''''x'''''}^{xx'x''} (\delta_{ab})^{-1} (\delta_{cd})^{-1} (\delta_{ef})^{-1} \\
& \times \int \frac{dp}{(2\pi)^d} \frac{e^{ip(x-x'')}}{\kappa p^2 + \gamma} \int \frac{\mathrm{d}q}{(2\pi)^d} \frac{e^{iq(x'''-x'''')}}{\kappa q^2 + \gamma} \int \frac{dr}{(2\pi)^d} \frac{e^{ir(x'''''-x')}}{\kappa r^2 + \gamma} \\
& \times \Big[\Big(Q^{(s)}_{bc}(x'') + Q^{(a)}_{bc}(x'') \Big) \delta^{x''x'''} \Big(Q^{(s)}_{de}(x'''') - Q^{(a)}_{de}(x'''') \Big) \delta^{x''''x'''''} \\
& \quad + \Big(Q^{(s)}_{bc}(x'') - Q^{(a)}_{bc}(x'') \Big) \delta^{x''x'''} \Big(Q^{(s)}_{de}(x'''') + Q^{(a)}_{de}(x'''') \Big) \delta^{x''''x'''''} \Big] .
\end{aligned}
$$

Evaluating this further,

$$\begin{aligned}
T_{2+7} &= 8\mu^2 \sum_{bce} \int_{\substack{xx' \\ x'''x''''}} \int \frac{dp\ dq\ dr}{(2\pi)^{3d}} \frac{e^{ip(x-x''')+iq(x'''-x'''')+ir(x''''-x')}}{(\kappa p^2+\gamma)(q^2+\gamma)(\kappa r^2+\gamma)} \\
&\qquad \times \left(Q^{(s)}_{bc}(x''') Q^{(s)}_{ce}(x'''') - Q^{(a)}_{bc}(x''') Q^{(a)}_{ce}(x'''') \right) \\
&= 8\mu^2 \sum_{bce} \int \frac{dp\ dq\ dr}{(2\pi)^{3d}} \frac{\delta(p)\delta(-r)}{(\kappa p^2+\gamma)(q^2+\gamma)(\kappa r^2+\gamma)} \\
&\qquad \times \left(Q^{(s)}_{bc}(q-p) Q^{(s)}_{ce}(r-q) - Q^{(a)}_{bc}(q-p) Q^{(a)}_{ce}(r-q) \right) \\
&= 8\mu^2 \sum_{bce} \int \frac{\mathrm{d}q}{(2\pi)^d} \frac{\left(Q^{(s)}_{bc}(q) Q^{(s)}_{ce}(-q) - Q^{(a)}_{bc}(q) Q^{(a)}_{ce}(-q) \right)}{\gamma^2(q^2+\gamma)} \\
T_{2+7} &= 8\mu^2 \sum_{bce} \int \frac{\mathrm{d}q}{(2\pi)^d} \frac{\left(Q^{(s)}_{bc}(q) Q^{(s)}_{ec}(-q) + Q^{(a)}_{bc}(q) Q^{(a)}_{ec}(-q) \right)}{\gamma^2(q^2+\gamma)}. \qquad \text{(D.1.21)}
\end{aligned}$$

Symmetry properties have been applied to reach the final step equation (D.1.21).

We similarly evaluate the combination of terms 4 and 6

$$\begin{aligned}
T_{4+6} &= 4\mu^2 \sum_{abcdef} \int_{\substack{xx'x'' \\ x'''x''''x'''''}} (\delta_{ab})^{-1} (\delta_{cd})^{-1} (\delta_{ef})^{-1} \\
&\quad \times \int \frac{dp}{(2\pi)^d} \frac{e^{ip(x-x'')}}{\kappa p^2+\gamma} \int \frac{dp}{(2\pi)^d} \frac{e^{iq(x'''-x'''')}}{\kappa q^2+\gamma} \int \frac{dr}{(2\pi)^d} \frac{e^{ir(x''''-x')}}{\kappa r^2+\gamma} \\
&\quad \times \Big[\left(Q^{(s)}_{bc}(x'') + Q^{(a)}_{bc}(x'') \right) \delta^{x''x'''} \left(\delta_{de} Q^{(2)}_{dd}(x'''') \right) \delta^{x''''x'''''} \\
&\qquad + \left(\delta_{bc} Q^{(2)}_{bb}(x'') \right) \delta^{x''x'''} \left(Q^{(s)}_{de}(x'''') - Q^{(a)}_{de}(x'''') \right) \delta^{x''''x'''''} \Big]
\end{aligned}$$

$$\begin{aligned}
T_{4+6} &= 4\mu^2 \sum_{abcdef} \int \frac{dp\ dq\ dr}{(2\pi)^{3d}} \frac{\delta(p)\delta(-r)(\delta_{ab})^{-1}(\delta_{cd})^{-1}(\delta_{ef})^{-1}}{(\kappa p^2+\gamma)(q^2+\gamma)(\kappa r^2+\gamma)} \\
&\quad \times \Big[\left(Q^{(s)}_{bc}(q-p) + Q^{(a)}_{bc}(q-p) \right) \left(\delta_{de} Q^{(2)}_{dd}(r-q) \right) \\
&\qquad + \left(\delta_{bc} Q^{(2)}_{bb}(q-p) \right) \left(Q^{(s)}_{de}(r-q) - Q^{(a)}_{de}(r-q) \right) \Big] \\
T_{4+6} &= 4\mu^2 \sum_{be} \int \frac{\mathrm{d}q}{(2\pi)^d} \frac{\left(Q^{(s)}_{be}(q) + Q^{(a)}_{be}(q) \right) \left(Q^{(2)}_{ee}(-q) \right)}{\gamma^2(q^2+\gamma)} \\
&\quad + 4\mu^2 \sum_{ce} \int \frac{\mathrm{d}q}{(2\pi)^d} \frac{\left(Q^{(2)}_{cc}(q) \right) \left(Q^{(s)}_{ce}(-q) - Q^{(a)}_{ce}(-q) \right)}{\gamma^2(q^2+\gamma)}. \qquad \text{(D.1.22)}
\end{aligned}$$

Similarly evaluating combination of terms 3 and 5 we have

$$\begin{aligned}
T_{3+5} &= 4\mu^2 \sum_{abcdef} \int_{\substack{xx'x'' \\ x'''x''''x'''''}} (\delta_{ab})^{-1} (\delta_{cd})^{-1} (\delta_{ef})^{-1} \\
&\times \int \frac{dp}{(2\pi)^d} \frac{e^{ip(x-x'')}}{\kappa p^2+\gamma} \int \frac{dp}{(2\pi)^d} \frac{e^{iq(x'''-x'''')}}{\kappa q^2+\gamma} \int \frac{dr}{(2\pi)^d} \frac{e^{ir(x'''''-x')}}{\kappa r^2+\gamma} \\
&\times \Big[\left(Q^{(s)}_{bc}(x'') - Q^{(a)}_{bc}(x'') \right) \delta^{x''x'''} \left(\delta_{de} Q^{(1)}_{dd}(x'''') \right) \delta^{x''''x'''''} \\
&\quad + \left(\delta_{bc} Q^{(1)}_{bb}(x'') \right) \delta^{x''x'''} \left(Q^{(s)}_{de}(x'''') + Q^{(a)}_{de}(x'''') \right) \delta^{x''''x'''''} \Big] \\
T_{3+5} &= 4\mu^2 \sum_{be} \int \frac{\mathrm{d}q}{(2\pi)^d} \frac{\left(Q^{(s)}_{be}(q) - Q^{(a)}_{be}(q) \right) \left(Q^{(1)}_{ee}(-q) \right)}{\gamma^2(q^2+\gamma)} \\
&\quad + 4\mu^2 \sum_{ce} \int \frac{\mathrm{d}q}{(2\pi)^d} \frac{\left(Q^{(1)}_{cc}(q) \right) \left(Q^{(s)}_{ce}(-q) + Q^{(a)}_{ce}(-q) \right)}{\gamma^2(q^2+\gamma)}. \qquad \text{(D.1.23)}
\end{aligned}$$

Concluding with evaluating the combination of terms terms 1 and 8 we have

$$\begin{aligned}
T_{1+8} &= 4\mu^2 \sum_{abcdef} \int_{\substack{xx'x'' \\ x'''x''''x'''''}} (\delta_{ab})^{-1} (\delta_{cd})^{-1} (\delta_{ef})^{-1} \delta_{bc}\delta_{de} \\
&\times \int \frac{dp}{(2\pi)^d} \frac{e^{ip(x-x'')}}{\kappa p^2+\gamma} \int \frac{dp}{(2\pi)^d} \frac{e^{iq(x'''-x'''')}}{\kappa q^2+\gamma} \int \frac{dr}{(2\pi)^d} \frac{e^{ir(x'''''-x')}}{\kappa r^2+\gamma} \\
&\times \Big[Q^{(2)}_{bb}(x'') \delta^{x''x'''} Q^{(2)}_{dd}(x'''') \delta^{x''''x'''''} \\
&\qquad + Q^{(1)}_{bb}(x'') \delta^{x''x'''} Q^{(1)}_{dd}(x'''') \delta^{x''''x'''''} \Big] \\
T_{1+8} &= 4\mu^2 \sum_{a} \int \frac{\mathrm{d}q}{(2\pi)^d} \frac{\left(Q^{(1)}_{aa}(q) Q^{(1)}_{aa}(-q) + Q^{(2)}_{aa}(q) Q^{(2)}_{aa}(-q) \right)}{\gamma^2(q^2+\gamma)}. \qquad \text{(D.1.24)}
\end{aligned}$$

Collecting terms together for Ξ from (D.1.24), (D.1.23), (D.1.22) and (D.1.21) we have

$$\Xi = T_{1+8} + T_{3+5} + T_{4+6} + T_{2+7} \qquad \text{(D.1.25)}$$

Finally collecting the results for Θ , Λ and Ξ from equations (D.1.13), (D.1.17) and (D.1.25), respectively, we obtain

$$\int \mathrm{d}x \mathrm{d}x' \begin{pmatrix} \boldsymbol{\mu} \\ \boldsymbol{\mu} \end{pmatrix}^{\mathsf{T}} \mathbb{M}^{-1}(x,x') \begin{pmatrix} \boldsymbol{\mu} \\ \boldsymbol{\mu} \end{pmatrix} = \Theta - \Lambda + \frac{1}{2}\Xi, \qquad \text{(D.1.26)}$$

equivalent to,

$$\begin{aligned}
&\int \mathrm{d}x\mathrm{d}x' \begin{pmatrix} \boldsymbol{\mu} \\ \boldsymbol{\mu} \end{pmatrix}^{\mathsf{T}} \mathbb{M}^{-1}(x,x') \begin{pmatrix} \boldsymbol{\mu} \\ \boldsymbol{\mu} \end{pmatrix} \\
&= \frac{2n\mu^2\delta(0)}{\gamma} - 2n\mu^2 \frac{\left(Q^{(1)}_{aa}(0) + Q^{(2)}_{aa}(0)\right)}{\gamma^2} - 4(n^2-n)\mu^2 \frac{Q^{(s)}_{bc}(0)}{\gamma^2} \\
&\quad + 4\mu^2 \sum_{bce} \int \frac{\mathrm{d}q}{(2\pi)^d} \frac{\left(Q^{(s)}_{bc}(q) Q^{(s)}_{ec}(-q) + Q^{(a)}_{bc}(q) Q^{(a)}_{ec}(-q)\right)}{\gamma^2(q^2+\gamma)} \\
&\quad + 2\mu^2 \sum_{be} \int \frac{\mathrm{d}q}{(2\pi)^d} \frac{\left(Q^{(s)}_{be}(q) + Q^{(a)}_{be}(q)\right)\left(Q^{(2)}_{ee}(-q)\right)}{\gamma^2(q^2+\gamma)} \\
&\quad + 2\mu^2 \sum_{ce} \int \frac{\mathrm{d}q}{(2\pi)^d} \frac{\left(Q^{(2)}_{cc}(q)\right)\left(Q^{(s)}_{ce}(-q) - Q^{(a)}_{ce}(-q)\right)}{\gamma^2(q^2+\gamma)} \\
&\quad + 2\mu^2 \sum_{be} \int \frac{\mathrm{d}q}{(2\pi)^d} \frac{\left(Q^{(s)}_{be}(q) - Q^{(a)}_{be}(q)\right)\left(Q^{(1)}_{ee}(-q)\right)}{\gamma^2(q^2+\gamma)} \\
&\quad + 2\mu^2 \sum_{ce} \int \frac{\mathrm{d}q}{(2\pi)^d} \frac{\left(Q^{(1)}_{cc}(q)\right)\left(Q^{(s)}_{ce}(-q) + Q^{(a)}_{ce}(-q)\right)}{\gamma^2(q^2+\gamma)} \\
&\quad + 2\mu^2 \sum_{a} \int \frac{\mathrm{d}q}{(2\pi)^d} \frac{\left(Q^{(1)}_{aa}(q) Q^{(1)}_{aa}(-q) + Q^{(2)}_{aa}(q) Q^{(2)}_{aa}(-q)\right)}{\gamma^2(q^2+\gamma)} \qquad \text{(D.1.27)}
\end{aligned}$$

This can be further reduced to

$$\begin{aligned}
&\int \mathrm{d}x\mathrm{d}x' \begin{pmatrix} \boldsymbol{\mu} \\ \boldsymbol{\mu} \end{pmatrix}^{\mathsf{T}} \mathbb{M}^{-1}(x,x') \begin{pmatrix} \boldsymbol{\mu} \\ \boldsymbol{\mu} \end{pmatrix} \\
&= \frac{2n\mu^2\delta(0)}{\gamma} - 4(n^2-n)\mu^2 \frac{Q^{(s)}_{bc}(0)}{\gamma^2} - 2n\mu^2 \frac{\left(Q^{(1)}_{aa}(0) + Q^{(2)}_{aa}(0)\right)}{\gamma^2} \\
&\quad + 2\mu^2 \sum_{a} \int \frac{\mathrm{d}q}{(2\pi)^d} \frac{\left(Q^{(1)}_{aa}(q) Q^{(1)}_{aa}(-q) + Q^{(2)}_{aa}(q) Q^{(2)}_{aa}(-q)\right)}{\gamma^2(q^2+\gamma)} \\
&\quad + 4\mu^2 \sum_{bce} \int \frac{\mathrm{d}q}{(2\pi)^d} \frac{\left(Q^{(s)}_{bc}(q) Q^{(s)}_{ec}(-q) + Q^{(a)}_{bc}(q) Q^{(a)}_{ec}(-q)\right)}{\gamma^2(q^2+\gamma)} \\
&\quad + 4\mu^2 \sum_{be} \int \frac{\mathrm{d}q}{(2\pi)^d} \frac{\left(Q^{(1)}_{ee}(-q) + Q^{(2)}_{ee}(-q)\right) Q^{(s)}_{eb}(q)}{\gamma^2(q^2+\gamma)}. \qquad \text{(D.1.28)}
\end{aligned}$$

D.2 Evaluation of $Z^n[Q_{ii}][d=1]$

In this section we perform substitution to the conclusion of the integration evaluation of the below quantity $\langle Z^n[Q_{ii}]\rangle$

$$\begin{aligned}\langle Z^n[Q_{ii}]\rangle \approx & -\frac{nL^d}{(2\pi)^{d/2}\Gamma(d/2)}\left\{\int_0^{\frac{1}{\sqrt{1/4\gamma}}} \mathrm{d}q\, q^{d-1}\ln\left[\frac{1}{\Delta}-\frac{2\mu^2}{\gamma^3}+\left(\frac{2\mu^2\kappa}{\gamma^4}+\frac{(4\pi)^{\alpha/2}}{48\pi^2\gamma\kappa}\right)q^2\right.\right.\\ &\left.-\frac{(4\pi)^{\alpha/2}}{8\pi^2}\left\{\frac{2}{\alpha}+\psi(1)-\ln(\gamma)\right\}\right]\\ &+\int_{\frac{1}{\sqrt{1/4\gamma}}}^{\Lambda}\mathrm{d}q\, q^{d-1}\ln\left[\frac{1}{\Delta}-\frac{2\mu^2}{\gamma^2\kappa q^2}-\frac{(4\pi)^{\alpha/2}}{8\pi^2\kappa}\left\{\frac{2}{\alpha}+\psi(1)-\ln(\gamma)+2\right.\right.\\ &\left.\left.\left.-\left(1+\frac{1}{2}\frac{4}{q^2}\right)\ln\left(1+\frac{q^2}{2\gamma}\right)\right\}\right]\right\}. \quad \text{(D.2.1)}\end{aligned}$$

In one dimension, $d=1$, $\langle Z^n[Q_{ii}]\rangle$ becomes

$$\begin{aligned}\approx & -\frac{nL}{\sqrt{2}\pi}\left\{\frac{\sqrt{\beta k\rho_0}\sqrt{-\frac{\beta^2k^2\left(\rho_0^3\left(\beta^3ck^3-\beta^3k^3\log\left(\frac{\beta k\rho_0}{\kappa}\right)-4\sqrt{\pi}\beta kR\right)+8\sqrt{\pi}\mu^2\right)}{R}}}{\sqrt{\kappa}\sqrt{\frac{\beta^2k^2}{R}}\sqrt{48\sqrt{\pi}\mu^2+\beta^3k^3\rho_0^3}}\times\right.\\ &2\sqrt{6}\tan^{-1}\left(\frac{\sqrt{\frac{2}{3}}\sqrt{\kappa}\sqrt{\frac{\beta^2k^2}{R}}\sqrt{\frac{\beta k\rho_0}{\kappa}}\sqrt{48\sqrt{\pi}\mu^2+\beta^3k^3\rho_0^3}}{\sqrt{\beta k\rho_0}\sqrt{-\frac{\beta^2k^2\left(\rho_0^3\left(\beta^3ck^3-\beta^3k^3\log\left(\frac{\beta k\rho_0}{\kappa}\right)-4\sqrt{\pi}\beta kR\right)+8\sqrt{\pi}\mu^2\right)}{R}}}\right)\\ &-\frac{\sqrt{\kappa}\sqrt{\frac{\beta^2k^2}{R}}\sqrt{\frac{\beta k\rho_0}{\kappa}}\sqrt{48\sqrt{\pi}\mu^2+\beta^3k^3\rho_0^3}}{\sqrt{\kappa}\sqrt{\frac{\beta^2k^2}{R}}\sqrt{48\sqrt{\pi}\mu^2+\beta^3k^3\rho_0^3}}\times\\ &\left(-2\log\left(-\frac{c}{-}+\frac{2}{3}+\frac{24\sqrt{\pi}\mu^2}{\beta^3k^3\rho_0^3}+\frac{4\sqrt{\pi}R}{\beta^2k^2}+\frac{\log\left(\frac{\beta k\rho_0}{\kappa}\right)}{}\right)+4+\log(\pi)\right)\\ &\left.+\int_{\sqrt{\frac{4\beta k\rho_0}{\kappa}}}^{\Lambda}\log\left(-\frac{b-\log\left(\frac{\beta k\rho_0}{\kappa}\right)-\left(\frac{2\beta k\rho_0}{\kappa q^2}+1\right)\log\left(\frac{\kappa q^2}{2\beta k\rho_0}+1\right)}{\sqrt{\pi}}-\frac{8\mu^2}{\beta^2\kappa k^2q^2\rho_0^2}+\frac{4R}{\beta^2k^2}\right)\,dq\right\}\end{aligned}$$

D.3 Evaluation of $Z^n[Q_{ij}^{(s)}[d=1]$

In this section we perform substitution to the conclusion of the integration evaluation of $\langle Z^n[Q_{ij}^{(s)}]\rangle$ in equation (4.3.8).

In one dimension, $d = 1$, (where we have combined with the similar term from the antisymmetric contribution below), $d = 1$, $\langle Z^n[Q_{ij}^{(s)}]\rangle$ becomes

$$
\begin{aligned}
\approx\ & +\frac{nL}{\sqrt{8\pi}}\left\{2\sqrt{\frac{\beta k\rho_0}{\kappa}}\log\left(-\frac{2\left(c-\log\left(\frac{\beta k\rho_0}{\kappa}\right)\right)}{\sqrt{\pi}}+\frac{4}{3\sqrt{\pi}}+\frac{4R}{\beta^2k^2}\right)\right. \\
& +\frac{4\sqrt{3}\sqrt{\beta k\rho_0}\sqrt{-\frac{\beta^2ck^2}{2R}+\sqrt{\pi}+\frac{\beta^2k^2\log\left(\frac{\beta k\rho_0}{\kappa}\right)}{2R}}}{\sqrt{\kappa}\sqrt{\frac{\beta^2k^2}{R}}} \\
& \qquad \times\tan^{-1}\left(\frac{\sqrt{\kappa}\sqrt{\frac{\beta^2k^2}{R}}\sqrt{\frac{\beta k\rho_0}{\kappa}}}{\sqrt{3}\sqrt{\beta k\rho_0}\sqrt{-\frac{\beta^2ck^2}{2R}+\sqrt{\pi}+\frac{\beta^2k^2\log\left(\frac{\beta k\rho_0}{\kappa}\right)}{2R}}}\right)-4\sqrt{\frac{\beta k\rho_0}{\kappa}} \\
& \left.+\int_{\sqrt{\frac{4\beta k\rho_0}{\kappa}}}^{\Lambda}\log\left(\frac{4R}{\beta^2k^2}-\frac{2\left(b-\log\left(\frac{\beta k\rho_0}{\kappa}\right)-\left(\frac{2\beta k\rho_0}{\kappa q^2}+1\right)\log\left(\frac{\kappa q^2}{2\beta k\rho_0}+1\right)\right)}{\sqrt{\pi}}\right)dq\right\}
\end{aligned}
$$

$$
-\frac{nL}{\sqrt{32}\pi}\left\{\frac{32\sqrt{\pi}\mu^2}{k^3\beta^3\sqrt{\frac{k^2\beta^2}{R}}\rho_0^3}\frac{1}{R\sqrt{\kappa}\sqrt{k^3\beta^3\rho_0^3+48\mu^2\sqrt{\pi}}}\right.
$$

$$
\left(\frac{1}{\left(k^3\beta^3\rho_0^3-16\left(-\frac{3ck^2\beta^2}{2R}+\frac{k^2\beta^2}{4R}+3\sqrt{\pi}\right)\mu^2-\frac{24k^2\beta^2\mu^2\log\left(\frac{k\beta\rho_0}{\kappa}\right)}{R}\right)}\right.
$$

$$
\frac{1}{\sqrt{\frac{k^5\log\left(\frac{k\beta\rho_0}{\kappa}\right)\rho_0^3\beta^5}{4R}-\frac{ck^5\rho_0^3\beta^5}{4R}+\sqrt{\pi}\left(k^3\beta^3\rho_0^3-\frac{2k^2\beta^2\mu^2}{R}\right)}}
$$

$$
\left[k^2\left(-\frac{3k^5\log\left(\frac{k\beta\rho_0}{\kappa}\right)\rho_0^3\beta^5}{R}+k^3\left(\frac{3ck^2\beta^2}{R}-\frac{k^2\beta^2}{4R}-12\sqrt{\pi}\right)\rho_0^3\beta^3+\frac{12k^2\mu^2\sqrt{\pi}\beta^2}{R}\right)\beta^2\right.
$$

$$
\times\tan^{-1}\left(\frac{\sqrt{\frac{k^2\beta^2}{R}}\sqrt{\kappa}\sqrt{\frac{k\beta\rho_0}{\kappa}}\sqrt{k^3\beta^3\rho_0^3+48\mu^2\sqrt{\pi}}}{\sqrt{6}\sqrt{k\beta\rho_0}\sqrt{\frac{k^5\log\left(\frac{k\beta\rho_0}{\kappa}\right)\rho_0^3\beta^5}{4R}-\frac{ck^5\rho_0^3\beta^5}{4R}+\sqrt{\pi}\left(k^3\beta^3\rho_0^3-\frac{2k^2\beta^2\mu^2}{R}\right)}}\right)
$$

$$
\left.\left.\sqrt{6}\sqrt{k\beta\rho_0}\mu^2\right]\right)-\sqrt{\frac{k^2\beta^2}{R}}\sqrt{\frac{k\beta\rho_0}{\kappa}}
$$

$$
+\frac{\sqrt{3}\tan^{-1}\left(\frac{\sqrt{\frac{k^2\beta^2}{R}}\sqrt{\kappa}\sqrt{\frac{k\beta\rho_0}{\kappa}}}{\sqrt{3}\sqrt{\frac{k^2\log\left(\frac{k\beta\rho_0}{\kappa}\right)\beta^2}{2R}-\frac{ck^2\beta^2}{2R}+\sqrt{\pi}}\sqrt{k\beta\rho_0}}\right)}{\sqrt{\kappa}\sqrt{\frac{k^2\log\left(\frac{k\beta\rho_0}{\kappa}\right)\beta^2}{2R}-\frac{ck^2\beta^2}{2R}+\sqrt{\pi}}}\times
$$

$$
\frac{\sqrt{k\beta\rho_0}\left(\frac{36k^4\mu^2\log^2\left(\frac{k\beta\rho_0}{\kappa}\right)\beta^4}{R^2}+k^3\left(\frac{(6c-1)k^2\beta^2}{4R}-3\sqrt{\pi}\right)\rho_0^3\beta^3\right.}{\left(-k^3\beta^3\rho_0^3+16\left(-\frac{3ck^2\beta^2}{2R}+\frac{k^2\beta^2}{4R}+3\sqrt{\pi}\right)\mu^2+\frac{24k^2\beta^2\mu^2\log\left(\frac{k\beta\rho_0}{\kappa}\right)}{R}\right)}
$$

$$
-\frac{3k^2\log\left(\frac{k\beta\rho_0}{\kappa}\right)\left(k^3\beta^3\rho_0^3+16\left(\frac{3ck^2\beta^2}{R}-\frac{k^2\beta^2}{4R}-6\sqrt{\pi}\right)\mu^2\right)\beta^2}{2R}
$$

$$
\left.\left.+8\left(\frac{(72c^2-12c+1)k^4\beta^4}{16R^2}+\frac{3(1-12c)k^2\sqrt{\pi}\beta^2}{2R}+18\pi\kappa^4\right)\mu^2\right)\right)
$$

$$
+\int_{\sqrt{\frac{4\beta k\rho_0}{\kappa}}}^{\Lambda}\frac{\frac{64\mu^4}{\beta^4k^4q^4\rho_0^4\left(-\frac{b-\log\left(\frac{\beta k\rho_0}{\kappa}\right)-\left(\frac{2\beta k\rho_0}{\kappa q^2}+1\right)\log\left(\frac{\kappa q^2}{2\beta k\rho_0}+1\right)}{\sqrt{\pi}}-\frac{8\mu^2}{\beta^2\kappa k^2q^2\rho_0^2}+\frac{4R}{\beta^2k^2}\right)}+\frac{16\mu^2}{\beta^2\kappa k^2q^2\rho_0^2}}{\frac{4R}{\beta^2k^2}-\frac{2\left(b-\log\left(\frac{\beta k\rho_0}{\kappa}\right)-\left(\frac{2\beta k\rho_0}{\kappa q^2}+1\right)\log\left(\frac{\kappa q^2}{2\beta k\rho_0}+1\right)\right)}{\sqrt{\pi}}}dq\right\}. \tag{D.3.1}
$$

D.4 Evaluation of $Z^n[Q_{ij}^{(a)}][d=1]$

In this section we perform substitution to the conclusion of the integration evaluation of $\langle Z^n[Q_{ij}^{(s)}]\rangle$ in equation (4.3.12). In one dimension, $d=1$, $\langle Z^n[Q_{ij}^{(a)}]\rangle$ becomes

$$\frac{3\sqrt{\frac{2}{\pi}}\mu^2 Ln}{\beta k\rho_0^3 R}\left(\frac{8\sqrt{\beta k\rho_0}\left(-\frac{3\beta^2ck^2}{2R}+3\sqrt{\pi}+\frac{3\beta^2k^2\log\left(\frac{\beta k\rho_0}{\kappa}\right)}{2R}+\frac{\beta^2k^2}{4R}\right)}{\sqrt{3}\sqrt{\kappa}\left(\frac{\beta^2k^2}{R}\right)^{3/2}\sqrt{-\frac{\beta^2ck^2}{2R}+\sqrt{\pi}+\frac{\beta^2k^2\log\left(\frac{\beta k\rho_0}{\kappa}\right)}{2R}}}\right.$$
$$\left.\times\tan^{-1}\left(\frac{\sqrt{\kappa}\sqrt{\frac{\beta^2k^2}{R}}\sqrt{\frac{\beta k\rho_0}{\kappa}}}{\sqrt{3}\sqrt{\beta k\rho_0}\sqrt{-\frac{\beta^2ck^2}{2R}+\sqrt{\pi}+\frac{\beta^2k^2\log\left(\frac{\beta k\rho_0}{\kappa}\right)}{2R}}}\right)-\frac{8R\sqrt{\frac{\beta k\rho_0}{\kappa}}}{\beta^2k^2}\right)$$
$$+\frac{nL}{\sqrt{8}\pi}\int_{\sqrt{\frac{4\beta k\rho_0}{\kappa}}}^{\Lambda}\frac{16\mu^2}{\beta^2k^2\rho_0^2\left(\frac{4R}{\beta^2k^2}-\frac{2\left(b-\log\left(\frac{\beta k\rho_0}{\kappa}\right)-\left(\frac{2\beta k\rho_0}{\kappa q^2}+1\right)\log\left(\frac{\kappa q^2}{2\beta k\rho_0}+1\right)\right)}{\sqrt{\pi}}\right)}dq \tag{D.4.1}$$